



DPTO. QUÍMICA ORGÁNICA
FACULTAD DE QUÍMICA
UNIVERSIDAD DE SEVILLA



INSTITUTO DE
INVESTIGACIONES QUÍMICAS
CONSEJO SUPERIOR DE
INVESTIGACIONES CIENTÍFICAS

Dynamization Strategies for the Atroposelective Synthesis of (Hetero)biaryls

Memoria presentada por el Licenciado
José Alberto Carmona Carmona
para optar al grado de Doctor en Química.

Sevilla, Julio 2019



**DEPARTAMENTO DE QUÍMICA ORGÁNICA
FACULTAD DE QUÍMICA - UNIVERSIDAD DE SEVILLA**



**INSTITUTO DE INVESTIGACIONES QUÍMICAS.
CONSEJO SUPERIOR DE INVESTIGACIONES CIENTÍFICAS**

VºBº La Directora de la Tesis

VºBº El Director de la Tesis

Fdo. Dra. Rosario Fernández Fernández,
Catedrática de Universidad
Departamento de Química Orgánica
Universidad de Sevilla

Fdo. Dr. José María Lassaletta Simón
Profesor de Investigación del CSIC
Instituto de Investigaciones Químicas

VºBº El Director de la Tesis

Fdo. Valentín Hornillos Gómez-Recuero
Investigador Ramón y Cajal
Departamento de Química Orgánica
Universidad de Sevilla

Summary/Resumen	12
Summary	12
Resumen.....	13
I. Introduction and Objectives.....	16
I.1. Asymmetric catalysis.....	16
I.1.2. Axial Chirality: Atropisomerism.	24
I.2. Atroposelective synthesis of axially chiral (hetero)biaryls.....	28
I.3. Atroposelective transformations for the synthesis of axially chiral (hetero)biaryls.	32
I.3.1. Desymmetrization.....	33
I.3.2. Kinetic Resolution (KR).....	37
I.3.2. Dynamic Kinetic Resolution (DKR).....	38
I.3.2.1. Bringmann's Biaryl " <i>Lactone Concept</i> ".....	40
I.3.2.2. Clayden's approach.	47
I.3.2. Dynamic Kinetic Asymmetric Transformation (DYKAT).....	49
I.4. Simultaneous generation of central and axial chirality in (hetero)biaryls.	55
I.5. Objectives.	65
II. Dynamic Kinetic Asymmetric Heck Reaction for the Synthesis of Heterobiaryls with Central and Axial Chirality.....	68
II.1. Introduction: Palladium-catalyzed cross-coupling reactions.....	68
II.2. Introduction: The Mizoroki-Heck reaction.	70
II.2.1. Precedents.....	70
II.2.2. Mechanism of the Heck reaction.....	75
II.3 Results and discussion.....	83
II.3.1. Synthesis of starting materials.....	84
II.3.2. Preliminary studies.....	86
II.3.3. Dynamic kinetic asymmetric Heck reaction with cyclic alkenes.....	87
II.3.4. Dynamic kinetic asymmetric Heck reaction with acyclic alkenes.....	100
II.3.5. Hydroarylation of 2,5-norbornadiene.....	105
II.3.6. Control experiments.....	106
II.3.7. Representative transformations.....	109

II.3.8. Mechanistic study	111
II.4 Conclusions.	119
II.5. Experimental Section.....	120
II.5.1. Synthesis of alcohols precursors to nonaflates substrates.	120
Synthesis of 1-(Isoquinolin-1-yl)-4-methylnaphthalen-2-ol	120
II.5.2. General procedure for the synthesis of nonaflates 3g and 3h.	121
Synthesis of 1-(Isoquinolin-1-yl)-4-methylnaphthalen-2-yl-1-nonaflate. 3g.....	121
Synthesis of 1-(Isoquinolin-1-yl)pyren-2-yl-1-nonaflate. 3h.....	122
II.5.3. General procedure for the Dynamic Kinetic Asymmetric Heck Reaction ...	122
Synthesis of (S)-1-{2-[(S)-2,3-Dihydrofuran-2-yl]naphthalen-1-yl}isoquinoline. 5b.....	123
Synthesis of (S)-1-{2-[(S)-2,5-Dihydrofuran-2-yl]naphthalen-1-yl}isoquinoline. 5'b	124
Synthesis of (S)-4-{2-[(S)-2,3-Dihydrofuran-2-yl]naphthalen-1-yl}quinazoline. 5c	125
Synthesis of (S)-1-{2-[(S)-2,3-Dihydrofuran-2-yl]naphthalen-1-yl}phthalazine. 5d	126
Synthesis of (S)-2-{2-[(S)-2,3-Dihydrofuran-2-yl]naphthalen-1-yl}-3- methylpyridine. 5e.....	127
Synthesis of (S)-1-{2-[(S)-2,3-Dihydrofuran-2-yl]-4-methoxynaphthalen-1- yl}isoquinoline. 5f.....	128
Synthesis of (S)-1-{2-[(S)-2,3-Dihydrofuran-2-yl]-4-methylnaphthalen-1- yl}isoquinoline. 5g	129
Synthesis of (S)-1-{2-[(S)-2,3-Dihydrofuran-2-yl]pyren-1-yl}isoquinoline. 5h. 130	
Synthesis of (S)-1-{2-[(S)-2,5-Dihydrofuran-2-yl]pyren-1-yl}isoquinoline. 5'h 131	
Synthesis of <i>N</i> -Boc protected (S)-1-{2-[(S)-2,3-dihydro-1 <i>H</i> -pyrrol-2- yl]naphthalen-1-yl}isoquinoline. 7b	132
Synthesis of <i>N</i> -Boc protected (S)-1-{2-[(S)-2,5-dihydro-1 <i>H</i> -pyrrol-2- yl]naphthalen-1-yl}isoquinoline. 7'b	133
Synthesis of <i>N</i> -Boc protected (S)-4-{2-[(S)-2,3-dihydro-1 <i>H</i> -pyrrol-2- yl]naphthalen-1-yl}quinazoline. 7c.....	134
Synthesis of <i>N</i> -Boc protected (S)-1-{2-[(S)-2,3-dihydro-1 <i>H</i> -pyrrol-2- yl]naphthalen-1-yl}phthalazine. 5d.....	135

Synthesis of <i>N</i> -Boc protected (<i>S</i>)-2-{2-[(<i>S</i>)-2,3-dihydro-1 <i>H</i> -pyrrol-2-yl]naphthalen-1-yl}-3-methylpyridine. 7e	136
Synthesis of <i>N</i> -Boc protected (<i>S</i>)-1-{2-[(<i>S</i>)-2,5-dihydro-1 <i>H</i> -pyrrol-2-yl]pyren-1-yl}isoquinoline. 7'h	137
Synthesis of (<i>S</i>)-1-[2-(1-Butoxyvinyl)naphthalen-1-yl]isoquinoline. 13b	138
Synthesis of (<i>S</i>)-4-[2-(1-Butoxyvinyl)naphthalen-1-yl]quinazoline. 13c	138
Synthesis of (<i>S</i>)-1-[2-(1-Ethoxyvinyl)naphthalen-1-yl]isoquinoline. 14b	139
Synthesis of (<i>S</i>)-1-{2-[1-(Cyclohexyloxy)vinyl]naphthalen-1-yl}isoquinoline. 15b	140
Synthesis of (<i>S</i>)-4-{2-[1-(Cyclohexyloxy)vinyl]naphthalen-1-yl}quinazoline. 15c	141
Synthesis of (<i>S</i>)-1-{2-[1-(2-Chloroethoxy)vinyl]naphthalen-1-yl}isoquinoline. 16b	142
Synthesis of (<i>S</i>)-2-{2-[1-(2-Chloroethoxy)vinyl]naphthalen-1-yl}-3-methylpyridine. 16e	143
Synthesis of (<i>S</i>)- <i>N</i> -{1-[1-(Isoquinolin-1-yl)naphthalen-2-yl]vinyl}- <i>N</i> -methylacetamide. 17b	144
II.5.4. Hydroarylation of 2,5-norbornadiene	145
Synthesis of (<i>S</i>)-1-{2-[(1 <i>S</i> ,2 <i>R</i> ,4 <i>S</i>)-Bicyclo[2.2.1]hept-5-en-2-yl]naphthalen-1-yl}isoquinoline. 18	145
Synthesis of (<i>R</i>)-1-{2-[(1 <i>R</i> ,2 <i>S</i> ,4 <i>R</i>)-Bicyclo[2.2.1]hept-5-en-2-yl]naphthalen-1-yl}isoquinoline hydrochloride. <i>ent</i> -18·HCl	146
II.5.5. Representative transformations from 7b.	147
Synthesis of (<i>S_a,S</i>)-1-{2-[(<i>S</i>)-3,4-Dihydro-2 <i>H</i> -pyrrol-2-yl]naphthalen-1-yl}isoquinoline. 20b	147
Synthesis of the Pd-20b complex. 21	148
Synthesis of (<i>S</i>)-1-{2-[(<i>S</i>)-Pyrrolidin-2-yl]naphthalen-1-yl}isoquinoline. 22b ..	149
II.5.6. Isolation of the Oxidative Addition Intermediate I ^{OA} _{L1} (OTf ⁻).	150
II.5.7. Reaction of Oxidative Addition Intermediate I ^{OA} _{L1} (OTf ⁻) with 2,3-dihydrofuran 4.	151
III. Dynamic Kinetic Resolution of Heterobiaryl Ketones by Zinc-catalyzed Asymmetric Hydrosilylation	154
III.1. Introduction	154
III.2. Results and Discussion.	162

III.2.1. Substrate design and synthesis.	162
III.2.2. Configurational stability analysis of the substrates	165
III.2.2.1. DFT calculations.	166
III.2.2.2. Racemization experiments.	167
III.2.3. Reaction conditions optimization.	170
III.2.4. Reaction scope.....	174
III.2.4. Representative transformations.	182
III.3. Conclusions.	185
General procedure for the synthesis of ligands L28-L33	186
Synthesis of (1 <i>S</i> ,2 <i>S</i>)- <i>N,N'</i> -Bis[4-(<i>tert</i> -butyl)benzyl]-1-phenyl-2-phosphanylethane-1,2-diamine. L30	186
III.4.2. General procedures for the synthesis of heterobiaryl ketones.	187
Synthesis of 1-[1-(Isoquinolin-1-yl)naphthalen-2-yl]ethan-1-one. 25a	188
Synthesis of 1-[1-(Quinazolin-4-yl)naphthalen-2-yl]ethan-1-one. 25b.....	188
Synthesis of 1-[1-(3-Methylpyridin-2-yl)naphthalen-2-yl]ethan-1-one. 25c	189
Synthesis of 1-[1-(isoquinolin-1-yl)-4-methylnaphthalen-2-yl]ethan-1-one. 25e	189
Synthesis of 1-[1-(Isoquinolin-1-yl)pyren-2-yl]ethan-1-one. 25f.	190
Synthesis of 1-[2-(Isoquinolin-1-yl)-3-methylphenyl]ethan-1-one. 25g.....	191
Synthesis of 1-[1-(3-Phenylisoquinolin-1-yl)naphthalen-2-yl]ethan-1-one. 25h	191
Synthesis of 1-[1-(Isoquinolin-1-yl)naphthalen-2-yl]propan-1-one. 25i.....	192
Synthesis of 1-[1-(isoquinolin-1-yl)naphthalen-2-yl]-3,3-dimethylbutan-1-one. 25j	192
Synthesis of Cyclohexyl[1-(isoquinolin-1-yl)naphthalen-2-yl]methanone. 25k.	193
III.4.3. General procedure for the Zn-catalyzed asymmetric hydrosilylation of heterobiaryl ketones.	194
Synthesis of 1-[1-(Isoquinolin-1-yl)naphthalen-2-yl]ethan-1-ol. 26a.....	195
Synthesis of 1-[3-(Methylpyridin-2-yl)naphthalen-2-yl]ethan-1-ol. 26c	196
Synthesis of 1-[1-(Isoquinolin-1-yl)-4-methylnaphthalen-2-yl]ethan-1-ol. 26e .	197
Synthesis of 1-[1-(Isoquinolin-1-yl)pyren-2-yl]ethan-1-ol. 26f.....	199
Synthesis of 1-[2-(Isoquinolin-1-yl)-3-methylphenyl]ethan-1-ol. 26g	200
Synthesis of 1-[1-(3-Phenylisoquinolin-1-yl)naphthalen-2-yl]ethan-1-ol. 26h...	202

Synthesis of 1-[1-(Isoquinolin-1-yl)naphthalen-2-yl]propan-1-ol. 26i	203
Synthesis of (<i>R</i>)-1-{1-[(<i>R</i>)-Isoquinolin-1-yl]naphthalen-2-yl}-3,3-dimethylbutan-1-ol. 26j	205
Synthesis of Cyclohexyl[1-(isoquinolin-1-yl)naphthalen-2-yl]methanol. 26k ...	205
III.3.3. Acetylation of more polar carbinol 3e.	207
Synthesis of (<i>1R</i>)-1-{1-[(<i>R</i>)-Quinazolin-4-yl]naphthalen-2-yl} ethyl acetate 3'e. 26'b	208
Synthesis of 1-[(<i>1R,3R</i>)-3-Methyl-3 <i>H,3'H</i> -spiro[naphtho(1,2- <i>c</i>)furan-1,4'-quinazolin]-3'-yl]ethan-1-one. (<i>R,R</i>)-26''b	208
Synthesis of 8-Butoxy-8-methyl-8 <i>H</i> -benzo[6,7]isoindolo[1,2- <i>a</i>]isoquinolin-7-ium chloride.	209
III.4.4. Representative transformations from 26a.	210
Synthesis of (<i>R</i>)-1-{2-[(<i>R</i>)-1-Hydroxyethyl]naphthalen-1-yl}isoquinoline 2-oxide. (<i>R_a,R</i>)-27a.....	210
Synthesis of (<i>R</i>)-1-{2-[(<i>S</i>)-1-Azidoethyl]naphthalen-1-yl}isoquinoline. (<i>R_a,S</i>)-28a	211
Synthesis of (<i>R</i>)-1-{1-[(<i>S</i>)-Isoquinolin-1-yl]naphthalen-2-yl}ethan-1-amine. (<i>R_a,S</i>)-29a	212
Synthesis of (<i>R</i>)-1-{2-[(<i>S</i>)-1-(4-Phenyl-1 <i>H</i> -1,2,3-triazol-1-yl)ethyl]naphthalen-1-yl}isoquinoline. (<i>R_a,S</i>)-30a	213
Synthesis of 1-[3,5-Bis(trifluoromethyl)phenyl]-3-{(<i>S</i>)-1-[1-((<i>R</i>)-isoquinolin-1-yl)naphthalen-2-yl]ethyl}urea. (<i>R_a,S</i>)-31a	214
IV. Catalytic Asymmetric synthesis of Axially Chiral Diamines by Reductive Amination and DKR	216
IV.1. Introduction.....	216
IV.1.1. Synthesis of axially chiral diamines, homologues of BINAM.	218
IV.1.2. Asymmetric Transfer Hydrogenation of imines.	222
IV.2. Results and discussion	228
IV.2.1. Substrates design and synthesis.	228
IV.2.2. Optimization of the reaction conditions.....	236
IV.2.3. Reaction scope.	240
IV.3. Conclusions.....	252
IV.4. Experimental Section.....	253

IV.4.1. General procedure for the synthesis of <i>N</i> -tosyl amines.....	253
Synthesis of <i>N</i> -(1-Bromonaphthalen-2-yl)-4-methylbenzenesulfonamide. 37b.	253
IV.4.2. Procedures for the cross-coupling reaction for the synthesis of substrates	
32A-F.	253
Synthesis of 5-Tosyl-5,6-dihydrobenzo[k]phenanthridin-6-ol. 32A.....	254
Synthesis of 6-Tosyl-5,6-dihydrobenzo[a]phenanthridin-5-ol. 32B	255
Synthesis of 1-Methyl-5-tosyl-5,6-dihydrophenanthridin-6-ol. 32C	256
Synthesis of 10-Methyl-5-tosyl-5,6-dihydrophenanthridin-6-ol. 32D	256
Synthesis of 1-(2-(Dimethylamino)phenyl)-2-naphthaldehyde. 32E.....	257
Synthesis of <i>N</i> -(2-(2-Acetylnaphthalen-1-yl)phenyl)-4-methylbenzenesulfonamide. 32F.....	258
IV.4.3. Synthesis of axially chiral diamines <i>via</i> Asymmetric Transfer Hydrogenation	
.....	258
Synthesis of (<i>R</i>)-4-Methyl- <i>N</i> -(2-(2-((propylamino)methyl)naphthalen-1-yl)phenyl)benzenesulfonamide. 34Aa.....	259
Synthesis of (<i>R</i>)- <i>N</i> -(2-(2-((Butylamino)methyl)naphthalen-1-yl)phenyl)-4-methylbenzenesulfonamide. 34Ab	260
Synthesis of (<i>R</i>)- <i>N</i> -(2-(2-((Cyclohexylamino)methyl)naphthalen-1-yl)phenyl)-4-methylbenzenesulfonamide. 34Ac	261
Synthesis of (<i>R</i>)- <i>N</i> -(2-(2-((Cyclopentylamino)methyl)naphthalen-1-yl)phenyl)-4-methylbenzenesulfonamide. 34Ae	262
Synthesis of (<i>R</i>)- <i>N</i> -(2-(2-(((Cyclopropylmethyl)amino)methyl)naphthalen-1-yl)phenyl)-4-methylbenzenesulfonamide. 34Ae	263
Synthesis of (<i>R</i>)- <i>N</i> -(2-(2-(((Cyclohexylmethyl)amino)methyl)naphthalen-1-yl)phenyl)-4-methylbenzenesulfonamide. 34Af	264
Synthesis of (<i>R</i>)- <i>N</i> -(2-(2-(((2-(1,3-Dioxolan-2-yl)ethyl)amino)methyl)naphthalen-1-yl)phenyl)-4-methylbenzenesulfonamide. 34Ag	265
Synthesis of (<i>R</i>)- <i>N</i> -(2-(2-((Allylamino)methyl)naphthalen-1-yl)phenyl)-4-methylbenzenesulfonamide. 34Ah	266
Synthesis of (<i>R</i>)-4-Methyl- <i>N</i> -(1-(2-((propylamino)methyl)phenyl)naphthalen-2-yl)benzenesulfonamide. 34Ba	267
Synthesis of (<i>R</i>)- <i>N</i> -(1-(2-((Butylamino)methyl)phenyl)naphthalen-2-yl)-4-methylbenzenesulfonamide. 34Bb	267

Synthesis of (<i>R</i>)- <i>N</i> -(1-(2-((Cyclohexylamino)methyl)phenyl)naphthalen-2-yl)-4-methylbenzenesulfonamide. 34Bc	268
Synthesis of (<i>R</i>)- <i>N</i> -(1-(2-(((Cyclohexylmethyl)amino)methyl)phenyl)naphthalen-2-yl)-4-methylbenzenesulfonamide. 34Bf	269
Synthesis of (<i>R</i>)- <i>N</i> -(1-(2-(((2-(1,3-Dioxolan-2-yl)ethyl)amino)methyl)phenyl)naphthalen-2-yl)-4-methylbenzenesulfonamide. 34Bg.....	270
Synthesis of (<i>R</i>)- <i>N</i> -(1-(2-((Allylamino)methyl)phenyl)naphthalen-2-yl)-4-methylbenzenesulfonamide. 34Bh.....	271
Synthesis of (<i>R</i>)-4-Methyl- <i>N</i> -(6-methyl-2'-((propylamino)methyl)-[1,1'-biphenyl]-2-yl)benzenesulfonamide. 34Ca.....	271
Synthesis of (<i>R</i>)- <i>N</i> -(2'-(((Cyclohexylmethyl)amino)methyl)-6'-methyl-[1,1'-biphenyl]-2-yl)-4-methylbenzenesulfonamide. 34Df	272
Synthesis of (<i>R</i>)-4-Methyl- <i>N</i> -(2-(2-(pyrrolidin-1-ylmethyl)naphthalen-1-yl)phenyl)benzenesulfonamide. 34Ak	273
Synthesis of <i>N,N</i> -Dimethyl-2-(2-((propylamino)methyl)naphthalen-1-yl)aniline. 34Ea	274
IV.4.4. General procedure for the reduction of carbonyls via asymmetric transfer hydrogenation.	274
Synthesis of (<i>R</i>)- <i>N</i> -(2-(2-(Hydroxymethyl)naphthalen-1-yl)phenyl)-4-methylbenzenesulfonamide. 42A.....	275
Synthesis of (1-(2-(Dimethylamino)phenyl)naphthalen-2-yl)methanol. 42E.....	275
Synthesis of (+)- <i>N</i> -(2-(2-(1-Hydroxyethyl)naphthalen-1-yl)phenyl)-4-methylbenzenesulfonamide. 42F	276
APPENDIX I: Abbreviations.....	277
APPENDIX II: General Methods	281

Summary/Resumen

Summary

The central objective in this PhD thesis has been the development of asymmetric catalysis methodologies for the atroposelective synthesis of (hetero)biaryls through dynamization strategies. These methodologies comprise resolution of both configurationally stable (DYKAT, for Dynamic Kinetic Asymmetric Transformation) or labile (DKR, for Dynamic Kinetic Resolution) heterobiaryl substrates. The obtained products possess appealing structures with potential applications as ligands for metal catalysis or precursors of bifunctional organocatalysts.

Along Chapter I, the general considerations and contextualization of the developed work are first disclosed. Additionally, the state of the art of the different strategies for the atroposelective synthesis of (hetero)biaryls is reviewed. For that purpose, those approaches involving any dynamization process for the synthesis of the enantioenriched functionalized (hetero)biaryls are specially considered.

In Chapter II, the first of the three developed methodologies during this PhD thesis is described. In this case, the Heck reaction (for which his discoverer was awarded with the Nobel Prize in Chemistry in 2010) has been combined with a DYKAT strategy, using configurationally stable heterobiaryl (pseudo)halides as substrates. This methodology has enabled the synthesis of highly functionalized heterobiaryls with the simultaneous generation of central and axial chirality elements, with an exquisite control on the regio-, diastereo-, and enantioselectivities.

In Chapter III an alternative methodology for the synthesis of heterobiaryls bearing central and axial chirality is described. In this case, an asymmetric reduction of configurationally labile heterobiaryl ketones *via* dynamic kinetic resolution (DKR) was performed. Specifically, the zinc-catalyzed asymmetric hydrosilylation using chiral diamines as ligands has been employed to obtain the corresponding heterobiaryl carbinols with excellent diastereo- and enantioselectivities.

Finally, the development of a methodology for the synthesis of axially chiral diamines is disclosed along Chapter IV. In this strategy, the configurational lability of heterobiaryl amins was exploited in Ru-catalyzed asymmetric transfer hydrogenation *via* dynamic kinetic resolution. This methodology is presented as an efficient pathway for the synthesis of homologues to BINAM and derivatives.

All the developed methodologies during this PhD thesis have allowed for the efficient synthesis of a wide variety of (hetero)biaryl structures bearing central and axial chirality elements.

Resumen

El objetivo principal de la presente Tesis Doctoral ha sido el desarrollo de metodologías catalíticas asimétricas para la síntesis atroposelectiva de (hetero)biarilos a través de estrategias de dinamización. Estas metodologías comprenden la resolución de sustratos (hetero)biarílicos configuracionalmente estables (DYKAT, por sus siglas en inglés: Dynamic Kinetic Asymmetric Transformation) o lábiles (DKR, por sus siglas en inglés: Dynamic Kinetic Resolution). Estos compuestos son altamente interesantes como ligandos para metales o como organocatalizadores.

A lo largo del capítulo I, se han desarrollado inicialmente las correspondientes consideraciones generales y puesta en contexto del trabajo. Además, se hace una revisión sobre el estado del arte en cuanto a las diferentes estrategias descritas para la síntesis atroposelectiva de (hetero)biarilos. Para ello, se tienen en cuenta todas las aproximaciones descritos, prestando especial atención a aquellas que involucran alguna estrategia de dinamización para obtener los (hetero)biarilos funcionalizados enantioméricamente enriquecidos.

En el capítulo II se describe la primera de las tres metodologías desarrolladas durante la presente tesis doctoral. En ella se ha hecho uso de la reacción de Heck asimétrica (gracias a la cual, su descubridor fue galardonado con el Premio Nobel de Química en 2010) junto con una estrategia de transformación asimétrica cinética dinámica (DYKAT),

utilizando (pseudo)haluros de heterobiarilo configuracionalmente estables como sustratos. Esta metodología ha permitido la síntesis de heterobiarilos altamente funcionalizados con la generación simultánea de quiralidad axial y central, y con un control exquisito sobre la regio-, diastereo- y enantioselectividad de la misma.

Por su parte, en el capítulo III se desarrolla una metodología alternativa para la síntesis de heterobiarilos con quiralidad axial y central basada en la reducción asimétrica de heterobiaril cetonas configuracionalmente lábiles (DKR). Concreamente, se ha empleado una reacción de hidrosililación asimétrica catalizada por complejos de zinc con diaminas quirales como ligandos, permitiendo obtener los correspondientes heterobiaril carbinoles con excelentes niveles de diastereo- y enantioselectividades.

Por último, a lo largo del capítulo IV se detalla una metodología para la síntesis de diaminas con quiralidad axial. En esta estrategia, se ha aprovechado la inestabilidad configuracional de los hemiaminales de partida, para llevar a cabo una resolución cinética dinámica (DKR) a través de una reacción de aminación reductora mediante transferencia de hidrógeno catalizada por complejos de rutenio. Esta metodología se presenta como una ruta eficiente para la síntesis de homólogos estructurales al BINAM y sus derivados.

Las metodologías desarrolladas a lo largo de esta Tesis Doctoral han permitido la síntesis eficiente y selectiva de una serie de (hetero)biarilos con quiralidad axial y central.

CHAPTER I

Introduction and Objectives

I. Introduction and Objectives.

I.1. Asymmetric catalysis.

Compounds of organic nature constitute the base of life existence. They comprise those which are mainly formed by carbon, hydrogen, nitrogen and oxygen atoms; however, other atoms like sulphur, phosphorous and halogens can be present in much lower amount. Organic Chemistry is the discipline responsible for the study of the synthesis and reactivity of these kind of compounds.

This term was first used in 1807 by Berzelius¹ in order to study those compounds derived directly from nature. By that time, it was thought that they held a special “vital force” that distinguished them from inorganic compounds, since they derived from living organisms. Furthermore, it was assumed that they could not be obtained synthetically and they could only be found directly in natural sources. It is because of this belief that Wöhler’s discovery in 1828² had such high importance. He was able to synthetically obtain urea, an organic compound isolable from animal urine, from two inorganic precursors such as ammonia and cyanic acid. It represented the first evidence of an organic compound synthesized in a laboratory and not obtained from natural sources, and many authors during history have considered Wöhler’s finding as the origin of modern organic chemistry³.

The understanding of how atoms are spatially displaced has also played a very important role in the development of organic chemistry as we know it nowadays. The branch of chemistry that deals with the spatial arrangement of atoms and groups in molecules, and the relation with their properties is named Stereochemistry.

In this context, a key concept is the symmetry, meaning for the property of an object of remaining invariant under a series of transformations as reflexion or rotation. However, in the framework of (organic) chemistry, it could be attributed more importance

¹ *Perspectives in Catalysis: In Commemoration of J. J. Berzelius*, ed. R. Larsson, CNK, Glerup, Lund, Sweden, **1981**.

² Wöhler, F. *Poggendorffs Ann.* **1828**, *12*, 253.

³ Cohen, P. S.; Cohen, S. M. *J. Chem. Educ.* **1996**, *73*, 883.

to the absence of symmetry, defined as asymmetry by the IUPAC (International Union of Pure and Applied Chemistry). Regarding to this chemical meaning of asymmetry, it is closely related to chirality, and it refers to the geometric property of a rigid object of not being superimposable on its mirror image. The classical example to illustrate this property are the left and right, our hands are chiral – our right hand is a mirror image of our left hand – as are most of life's constituting molecules. However, there are many other examples of objects that also present chirality (Figure I.1).

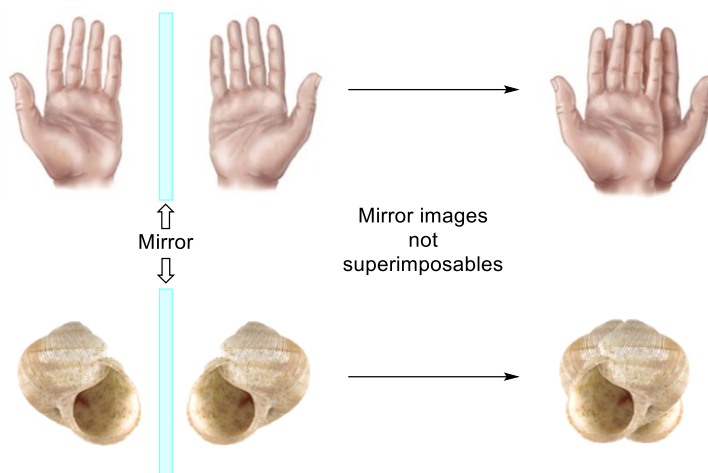


Figure I.1 – Illustration for chiral objects.

The most relevant contributions to the area of stereochemistry were made initially by Jean-Baptiste Biot⁴, followed by Louis Pasteur⁵ and later Jacobus van't Hoff⁶ and Charles Le Bel⁷. In general terms, the first established that certain organic compounds are able to rotate the plane of polarization of light. Then, Louis Pasteur correlated this observation with an asymmetric spatial arrangement of the atoms within molecules. Few years later, van't Hoff and Le Bel arranged the four valences of the carbon atom in a

⁴ Biot, J. B. *Bull. Soc. Philomath. Paris* **1815**, 190.

⁵ Pasteur, L. *Ann. Chim. Phys.* **1850**, 28, 56.

⁶ Van't Hoff, J. H. *Arch. Neerl. Sci. Exactes Nat.* **1874**, 9, 445.

⁷ Le-Bel, J. A. *Bull. Soc. Chim. France* **1874**, 22, 337.

tetrahedral fashion, setting the subsequent ability of organic molecules to exist in mirror image forms.

As mentioned, chiral molecules are not superimposable on their mirror images, and the pair of those mirror images conform what are called enantiomers. It is well-known that both enantiomers present different chemical properties, but the identical physical properties, except for their ability to rotate plane-polarized light by equal amounts but in opposite directions (D or L, depending if the light is rotated to the right or left side, respectively).

Nature represents the most evident proof of the great importance of chirality. Some examples are the amino acids that constitute proteins of living beings, which are chiral molecules exclusively from L-configuration. Additionally, many metabolisms of living organisms depend upon specific enzymes, hormones and other receptors, for a precise enantiomer of a particular molecule. Therefore, if the enantiomer that reaches this receptor is not the proper one, the metabolic route would not be initiated, or even, an undesired metabolism could occur.

There are several examples of biologically active compounds that present different properties depending on which enantiomer is assimilated by the organism. For instance, the most notorious case in this context is represented by thalidomide. During the late 1950s this drug was prescribed to pregnant women as a sedative and to decrease the morning sickness. However, it was provided in its racemic mixture and it was later found that the desired bioactivity was provided by the (*S*)-thalidomide; whereas the opposite enantiomer, (*R*)-thalidomide was responsible for teratogenic deformities in children born after their mothers used it during pregnancies. Moreover, it was later discovered that racemization of the drug takes place *in vivo* and, therefore, it was taken off the market in 1961 (Figure I.2).

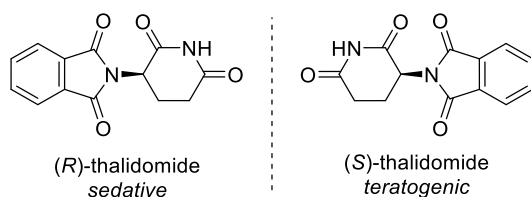


Figure I.2 – Enantiomers of thalidomide and their different biological properties.

Nonetheless, there are other examples in which the difference between both enantiomers is not so dramatic, but existing, and some of these pairs of enantiomers are displayed on Figure I.3. For example, L-DOPA (also known as levodopa) is employed for the treatment of Parkinson disease when transformed in dopamine by a L-amino acid decarboxylase enzyme. However, its enantiomer D-DOPA is biologically inactive and could be dangerous if accumulated. An additional well-known example is that of limonene, for which each enantiomer presents different organoleptic properties, while (*R*)-limonene smells like orange, (*S*)-limonene does it to lemons. The case of propranolol can also be mentioned: the (*S*)-propranolol is a β -blocker used to overcome anxiety issues (commonly known, in Spain, under the commercial name of Sumial) and to treat hypertension, while its *R* enantiomer is employed as a contraceptive,

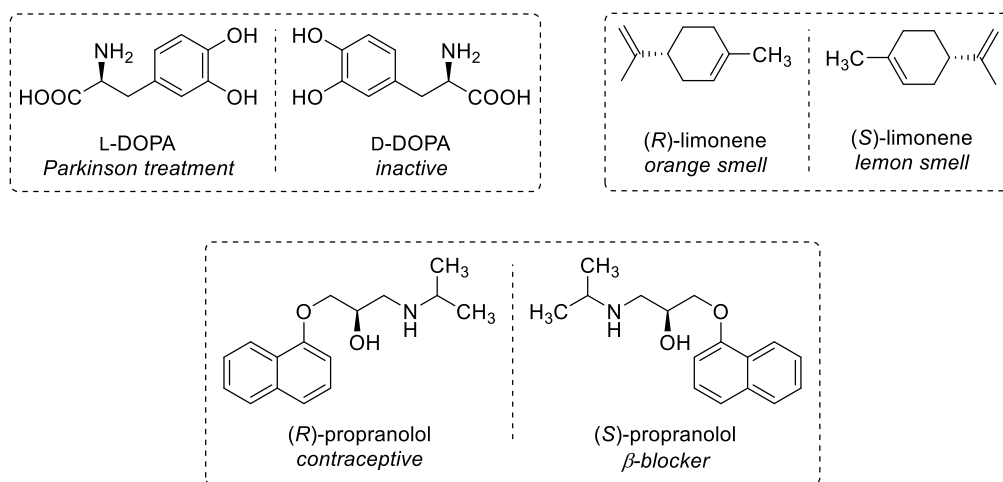


Figure I.3 – Different compounds with enantiomer-depending properties.

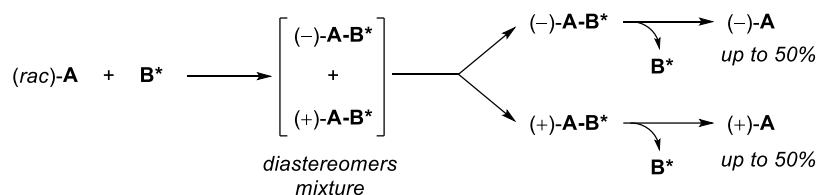
Considering these examples, among others, it is evident that the pharmaceutical industry presents a very high interest on methods that allow the selective synthesis of one

of the two possible enantiomers of a given compound. However, also in the cosmetics and agrochemical industries, enantiomerically pure compounds have an important presence.

In this context, the development of enantioselective synthetic methods is highly desirable. These methods can be classified along three different approaches:

- *Chiral pool*:⁸ this is based on the exploitation of natural enantiomerically pure starting materials (*i.e.* natural L-amino acids or D-monosaccharides) so that the absolute configuration of the final products is given by that of the substrates. This strategy presents *a priori* two main drawbacks: (i) first, the need of stoichiometric amounts of the enantiopure substrate, and (ii) second, the fact that the desired configuration is not always present in natural products.

- *Resolution of racemic mixtures*:⁹ consisting on the reaction of an enantiopure reagent and a racemic mixture, obtaining a mixture of diastereomers that would be further separated due to their different physical properties. Then, the enantiopure reagent could be removed, if possible, in order to obtain the enantiomerically pure starting material (Scheme I.1). This method presents a huge limitation since a maximum of only 50% yield can be afforded.



Scheme I.1 – Resolution of racemic mixture by diastereomers separation.

- *Asymmetric synthesis*:¹⁰ consists on the construction of chiral elements from an achiral (or racemic) substrate. The chirality source could come from either a

⁸ *Classics in Total Synthesis III*; Nicolau, K. C.; Snyder, S. A., Eds.; Wiley-VCH: Weinheim, **2011**.

⁹ Anderson, N. G. *Org. Proc. Res. Dev.* **2005**, *9*, 800.

¹⁰ (a) *Asymmetric Synthesis*; Aitken, R. A.; Kilényi, S. N., Eds.; Chapman & Hall: Cambridge, **1992**.
 (b) *Comprehensive Asymmetric Catalysis*; Jacobsen, E. N.; Pfaltz, A.; Yamamoto, H., Eds.; Springer: Berlin, **1999**.

chiral auxiliary¹¹ or a catalyst that could be enzymatic (biocatalysis) or non-enzymatic, and the latter could be based on metals (organometallic catalysis) or not (organocatalysis).

The catalytic asymmetric synthesis approach presents the higher potential and applicability since only sub-stoichiometric amounts of the catalyst are needed to induce chirality in the final products, which results in atom-efficient processes.¹² However, as mentioned above, the nature of the catalyst leads to different strategies:

- A. *Biocatalysis*:¹³ if specific enzymes or microorganisms are employed as catalysts. These systems present several benefits, such the mild conditions usually employed and high selectivities achieved, which might also become a detriment on its applicability because of the high specificity of enzymes.
- B. *Organometallic catalysis*:¹⁴ in this case, the vast majority of the catalysts employed are based on chiral organic ligands coordinated to a metal centre.
- C. *Organocatalysis*:¹⁵ if the catalyst is based on relatively low molecular weight organic molecules without metal atoms on their structure, which are usually air-stable, and do not require careful reaction conditions as is often the case in metal-based catalysts (such as anhydrous solvents, inert air,...).

Despite the number of alternative approaches and strategies for the synthesis of enantiomerically pure compounds, most of the asymmetric catalysts developed are still

¹¹ Evans, D. A.; Helmchen, G.; Rueping, M. Chiral Auxiliaries in Asymmetric Synthesis. In *Asymmetric Synthesis-The Essentials*; Christmann, M.; Bräse, S., Eds.; Wiley-VCH: Weinheim, **2007**.

¹² (a) Sheldon, R. A. *Pure Appl. Chem.* **2000**, 72,1233. (b)Trost, B. M. *Science* **1991**, 254, 1471.

¹³ (a) *Biotransformations in Organic Synthesis*; Faber, K., Ed.; Springer-Verlag: Berlin, **2011**. (b) Hudlicky, T.; Reid, J. W. *Chem. Soc. Rev.* **2009**, 38, 3117.

¹⁴ (a) Murai, S.; Activation of Unreactive Bonds and Organic Synthesis. In *Topics in Organometallic Chemistry*; Beller, M.; Dixneuf, P. H.; Dupont, J.; Fürstner, A.; Glorius, F.; Gooßen, L. J.; Nolan, S. P.; Okuda, J.; Oro, L. A.; Willis, M.; Zhou, Q.-L., Eds.; Springer-Verlag: Berlin, **1999**. (b) Ma, J.-A.; Cahard, D. *Angew. Chem. Int. Ed.* **2004**, 43, 4566.

¹⁵ (a) *Enantioselective Organocatalysis*; Dalko, P., Ed.; Wiley-VCH: Weinheim, **2007**; (b) *Asymmetric Organocatalysis, From Biomimetic Concepts to Applications in Asymmetric Synthesis*; Berkessel, A.; Gröger, H., Eds.; Wiley-VCH: Weinheim, **2005**.

based on organometallic species. This strategy presents a higher modularity since almost unlimited structural modifications can be introduced on the ligand moieties, while the metal centre can also be modified in order to tune the desired reactivity.

The enormous importance of asymmetric catalysis was manifested in 2001, with the Nobel Prize in Chemistry awarded to Knowles,¹⁶ Noyori¹⁷ and Sharpless¹⁸ for their contributions to the field of asymmetric hydrogenations and oxidations. The breakthrough came in 1968 when William S. Knowles discovered that it was possible to use a transition metal based chiral catalyst that could transfer chirality to a non-chiral substrate in order to obtain a chiral product. In particular, the reaction performed was an asymmetric hydrogenation of olefins by rhodium/chiral complexes.¹⁹ Later, Noyori realised about the need for a more general catalyst that would broaden the applications of the asymmetric hydrogenation reactions, and found that Ru(II)-BINAP complexes succeeded in the asymmetric hydrogenation of many type of molecules with different functional groups.²⁰ In parallel, Sharpless also realised about the need for an efficient catalyst to perform asymmetric oxidations, and his work in this field was exemplified by his chiral epoxidation reaction.²¹

As mentioned previously, the discoveries by van't Hoff and Le Bel about the tetrahedral arrangement of carbon atom valences set the bases for what it is known as an stereocentre. However, this the most common type of chirality that can be found in molecules, but not the only one. There are also other sources of chirality, that are summarized next:

- Central chirality: in a general way, an stereogenic centre is characterised by an atom that has four different groups bonded. The most well-known case in organic

¹⁶ Knowles, W. S. *Angew. Chem. Int. Ed.* **2002**, *41*, 1998.

¹⁷ Noyori, R. *Angew. Chem. Int. Ed.* **2002**, *41*, 2008.

¹⁸ Sharpless, K. B. *Angew. Chem. Int. Ed.* **2002**, *41*, 2024.

¹⁹ Knowles, W. S.; Sabacky, M. S. *Chem. Commun. (London)*, **1968**, 1445.

²⁰ Noyori, R.; Ohta, M.; Hsiao, Y.; Kitamura, M.; Ohta, T.; Takaya, H. *J. Am. Chem. Soc.* **1986**, *108*, 7117.

²¹ Sharpless, K. B.; Michaelson, R. C. *J. Am. Chem. Soc.* **1973**, *95*, 6136.

chemistry are the central chirality by tetrahedral carbon atoms (Figure I.4A), but there are other atoms different than carbon that can appear as a stereogenic centre. Amines are not chiral, because they rapidly invert at room temperature (Figure I.4B). However, asymmetric quaternary ammonium salts,²² and compounds with a stereogenic phosphorous²³ and sulphur²⁴ centres are also chiral (Figure I.4C).

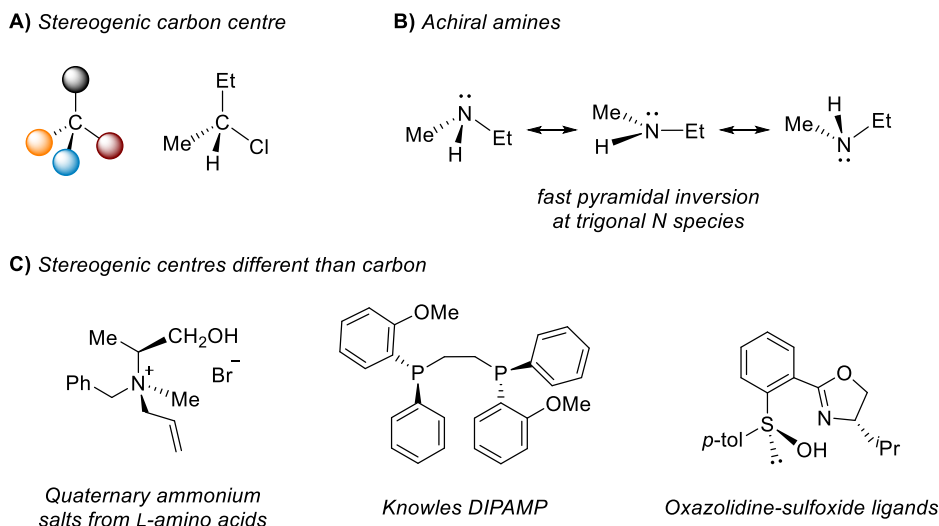


Figure I.4 – Examples of stereogenic centres.

- Axial chirality: refers to stereoisomerism resulting from the non-planar arrangement of four groups in pairs around a chiral axis. Depending on the nature of this axis, it can be found in allenes, spiro compounds or *ortho*-substituted (hetero)biaryls. The stereoisomers from the latter case, given the restricted rotation around a single bond due to steric factors, are also known as atropisomers (from greek, *ἀτροπος*, *atropos*, meaning "without turn") (Figure I.5A).

²² Wua, H.-F.; Lin, W.-B.; Xia, L.-Z.; Luo, Y.-G.; Chen, X.-Z.; Li, G.-Y.; Zhang, G.-L.; Pan, X.-F. *Helv. Chim. Acta* **2009**, *92*, 677.

²³ (a) Knowles, W. S. *J. Chem. Educ.* **1986**, *63*, 222. (b) DiRocco, D. A.; Ji, Y.; Sherer, E. C.; Klapars, A.; Reibarkh, M.; Dropinski, J.; Mathew, R.; Maligres, P.; Hyde, A. M.; Limanto, J.; Brunskill, A.; Ruck, R. T.; Campeau, L.-C.; Davies, I. W. *Science* **2017**, *356*, 426.

²⁴ (a) Trost, B. M.; Rao, M. *Angew. Chem. Int. Ed.* **2015**, *54*, 5026. (b) Otocka, S.; Kwiatkowska, M.; Madalińska, L.; Kiełbasiński, P. *Chem. Rev.* **2017**, *117*, 4147.

- Planar chirality: corresponds to the stereoisomerism resulting from the arrangement of out-of-plane groups with respect to a plane (chiral plane). This chirality expression is seen in some cyclophanes or metallocenes (Figure I.5B).

- Helical chirality: this is a particular case axial chirality, inherent from their three-dimensional shape. Is typical from helicenes, *ortho*-condensed polycyclic aromatic compounds in which benzene rings or other aromatics are angularly annulated (Figure I.5C).

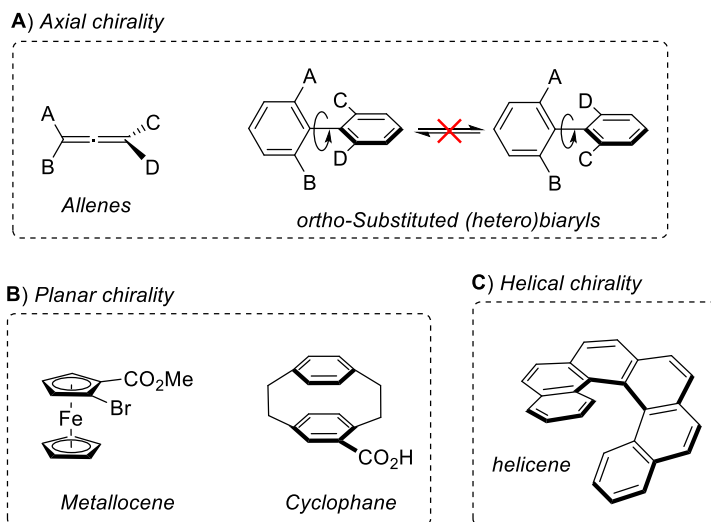


Figure I.5 – Types of chirality.

This PhD thesis is aimed at the development of synthetic procedures for the generation, principally, of axial chirality. Therefore, this type of chirality will be discussed deep .in the following sections.

I.1.2. Axial Chirality: Atropisomerism.

A particularly interesting area within the asymmetric catalysis concerns the enantioselective synthesis of compounds presenting axial chirality.

The first example of atropisomeric compounds was reported by Christie and Kenner in 1922²⁵ when they were able to isolate both atropisomers of 6,6'-dinitro-[1,1'-biphenyl]-2,2'-dicarboxylic acid from the racemic mixture after fractional crystallization using brucine as resolution agent (Figure I.6).

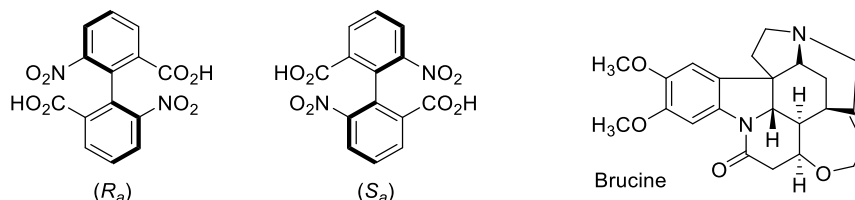


Figure I.6 – First report showing the resolution of atropisomers.

Atropisomers are stereoisomers that can be interconverted by rotation about single bonds but where the rotational barrier (or atropisomerization barrier) is large enough to avoid the interconversion at room temperature, and they can be therefore separated. The rotational barrier is related to the configurational stability of the stereogenic axis, and this stability depends upon the substitutions at the *ortho* positions around the axis (6,6' and 2,2'): the bulkier the substituents, the higher the stability.

Regarding the configuration in compounds with axial chirality, it is specified by the stereodescriptors R_a and S_a (the subscript a refers to *axial*), or M and P notations, for each atropisomer. The use of the first one is more extended, while the latter is generally used for helical chirality. Nevertheless, if the stereogenic axis is the only chirality element in the molecule, the subscript a can be omitted. The assignment of this absolute configuration has to be done as follows:

1. According to Cahn-Ingold-Prelog rules, the substituents of each aromatic fragment *ortho* to the stereogenic axis are ordered separately. The aromatic unit bearing the highest atomic number substituent would have the priority numbers 1 and 2, and the other aryl, 3 and 4.

²⁵ Christie, G. H.; Kenner, J. *J. Chem. Soc.* **1922**, 121, 614.

- Then, the molecule is viewed in Newman projection along the axis, setting the aromatic unit with the highest priority in front.
- Finally, as for the stereogenic centres, the direction of a line from priority 1 to 3 across 2, determines the configuration of the stereogenic axis. If it is clockwise, configuration R_a is assigned, and anti-clockwise means S_a configuration (Figure I.7).

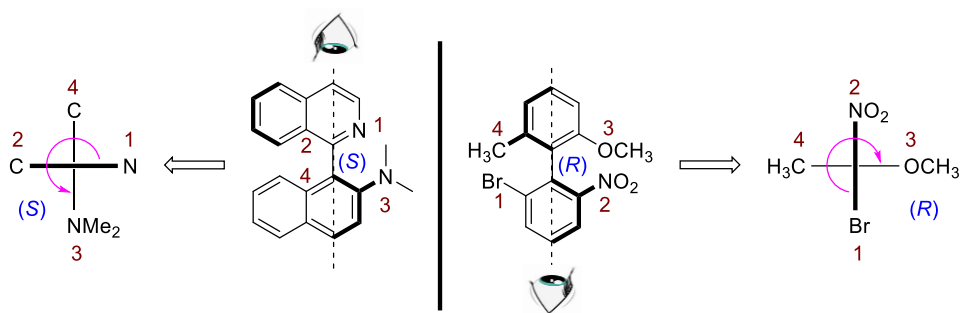


Figure I.7 – Assignment of the stereogenic axis configuration.

Axially chiral biaryls are widely used as the key structural motif of chiral ligands and catalysts in asymmetric synthesis.²⁶ For instance, in two of the named “privileged chiral ligands and catalysts”, BINAP (2,2'-bis(diphenylphosphino)-1,1'-binaphthyl) and BINOL (1,1'-bi-2-naphthol), the chirality source is an stereogenic axis (Figure I.8).²⁷

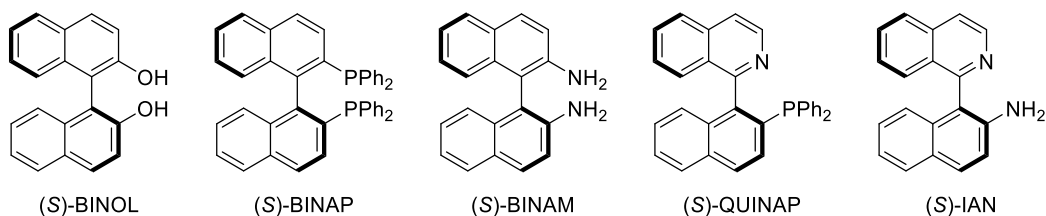


Figure I.8 – Examples of axially chiral (hetero)biaryls used as ligands or catalysts in asymmetric catalysis.

²⁶ For selected reviews and articles about axially chiral biaryls as ligands, see: (a) McCarthy, M.; Guiry, P. J. *Tetrahedron* **2001**, *57*, 3809. (b) Jindal, G.; Sunoj, R. B. *Angew. Chem. Int. Ed.* **2014**, *53*, 4432. (c) Zhang, L.; Xiang, S.-H.; Wang, J.; Xiao, J.; Wang, J.-Q.; Tan, B. *Nat. Comm.* **2019**, *10*, 566.

²⁷ Yoon, T. P.; Jacobsen, E. N. *Science* **2003**, *299*, 1691.

Additionally, these structures are also a very important motif observed in biologically active compounds.²⁸ Some of the most representative examples are shown in Figure I.9. Vancomycin is an antibiotic prescribed to fight bacteria from intestines. (*R*)-Gossypol, a natural product from cotton seeds, is an effective non-hormonal male contraceptive, however, it has also been documented to have irreversible effects on male fertility and is not recommended for this use. Moreover, (*R*)-gossypol is under investigations due to its capability to induce apoptosis and a cytoprotective form of autophagy in bladder cancer.²⁹

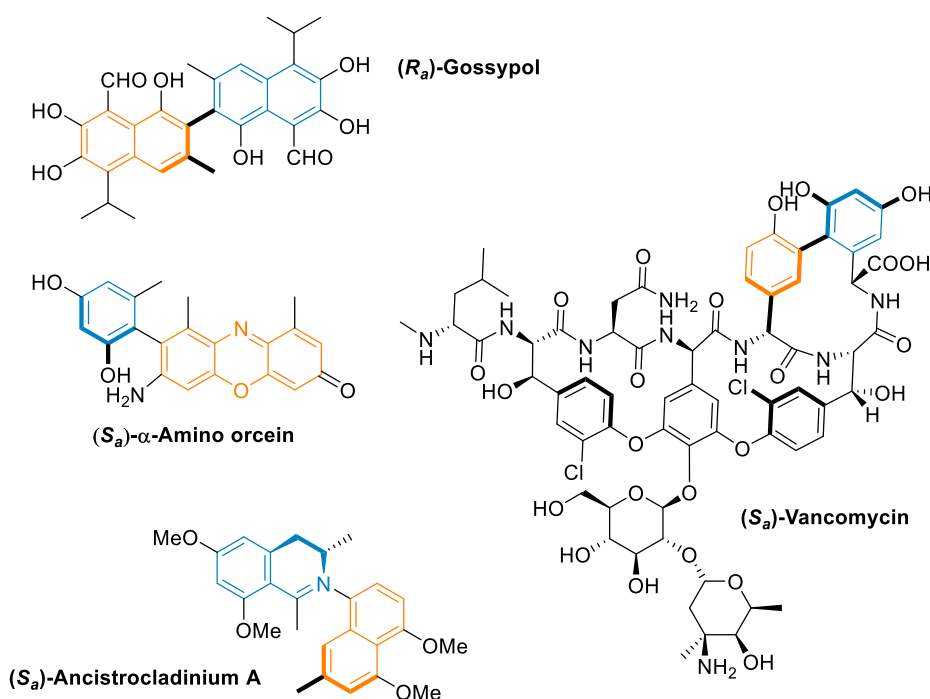


Figure I.9 – Examples of biologically active compounds bearing an stereogenic axis.

²⁸ For selected examples of biologically active compounds with axial chirality, see: (a) Bringmann, G.; Gulder, T.; Gulder, T. A. M.; Breuning, M. *Chem. Rev.* **2011**, *111*, 563. (b) Smyth, J. E.; Butler, N. M.; Keller, P. A. *Nat. Proc. Prep.* **2015**, *32*, 1562. (c) Bringmann, G.; Günther, C.; Ochse, M.; Schupp, O.; Tasler, S. Biaryls in Nature. In *Progress in the Chemistry of Organic Natural Products*; Herz, W.; Falk, H.; Kirby, G. W.; Moore R. E., Eds.; Springer: Vienna, **2001**; Vol. 82; pp. 1–249.

²⁹ Mani, J.; Vallo, S.; Rakel, S.; Antonietti, P.; Gessler, F.; Blaheta, R.; Bartsch, G.; Michaelis, M.; Cinatl, J.; Haferkamp, A.; Kögel, D. *BMC Cancer* **2015**, *15*, 224.

Other examples includes α -amino orcein, extracted from several lichen species, which is a reddish-brown dye used as a stain in microscopy to visualize chromosomes, Hepatitis B surface antigens, and copper-associated proteins. The last example depicted, Ancistrocladinium A, with *S* configuration at the stereogenic axis, has shown to be an effective anti-leishmanial activity.³⁰

As seen, the ability of natural receptors to possess differential binding affinities between atropisomers is an important factor when considering active and inactive atropisomeric drug.

I.2. Atroposelective synthesis of axially chiral (hetero)biaryls.

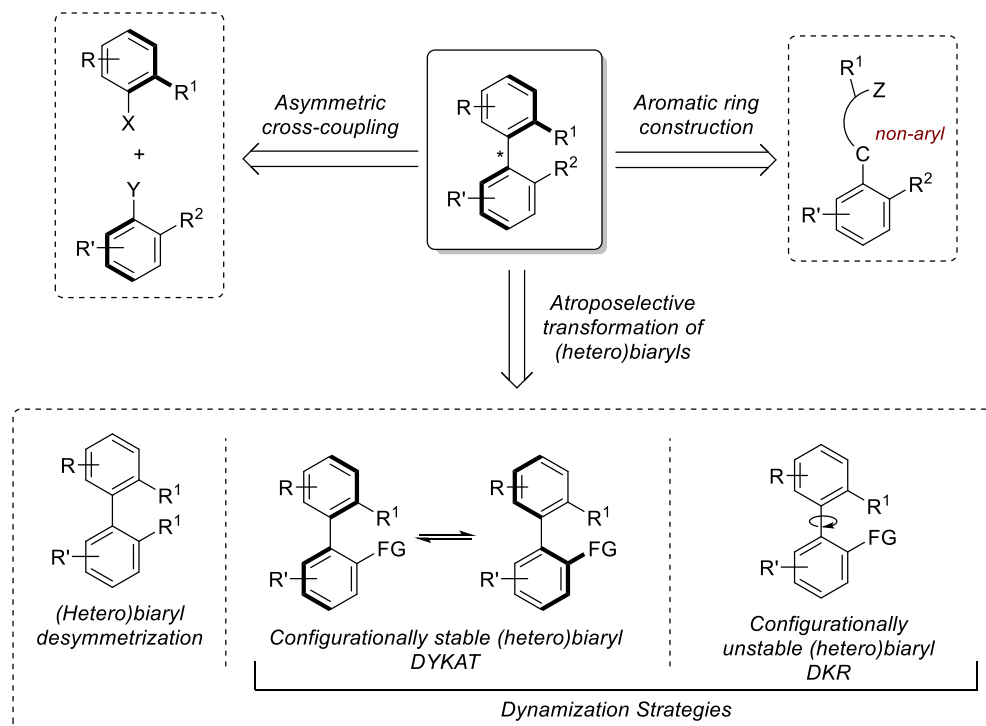
Owing to the importance of axially chiral (hetero)biaryl compounds, many excellent methods for their directed, atroposelective construction have been developed. However, it is still a hot topic that occupies the interest of many research groups in asymmetric catalysis, in order to develop new methods providing access to new structures which, eventually, would find new applications.

Fundamentally, there are three different approaches for the atroposelective synthesis of axially chiral (hetero)biaryl derivatives (Scheme I.2).³¹ The most straightforward method consists on the direct formation of the axis by a C–C asymmetric cross-coupling. The second approach comprises the *de novo* construction of one of the aromatic rings, and two main possibilities have been developed: (i) Rh- or Co-catalyzed [2+2+2] cycloaddition, and (ii) generation of an stereocentre followed by central-to-axial chirality transfer. Alternatively, the third approach consists on the atroposelective transformation of an already existing (hetero)biaryl system. The latter strategy, in turn, can

³⁰ Bringmann, G.; Kajahn, I.; Reichert, M.; Pedersen, S. E. H.; Faber, J. H.; Gulder, T.; Brun, R.; Christensen, S. B.; Ponte-Sucre, A.; Moll, H.; Heubl, G.; Mudogo, V. *J. Org. Chem.* **2006**, *71*, 9348.

³¹ (a) Bringmann, G.; Mortimer, A. J. P.; Keller, P. A.; Gresser, M. J.; Garner, J.; Breuning, M. *Angew. Chem. Int. Ed.* **2005**, *44*, 5384. (b) Loxq, P.; Manoury, E.; Poli, R.; Deydier, E.; Labande, A. *Coord. Chem. Rev.* **2016**, *308*, 131.

be divided in two main blocks depending on whether a dynamization process is involved or not.



Scheme 1.2 – Possible routes to access axially chiral (hetero)biaryls.

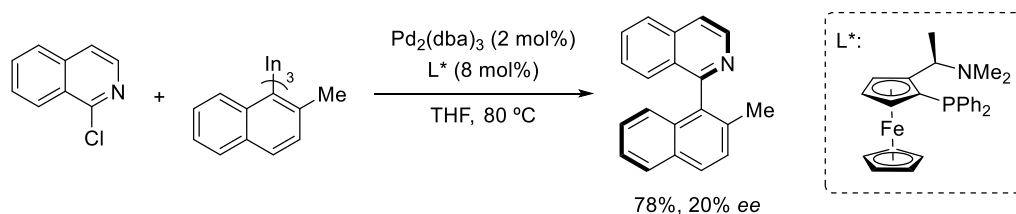
The direct asymmetric cross-coupling for the construction of the stereogenic axis has been widely studied over the last two decades, and essentially, could be tackled through three different alternatives: (i) atroposelective cross-couplings, (ii) oxidative cross-couplings, and (iii) organocatalytic atroposelective reactions.

The two latter strategies have been employed for the synthesis of BINOL³² and BINAM derivatives, respectively. The synthesis of BINAM derivatives, and their limitations, will be discussed later along Chapter IV.

³² For selected oxidative coupling reactions for the synthesis of BINOL and derivatives, see: (a) Li, X.; Yang, J.; Kozłowski, M. C. *Org. Lett.* **2001**, 3, 1137. (b) Kim, K. H.; Lee, D.-W.; Lee, Y.-S.; Ko, D.-H.; Ha, D.-C. *Tetrahedron* **2004**, 60, 9037. (c) Egami, H.; Katsuki, T. *J. Am. Chem. Soc.* **2009**, 131, 6082.

The atroposelective cross-coupling for the synthesis of the axis is the most extended approach to obtain axially chiral biaryls. Most of the reported examples are based on Pd-catalyzed Suzuki-Miyaura reaction,³³ but other cross-couplings, as Kumada³⁴ or Ullmann reactions³⁵ have also been applied. The former strategy is considered the main approach, due to the functional groups tolerance and compatibility with many reaction media.

However, the reported methodologies based on this strategy failed for the synthesis of axially chiral heterobiaryls, a fact that can be attributed to the interferences caused by coordination of the substrate to the metal catalyst, and to the low configurational stability of the resulting products at the relatively high temperatures usually required to perform this type of reactions. For instance, there is only one precedent to the date, reported by Sarandeses and co-workers in which a single heterobiaryl product was obtained with a disappointing 20% of enantiomeric excess (Scheme I.3).



Scheme I.3 – Sarandeses's cross-coupling reaction for the atroposelective synthesis of heterobiaryls.

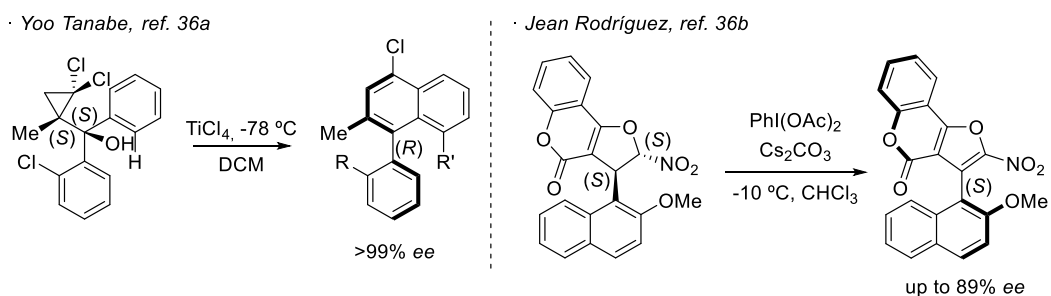
The second approach mentioned above for the synthesis of axially chiral biaryls consists on the formation of the stereogenic axis by a cyclization reaction. In this case, a preformed aryl–C single bond is transformed in an atroposelective manner into the biaryl axis upon construction of the second aromatic unit from an attached substituent, bearing an

³³ For selected examples of atroposelective Pd-catalyzed Suzuki-Miyaura cross-couplings, see: (a) Pan, C.; Zhu, Z.; Zhang, M.; Gu, Z. *Angew. Chem. Int. Ed.* **2017**, *56*, 4777. (b) Shen, X.; Jones, G. O.; Watson, D. A.; Bhayana, B.; Buchwald, S. L. *J. Am. Chem. Soc.* **2010**, *132*, 11278. (c) Uozumi, Y.; Matsuura, Y.; Arakawa, T.; Yamada, Y. M. A. *Angew. Chem., Int. Ed.* **2009**, *48*, 2708. (d) Bermejo, A.; Ros, A.; Fernández, R.; Lassaletta, J. M. *J. Am. Chem. Soc.* **2008**, *130*, 15798. (e) Zhang, D.; Wang, Q. *Coord. Chem. Rev.* **2015**, *286*, 1.

³⁴ Hayashi, T.; Hayashizaki, K.; Kiyoi, T.; Ito, I. *J. Am. Chem. Soc.* **1988**, *110*, 8153.

³⁵ Wu, W.; Wang, S.; Zhou, Y.; He, Y.; Zhuang, Y.; Li, L.; Wan, P.; Wang, L.; Zhou, Z.; Qiu, L. *Adv. Synth. Catal.* **2012**, *354*, 2395.

stereogenic element, usually an stereogenic centre. Thus, a process of central-to-axial chirality transfer takes place since the stereogenic centre is lost in the cyclization, and the chiral information is transferred to the axis (Scheme I.4).³⁶



Scheme I.4 – Central-to-axial chirality transfer examples.

Alternatively, *de novo* ring construction can be achieved through an atroposelective [2+2+2] cycloaddition. This reaction has been studied mainly with transition metals from Group 9 (Co,³⁷ Rh³⁸ and Ir³⁹) in combination with chiral (bis)phosphine ligands, and scarce examples have been developed with different metals, or even organocatalyzed cycloadditions (Scheme I.5A). In contrast to the asymmetric cross-coupling reactions, this methodology has been extended for the synthesis of heterobiaryls with axial chirality (Scheme I.5B).⁴⁰ This alternative has also been considered as a reliable method for the atroposelective synthesis of (hetero)biaryls.

³⁶ (a) Nishii, Y.; Wakasugi, K.; Koga, K.; Tanabe, Y. *J. Am. Chem. Soc.* **2004**, *126*, 5358. (b) Raut, V. S.; Jean, M.; Vanthuyne, N.; Roussel, C.; Constantieux, T.; Bressy, C.; Bugaut, X.; Bonne, D.; Rodriguez, J. *J. Am. Chem. Soc.* **2017**, *139*, 2140.

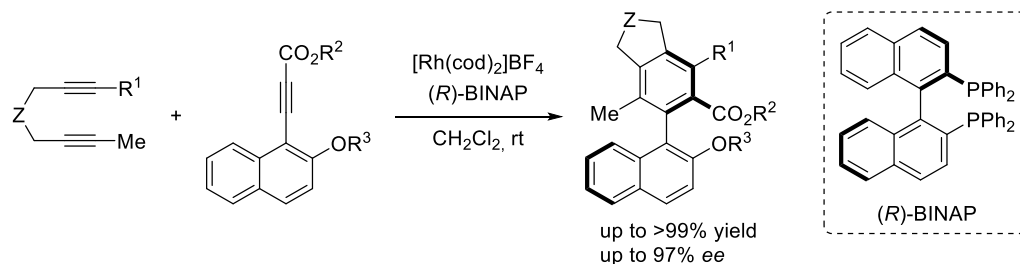
³⁷ Heller, B.; Gutnov, A.; Fischer, C.; Drexler, H.-J.; Spannenberg, A.; Redkin, D.; Sundermann, C.; Sundermann, B. *Chem. Eur. J.* **2007**, *13*, 1117.

³⁸ (a) Ogaki, S.; Shibata, Y.; Noguchi, K.; Tanaka, K. *J. Org. Chem.* **2011**, *76*, 1926. (b) Nishida, G.; Suzuki, N.; Noguchi, K.; Tanaka, K. *Org. Lett.* **2006**, *8*, 3489.

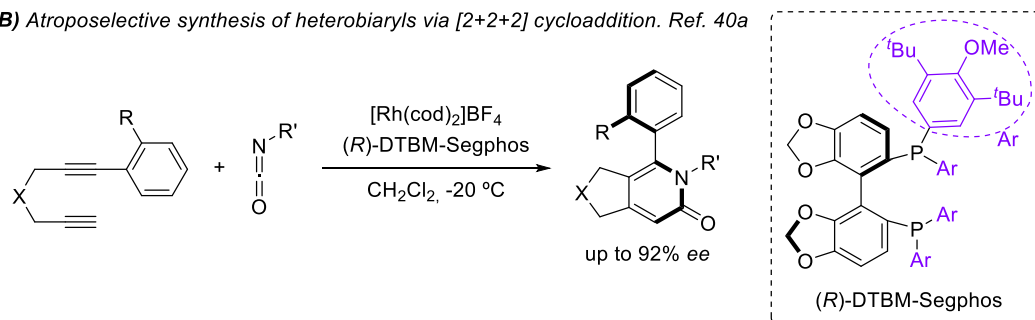
³⁹ (a) Shibata, T.; Fujimoto, T.; Yokota, K.; Takagi, K. *J. Am. Chem. Soc.* **2004**, *126*, 8382. (b) Shibata, T.; Yoshida, S.; Arai, Y.; Otsuka, M.; Endo, K. *Tetrahedron* **2008**, *64*, 821.

⁴⁰ (a) Tanaka, K.; Wada, A.; Noguchi, K. *Org. Lett.* **2005**, *7*, 4737. (b) Liu, Y.; Wu, X.; Li, S.; Xue, L.; Shan, C.; Zhao, Z.; Yan, H. *Angew. Chem. Int. Ed.* **2018**, *57*, 6491. (c) Sakiyama, N.; Hojo, D.; Noguchi, K.; Tanaka, K. *Chem. Eur. J.* **2011**, *17*, 1428.

A) Atroposelective synthesis of biaryls via [2+2+2] cycloaddition. Ref. 38a



B) Atroposelective synthesis of heterobiaryls via [2+2+2] cycloaddition. Ref. 40a



Scheme 1.5 – Tanaka's group contributions to rhodium-catalyzed [2+2+2] cycloaddition reactions for the atroposelective construction of the stereogenic axis in (hetero)biaryl systems.

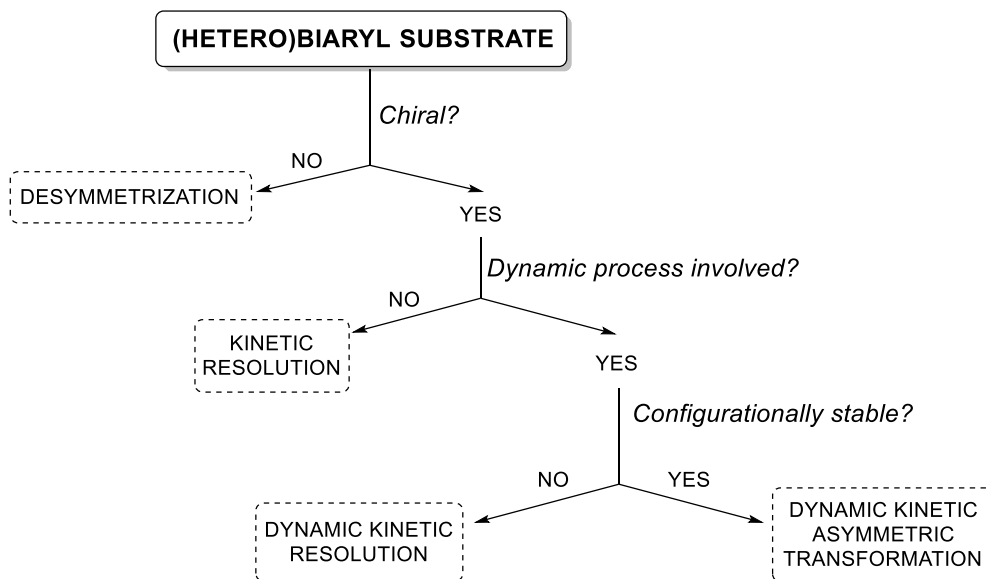
Besides the described approaches for the construction of the stereogenic axis, either by a cross-coupling or a cyclization reaction, an important strategy is that based on an atroposelective transformation of an already existing (hetero)biaryl. This is an elegant alternative to obtain this type of highly functionalized compounds, and given its importance in the context of this PhD thesis, it will be discussed in the next separate section.

I.3. Atroposelective transformations for the synthesis of axially chiral (hetero)biaryls.

As commented above, the construction of the targeted axially chiral (hetero)biaryls in this strategy is based on the introduction of the stereochemical information at a preformed biaryl structure, and hence, the starting compounds could be considered as pro-stereogenic.

Four possible approaches can be described considering three main factors: (i) if the (hetero)biaryl substrate is chiral or achiral, (ii) its configurational stability, and (iii) if a

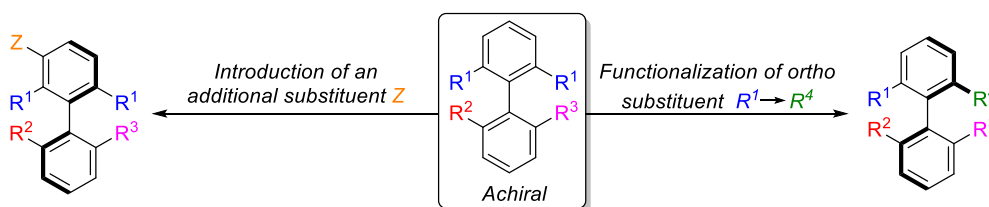
dynamization process is involved in the reaction, and its nature. Therefore, regarding this criteria, the different approaches are depicted in Scheme I.6.



Scheme I.6 – Different strategies for the atroposelective transformation of (hetero)biaryl substrates.

I.3.1. Desymmetrization.

It is the only strategy based on the use of an achiral substrate. For instance, the (hetero)biaryl substrate employed in this case is a meso compound, as it contains an prostereogenic axis but also a mirror plane, and therefore, its chirality is lost and it does not rotate plane polarized light.

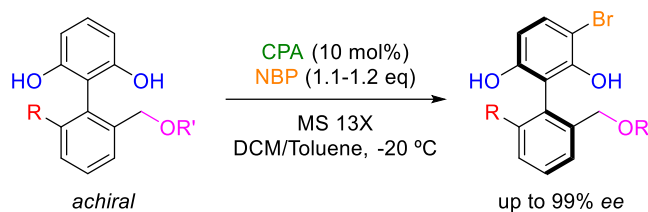


Scheme I.7 – Possible desymmetrization routes for the asymmetric synthesis of (hetero)biaryls.

In order to obtain an stereogenic axis with a given configuration, the plane of symmetry from the molecule must be eliminated, and there are two different ways to afford this (Scheme I.7).

A. Introduction of an additional substituent.

If an additional functionality is introduced in the (hetero)aromatic fragment responsible for the existence of the mirror plane, the symmetry would be lost, and the now configurationally stable stereogenic axis would be generated. A representative example of this alternative was reported by the group of Akiyama, for the enantioselective synthesis of biaryls through an asymmetric bromination catalyzed by a chiral phosphoric acid (CPA), using *N*-bromothalimide (NBP) (Scheme I.8).⁴¹



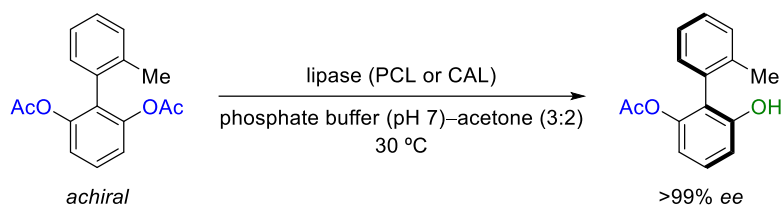
Scheme I.8 – Strategy for the desymmetrization of biaryls developed Akiyama.

B. Functionalization of *ortho* substituents.

The second approach is based on the transformation of one of the enantiotopic *ortho* substituents into a different group (R^1 to R^4 , in Scheme I.7) that results in the resolution of the stereogenic axis and the loss of symmetry elements at the molecule. This could be exemplified in the work developed by Matsumoto and co-workers for the enantioselective enzymatic hydrolysis of biaryl diacetates (Scheme I.9).⁴²

⁴¹ Mori, K.; Ichikawa, Y.; Kobayashi, M.; Shibata, Y.; Yamanaka, M.; Akiyama, T. *J. Am. Chem. Soc.* **2013**, *135*, 3964.

⁴² Matsumoto, T.; Konegawa, T.; Nakamura, T.; Suzuki, K. *Synlett* **2002**, 122.



Scheme I.9 – Biaryl desymmetrization strategy developed by the group of Matsumoto.

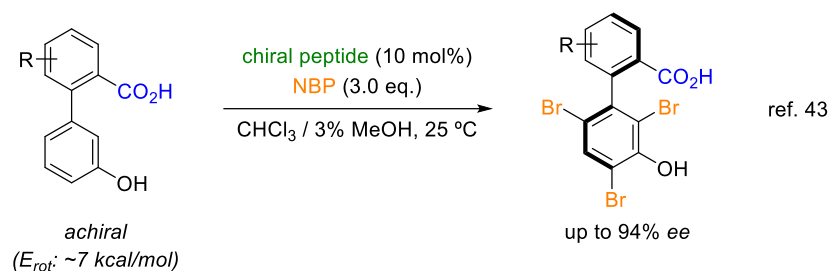
In addition to these two strategies mentioned above, there are also other examples of atroposelective synthesis of (hetero)biaryls that could generate some debate about whether they are considered dynamic kinetic resolutions or desymmetrizations. One of them, consists on a peptide-catalyzed asymmetric bromination of biaryls developed by the group of Miller (Scheme I.10A).⁴³ Despite the authors described the process as a dynamic kinetic resolution (DKR), we consider that it fits better as a desymmetrization because of the following reasons: (i) first, to be considered as a DKR, both atropisomers of the substrate should be detectable, but it is not possible due to its very low rotational barrier (~ 7 kcal/mol), and (ii), second, given this fast interconversion it could be assigned a formal co-planarity of both aromatic fragments, and in this way there would be a plane of symmetry along them.

Furthermore, there is another methodology for the atroposelective synthesis of axially chiral (hetero)biaryls that can be assigned as a desymmetrization of a prostereogenic (hetero)biaryl compounds that concerns the C–H activation of substrates containing a configurationally unstable stereogenic axis. In this case, the substrate presents such a low rotational barrier that could be considered as achiral (planar), but the introduction of an additional *ortho*-substituent *via* asymmetric C–H activation leads to now configurationally stable (hetero)biaryl compounds (Scheme I.10B).⁴⁴

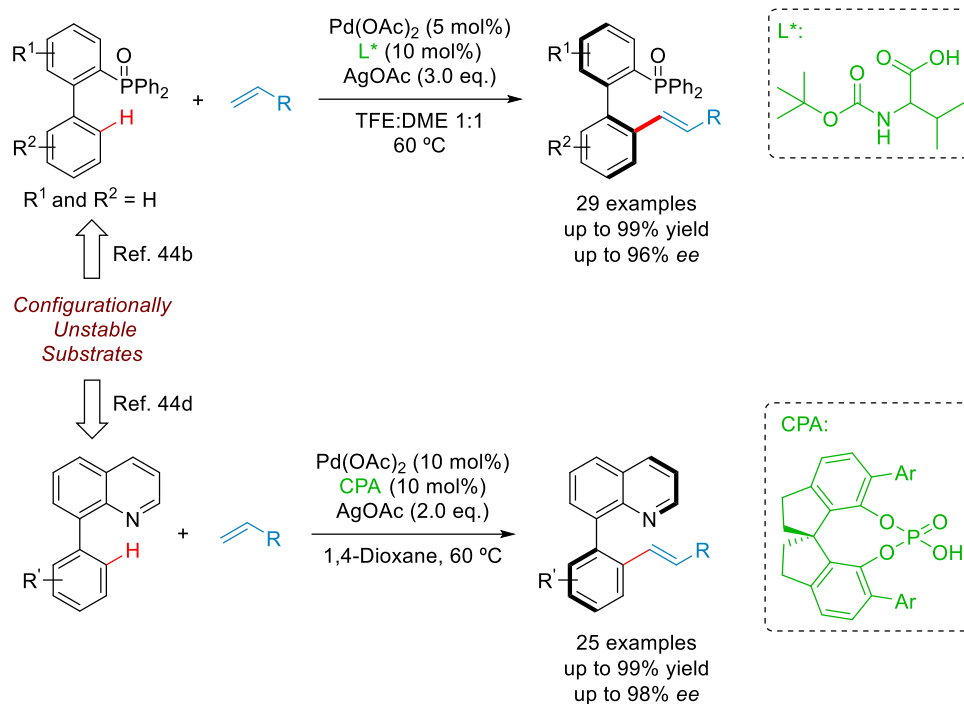
⁴³ Gustafson, J. L.; Lim, D.; Miller, S. J. *Science* **2010**, *328*, 1251.

⁴⁴ For recent examples of atroposelective C–H activation, see: (a) Hazra, C. K.; Dherbassy, Q.; Wencel-Delord, J.; Colobert, F. *Angew. Chem. Int. Ed.* **2014**, *53*, 13871. (b) Li, S.-X.; Ma, Y.-N.; Yang, S.-D. *Org. Lett.* **2017**, *19*, 1482. (c) Liao, G.; Yao, Q.-J.; Zhang, Z.-Z.; Wu, Y.-J.; Huang, D.-Y.; Shi, B.-F. *Angew. Chem. Int. Ed.* **2018**, *57*, 3661. (d) Luo, J.; Zhang, T.; Wang, L.; Liao, G.; Yao, Q.-J.; Wu, Y.-J.; Zhan, B.-B.; Lan, L.; Lin, X.-F.; Shi, B.-F. *Angew. Chem. Int. Ed.* **2019**, *58*, 6708.

A) Atroposelective organocatalyzed bromination



B) Atroposelective Pd-catalyzed C-H activations



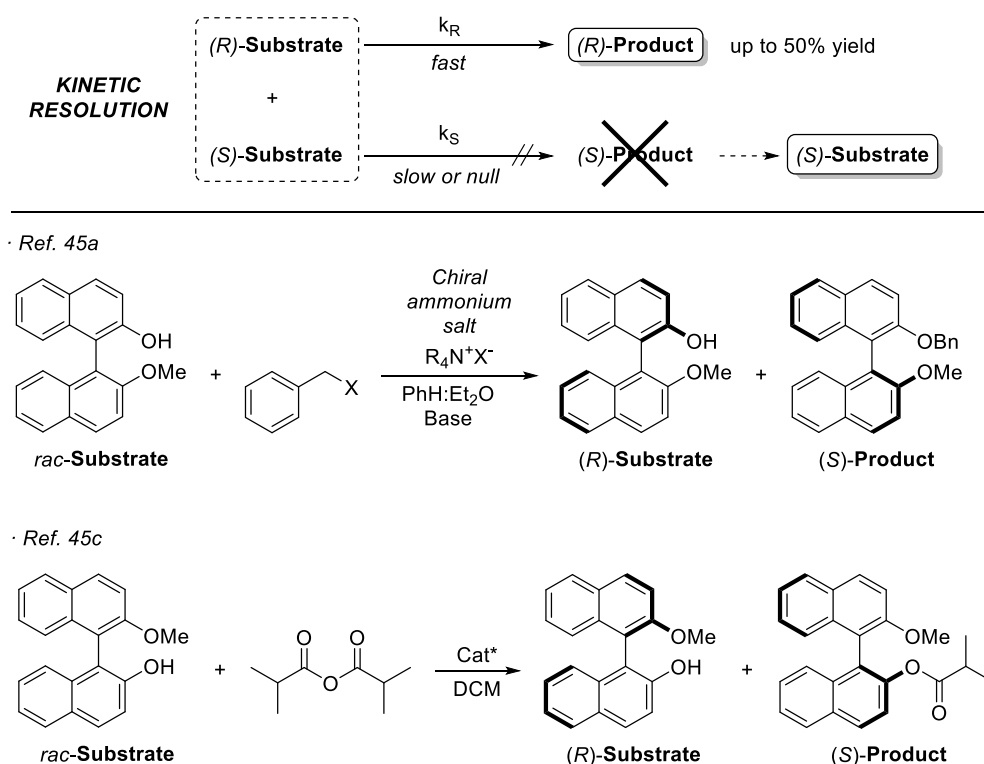
Scheme I.10 –Desymmetrization strategies for the synthesis of axially chiral (hetero)biaryls.

Despite these approaches could generate a debate about the fundamental strategy involved, along this PhD thesis they would be considered as desymmetrizations because of the above mentioned reasons.

I.3.2. Kinetic Resolution (KR).

Alternatively, if the starting substrate is chiral but there is no dynamic process involved in the stereochemical outcome of the reaction, then, a kinetic resolution (KR) could take place.

In this case, the strategy is based on the different rates of reactivity of the two atropisomers of the substrate. Ideally, one of the atropisomers from the racemic mixture is fully transformed into the desired product, while the other is recovered unreacted (Scheme I.11).



Scheme I.11 – Atroposelective synthesis of biaryls, kinetic resolution approach: concept and examples.

This strategy represents one of the most common methods for the synthesis of enantioenriched biaryls, and has been extensively applied to the synthesis of BINOL, BINAM and NOBIN derivatives.⁴⁵

In an ideal kinetic resolution, the main drawback is that the desired enantioenriched product can only be obtained with up to 50% yield, since only one atropisomer from the racemic mixture is reactive under KR conditions. Nonetheless, it is possible that a small amount of the less reactive atropisomer is converted into desired product, leading to more than 50% yield but also decreasing the enantiomeric excess of the major product.

This limitation can be solved if there is a possible route through which both atropisomers of the substrate can interconvert into each other. It means that there is a dynamic process involved in the stereochemical outcome of the reaction. Then, two different approaches can be distinguished depending on the nature of the dynamic process: dynamic kinetic resolution (DKR), or dynamic kinetic asymmetric transformation (DYKAT).

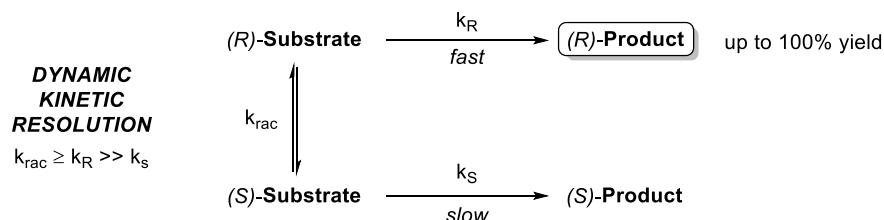
This PhD thesis, will focus on the development of novel dynamization strategies (DKRs and DYKATs) for the synthesis of axially chiral (hetero)biaryls.

I.3.2. Dynamic Kinetic Resolution (DKR).

In this case, the substrate is able to racemize, ensuring the constant transformation of the less reactive atropisomer into the more reactive one, and then to the desired enantioenriched product. This interconversion process enables the transformation of both atropisomers into a single stereoisomeric product in quantitative theoretical yield (Scheme I.12).

⁴⁵ For selected examples for the synthesis of BINOL and derivatives *via* KR, see: (a) Jones, B. A.; Balan, T.; Jolliffe, J. D.; Campbell, C. D.; Smith, M. D. *Angew. Chem. Int. Ed.* **2019**, *58*, 4596. (b) Lu, S.; Poh, B. S.; Zhao, Y. *Angew. Chem. Int. Ed.* **2014**, *53*, 11041. (c) Ma, G.; Deng, Y.; Sibi, M. P. *Angew. Chem. Int. Ed.* **2014**, *53*, 11818. (d) Aoyama, H.; Tokunaga, M.; Kiyosu, J.; Iwasawa, T.; Obora, Y.; Tsuji, Y. *J. Am. Chem. Soc.* **2005**, *127*, 10474.

As for kinetic resolutions, in DRKs the reaction rates for the two atropisomers of the substrate are different, but their interconversion is also possible. For an efficient DKR to occur, the racemization rate (k_{rac} , in Scheme I.12) needs to be equal or higher than the reaction rate for the more reactive atropisomer (k_{R} , in Scheme I.12).



Scheme I.12 – Dynamic kinetic resolution concept.

In a dynamic kinetic resolution, this racemization process does not necessarily involve a chiral catalyst. In general terms, the DKR will give higher enantiomeric excesses than the classic KR because the continuous racemization on the substrate will prevent the build-up of the opposite atropisomer from the starting material that affects negatively the KR.

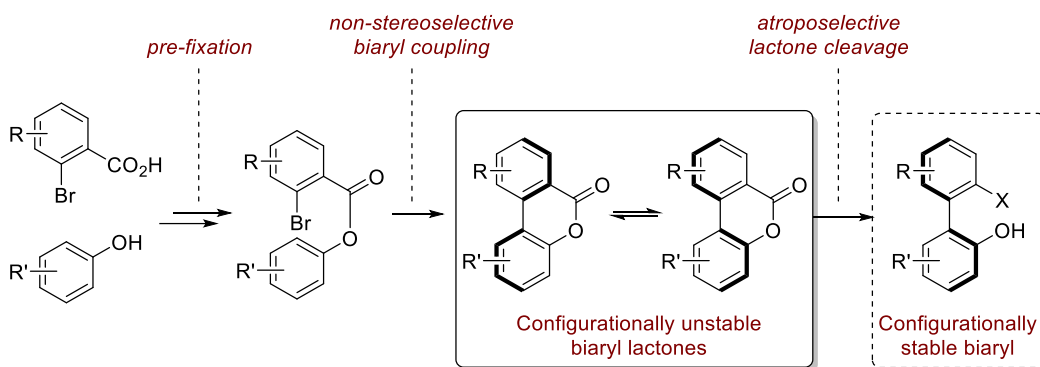
Several important reviews focusing on the theory and practical applications of DKR have been reported,⁴⁶ but the DKR approaches to obtain enantiomerically pure (hetero)biaryls have been reported to a lesser extent.

In the next section, DKR strategies for the atroposelective synthesis of (hetero)biaryls will be discussed. In particular, those dynamic processes in which the interconversion of both atropisomers of the starting (hetero)biaryl derivative is facilitated by formation of six-membered cyclic intermediates or transition states will be discussed.

⁴⁶ For selected reviews on DKR, see: (a) Pellissier, H. *Adv. Synth. Catal.* **2011**, 353, 659. (b) Pellissier, H. *Tetrahedron* **2008**, 64, 1563. (c) Steinreiber, J.; Faber, K.; Griengl, H. *Chem. Eur. J.* **2008**, 14, 8060. (d) Huerta, F. F.; Minidis, A. B. E.; Bäckvall, J.-E. *Chem. Soc. Rev.* **2001**, 30, 321.

I.3.2.1. Bringmann's Biaryl "Lactone Concept".

This concept was first introduced by Gerhard Bringmann, in 1992, when they reported an atropo-enantioselective lactone ring opening with a chiral hydride transfer reagent derived from a borane species.⁴⁷ This approach is based on the formation of a lactone bridge responsible for the configurational instability of the biaryl axis, providing a rapid atropisomerization equilibrium. Then, an atroposelective transformation is performed to cleave the lactone bridge, leading to the corresponding, now configurationally stable, axially chiral biaryl compounds (Scheme I.13).



Scheme I.13 – The concept of the "lactone strategy".

This methodology constitutes a very powerful tool that has been widely applied in the total synthesis of natural products containing an stereogenic axis (Figure I.10).⁴⁸

⁴⁷ Seminal work: Bringmann, G.; Hartung, T. *Angew. Chem. Int. Ed.* **1992**, *31*, 761.

⁴⁸ (a) Bringmann, G.; Breuning, M.; Tasler, S. *Synthesis* **1999**, *4*, 525. (b) Bringmann, G.; Tasler, S.; Pfeifer, R. M.; Breuning, M. *J. Organomet. Chem.* **2002**, *661*, 49. (c) Bringmann, G.; Tasler, S.; Endress, H.; Mühlbacher, J. *Chem. Commun.* **2001**, 761.

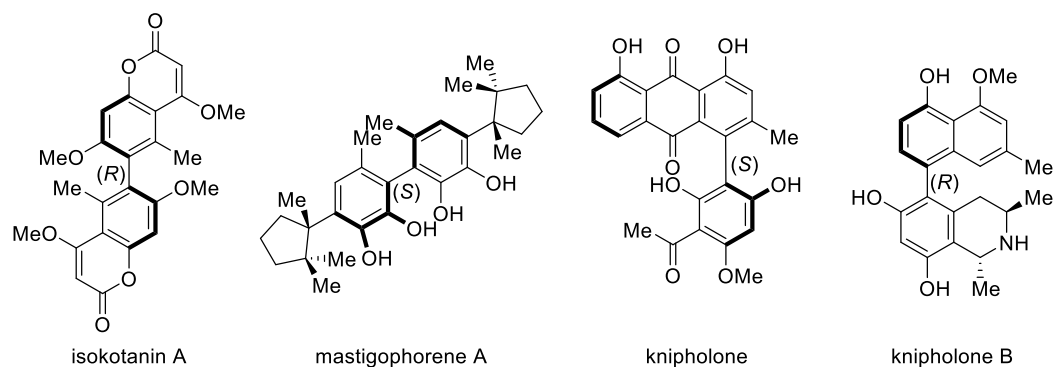
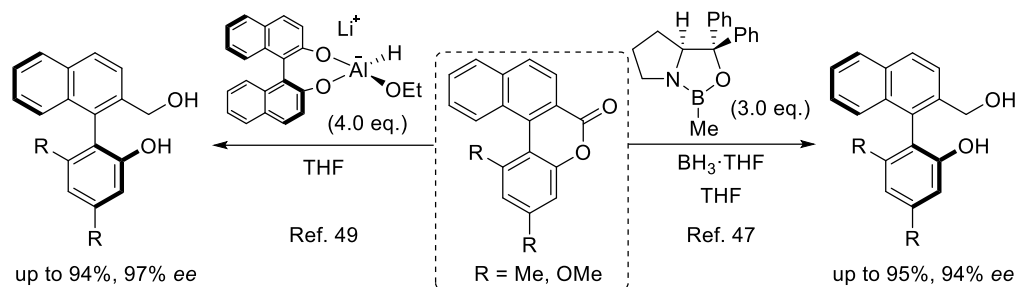


Figure I.10 – Representative examples of axially chiral natural products synthesised through “lactone strategy”.

Despite most of the developed strategies for the lactone ring cleavage consist on the reduction of the carbonyl functionality (Scheme I.14),^{47,49} not only hydrides could be employed as nucleophiles.



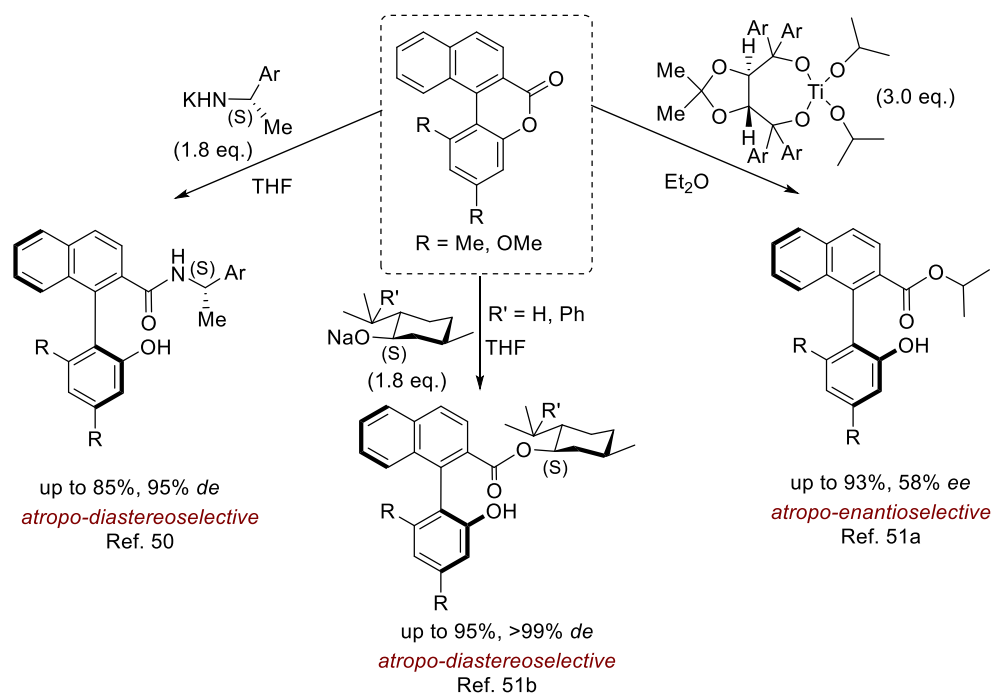
Scheme I.14 – Atroposelective cleavage of bridged biaryl lactones using hydride as nucleophile.

In this context, Bringmann’s group has also employed different *N*-⁵⁰ and *O*-nucleophiles⁵¹ for the atropo-enantio- and atropo-diastereoselective cleavage of configurationally unstable biaryl lactones (Scheme I.15).

⁴⁹ Bringmann, G.; Hartung, T. *Tetrahedron* **1993**, *49*, 7891.

⁵⁰ Bringmann, G.; Breuning, M.; Tasler, S.; Endress, H.; Ewers, C. L. J.; Göbel, L.; Peters, K.; Peters, E.-M. *Chem. Eur. J.* **1999**, *5*, 3029.

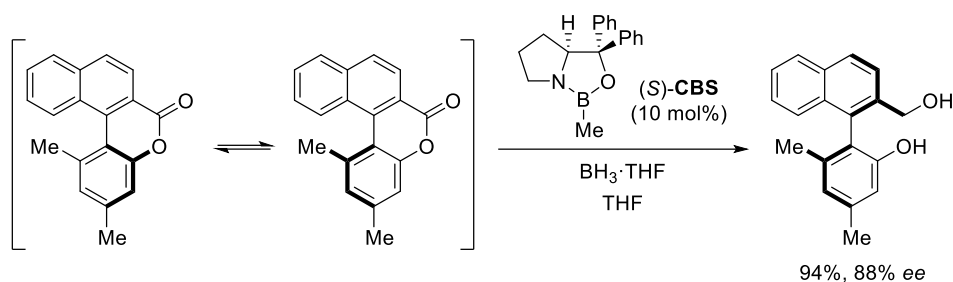
⁵¹ (a) Seebach, D.; Jaeschke, G.; Gottwald, K.; Matsuda, K.; Formisano, R.; Chaplin, D. A.; Breuning, M.; Bringmann, G. *Tetrahedron* **1997**, *53*, 7539. (b) Bringmann, G.; Breuning, M.; Walter, R.; Wuzik, A.; Peters, K.; Peters, E.-M. *Eur. J. Org. Chem.* **1999**, 3047.



Scheme I.15 – Chiral nucleophiles different than hydride reported by Bringmann for the lactone strategy.

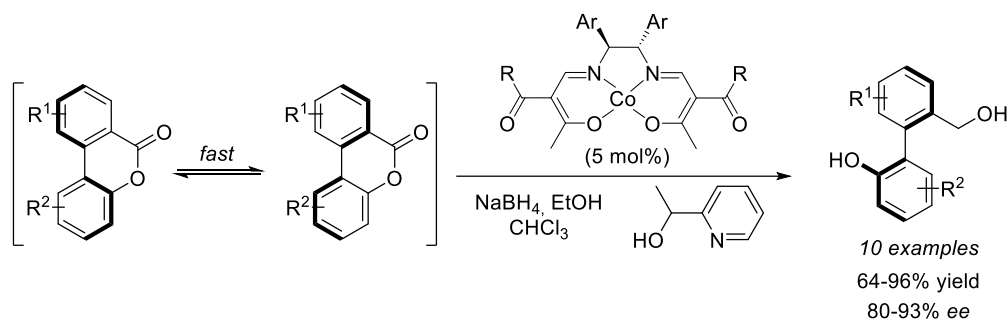
However, this strategy initially showed an important limitation regarding the need of stoichiometric amounts of the chiral nucleophile responsible for the lactone bridge cleavage. For instance, in 2002, ten years after the first report on this biaryl lactone bridge cleavage strategy, the first example of a catalytic reduction of biaryl lactones with 10 mol% of the Corey-Bakshi-Shibata (CBS) reagent was reported by Bringmann and co-workers (Scheme I.16).⁵² However, the reaction showed a slight decrease on the enantiomeric excess from 94 to 88 % when the CBS amount was reduced from 3.0 eq. to 0.1 eq., respectively (see Schemes I.14 vs I.16).

⁵² Bringmann, G.; Breuning, M.; Henschel, P.; Hinrichs, J. *Org. Synth.* **2002**, 79, 72.



Scheme I.16 – First catalytic atropo-enantioselective biaryl synthesis through the “lactone strategy”.

This achievement supposed an important progress to the lactone strategy and captured the attention of other authors aiming to expand the synthetic utility of this tool. In 2008, Yamada and co-workers developed an improved catalytic atropo-enantioselective reduction of biaryl lactones for the synthesis of axially chiral biaryls (Scheme I.17).⁵³

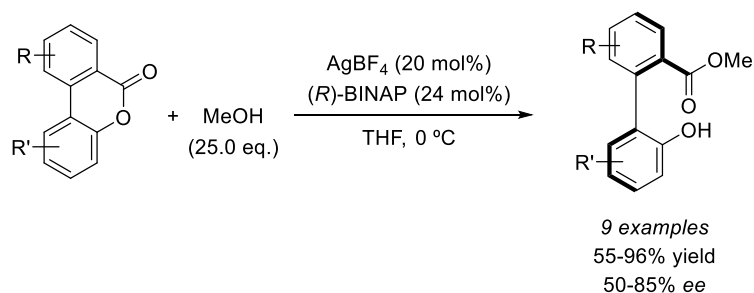


Scheme I.17 – Yamada's report on the atroposelective Co-catalyzed biaryl lactone bridge reduction.

This contribution expanded the scope of biaryl structures that was limited to only two examples in the original Bringmann's report. In this case, sodium borohydride was employed to generate a chiral Co-H complex responsible for the reduction of the carbonyl functionality. Additional HPLC analysis of the starting biaryl lactone at different temperatures helped the authors to determine that at 30 °C the atropisomerization of the substrate was taking place fast enough to allow for an efficient dynamic kinetic resolution to occur.

⁵³ Ashizawa, T.; Tanaka, S.; Yamada, T. *Org. Lett.* **2008**, *10*, 2521.

Inspired by this work and the previous report by Bringmann in the atropo-enantioselective ring-opening of biaryl lactones catalyzed by $(i\text{PrO})_2\text{Ti}$ -TADDOL-ates acting as *O*-nucleophiles,^{51a} the group of Yamada developed a silver-catalysed atroposelective ring-opening of biaryl lactones with methanol, although a large excess of the nucleophile was required (Scheme I.18).⁵⁴

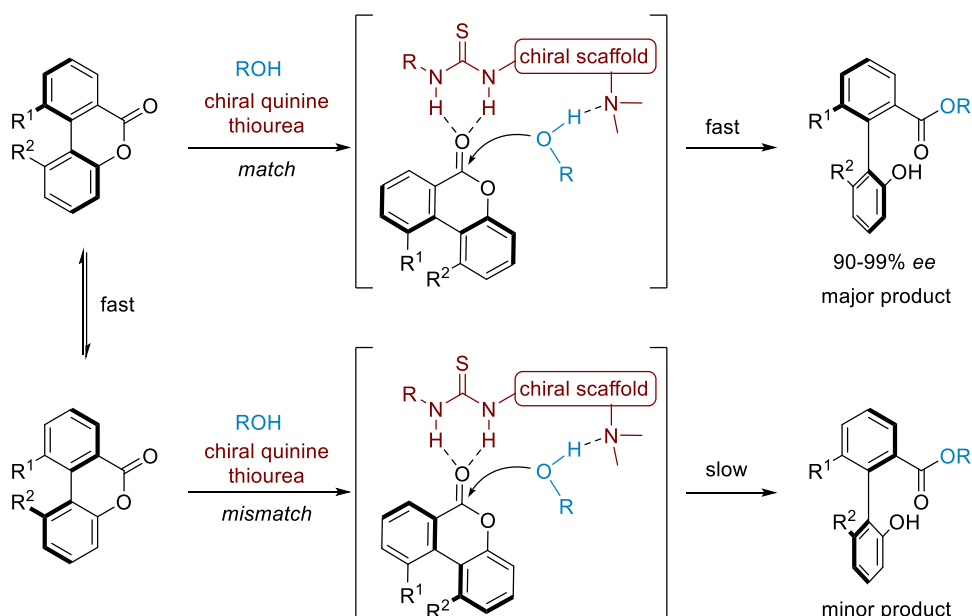


Scheme I.18 – Atroposelective biaryl lactone ring-opening using methanol as *O*-nucleophile.

A major breakthrough in the field was reported in 2016 by the group of Wei Wang, who reported a catalytic atroposelective transesterification of Bringmann lactones with enantiomeric excesses up to 99% using a chiral bifunctional quinine-based thiourea organocatalyst. In this report, the authors highlighted the effect of a synergistic activation mode of the thiourea as H-bond donor to the carbonyl, and the sp^3 nitrogen at quinine as H-bond acceptor to activate the alcohol, crucial to achieve such high selectivities (Scheme I.19).⁵⁵

⁵⁴ Ashizawa, T.; Yamada, T. *Chem. Lett.* **2009**, 38, 246.

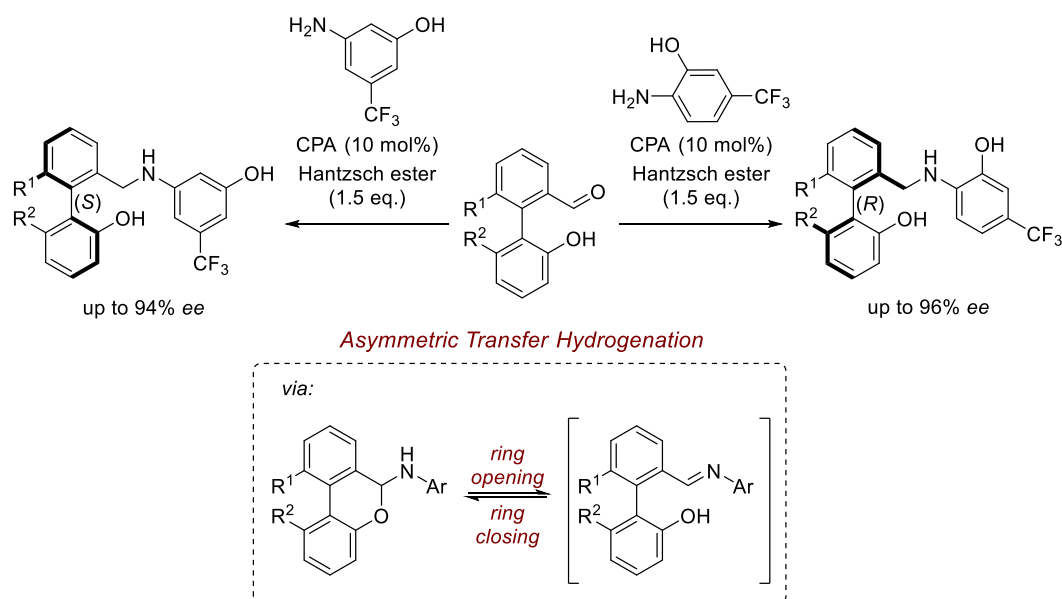
⁵⁵ Yu, C.; Huang, H.; Li, X.; Zhang, Y.; Wang, W. *J. Am. Chem. Soc.* **2016**, 138, 6956.



Scheme 1.19 – Highly atropo-enantioselective metal-free transesterification of biaryl lactones by Wang *et al.*

By the same time, Akiyama and co-workers, developed an enantiodivergent atroposelective synthesis of axially chiral biaryl hemiaminals by asymmetric transfer hydrogenation catalyzed by a chiral phosphoric acid (CPA), also based on the Bringmann's concept but with a significant difference. In that work, the authors demonstrated that the imine resulting from condensation of a cyclic biaryl acetal with an amine (hydroxyaniline) is also configurationally labile through the formation of an *N,O*-acetal in equilibrium with the open form, which is then reduced by using the Hantzsch ester and a CPA. Interestingly, it is possible to control the configuration of the final product by the proper choice of the hydroxyaniline derivative: whereas *o*-hydroxyanilines favoured the formation of the *R* isomer, the use of the *m*-hydroxyanilines reversed the atroposelectivity to furnish the *S* isomer of the biaryl, in both cases with high enantioselectivities (Scheme 1.20).⁵⁶

⁵⁶ Mori, K.; Itakura, T.; Akiyama, T. *Angew. Chem. Int. Ed.* **2016**, *55*, 11642.



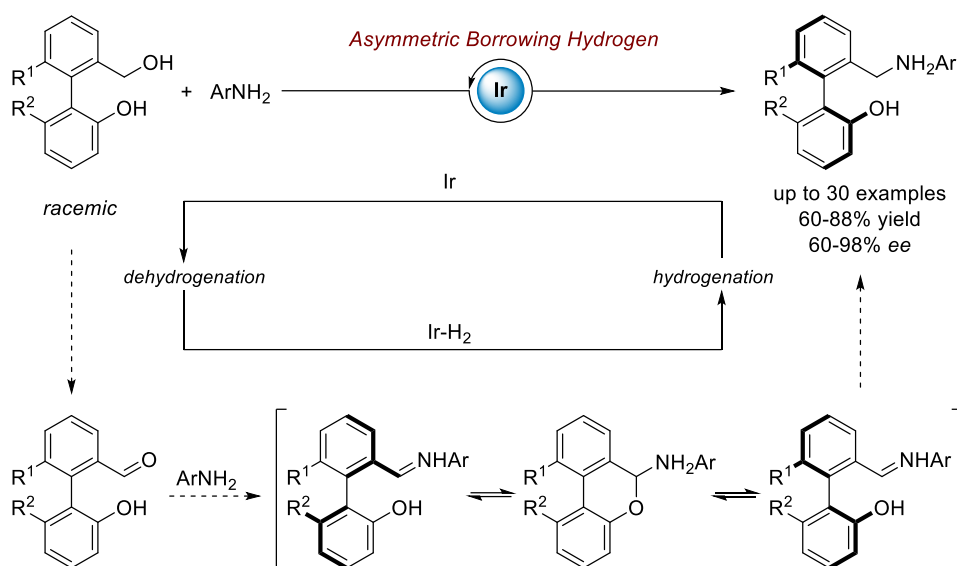
Scheme I.20 – Enantiodivergent atroposelective synthesis of axially chiral biaryl amine-alcohols by the group of Akiyama.

This catalytic methodology was applied to the synthesis of axially chiral amino-alcohols in excellent yields and enantioselectivities. These frameworks exhibit interesting properties as catalysts, for example by promoting the asymmetric addition of organozinc reagents to aldehydes yielding the corresponding chiral products with high enantioselectivities.⁵⁷

Continuing with these studies, Jian Wang and co-workers developed a hydrogen borrowing reaction followed by a hydrogen transfer approach for the synthesis of similar compounds with an additional expansion of the scope (Scheme I.21).⁵⁸ Indeed, these authors were able to synthesize up to 30 axially chiral amino-alcohols, introducing several structural variations both at the biaryl frame, and at the aromatic amine substituents.

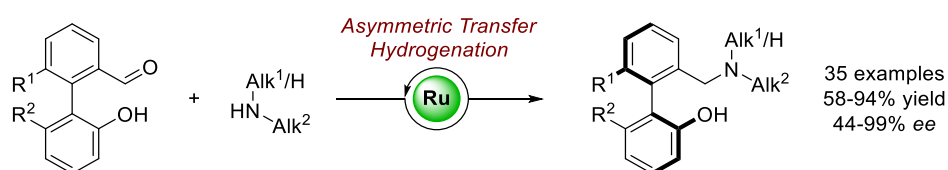
⁵⁷ (a) Ko, D.-H.; Kim, K. H.; Ha, D.-C. *Org. Lett.* **2002**, *4*, 3759. (b) Kang, S.-W.; Ko, D.-H.; Kim, K. H.; Ha, D.-C. *Org. Lett.* **2003**, *5*, 4517.

⁵⁸ Zhang, J.; Wang, J. *Angew. Chem. Int. Ed.* **2018**, *130*, 474.



Scheme I.21 –Hydrogen borrowing approach developed by Wang and co-workers.

Additionally, the same authors reported in parallel an alternative method for the synthesis of axially chiral amino-alcohols based on a ruthenium-catalyzed atroposelective reductive amination *via* dynamic kinetic resolution (Scheme I.22).⁵⁹



Scheme I.22 – Ru-catalyzed synthesis of axially chiral amino-alcohols.

Moreover, this methodology expanded the scope to alkyl amines, both primary and secondary and allowed for the synthesis of these structures in good to excellent yields and enantioselectivities.

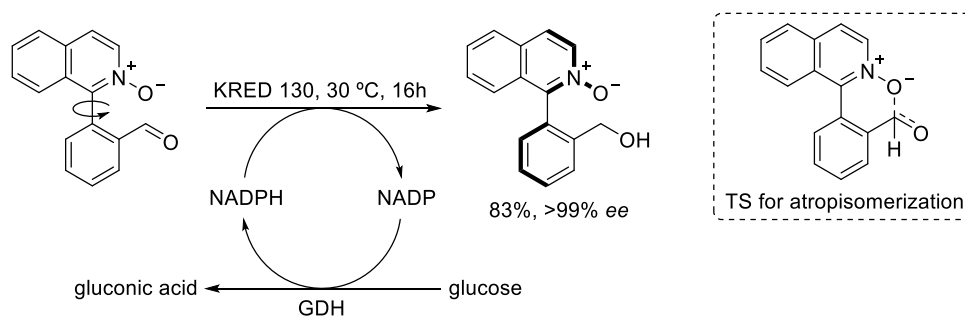
I.3.2.2. Clayden's approach.

In the labilization mechanism occurring at Bringmann's biaryl "lactone strategy" a covalently attached bridged lactone ring is cleaved by a chiral nucleophile, while the system

⁵⁹ Guo, D.; Zhang, J.; Zhang, B.; Wang, J. *Org. Lett.* **2018**, *20*, 6284.

described by Akiyama relies on the labilization promoted by formation of a cyclic intermediate (hemiaminal). In contrast, the next strategy relies on the labilization facilitated by six-membered ring transition states for the atropisomerization event.

In 2016, Clayden and co-workers developed a biocatalytic reduction for the atropo-enantioselective synthesis of axially chiral heterobiaryl *N*-oxides *via* dynamic kinetic resolution (Scheme I.23).⁶⁰ Particularly, a ketoreductase (KRED 130) is used for the reduction of a configurationally unstable heterobiaryl ketone under mild conditions, while glucose is oxidized to gluconic acid.

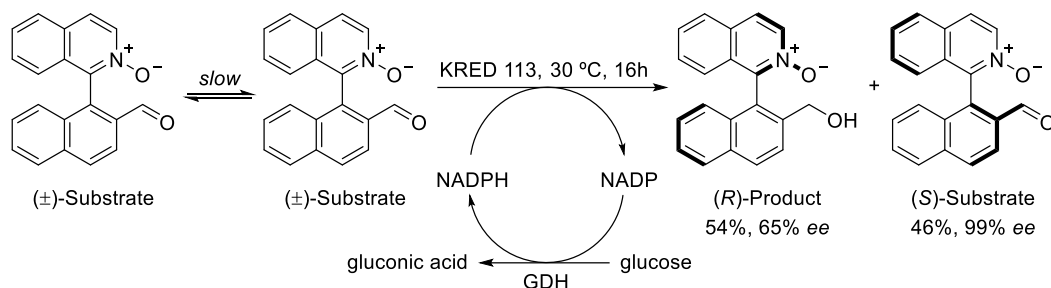


Scheme I.23 – Biocatalytic reduction and DKR developed by Clayden et al.

In this report, the dynamization process through which the atropisomerization of the substrate takes place involves an intramolecular interaction between the *N*-oxide oxygen atom and the aldehyde carbonyl atom, in a six-membered transition state that was supported by molecular modelling, in a close resembling to the mechanism for atropisomerization at Bringmann's lactones. However, in contrast to the latter, there is no covalent bond formation in Clayden's system, but a TS with a bonding interaction can be used instead. It is also worth to mention that Clayden et al. determined that the reaction with the corresponding aldehyde derived from naphthylisoquinoline *N*-oxide was not efficient due to the low racemization rate for this hindered tetra-*ortho*-substituted system, simply providing a kinetic resolution (Scheme I.24). Furthermore, when the substrate was

⁶⁰ Staniland, S.; Adams, R. W.; McDouall, J. J. W.; Maffucci, I.; Contini, A.; Grainger, D. M.; Turner, N. J.; Clayden, J. *Angew. Chem. Int. Ed.* **2016**, *55*, 10755.

heated over 100 °C in order to determine the racemization rate, the product decomposition occurs before the racemization.



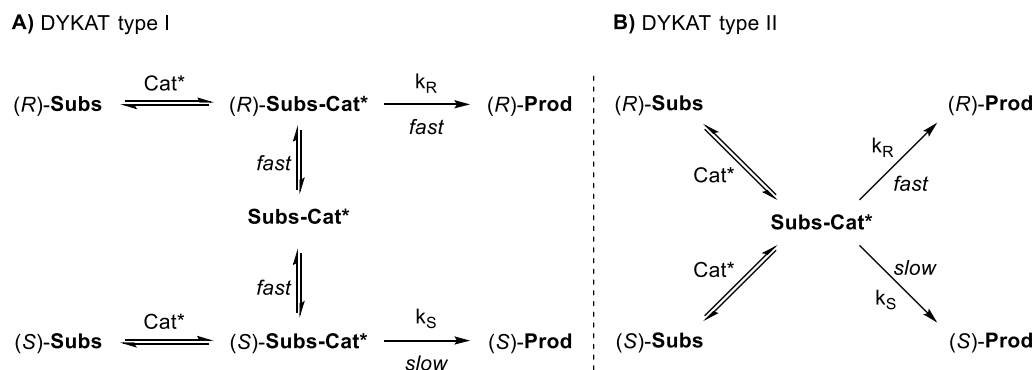
Scheme I.24 – Biocatalytic reduction and kinetic resolution at hindered systems.

Therefore, it can be concluded that, in the analysed systems, the labilization process through six-membered cyclic transition states (or intermediates) is not as efficient as those proceeding through covalently bonded intermediates. As a practical consequence, the substrate cannot be tetrasubstituted at *ortho* positions around the stereogenic axis in order to make possible an efficient DKR.

I.3.2. Dynamic Kinetic Asymmetric Transformation (DYKAT).

Compared to the previous strategy, in a dynamic kinetic asymmetric transformation the starting substrate is configurationally stable since the rotational barrier is high enough to avoid the spontaneous interconversion between both atropisomers, while the reaction conditions do not alter this situation. Therefore, the racemization event should be mediated by a chiral catalyst, involving the formation of either diastereomeric intermediates in which the configurational stability is compromised (DYKAT type I, Scheme I.25A), or a common intermediate (DYKAT type II, Scheme I.25B).⁶¹

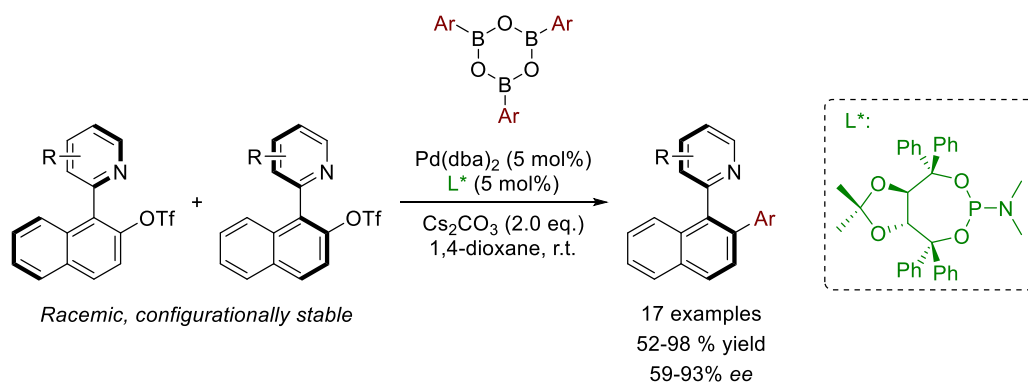
⁶¹ Steinreiber, J.; Faber, K.; Griengl, H. *Chem. Eur. J.* **2008**, *14*, 8060.



Scheme I.25 – Dynamic kinetic asymmetric transformation concept.

With respect to the application of this DYKAT strategy for the synthesis of axially chiral compounds, all the reported examples are, to the best of our knowledge, based on heterobiaryl structures.

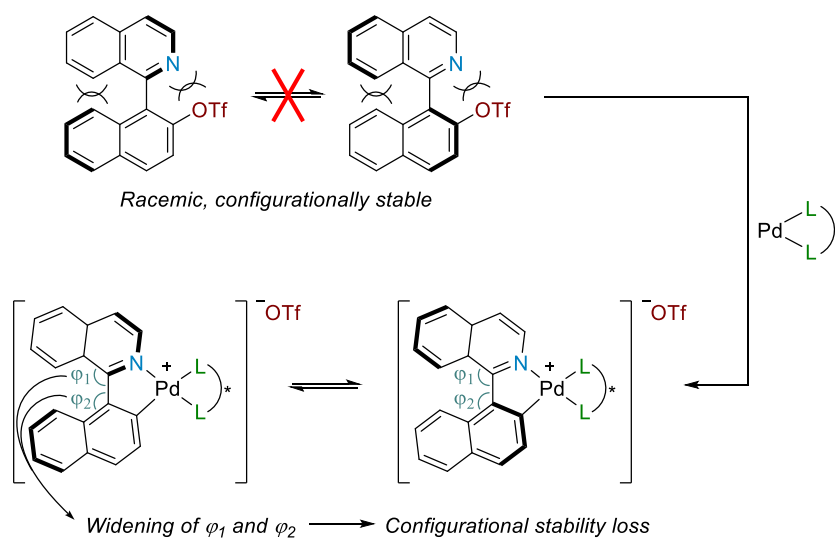
In this context, our research group reported in 2013 the first example of an atroposelective synthesis of axially chiral heterobiaryls based on a DYKAT approach.⁶² As a first example of this strategy, a palladium-catalyzed asymmetric arylation of heterobiaryl triflates with arylboroxines using a TADDOL-derived phosphoramidite as ligand was developed (Scheme I.26).



Scheme I.26 – Dynamic kinetic asymmetric cross-coupling for the synthesis of axially chiral heterobiaryls.

⁶² Ros, A.; Estepa, B.; Ramírez-López, P.; Álvarez, E.; Fernández, R.; Lassaletta, J. M. *J. Am. Chem. Soc.* **2013**, *135*, 15730.

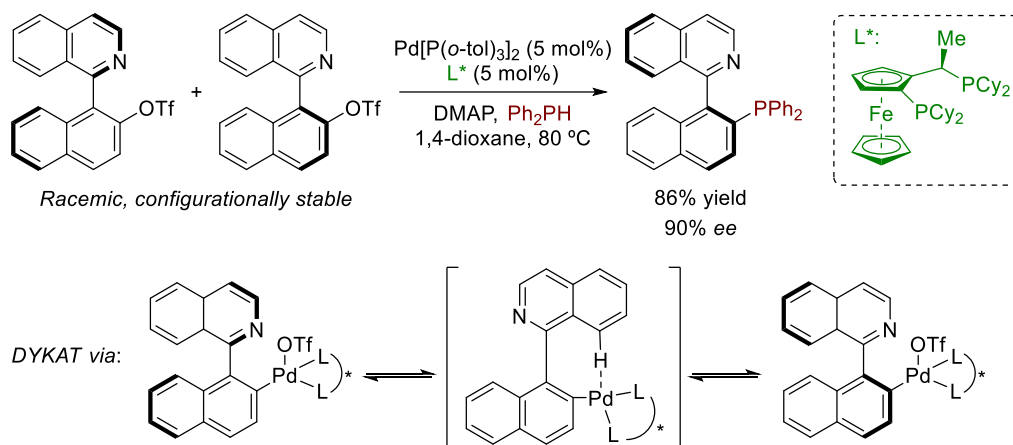
In this case, the starting heterobiaryl triflates are configurationally stable; the interconversion between both atropisomers is not possible at normal reaction temperatures. However, the Suzuki cross-coupling reaction involves first an oxidative addition step of the Pd into aryl–OTf bond, and given the poor coordinating ability of the resulting triflate anion, the isoquinoliyl/pyridyl nitrogen is expected to be incorporated to the coordination sphere of the metal centre. This results in the formation of a five-membered ring, with the subsequent widening of the angles involved in the configurational stability of the stereogenic axis; thus, making possible the interconversion between both diastereomeric intermediates (Scheme I.27).



Scheme I.27 – Atropisomerization mechanism proposed by our group.

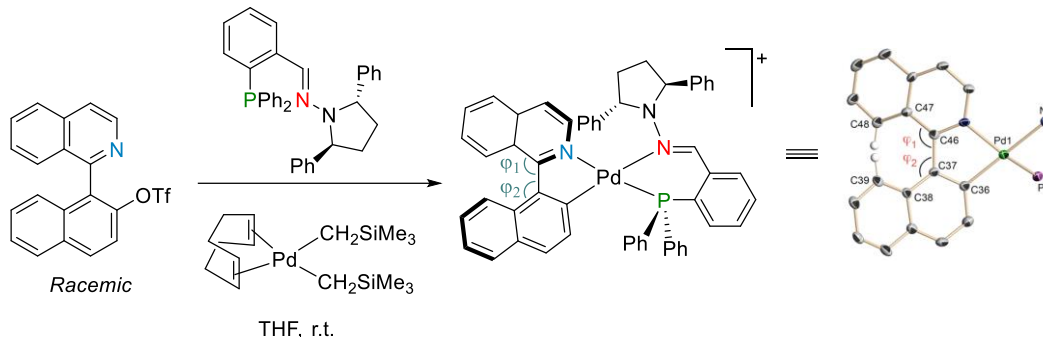
In parallel, a similar strategy by Stoltz and Virgil for the atropo-enantioselective synthesis of QUINAP was simultaneously reported (Scheme I.28).⁶³

⁶³ Bhat, V.; Wang, S.; Stoltz, B. M.; Virgil, S. C. *J. Am. Chem. Soc.* **2013**, *135*, 16829.



Scheme I.28 – Synthesis of QUINAP through DYKAT approach developed by Stoltz's and Virgil's group, and their proposed mechanism.

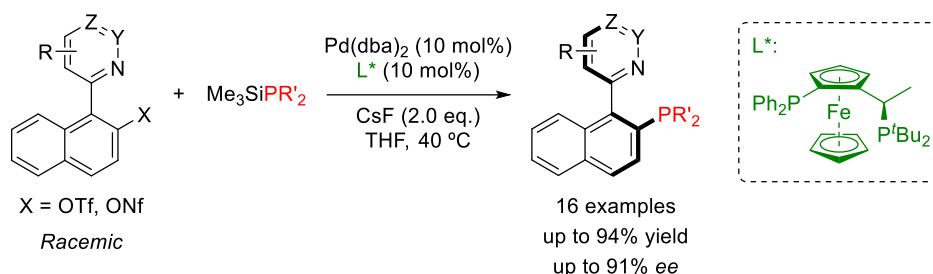
However, the authors proposed a different mechanism for the isomerization of the diastereomeric species, in which the key racemization event takes place through an intermediate where a stabilizing agostic interaction occurs between the isoquinoline peri-hydrogen and the cationic palladium atom resulting in a chelated structure (Scheme I.28). Nonetheless, this proposal is highly speculative compared to the previously described by our research group, that was convincingly supported by the isolation of the oxidative addition intermediate and its single crystal X-ray analysis (Scheme I.29).



Scheme I.29 – Isolated oxidative addition intermediate in the DYKAT approach.

This dynamic kinetic asymmetric transformation strategy for the synthesis of axially chiral heterobiaryls developed by our group was later extended to different cross-coupling reactions.

Furthermore, it was also developed an alternative methodology for the synthesis of QUINAP and its derivatives, that resulted more versatile and efficient than the previous reported by Stoltz and Virgil.⁶⁴ This methodology allowed for the synthesis of a wide variety of axially chiral heterobiaryls, with potential as P,N ligands such as QUINAP and analogues with high levels of enantioselectivity (Scheme I.30).



Scheme I.30 – Dynamic kinetic asymmetric C–P cross-coupling.

The atropisomerization mechanism previously reported, involving a five-membered cationic palladacycle oxidative addition intermediates was further evidenced in this case. For instance, DFT calculations determined that there exists a much higher stabilization of the intermediates when isoquinolyl nitrogen is coordinated to Pd, compared to the agostic Pd–H interaction proposed by Virgil and Stoltz ($\Delta G = +9.3$ kcal/mol), allowing to discard the latter (Figure I.11).

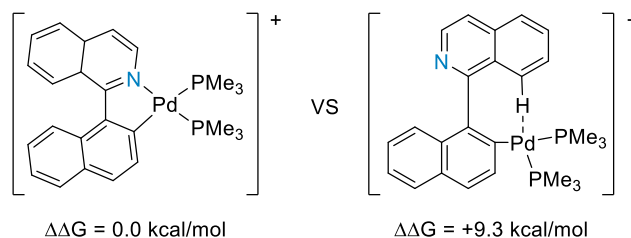
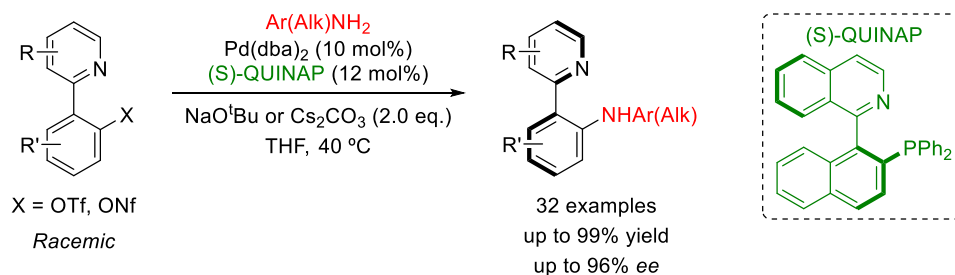


Figure I.11 – Comparison of the stabilizing interactions on the atropisomerization mechanism proposed by Fernández and Lassaletta vs Virgil and Stoltz.

Interestingly, the next extension of the strategy, a C–N atroposelective cross-coupling through a Pd-catalyzed dynamic kinetic asymmetric Buchwald-Hartwig

⁶⁴ Ramírez-López, P.; Ros, A.; Estepa, B.; Fernández, R.; Fiser, B.; Gómez-Bengo, E.; Lassaletta, J. M. *ACS Catal.* **2016**, *6*, 3955.

amination using QUINAP as ligand made use of the axially chiral P,N ligands prepared through the previously described methodology (Scheme I.31).⁶⁵



Scheme I.31 – Dynamic kinetic asymmetric C–N cross-coupling via Buchwald-Hartwig amination.

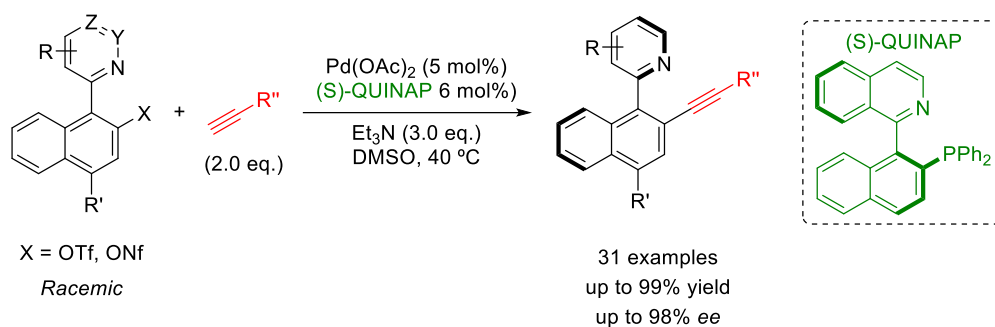
Once again, the atropisomerization occurs at the oxidative addition cationic intermediate involving the coordination of isoquinolyl/pyridyl nitrogen to the Pd centre. In fact, when the reaction was performed with the corresponding heterobiaryl bromide (instead of sulfonate), a complex mixture of diastereomeric oxidative addition intermediates was formed including cationic and neutral forms. From this mixture crystals of the latter, suitable for X-ray diffraction analysis were isolated. As expected the bromide remained partially coordinated to palladium, and the isoquinoline/naphthyl rings arranged almost perpendicularly. This result indicates that the higher coordinating ability of bromide with respect to triflate prevents the coordination of the isoquinolyl nitrogen. In the presence of NaOtBu, however, sodium bromide precipitates and the cationic intermediate thereby formed enables the reaction to proceed in a similar manner as with the sulfonate analogues.

(S)-QUINAP was also the ligand that provided the best results on the dynamic kinetic asymmetric alkynylation of configurationally stable heterobiaryl sulfonates, also developed in our research group.⁶⁶ This methodology was used for the synthesis of axially chiral heterobiaryl alkynes with a broad reaction scope, under very mild conditions using a Cu-free atroposelective Sonogashira cross-coupling (Scheme I.32). This methodology

⁶⁵ Ramírez-López, P.; Ros, A.; Romero-Arenas, A.; Iglesias-Sigüenza, J.; Fernández, R.; Lassaletta, J. M. *J. Am. Chem. Soc.* **2016**, *138*, 12053.

⁶⁶ Hornillos, V.; Ros, A.; Ramírez-López, P.; Iglesias-Sigüenza, J.; Fernández, R.; Lassaletta, J. M. *Chem. Commun.* **2016**, *52*, 14121.

tolerates the use of aromatic and aliphatic terminal alkynes as coupling partners for the heterobiaryl sulfonates, and the catalyst loading could be decreased to 1 mol% when the reaction was performed at 2 mmol or larger scale.



Scheme 1.32 – Dynamic kinetic asymmetric alkylation of heterobiaryl sulfonates reported by Hornillos, Fernández and Lassaletta.

The growing number of reports focusing on different strategies for the atroposelective synthesis of axially chiral (hetero)biaryls reflect the importance of this class of chirality and compounds. In this context, the development of methodologies for the simultaneous generation of an additional element of chirality, such as a stereogenic centre, represent a more challenging goal.

I.4. Simultaneous generation of central and axial chirality in (hetero)biaryls.

This section will focus on the discussion of the existing methodologies for the synthesis of (hetero)biaryls with the simultaneous generation of central and axial chirality elements. The applications of (hetero)biaryls bearing both central and axial chirality as ligands for metals and catalysts has been illustrated in different occasions.⁶⁷ However, their

⁶⁷ For selected examples, see: (a) Race, N. J.; Faulkner, A.; Fumagalli, G.; Yamauchi, T.; Scott, J. S.; Rydén-Landergren, M.; Sparkes, H. A.; Bower, J. F. *Chem. Sci.* **2017**, *8*, 1981. (b) Zhang, J.-W.; Xu, J.-H.; Cheng, D.-J.; Shi, C.; Liu, X.-Y.; Tan, B. *Nat. Commun.* **2016**, *7*, 10677. (c) Wang, S.; Li, J.; Miao, T.; Wu, W.; Li, Q.; Zhuang, Y.; Zhou, Z.; Qiu, L. *Org. Lett.* **2012**, *14*, 1966. (d) Shibatomi, K.; Soga, Y.; Narayama, A.; Fujisawa, I.; Iwasa, S. *J. Am. Chem. Soc.* **2012**, *134*, 9836. (e) Nareddy, P.; Mantilli, L.; Guénee, L.; Mazet, C. *Angew. Chem. Int. Ed.* **2012**, *51*, 3826. (f) Wang, D.-Y.; Hu, X.-P.; Huang, J.-D.; Deng, J.; Yu, S.-B.; Duan, Z.-C.; Xu, X.-F.; Zheng, Z. *Angew. Chem. Int. Ed.* **2007**, *46*, 7810. (g) Denmark, S. E.; Fan, Y. *Tetrahedron: Asymmetry* **2006**, *17*, 687.

synthesis usually requires complex multistep procedures, and there are scarce examples of catalytic strategies for that purpose.

The existing methodologies could be classified according to the kind of transformation through which the desired chirality elements are generated.

A. Formation of bridged biaryl structures.

The high relevance of bridged biaryl skeletons, such as dibenzoazepines and derivatives, in biological systems is well documented. Then, their synthesis is a topic of current interest. Moreover, the possibility of introducing different chirality elements is highly appealing.

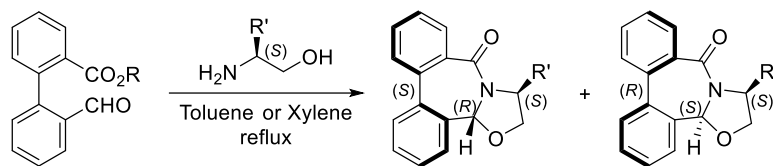
To the best of our knowledge, the first method dealing with the simultaneous generation of central and axial chirality in biaryl structures was reported in 2007 by the group of Wallace.⁶⁸ In this work, the authors developed a methodology for the formation of biaryl-fused lactams from configurationally unstable biaryl structures and commercially available aminoalcohols (Scheme I.33A).

Additionally, the same research group extended this strategy for the synthesis of dibenzazepine derivatives with switchable axial chirality.⁶⁹ They observed that when the secondary amine was *N*-Boc protected, the configuration at the stereogenic axis was inverted in a reversible process (Scheme I.33B).

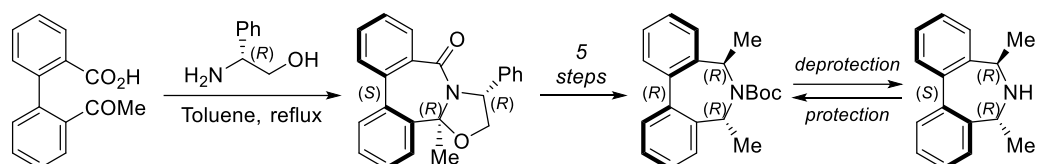
⁶⁸ Edwards, D. J.; House, D.; Sheldrake, H. M.; Stone, S. J.; Wallace, T. W. *Org. Biomol. Chem.* **2007**, *5*, 2658.

⁶⁹ Pira, S. L.; Wallace, T. W.; Graham, J. P. *Org. Lett.* **2009**, *11*, 1663.

A) Wallace, T. W., 2007. *Ref. 68*

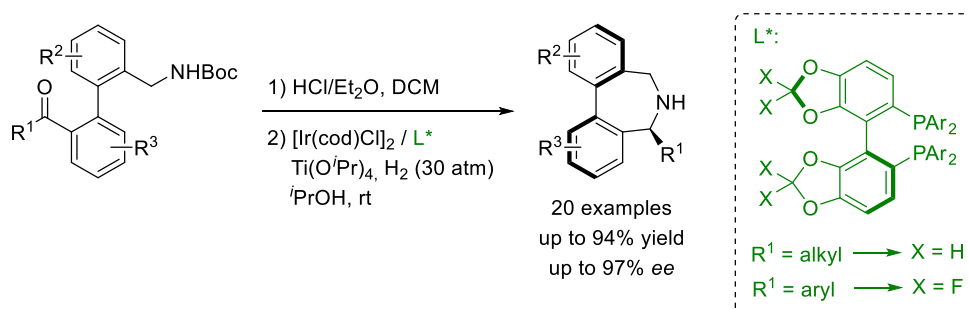


B) Wallace, T. W., 2009. *Ref. 69*



Scheme I.33 – Cyclization approaches developed by Wallace's group.

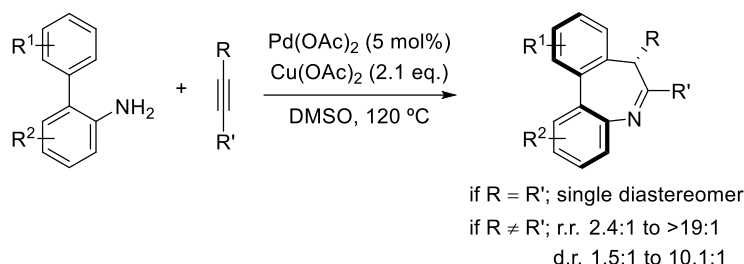
Also very recently, the group of Yin and Zhang has reported an intramolecular asymmetric reductive amination of bridged biaryl derivatives for the synthesis of dibenzo[*c,e*]azepines (Scheme I.34).⁷⁰ Despite the final products are similar to those synthesized by Wallace, this strategy consists on an intramolecular cyclization. Moreover, there is no need of a stoichiometric chiral reagent; a chiral Ir-catalyst is responsible for the asymmetric reduction of the corresponding imine formed after N-Boc cleavage and intramolecular condensation.



*Scheme I.34 – Yin and Zhang's asymmetric reductive amination for the synthesis of dibenzo[*c,e*]azepines.*

⁷⁰ Yang, T.; Guo, X.; Yin, Q.; Zhang, X. *Chem. Sci.* **2019**, *10*, 2473.

A previous work for the diastereoselective synthesis of central and axially chiral dibenzo[*b,d*]azepines was reported by the group of Luan consisting on a [5+2] oxidative annulation between *o*-arylanilines and alkynes (Scheme I.35).⁷¹



Scheme I.35 – Diastereoselective [5+2] oxidative annulation for the synthesis of dibenzo[*b,d*]azepines.

When symmetrical alkynes were employed, a single diastereomer was obtained; while the use of unsymmetrical alkynes, resulted in a mixture of regio- and diastereomers in variable ratios.

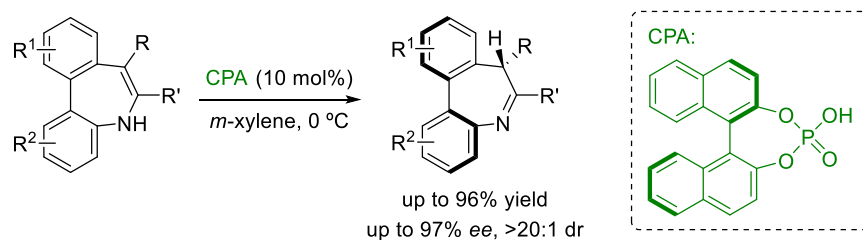
B. Modification of bridged biaryl structures.

An alternative that has also been recently exploited is the modification of already existing achiral or configurationally unstable bridged biaryl structures.

In this regard, based on their previous work, Luan and co-workers reported a catalytic enantioselective enamine–imine tautomerization.⁷² These metastable enamines, which were synthesized through an alternative route, have been shown to convert, under acidic conditions, to the corresponding structurally and thermodynamically stable imine form. Therefore, the treatment of these enamines with a BINOL derived chiral phosphoric acid (CPA), results in the enantioselective tautomerization to the imine with the simultaneous establishment of central and axial chirality in good yields and excellent diastereo- and enantioselectivities (Scheme I.36).

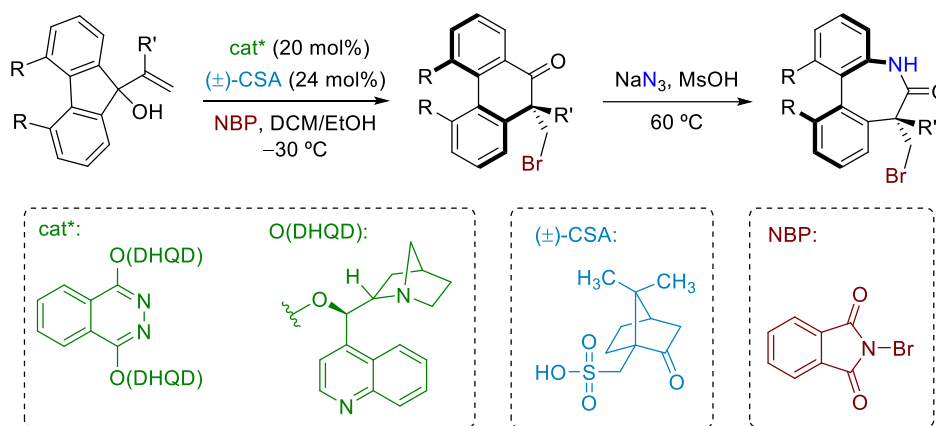
⁷¹ Zuo, Z.; Liu, J.; Nan, J.; Fan, L.; Sun, W.; Wang, Y.; Luan, X. *Angew. Chem. Int. Ed.* **2015**, *54*, 15385.

⁷² Liu, J.; Yang, X.; Zuo, Z.; Nan, J.; Wang, Y.; Luan, X. *Org. Lett.* **2018**, *20*, 244.



Scheme I.36 – CPA-catalyzed enantioselective enamine-imine tautomerization.

Another methodology to access central and axially chiral biaryl structures based on a transformation on a bridged structure has also been described. In 2017, Yeung et al. reported an organocatalytic enantioselective semipinacol rearrangement which, combined with a dynamic kinetic resolution, allowed for the synthesis of the desired products (Scheme I.37).⁷³



Scheme I.37 – Organocatalyzed enantioselective semipinacol rearrangement developed by Yeung et al.

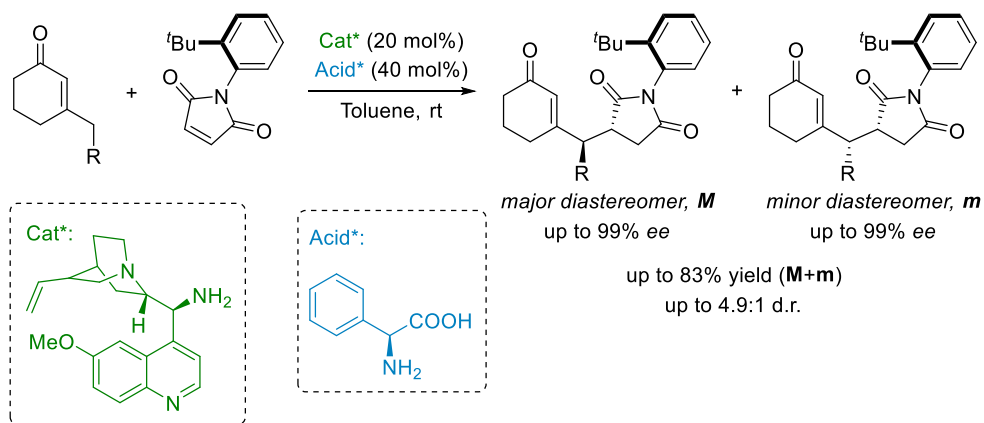
Moreover, these biaryls can be subjected to a second ring expansion through an intramolecular Schmidt reaction to afford the corresponding dibenzolactams, with the inverted configuration at the stereogenic axis (Scheme I.37).

C. Desymmetrization reactions.

⁷³ Liu, Y.; Tse, Y.-L. S.; Kwong, F. Y.; Yeung, Y.-Y. *ACS Catal.* **2017**, *7*, 4435.

Another alternative for the simultaneous construction of central and axial chirality is based on the desymmetrization of already existing biaryl structures.

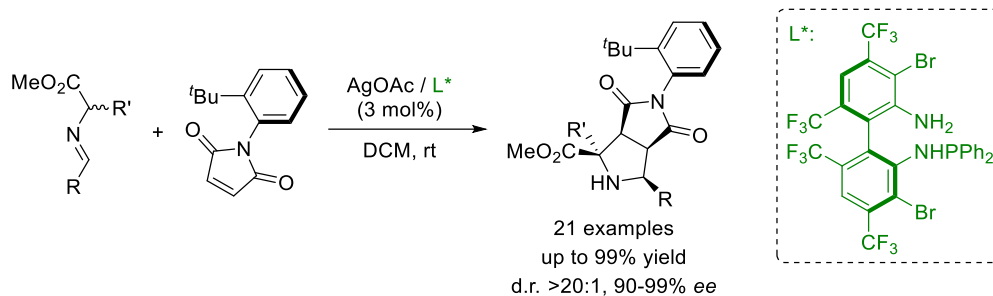
In this context, *N*-arylmaleimide architectures have attracted a particular interest. The first work in this regard was reported in 2014 by the group of Bencivenni, who developed an amino-catalytic desymmetrization of *N*-arylmaleimides *via* vinylogous Michael addition. The desymmetrization occurs through the introduction of an additional substituent in order to eliminate the mirror plane existing at the meso-substrate (see Scheme I.7). The cyclohexenone is activated by a quinine derived primary amine, and the resulting enamine intermediate adds to the *N*-arylmaleimide with the simultaneous installation of an stereogenic axis and two stereocentres with moderate diastereoselectivities and excellent enantioselectivities (Scheme I.38).



Scheme I.38 – *N*-Arylmaleimide desymmetrization for the construction of central and axial chirality.

Another interesting work dealing with the desymmetrization of *N*-arylmaleimides was reported two years later by the group of Wang.⁷⁴ In contrast to the above described method, this strategy is based on a Ag(I)-catalyzed 1,3-dipolar cycloaddition of azomethine ylides (Scheme I.39).

⁷⁴ Liu, H.-C.; Tao, H.-Y.; Cong, H.; Wang, C.-J. *J. Org. Chem.* **2016**, *81*, 3752.



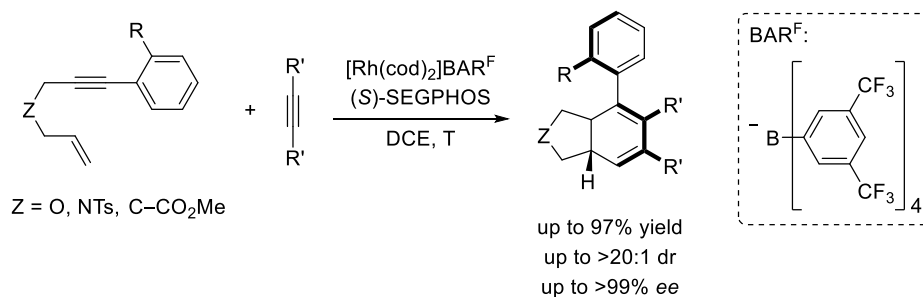
Scheme 1.39 – Desymmetrization of *N*-arylmaleimides via 1,3-dipolar Ag(I)-catalyzed cycloaddition.

This methodology allows for the preparation of enantioenriched octahydropyrrolo[3,4-*c*]pyrrole derivatives containing four adjacent stereocenters and one N–C stereogenic axis with an excellent control on diastereo- and enantioselectivities.

D. De novo construction of the stereogenic axis.

An extended approach applied to the topic at issue consists on the *de novo* construction of the stereogenic axis through different synthetic routes.

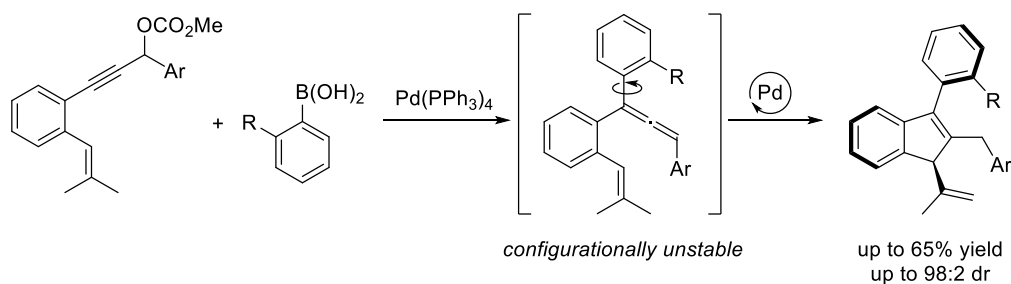
Thus, Shibata's group developed the Rh-catalyzed intermolecular [2+2+2] cycloaddition for the synthesis of bicyclic cyclohexa-1,3-dienes with both axial and central chirality with high diastereo- and enantioselectivities (Scheme 1.40).⁷⁵ This methodology represents the first example of a transition metal-catalyzed cycloaddition reaction for the generation of two different chiral motifs.



Scheme 1.40 – Shibata's [2+2+2] cycloaddition for the construction of central and axial chirality.

⁷⁵ Shibata, T.; Otomo, M.; Tahara, Y.; Endo, K. *Org. Biomol. Chem.*, **2008**, *6*, 4296.

A few years later, in 2016, Nechab and co-workers reported an atroposelective palladium tandem catalysis for the synthesis of central and axially chiral indenenes,⁷⁶ a core with a broad spectrum of applications. This methodology involves the conversion of propargylic carbonates into allenes via Pd-catalyzed coupling with aryl boronic acids, followed by tandem intramolecular palladium-assisted Alder-ene cyclization, with good diastereocontrol in the formation of indenenes containing two stereogenic elements, although in moderate yields (Scheme I.41).

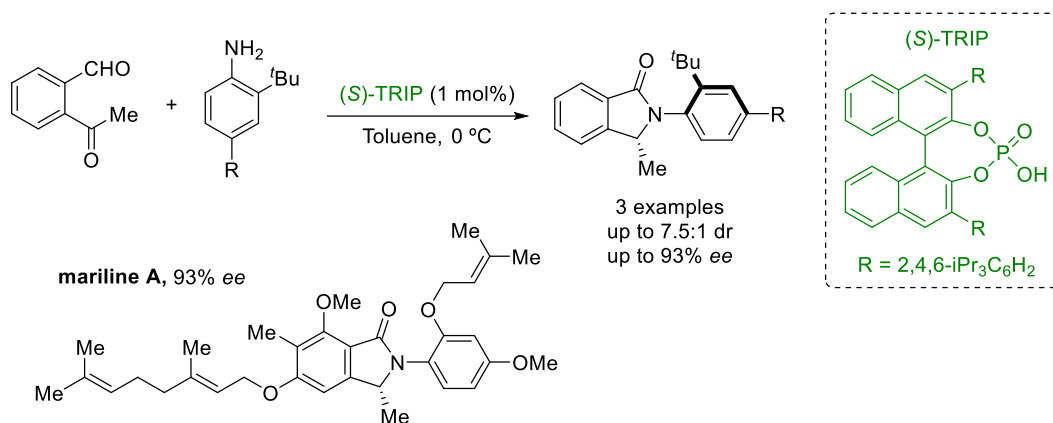


Scheme I.41 – Tandem Pd-catalysis for the synthesis of indenenes with central and axial chirality.

These compounds present structural similarities to indolines which are also present in many bioactive substances. For that reason, Seidel's group developed a catalytic enantioselective methodology for the synthesis of isoindolines with central and axial chirality elements from two achiral substrates, *ortho*-acyl benzaldehyde and *ortho*-substituted anilines (Scheme I.42).⁷⁷ This methodology was applied to the total synthesis of axially chiral mariline A in 5% overall yield and 93% *ee* after 10 reaction steps.

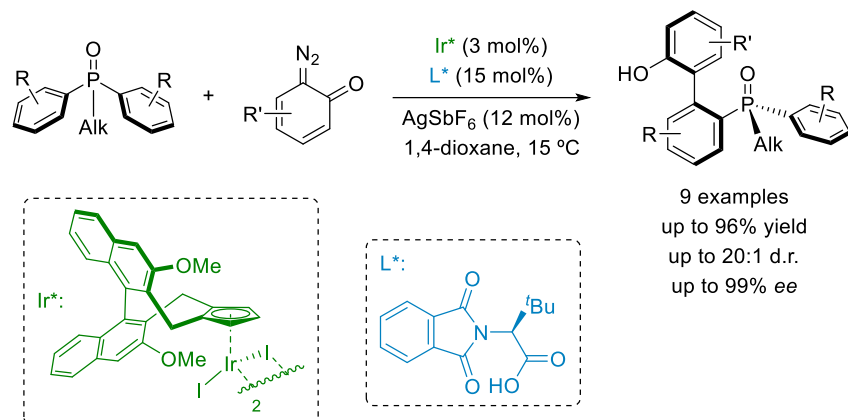
⁷⁶ Borie, C.; Vanthuyne, N.; Bertrand, M. P.; Siri, D.; Nechab, M. *ACS Catal.* **2016**, *6*, 1559.

⁷⁷ Min, C.; Lin, Y.; Seidel, D. *Angew. Chem. Int. Ed.* **2017**, *56*, 15353.



Scheme I.42 – Synthesis of central and axially chiral isoindoline skeletons developed by Nechab's group.

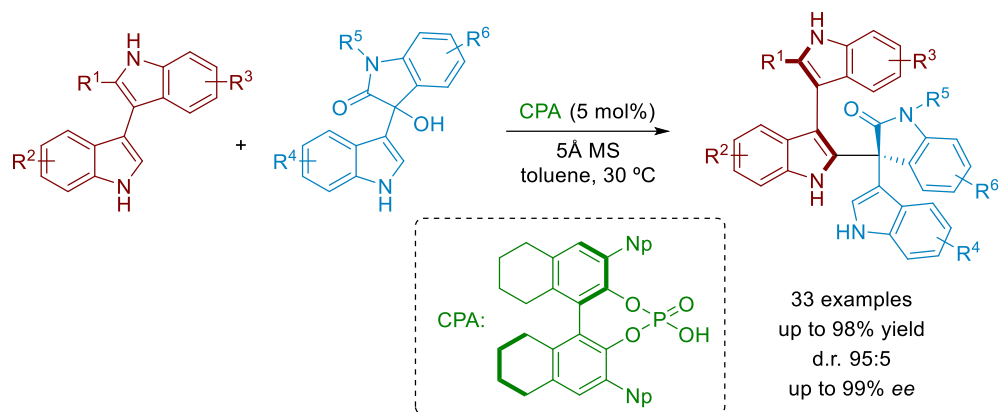
A very interesting contribution was reported in 2018 by the group of Cramer and co-workers, which developed a methodology for the synthesis of biaryl phosphine oxides bearing axial chirality and a *P*-stereogenic centre through an Ir-catalyzed C–H arylation reaction (Scheme I.43).⁷⁸ Depending on the structure of the substrates, the corresponding biaryls bearing only *P*- or axial chirality could also be accessed. Further reduction leads to chiral biaryl monodentate P-ligands with well-established importance in the field of asymmetric catalysis.



Scheme I.43 – Atropo-enantioselective C–H arylation methodology for the synthesis of *P*- and axially chiral biaryls.

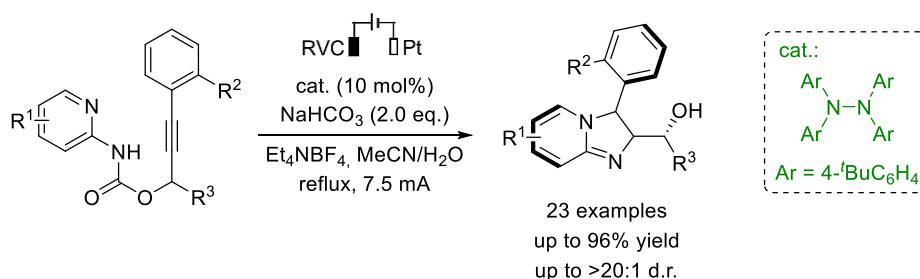
⁷⁸ Jang, Y.-S.; Woźniak, L.; Pedroni, J.; Cramer, N. *Angew. Chem. Int. Ed.* **2018**, *57*, 12901.

Additionally, the catalytic asymmetric construction of axially chiral 3,3'-bisindole skeletons has been published by the group of Shi (Scheme I.44).⁷⁹ These structures are present in many natural alkaloids and other biologically relevant compounds. The method represents the first organocatalyzed asymmetric construction of 3,3'-bisindole skeletons with both axial and central chirality.



Scheme I.44 – Asymmetric synthesis of 3,3'-bisindole skeletons bearing central and axial chirality.

In a different context, the electrochemically catalyzed cyclization cascade for the synthesis of imidazopyridine moieties bearing both central and axial chirality elements was also very recently reported by Xu et al. The method makes use of a reticulated vitreous carbon (RVC) anode and a platinum plate cathode (Scheme I.45).⁸⁰



Scheme I.45 – Atroposelective electrochemically induced cyclization developed by Xu's group.

⁷⁹ Ma, C.; Jiang, F.; Sheng, F.-T.; Jiao, Y.; Mei, G.-J.; Shi, F. *Angew. Chem. Int. Ed.* **2019**, *58*, 3014.

⁸⁰ Yan, H.; Mao, Z.-Y.; Hou, Z.-W.; Song, J.; Xu, H. *C. Beilstein J. Org. Chem.* **2019**, *15*, 795.

To conclude, the literature collected to cover the area of simultaneous generation of central and axial chirality elements in biaryl structures reveals a growing interest, with very recent contributions and many potential applications, but there is obviously need for additional developments, in particular for the synthesis of functionalized (hetero)biaryl skeletons with potential applications in Asymmetric Catalysis. In this PhD thesis, several strategies have been designed to accomplish this challenging goal.

I.5. Objectives.

The central objective of this PhD Thesis has been the development of catalytic methods that allow for the atroposelective synthesis of functionalized (hetero)biaryls using novel dynamization (racemization) strategies. Depending on the nature of the substrates, these methods can be classified as **DYKAT** (**DY**namic **K**inetic **A**symmetric **T**ransformations), if configurationally stable substrates are employed (Chapter II) or as **Dynamic Kinetic Resolutions (DKR)**, for the use of configurationally labile (hetero)biaryl derivatives (Chapters III and IV). In this context, we also aimed to take advantage of these strategies for the simultaneous generation of central and axial chirality elements in (hetero)biaryl structures, as highly functionalized (hetero)biaryl skeletons with potential applications as ligands for metal catalysis and organocatalysts. The specific objectives pursued along the Thesis are listed below:

- The development of a dynamic kinetic asymmetric Heck reaction using configurationally stable heterobiaryl sulfonates (Chapter II).
- The asymmetric hydrosilylation reaction of configurationally labile heterobiaryl ketones *via* dynamic kinetic resolution (Chapter III).
- The asymmetric Ru-catalyzed asymmetric transfer hydrogenation of biaryl aminals *via* dynamic kinetic resolution (Chapter IV).

CHAPTER II

*Dynamic Kinetic Asymmetric Heck
Reaction for the Simultaneous Generation
of Central and Axial Chirality*

Journal of the American Chemical Society **2018**, *140*, 11067.

II. Dynamic Kinetic Asymmetric Heck Reaction for the Synthesis of Heterobiaryls with Central and Axial Chirality.

II.1. Introduction: Palladium-catalyzed cross-coupling reactions.

Organic molecules are mainly formed by carbon-carbon bonds. In fact, the majority of synthetic Organic Chemistry challenges are related to the built up of complex structures from simpler molecules, which will, of course, involve the construction of carbon-carbon bonds.

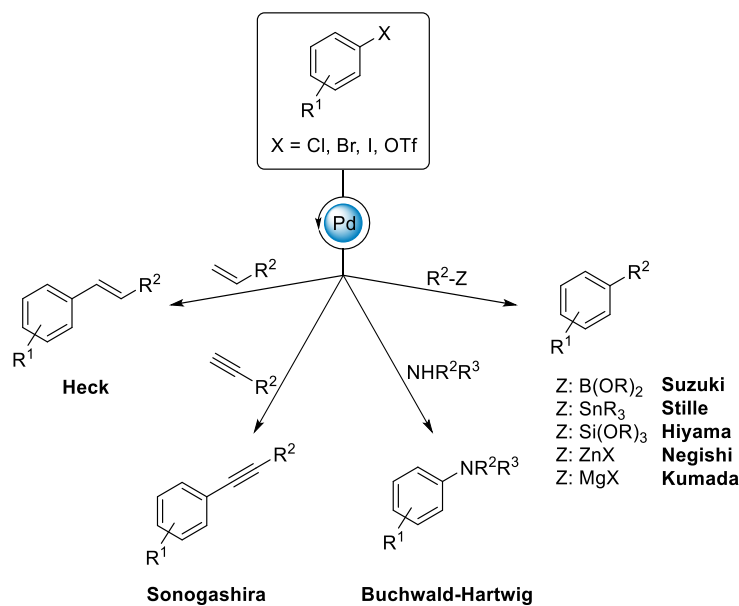
In this context, a very powerful methodology for the formation of C–C bonds consists on metal-catalyzed cross-coupling reactions. In general, these cross-coupling reactions take place between organic electrophiles, typically aryl (pseudo)halides, and different carbon nucleophiles catalyzed by transition metal complexes.

The huge importance of Pd-catalyzed cross-coupling reactions in the progress of modern chemistry was reflected when the pioneers of the development to this reactivity, Richard Heck, Akira Suzuki, Eiichi Negishi, were awarded with the Nobel Prize in Chemistry in 2010.⁸¹ Richard F. Heck first introduced these reactions in the late 1960s with the use of stoichiometric or catalytic amounts of palladium for the functionalization of olefins⁸². Since then, the inclusion of palladium as catalyst has provided an increasing number of remarkable reactions with an extraordinary potential and applicability in the field (Scheme II.1) that have been widely studied and developed during the last decades both in academic and industrial laboratories.⁸³

⁸¹ (a) Wu, X-F.; Anbarasan, P.; Neumann, H.; Beller, M. *Angew. Chem. Int. Ed.* **2010**, *49*, 9047. (b) Johansson Seechurn, C. C. C.; Kitching, M. O.; Colacot, T. J.; Snieckus, V. *Angew. Chem. Int. Ed.* **2012**, *51*, 5062.

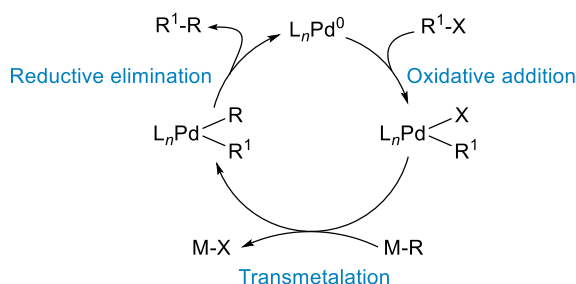
⁸² Heck, R. F. *J. Am. Chem. Soc.* **1968**, *90*, 5518.

⁸³ For a revision see: (a) Biffis, A.; Centomo, P.; Del Zotto, A.; Zecca, M. *Chem. Rev.* **2018**, *118*, 2249. (b) de Meijere, A.; Bräse, S.; Oestreich, M. (Eds.). (2014). *Metal-Catalyzed Cross-Coupling Reactions and more* (Vol. 1). Weinheim: Wiley-VCH. (c) Molnár, Á. (Ed). (2013). *Palladium-Catalyzed Coupling Reactions: Practical Aspects and Future Developments*. Weinheim: Wiley-VCH. (d) Xue, L.; Lin, Z. *Chem. Soc. Rev.* **2009**, *39*, 1692. (e) Nicolaou, K. C.; Bulger, P. G.; Sarlah, D. *Angew. Chem. Int. Ed.* **2005**, *44*, 4442.



Scheme II.1 – Palladium catalyzed cross-coupling reactions.

These cross-coupling reactions present a general reaction pathway with three common main steps: (a) Oxidative addition, (b) Transmetalation, and (c) Reductive elimination (Scheme II.2). Nonetheless, the Heck reaction presents additional peculiarities that will be explained further on.



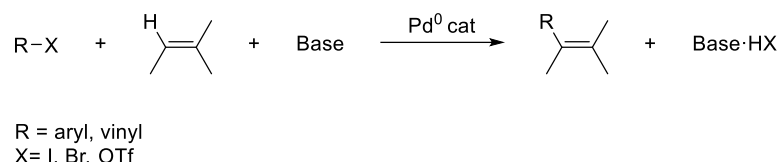
Scheme II.2 – Common reaction steps for the cross-coupling reactions.

As mentioned above, this chapter will focus on the dynamic kinetic asymmetric transformation of heterobiaryl sulfonates by an asymmetric Heck reaction. This reaction is also known as the Mizoroki-Heck reaction, since Mizoroki first found out this reactivity, although he could not continue his research because of his early death.

II.2. Introduction: The Mizoroki-Heck reaction.

II.2.1. Precedents.

In the early 1970's Mizoroki⁸⁴ and Heck⁸⁵ independently reported the first examples of palladium-catalyzed arylation or alkenylation of alkenes.



Scheme II.3 – General scheme for the Mizoroki-Heck reaction.

This methodology, referred to as the Mizoroki-Heck reaction (from now on, Heck reaction), consists on a fundamental palladium-catalyzed C–C bond-forming transformation with numerous applications in the synthesis of natural products and valuable synthetic intermediates. It also provides the most efficient route for the vinylation of aryl/vinyl halides or triflates in the presence of a base.⁸⁶ It has drawn much attention due to its high efficiency and simplicity; this methodology is very attractive from a synthetic perspective due to its extraordinary chemoselectivity and mild reaction conditions together with the low toxicity and relatively low cost of the reagents involved.

Surprisingly, the first asymmetric version had to wait until 1989, when the groups of Shibasaki⁸⁷ and Overman⁸⁸ independently developed the first examples of intramolecular asymmetric Heck reaction (Scheme II.4A). Few years later, Hayashi and co-workers also reported the first intermolecular asymmetric variant (Scheme II.4B).⁸⁹

⁸⁴ Mizoroki, T.; Mori, K.; Ozaki, A. *Bull. Chem. Soc. Jpn.* **1971**, *44*, 581.

⁸⁵ Heck, R. F.; Nolley, J. P. *J. Org. Chem.* **1972**, *37*, 2320.

⁸⁶ (a) Heck, R. F., *Acc. Chem. Res.*, **1979**, *12*, 146. (b) *The Mizoroki-Heck Reaction*; Oestreich, M., Ed.; Wiley: New York, **2009**. (c) Braše, S.; de Meijere, A. In *Metal-Catalyzed Cross-Coupling Reactions*; de Meijere, A.; Bräse, S.; Oestreich, M., Eds.; Wiley-VCH: Weinheim, **2014**; pp 533-633.

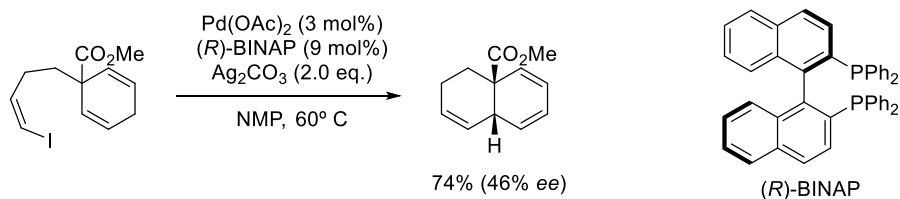
⁸⁷ Sato, Y.; Sodeoka, M.; Shibasaki, M. *J. Org. Chem.* **1989**, *54*, 4738.

⁸⁸ Carpenter, N. E.; Kucera, D. J.; Overman, L. E. *J. Org. Chem.* **1989**, *54*, 5846.

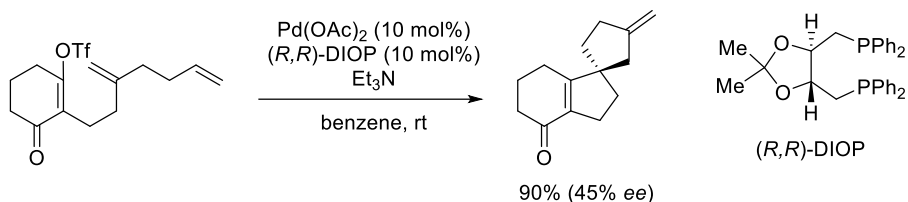
⁸⁹ Ozawa, F.; Kulbo, A.; Hayashi, T. *J. Am. Chem. Soc.* **1991**, *113*, 1417.

A) Seminal asymmetric Heck reaction

Shibasaki et al. (1989)

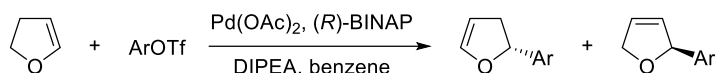


Overman et al. (1989)



B) Seminal intermolecular asymmetric Heck reaction

Hayashi et al. (1991)



Scheme II.4 – First examples for intra- and intermolecular asymmetric Heck reaction.

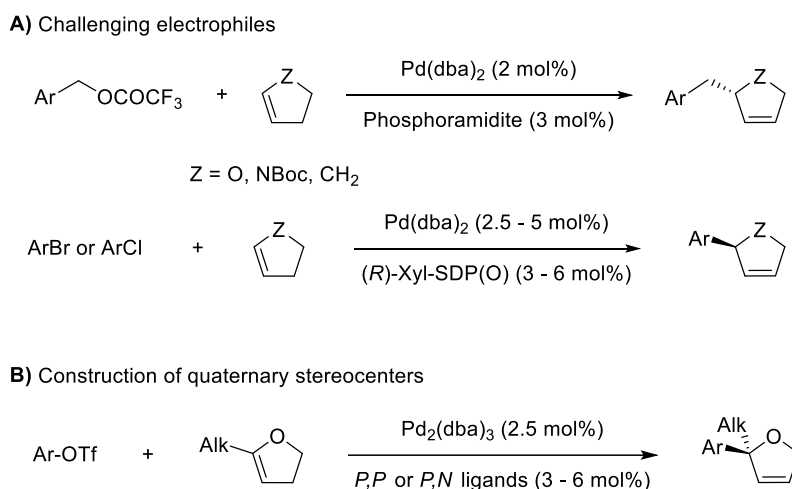
It should be noted that, despite its high potential, this coupling reaction has been often employed as a benchmark to validate the design of novel chiral ligands and catalysts rather than finding suitable applications in stereoselective organic synthesis.⁹⁰ Only very recently, the synthetic utility of the asymmetric Heck reaction has been exploited because of the outstanding performance of chiral mixed phosphine/phosphine oxide ligands in several representative transformations.⁹¹

⁹⁰ (a) Loiseleur, O.; Hayashi, M.; Keenan, M.; Schmees, N.; Pfaltz, A. *J. Organomet. Chem.* **1999**, 576, 16. (b) Tietze, L. F.; Ila, H.; Bell, H. P. *Chem. Rev.* 2004, 104, 3453. (c) McCartney, D.; Guiry, P. J. *Chem. Soc. Rev.* **2011**, 40, 5122. (d) Shibasaki, M.; Vogl, E. M.; Ohshima, T. *Adv. Synth. Catal.* **2004**, 346, 1533.

⁹¹ (a) Wöste, T. H.; Oestreich, M. *Chem. Eur. J.* **2011**, 17, 11914. (b) Hu, J.; Hirao, H.; Li, Y.; Zhou, J. *Angew. Chem. Int. Ed.* **2013**, 52, 8676. (c) Hu, J.; Lu, Y.; Li, Y.; Zhou, J. *Chem. Commun.* **2013**, 49, 9425.

Additionally, the group of Zhou expanded the scope of the intermolecular Heck reaction. They developed new strategies to enable the use of previously elusive substrates such as benzylic electrophiles⁹² or aryl halides⁹³ in asymmetric intermolecular Heck reactions, overcoming the difficulty of displacing a halide with a neutral olefin on Pd centres (Scheme II.5A).

Moreover, the groups of Hou⁹⁴ and Mazet⁹⁵ independently developed methodologies for the construction of quaternary stereocenters from trisubstituted dihydrofurans in high yields and excellent enantioselectivities using an asymmetric Heck reaction (Scheme II.5B). So far, the only previous report for an asymmetric Heck reaction of 5-methyl-2,3-dihydrofuran with PhOTf afforded the corresponding Heck product in 38% yield and 98% *ee*.⁹⁶



Scheme II.5 – Asymmetric Heck reaction with challenging substrates for the construction of tertiary and quaternary stereocentres.

⁹² Yang, Z.; Zhou, J. *J. Am. Chem. Soc.* **2012**, *134*, 11833.

⁹³ Wu, C.; Zhou, J. *J. Am. Chem. Soc.* **2014**, *136*, 650.

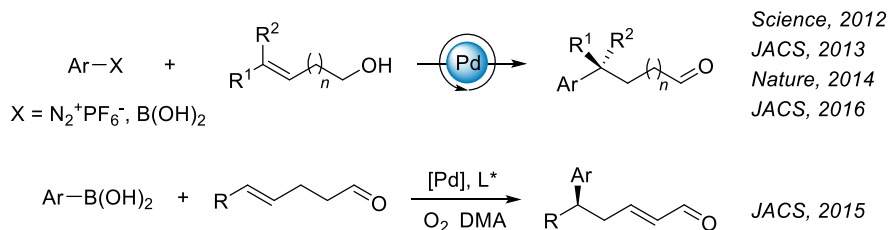
⁹⁴ Zhang, Q.-S.; Wan, S.-L.; Chen, D.; Ding, C.-H.; Hou, X.-L. *Chem. Commun.* **2015**, *51*, 12235.

⁹⁵ Borrajo-Calleja, G. M.; Bizet, V.; Bürgi, T.; Mazet, C. *Chem. Sci.* **2015**, *6*, 4807.

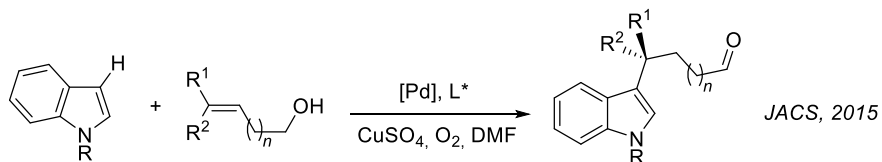
⁹⁶ Tschoerner, M.; Albinati, A.; Pregosin, P. S. *Organometallics*, **1999**, *18*, 670.

In 2012, the group of Sigman developed a redox-relay Heck reaction where the relay by palladium is controlled by a thermodynamic sink (an alcohol) on the substrate.⁹⁷ The unsaturation of the alkene is transferred to the alcohol to form aldehydes or ketones. This method installs stereogenic centers in remote positions from the resulting carbonyl group, thus expanding the synthetic value of the Heck reaction. The strategy was also extended by Sigman's group to oxidative Heck reaction using boronic acids⁹⁸ as reactants, allowing for the synthesis of quaternary stereocentres and α,β -unsaturated carbonyls with an stereocentre at δ position (Scheme II.6A). Additionally, the same group developed an enantioselective dehydrogenative redox-relay Heck reaction for the synthesis of indoles functionalized with quaternary stereocentres (Scheme II.6B).⁹⁹

A) Redox-relay enantioselective Heck arylations



B) Dehydrogenative enantioselective redox-relay Heck reaction



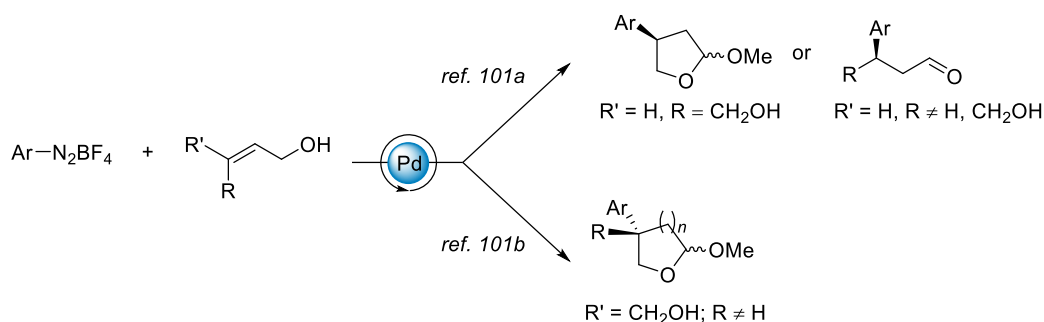
Scheme II.6 – Sigman's contribution to redox-relay Heck reaction.

⁹⁷ Werner, E. W.; Mei, T.-S.; Burckle, A. J.; Sigman, M. S. *Science* **2012**, 338, 1455

⁹⁸ (a) Mei, T.-S.; Werner, E. W.; Burckle, A. J.; Sigman, M. S. *J. Am. Chem. Soc.* **2013**, 135, 6830. (b) Mei, T.-S.; Patel, H. H.; Sigman, M. S. *Nature* **2014**, 508, 340. (c) Zhang, C.; Santiago, C. B.; Kou, L.; Sigman, M. S. *J. Am. Chem. Soc.* **2015**, 137, 7290. (d) Chen, Z. M.; Hilton, M. J.; Sigman, M. S. *J. Am. Chem. Soc.* **2016**, 138, 11461.

⁹⁹ Zhang, C.; Santiago, C. B.; Crawford, J. M.; Sigman, M. S. *J. Am. Chem. Soc.* **2015**, 137, 15668

At the same time, Correia's group extended this redox-relay methodology to Heck-Matsuda¹⁰⁰ reactions with alkenyl alcohols for the synthesis of heterocycles functionalized with tertiary or quaternary stereocentres (Scheme II.7).¹⁰¹



Scheme II.7 – Redox-relay enantioselective Heck-Matsuda reaction developed by Correia's group.

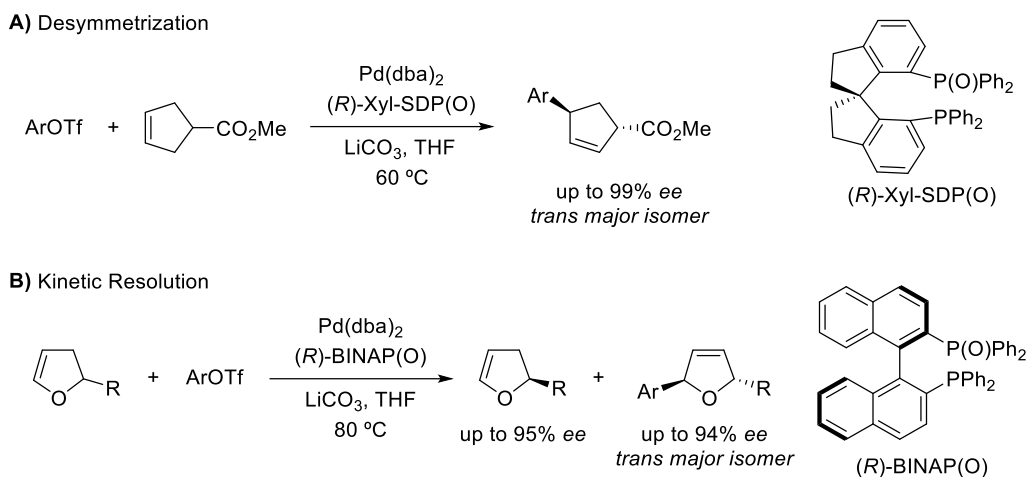
It is also worth to mention the desymmetrization of substituted cyclopentenes *via* an asymmetric Heck reaction developed by Zhou and co-workers, a process that was stereoselective only when a (bis)phosphine monoxide ligand was employed, providing the *trans* disubstituted cyclopentenes in high selectivities (Scheme II.8A).¹⁰² This family of ligands was also studied by the group of Hou for the kinetic resolution of 2-substituted-2,3-dihydrofurans *via* Pd-catalyzed asymmetric Heck reaction, leading to optically active 2-substituted-dihydrofurans and *trans*-2,5-disubstituted dihydrofurans in high yield and good enantioselectivities (Scheme II.8B).¹⁰³

¹⁰⁰ Kikukawa, K.; Matsuda, T. *Chem. Lett.* **1977**, 6, 159.

¹⁰¹ (a) Oliveira, C. C.; Angnes, R. A.; Correia, C. R. D. *J. Org. Chem.* **2013**, 78, 4373. (b) Oliveira, C. C.; Pfaltz, A.; Correia, C. R. D. *Angew. Chem., Int. Ed.* **2015**, 54, 14036. (c) Kattela, S.; Heerdt, G.; Correia, C. R. D. *Adv. Synth. Catal.* **2017**, 359, 260.

¹⁰² Liu, S.; Zhou, J. *Chem. Commun.* **2013**, 49, 11758.

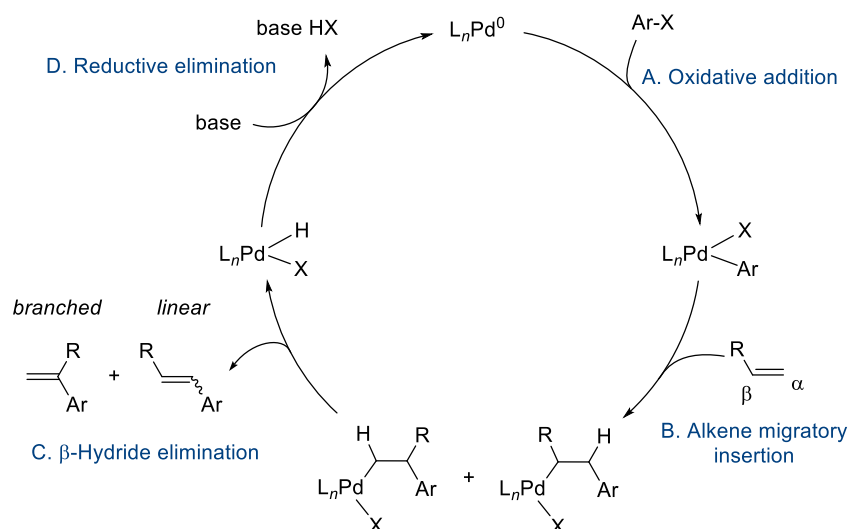
¹⁰³ Li, H.; Wan, S.-L.; Ding, C.-H.; Xu, B.; Hou, X.-L. *RSC Adv.* **2015**, 5, 75411.



Scheme II.8 – Strategies for the desymmetrization and kinetic resolution of substituted cyclic alkenes based on a Pd-catalyzed asymmetric Heck reaction.

II.2.2. Mechanism of the Heck reaction

As mentioned above, the Heck reaction presents some important mechanistic differences with respect to other cross-coupling reactions. All of them start with an oxidative addition step affording a common aryl palladium(II) intermediate. However, the next steps are different. In cross-coupling reactions, where stronger nucleophiles are commonly used, the substitution of the halide atom in the coordination sphere occurs via a neutral pathway. In Heck reactions, however, the weaker alkene nucleophile cannot directly substitute the halide, and there are consequently two possibilities for the reaction to proceed. One of them is to substitute a neutral ancillary ligand involving a prior dissociation of an hemilabile ligand (neutral pathway) and the second is to abstract the halide from the cationic palladium(II) with the help of a halide scavenger (cationic pathway).



Scheme II.9 – General catalytic cycle for the Heck reaction.

Furthermore, the catalytic cycle for the Heck reaction does not proceed through a transmetalation step since there is no carbon-metal bond, and thus, *syn*-addition (insertion) and β -hydride elimination take place instead (Scheme II.9).^{83c}

Details for these elemental steps are given below.

A. Oxidative addition

The first step of the catalytic cycle consists on an oxidative addition of the aryl halide to the 14 electrons $Pd(0)$ source, providing the 16 electrons $Pd(II)$ intermediates with square planar geometry. Often this is the rate determining step, and follows the next reactivity trend depending on the halide employed: $ArI > ArOTf > ArBr \gg ArCl$.^{83b,104} This order of reactivity has also been experimentally observed through the Hammett parameter of the corresponding aryl halides to $Pd(0)$ species, and can be related to the reactivity of this halides towards oxidative addition.¹⁰⁵ When strong σ -donor ligands like phosphines or *N*-heterocyclic carbenes (NHCs) are employed, this step can also be

¹⁰⁴ Jutand, A.; Négri, S.; de Vries, J. G. *Eur. J. Inorg. Chem.* **2002**, 7, 1711.

¹⁰⁵ Knowles, J. P.; Whiting, A. *Org. Biomol. Chem.* **2007**, 5, 31.

accelerated, since the additional electron density provided by such ligands facilitates the oxidation of the metal.

B. Alkene migratory insertion

After oxidative addition, the *trans*-ArPdXL₂ intermediate is ready for coordination and insertion of the alkene in the Pd–Ar bond in a *syn* manner. As mentioned above, this step can proceed over two different routes, (i) cationic pathway or (ii) neutral pathway (Scheme II.10).¹⁰⁶

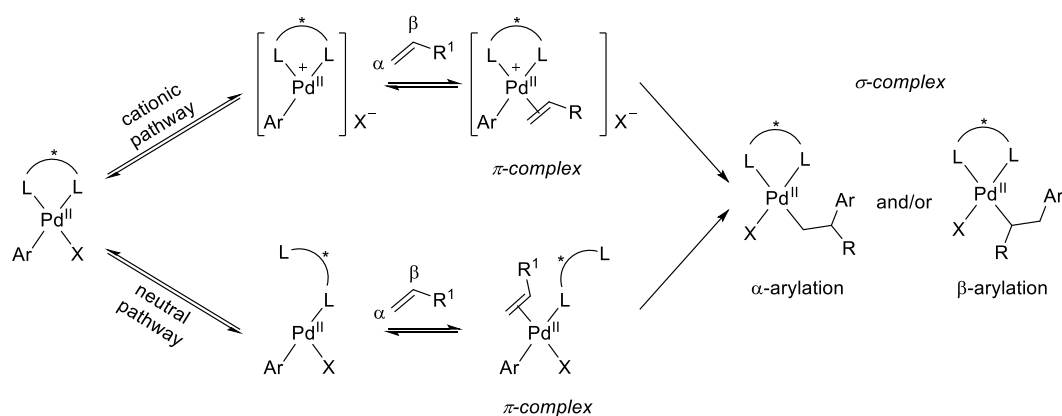
- (i) Cationic pathway: takes place if there is a (pseudo)halide that detaches the metal centre, thus leaving a coordination vacant site on the metal. It occurs when poorly coordinating pseudohalides (i.e. OTf, OAc) are employed or halide abstractors (i.e. Ag or Tl salts) are added. Since the chiral bidentate ligand remains fully coordinated, the chances for a good asymmetric induction are increased.
- (ii) Neutral pathway: in this case, there is a dissociation of one ligand prior the insertion of the alkene. It is favoured by the use of strong σ -donor halides acting as ligands. In contrast to the cationic route, the dissociation of one chelating arm of the ligand tends to result in a lower asymmetric induction in the final products.

This step is crucial with respect to enantioselectivity and therefore, the nature of X in Ar–X (and consequently the Pd–X bond strength in the oxidative addition intermediate) is an important factor.

The nature of the alkene is also a relevant aspect to consider: for electron poor olefins, which are weaker nucleophiles, it is easier to displace a neutral ancillary ligand rather than the halide and therefore the neutral pathway is facilitated; while the stronger nucleophilicity of electron-rich olefins favours the cationic route, ensuring that the

¹⁰⁶ Deeth, R. J.; Smith, A.; Brown, J. M. *J. Am. Chem. Soc.* **2004**, 126, 7144.

displacement of halide could be afforded.¹⁰⁷ As mentioned above, the cationic pathway gives rise to higher levels of enantioselectivity in general terms and, therefore electron rich alkenes are more suitable for the asymmetric Heck reaction.



Scheme II.10 – Cationic vs neutral alkene insertion pathways.

The next step after alkene coordination (π -complex) consists on the insertion of the olefin into the Ar–Pd bond.

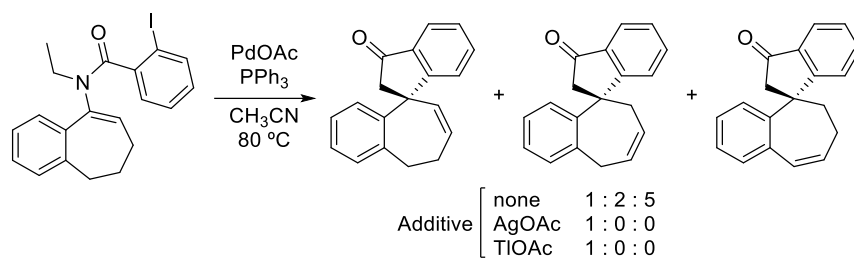
This step controls the regioselectivity of the Heck reaction, since two isomeric σ -complexes can be formed depending on an α or β arylation of the alkene, further leading to the branched or linear arylated alkene, respectively, after the β -hydride elimination step. (Scheme II.10). The nature of π -complex is crucial in this aspect; a cationic π -complex leads to an increase of the polarization at the Pd–Ar bond and a selective migration of the aryl moiety (formally acting as anion) occurs at the more electrophilic carbon from the alkene, thus, leading preferentially to α -arylation and further branched product.¹⁰⁸

C. β -Hydride elimination

This step leads to the final product. As occurred with the alkene insertion, β -hydride elimination is a *syn* process, so an internal C–C bond rotation in the σ -

¹⁰⁷ Cabri, W.; Candiani, I.; DeBernardinis, S.; Francalanci, F.; Penco, S.; Santi, R. *J. Org. Chem.* **1991**, *56*, 5796.

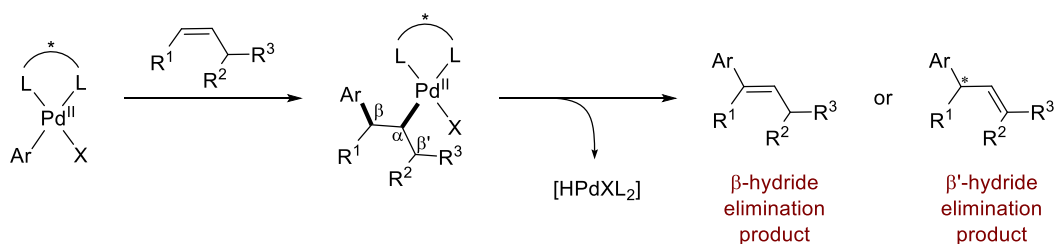
¹⁰⁸ (a) Cabri, W.; Candiani, I. *Acc. Chem. Res.* **1995**, *28*, 2. (b) Andappan, M. M. S.; Nilsson, P.; von Schenck, H.; Larhed, M. *J. Org. Chem.* **2004**, *69*, 5212.



Scheme II.12 – Effect of halide abstractor additives in double bond migration.

(Bis)phosphine oxides can also help to increase selectivity since they are poorer σ -donor ligands and result in more electron-deficient, cationic Pd centres. This fact facilitates a fast deprotonation of Pd–H species versus olefin insertion, essential to regenerate Pd(0) species and minimize double bond migration.¹¹⁰

Another problem in terms of regioselectivity may occur during this step when acyclic olefins are used, due to the possible β - and β' -hydride elimination competition leading to isomeric products (Scheme II.13).

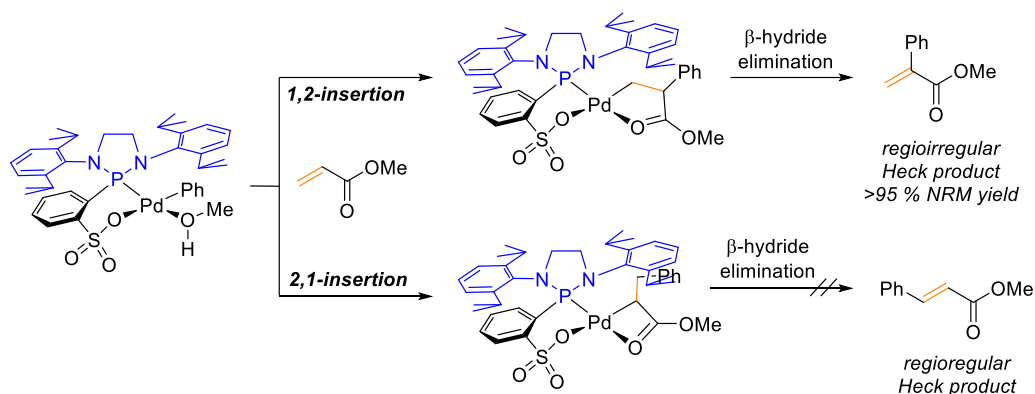


Scheme II.13 – Competing β - and β' -hydride elimination products.

Most of the reported Heck reactions employ simple biased acrylate esters as substrates to prevent this competition. These acrylate esters present a high unsymmetrical steric and electronic environment, helping to prevent also regioselectivity issues during alkene migratory insertion step. As the main drawback, these systems present a limitation for the generation of either tertiary or quaternary chiral stereocentres because of the suppression of β' -hydride elimination pathway.^{90d} Remarkably, regarding the arylation of

¹¹⁰ (a) Hills, I. D.; Fu, G.; *J. Am. Chem. Soc.* **2004**, 126, 13178. (b) Wheatley, B. M. M.; Keay, B. *A. J. Org. Chem.* **2007**, 72, 7253.

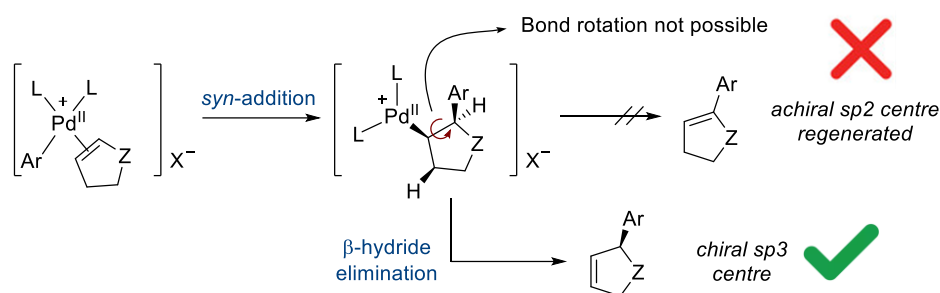
these simple acrylate esters, there is one precedent in the literature in which the regioselectivity can be inverted by the introduction of structural modifications at the ligand to destabilize the transition state for the 2,1-insertion *via* steric repulsions. In this way, the regioselectivity of the insertion of methyl acrylate into the Pd–C(Ph) bond can be inverted entirely to yield the opposite (*regioirregular*) products in stoichiometric reactions (Scheme II.14).¹¹¹



Scheme II.14 – Selective formation of regioirregular Heck products by catalyst design.

An additional problem for the generation of a stereogenic centre is that the sp^3 carbon formed in the migratory *syn*-insertion step could be converted back to an sp^2 centre after β -hydride elimination. However, since this is a *syn*-process, the hydrogen atom at this sp^3 centre is not *syn* to Pd, so that the β -hydride elimination can only take place towards the opposite position. Therefore, a chiral centre would be generated at the arylated position. This situation applies for endocyclic alkenes, as the hydrogen at the functionalised sp^3 centre will always be *anti* to the Pd, and an internal C–C bond rotation of the Pd intermediate species is not feasible (Scheme II.15).

¹¹¹ Wucher, P.; Caporaso, L.; Roesle, P.; Ragone, F.; Cavallo, L.; Mecking, S.; Göttker-Schnetmann, I. *Proc Natl Acad Sci USA* **2011**, *108*, 8955.

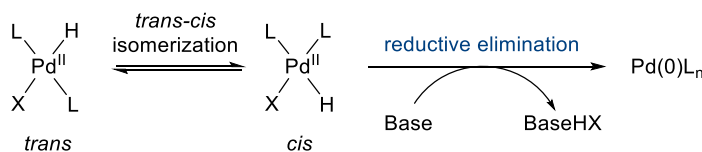


Scheme II.15 – Generation of chiral sp^3 centres in asymmetric Heck reactions with endocyclic alkenes.

D. Reductive elimination

It could be seen as the opposite to oxidative addition, and represents the last step of the catalytic cycle. After dissociation from the arylated alkene, the hydridopalladium(II) halide undergoes a reductive elimination to regenerate the catalytically active Pd(0) complex. Despite this process could be thought as a direct elimination to generate hydrogen halide and above mentioned Pd(0) complex, it can also be promoted by a base. Actually, in 1998, Brown and co-workers demonstrated through DFT studies that the base-promoted elimination was more energetically favoured than the mechanism that considers a direct reductive elimination.¹¹²

The groups to be eliminated need to be *cis* positioned. So, if they present a *trans* arrangement, a previous isomerization of the XL_nPdH complex has to take place prior to the reductive elimination step (Scheme II.16).



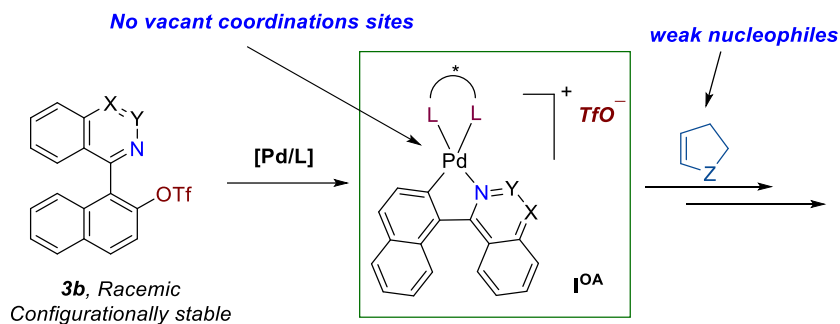
Scheme II.16 – XL_nPdH complex *trans-cis* isomerization.

¹¹² Deeth, R. J.; Smith, A.; Hii, K. K.; Brown, J. M. *Tetrahedron Lett.* **1998**, 39, 3229.

II.3 Results and discussion.

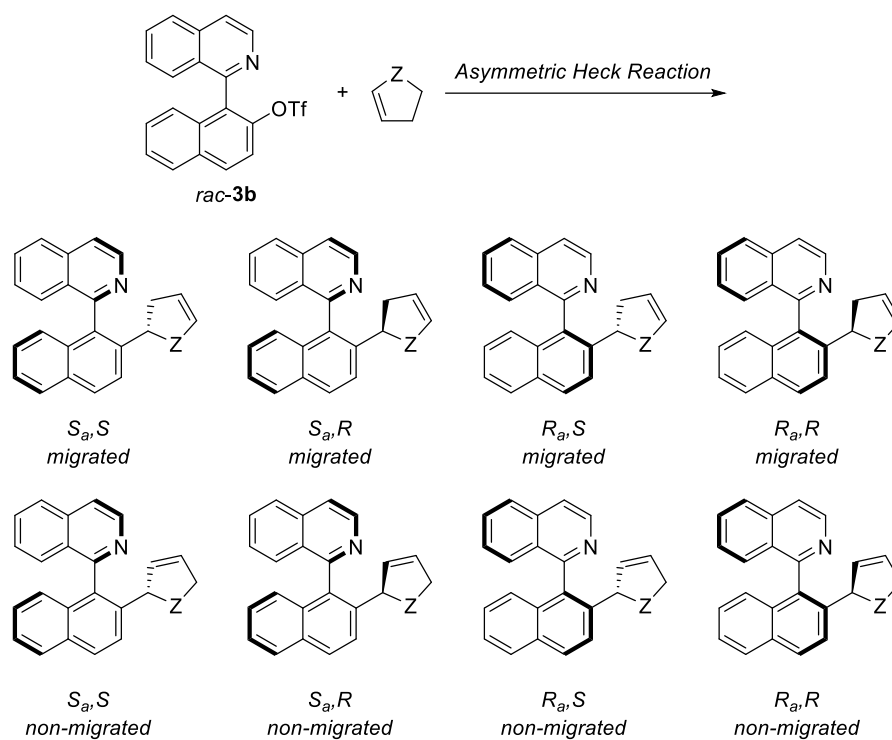
In this context, an asymmetric Heck reaction combined with the dynamic kinetic asymmetric transformation strategy (see Chapter I), envisioned in the frame of our interest in the synthesis of functional axially chiral heterobiaryls, appears as an appealing strategy for the synthesis of derivatives with central and axial stereogenic elements. This transformation, however, is particularly challenging for two main reasons.

First, when an heterobiaryl sulfonate such as **3b** is used as substrate, the oxidative addition intermediate (**I^{OA}**) has no vacant coordination sites, in contrast with the common cationic Heck reaction pathway. This happens because the relatively good isoquinoly/pyridyl *N* ligand displaces the poor coordinating triflate/nonaflate, leading to a relatively stable palladacyclic intermediate. Now this good *N*-ligand must be further displaced by a neutral olefin on the Pd(II) centre (Scheme II.17).



Scheme II.17 – Main problems raised from the present hypothesis.

A second potential problem is that the reaction with endocyclic olefins can afford up to eight different Heck isomeric products considering the formation of two stereogenic elements and the possible double bond migration (Scheme II.18); a formidable challenge from the perspective of stereocontrol.



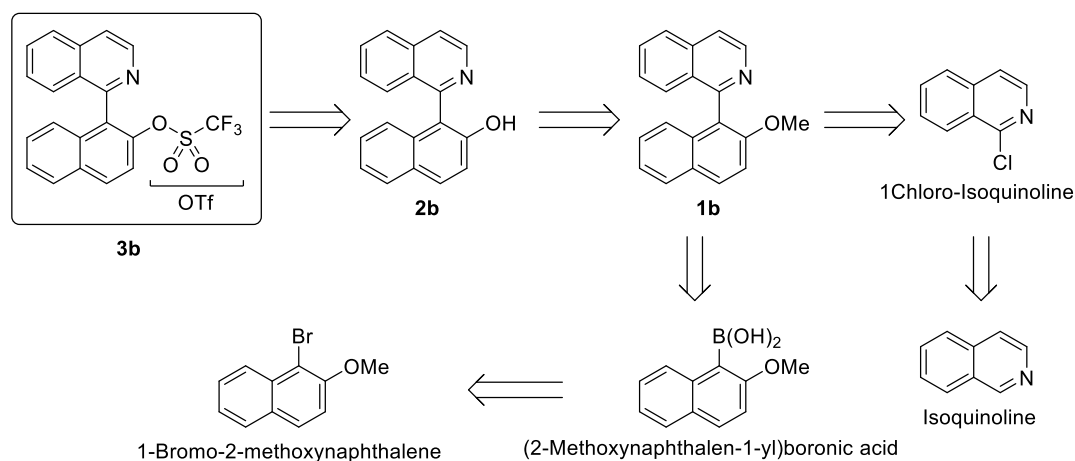
Scheme II.18 – The possible isomeric products of the reaction between **3b** and 5-membered endocyclic alkenes.

Therefore, the choice of the chiral ligand and reaction conditions will be decisive to control the stereoselectivity of a single isomer, or at least, to minimize stereodiversity.

From here on, all the experimental work carried out for this chapter, as well as the conclusions obtained will be detailed and discussed.

II.3.1. Synthesis of starting materials

This chapter deals with the study of a dynamic kinetic asymmetric Heck reaction using racemic heterobiaryl sulfonates. Therefore, the first point to detail must be the synthesis of these substrates and their precursors. A retrosynthetic analysis of these structures suggests that the route displayed on Scheme II.19 should be followed.

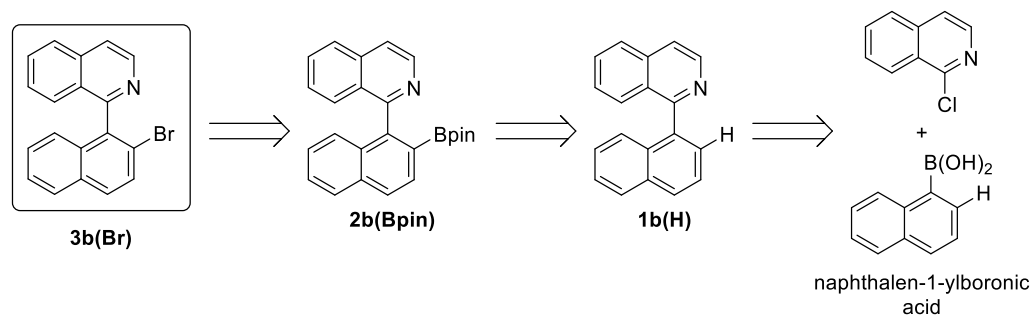


Scheme II.19 – Retrosynthetic analysis for accessing naphthylisoquinoline triflate **3b**.

Nevertheless, the synthesis of the majority of these heterobiaryl sulfonates have been previously described in literature,^{62,64,66} and therefore, the corresponding procedures were extended to synthesize the non-described substrates and precursors.

For mechanistic considerations (*vide infra*), the heterobiaryl bromide **3b(Br)** has been employed instead of sulfonate **3b**, and the synthetic route was different. In this case, the boronic acid coupling partner was not *ortho*-substituted with a methoxy group, but a hydrogen atom. After Suzuki cross-coupling reaction, the resulting product was subjected to nitrogen-directed iridium-catalyzed borylation, following a methodology previously developed by our group,¹¹³ and further treatment with copper(II) bromide, to afford the desired heterobiaryl bromide **3b(Br)** (Scheme II.20).

¹¹³ Ros, A.; Estepa, B.; López-Rodríguez, R.; Álvarez, E.; Fernández, R.; Lassaletta, J. M. *Angew. Chem. Int. Ed.* **2011**, 50, 11724.

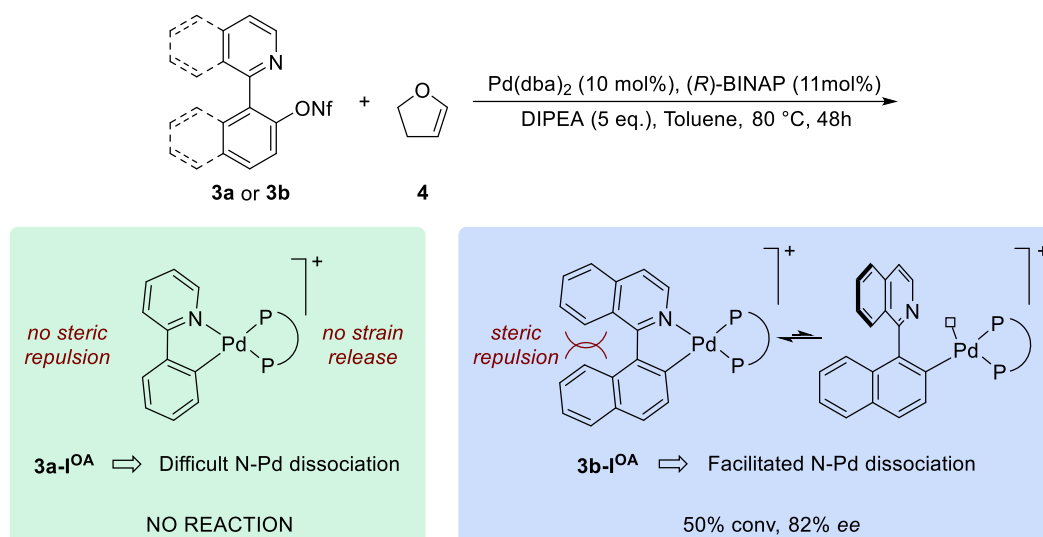


Scheme II.20 – Retrosynthetic analysis for accessing naphthylisoquinoline bromide **3b(Br)**.

II.3.2. Preliminary studies

In a preliminary experiment, it was observed that the reaction of 2-(pyridin-2-yl)phenyl nonaflate **3a** and 2,3-dihydrofuran **4** provides no reaction product under common asymmetric Heck conditions [$\text{Pd}(\text{dba})_2/(R)\text{-BINAP}$, DIPEA, toluene, 80 °C] (Scheme II.21). This fact confirmed our initial concerns of a difficult displacement of the pyridine N atom by a neutral olefin. It was assumed that, in this case, when $R = R' = \text{H}$, a very stable oxidative addition cationic palladacycle intermediate **3a-I^{OA}** is formed, which does not dissociate to allow coordination of the olefin and further migratory insertion. This hypothesis was confirmed when the same experiment was performed using stoichiometric amounts of Pd-catalyst, and ^{31}P -NMR analysis of reaction mixture showed mainly the presence of two doublets at 41.1 ppm and 14.7 ppm ($J = 47.0$ Hz), corresponding to the unsymmetrical phosphine ligands on **I^{OA}**.

Despite this discouraging result, we anticipated that the use of 1-(isoquinolin-1-yl)naphthalene-2-yl nonaflate **3b**, would result in a more strained **3b-I^{OA}** palladacycle. In contrast with **3a-I^{OA}** this would no longer constitute a thermodynamic sink, and dissociation of the N-Pd bond would be favoured by release of that steric strain (Scheme II.21). In fact, the reaction of **3b** and **4** under the same conditions provided the desired product as a 10:1 mixture of regioisomers **5b:5'b** (from here on, this ratio would be referred as to S factor), and a promising 82% *ee* for the major isomer **5b** (entry 6, Table II.1).



Scheme II.21 – Preliminary experiments. Proof of concept.

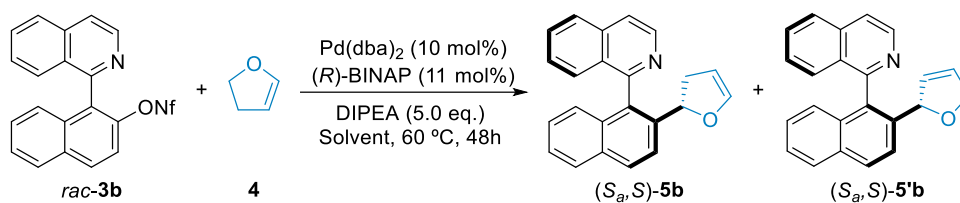
II.3.3. Dynamic kinetic asymmetric Heck reaction with cyclic alkenes

With the confirmed proof of concept in hands, we then moved to optimize the methodology. 2,3-Dihydrofuran **4** is by far the most employed cyclic olefin when a new ligand, catalyst or substrate has to be studied in an asymmetric intermolecular Heck reaction.^{91a,114} Therefore, the asymmetric alkenylation of 1-(isoquinolin-1-yl)naphthalene-2-yl nonaflate **3b** with **4** was selected as the model reaction in order to study the optimization of the reaction parameters.

Initially, we explored the influence of the anhydrous solvent to find the best one in terms of reactivity and selectivity, maintaining constant [Pd(dba)₂]/(R)-BINAP] as catalyst, and DIPEA as base, at 60 °C (Table II.1).

¹¹⁴ For a recent revision, see: (a) Oestreich, M. *Angew. Chem., Int. Ed.* **2014**, *53*, 2282. (b) Rubina, M.; Sherrill, W. M.; Barkov, A. Y.; Rubin, M. *Beilstein J. Org. Chem.* **2014**, *10*, 1536.

Table II.1 – Solvent screening.

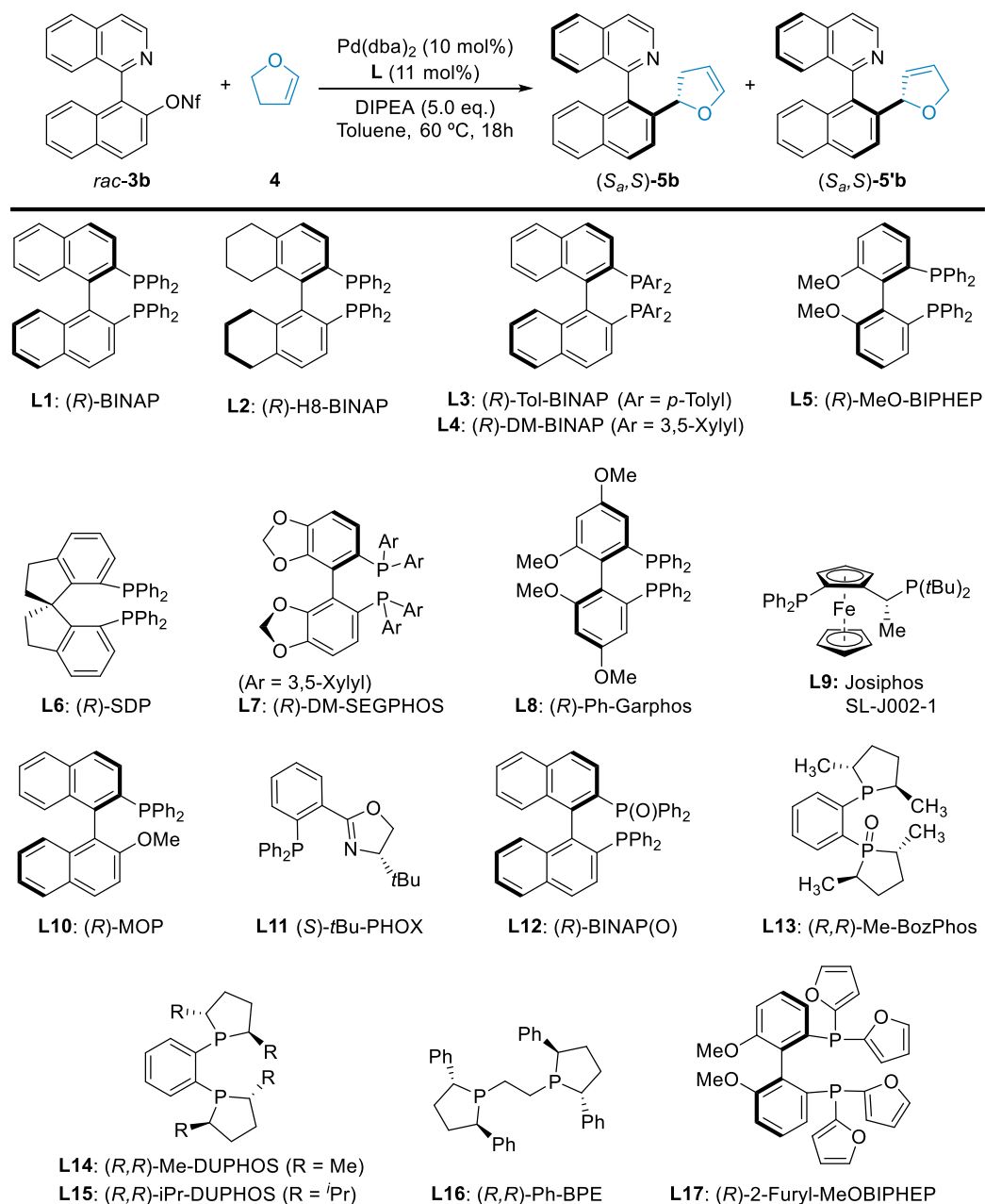


Entry ^a	Solvent	Conv (%) ^b	S (5b : 5'b) ^b	ee (%) ^c
1	1,4-Dioxane	15	n.d.	n.d.
2	DMSO	26	3:1	n.d.
3	MeOH	<5	n.d.	n.d.
4	DMF	25	5:1	n.d.
5	Toluene	28	6:1	88
6^d	Toluene	50	10:1	82

^a Reaction performed at 0.1 mmol of *rac*-**3b** and 0.8 mmol of **4**. ^b Determined by ¹H-NMR spectroscopy. ^c Determined by chiral HPLC analysis. ^d Reaction temperature: 80 °C.

From the screening of solvents, it is clear that toluene provides the best results in general terms (entries 5 and 6, Table II.1). Next, using toluene as solvent, a variety of commercially available ligands often employed in the asymmetric Heck reaction were tested, and the results were analysed after 18h (Table II.2).

Table II.2 – Commercial ligands screening.



Entry ^a	Ligand (L)	Conv (%) ^b	S (5b:5'b) ^b	ee (%) ^c
1	(R)-H8-BINAP (L2)	27	11:1	82
2	(R)-Tol-BINAP (L3)	16	8:1	96
3	(R)-DM-BINAP (L4)	22	6:1	99
4	(R)-MeO-BIPHEP (L5)	11	n.d.	n.d.
5	(R)-SDP (L6)	n.r.	n.d.	n.d.
6	(R)-DM-SEGPHOS (L7)	19	7:1	n.d.
7	(R)-Ph-Garphos (L8)	7	n.d.	n.d.
8	SL-J002-1 (L9)	<5	n.d.	n.d.
9	(R)-MOP (L10)	40	>1:20	13
10	(S)- <i>t</i> Bu-PHOX (L11)	<5	n.d.	n.d.
11	(R)-BINAP(O) (L12)	<5	n.d.	n.d.
12	(R,R)-Me-BozPhos (L13)	<5	n.d.	n.d.
13	(R,R)-Me-DUPHOS (L14)	52	>20:1	89
14	(R,R)- <i>i</i> Pr-DUPHOS (L15)	5	n.d.	n.d.
15	(S,S)-Ph-BPE (L16)	n.r.	n.d.	n.d.
16	(R)-2-Furyl-MeOBIPHEP (L17)	5	n.d.	n.d.

^a Reaction performed at 0.1 mmol of *rac*-3b and 0.8 mmol of 4. ^b Determined by ¹H-NMR spectroscopy. ^c Determined by chiral HPLC analysis.

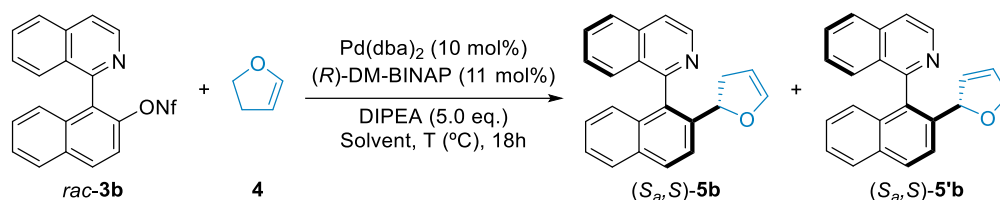
Interestingly, BINAP derivatives provided the best results in terms of selectivities (entries 1 to 3, Table II.2). In particular, (R)-DM-BINAP gave excellent enantiomeric excess of 5b and a good 5b:5'b selectivity, although the conversion remained low.

No improvements were observed using related P,P ligands (entries 4 to 7, Table II.2), while Josiphos derivative L9 was unproductive (entry 8, Table II.2). Not surprisingly, hemilabile ligand L10 afforded the non-isomerized Heck product 5'b exclusively with high regioselectivity, although in low ee (entry 9, Table II.2). Remarkably, ligands L11, L12 or L13 were ineffective (entries 10 to 12, Table II.2), even though less σ -donating P,N and P,O ligands might favour a faster alkene insertion due to the more electrophilic character of the cationic palladium(II) centres. In this case, however, a stronger binding of the

isoquinoline nitrogen caused by the higher electrophilicity of cationic Pd(II) species, would prevent further coordination of the olefin. Although (*R,R*)-Me-DUPHOS **L14** showed higher reactivity, the enantioselectivity suffered a slight decrease (entry 13, Table II.2).

As mentioned above, (*R*)-DM-BINAP was identified from this screening as the most promising ligand in terms of enantioselectivity. Therefore, other reaction parameters were modified in order to improve the reactivity and regioselectivity, using this ligand (Table II.3).

Table II.3 – Optimization of other reaction parameters.



Entry ^a	Solvent/T (°C)	Other variations	Conv (%) ^b	S (5b:5'b) ^b	ee (%) ^c
1	Toluene / 70	-	60	11:1	98
2	Toluene / 80	-	>99	>20:1	97
3	DMF / 80	-	81	18:1	96
4	Toluene / 80	[Pd-L] (5 mol%) 20h	96 (90% yield)	>20:1	97
5	Toluene / 80	[Pd-L] (5 mol%) Pd(OAc) ₂	26	5:1	97
6	Toluene / 80	[Pd-L] (5 mol%) Et ₃ N	>99	5:1	97

^a Reaction performed at 0.1 mmol of *rac*-**3b** and 0.8 mmol of **4**. ^b Determined by ¹H-NMR spectroscopy. ^c Determined by chiral HPLC analysis.

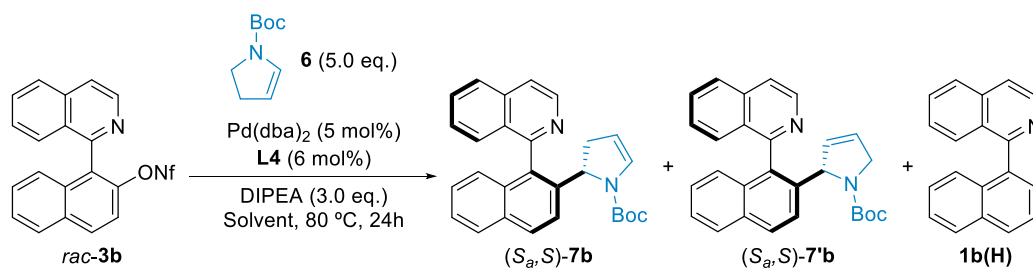
To our delight, it was observed that increasing the temperature to 80 °C, resulted in a complete conversion without significantly compromising the enantioselectivity. Furthermore, the regioselectivity was also improved and only **5b** was obtained, with no traces of **5'b** observed by ¹H-NMR analysis (entry 2, Table II.3). The use of DMF as solvent at 80 °C (entry 3, Table II.3), which provided the best regioselectivity values under the first

explored conditions (entry 4, Table II.1), did not improve the results obtained with toluene. Moreover, the catalyst loading could be decreased to 5 mol% of Pd(dba)₂ + 6 mol% (*R*)-DM-BINAP (effective, 5 mol% of catalyst), providing similar results (entry 4, Table II.3). No improvement was observed by using different palladium source or base as Pd(OAc)₂, or Et₃N, respectively.

To conclude, the optimal conditions to explore the scope of the asymmetric Heck reaction with heterobiaryl sulfonates **3** (0.1 mmol) and **4** (8.0 eq.) conform the use of Pd(dba)₂ (5 mol%), (*R*)-DM-BINAP (6 mol%), DIPEA (5.0 eq.) and toluene (0.5 mL) at 80 °C.

Importantly, this methodology could be also extended to other endocyclic olefins such as, *N*-Boc-2,3-dihydropyrrole **6**. However, under the optimized conditions for 2,3-dihydrofuran, a decrease in the **7b**/**7'b** selectivity (*S* factor) was observed, and an additional optimization of the reaction conditions, particularly solvents, was required (Table II.4).

Table II.4 – Solvent screening for the reaction between *rac*-**3b** and **6**.



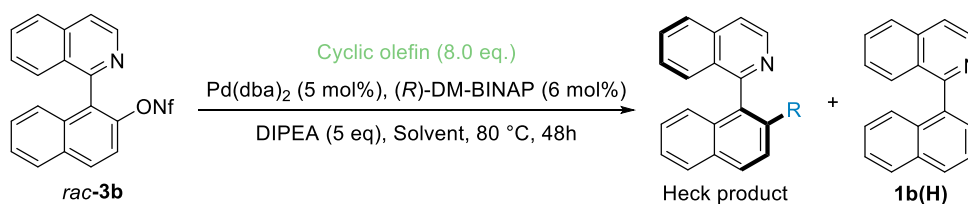
Entry ^a	Solvent	Variations	<i>rac</i> - 3b : 7b : 7'b : 1b(H) ^b	ee (%) ^c
1	Toluene	-	6:[55:17]:22	98
2	DMF	-	35:[43:14]:8	n.d.
3	DMSO	-	1.2:[80:16]:2.8	98
4	DMSO	[Pd-L] (10 mol%)	2:[80:13]:5	98
5	DMSO	36h	0:[81:14]:5	98

^a Reaction performed at 0.1 mmol of *rac*-**3b** and 0.5 mmol of **6**. ^b Determined by ¹H-NMR spectroscopy. ^c Determined by chiral HPLC analysis.

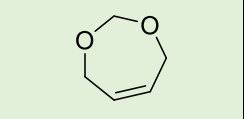
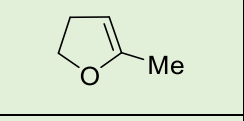
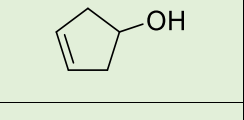
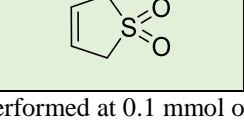
Under the optimized conditions for 2,3-dihydrofuran **4**, a decrease in *S* selectivity factor was observed. Additionally, dehalogenated product **1b(H)** was also observed, and not all *rac*-**3b** was consumed (entry 1, Table II.4). Nonetheless, this reaction showed excellent enantioselectivities but moderate regioselectivities. Using DMF as solvent lower reactivity was observed (entry 2, Table II.4). Fortunately, the use of DMSO led to full conversion to the desired products **7b** and **7b'**, together with a significant decrease of **1b(H)** (entry 3, Table II.4). On the other hand, a longer reaction time of 36h was required to observe full conversion (entry 4, Table II.4), although a slightly increase in the formation of **1b(H)** was also observed. Nevertheless, the consumption of *rac*-**3b** (entries 5 vs 3, Table II.4) was preferred to facilitate the further purification process.

Once the asymmetric alkenylation reactions of *rac*-**3b** with both 2,3-dihydrofuran and *N*-Boc-2,3-dihydropyrrole were optimized, the next step was to extend the methodology to other endocyclic olefins (Table II.5). However, some limitations were found in this case.

Table II.5 – Limitations of the method using other endocyclic olefins.



Entry ^a	Cyclic olefin	Solvent	Heck product (%) ^b	1b(H) (%) ^b
1		Toluene	-	>95
2		DMSO	85% yield. Low <i>S</i> and <i>ee</i>	-
3		Toluene	-	>95
4		DMSO	n.r.	n.r.
5		Toluene	-	>95
6		DMSO	n.r.	n.r.

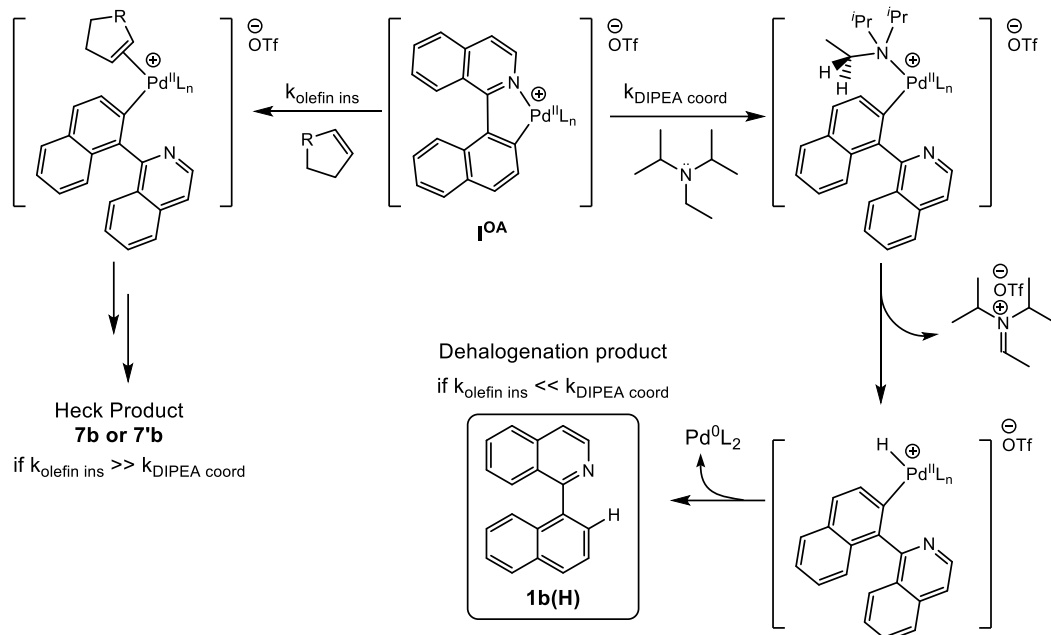
7		Toluene	31	69
8		DMSO	-	73
9		Toluene	-	36
10		DMSO	-	39
11		Toluene	-	>95
12		DMSO	46 (complex mixture)	54
13		Toluene	-	41
14		DMSO	-	>95

^a Reaction performed at 0.1 mmol of *rac*-**3b**. ^b Determined by ¹H-NMR spectroscopy.

Under the optimized conditions for the reaction of *rac*-**3b** with either **4** or **6**, reactions performed with these cyclic olefins failed to give any products other than dehalogenation **1b(H)**. We attribute this lack of reactivity to the fact that the less electron-rich olefins now employed are not capable to displace the isoquinolyl N atom in the **I^{OA}** intermediate. Another contribution to their low reactivity could be related to the high level of steric crowding at this **I^{OA}** palladacycle.

Regarding the dehalogenation process, it could be rationalized considering DIPEA as a base and a hydride source, promoting a Pd-catalyzed dehalogenation reaction (Scheme II.22).¹¹⁵ In order to prevent this route, the use of an inorganic base as LiOAc was alternatively considered.¹⁰⁷ Unfortunately, no reaction was observed under this conditions.

¹¹⁵ (a) Coquerel, Y.; Bremond, P.; Rodriguez, J. *J. Organomet. Chem.* **2007**, *692*, 4805. (b) Xue, F. L.; Qi, J.; Peng, P.; Mo, G. Z.; Wang, Z. Y. *Lett. Org. Chem.* **2014**, *11*, 64. (c) Zawisza, A. M.; Muzart, J. *Tetrahedron Lett.* **2007**, *48*, 6738.



Scheme II.22 – Mechanism proposed for the Pd-catalyzed dehalogenation event.

Considering these limitations, we focused on the use of 2,3-dihydrofuran **4** and *N*-Boc-2,3-dihydropyrrole **6** cyclic olefin representatives. Notwithstanding, these two olefins can give access to a wide variety of highly functionalized products.

Hence, the next step consisted on the introduction of structural modifications on the heterobiaryl sulfonate moiety and the study of the alkenylation under optimized conditions with the above mentioned olefins. These structural variations were divided on two main groups, depending on which fragment of the heterobiaryl is modified. With respect to the heteroaromatic counterpart, quinazoline (**3c**), phthalazine (**3d**) and picoline (**3e**) analogues were synthesized. And maintaining the isoquinoline fragment, different substitutions patterns could also be introduced on the naphthalene ring (**3f-i**) (Figure II.1).

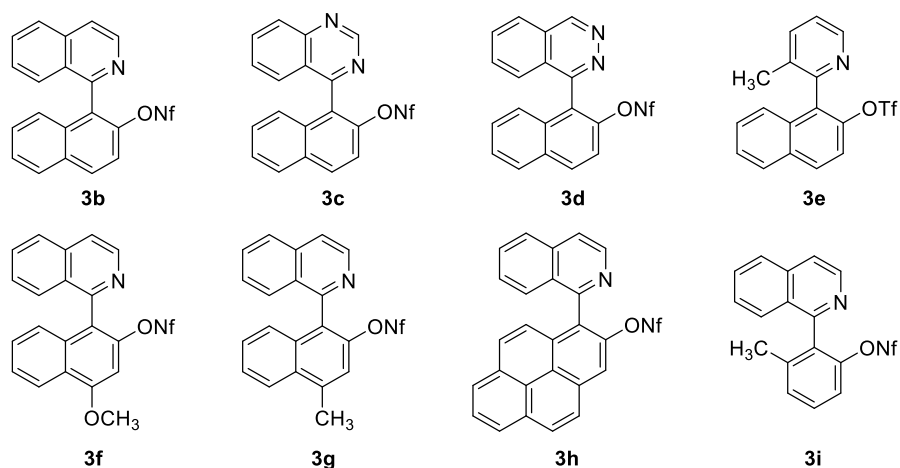
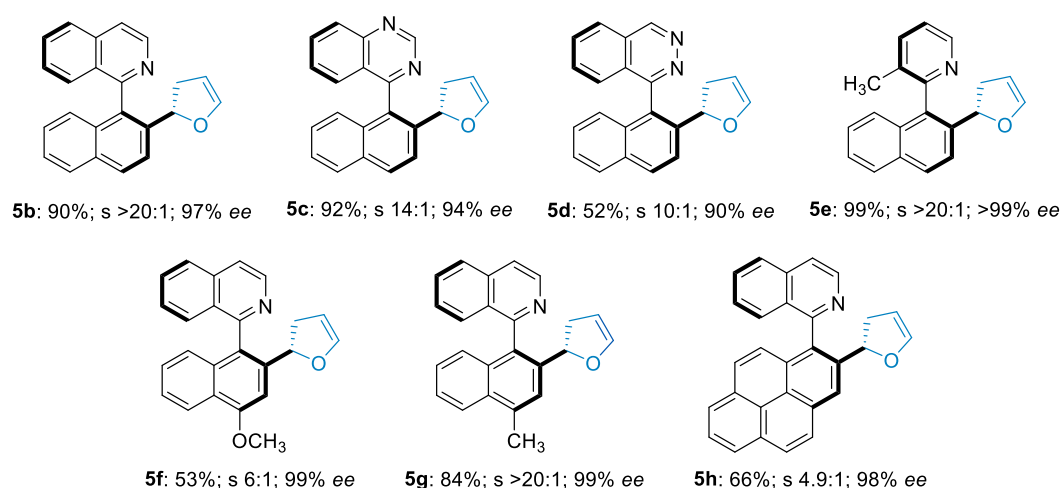
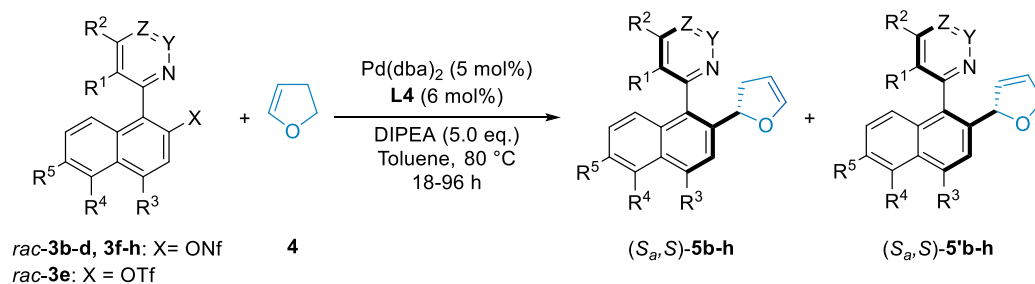


Figure II.1 – Library of synthesized heterobiaryl sulfonates.

It has been observed that both heterobiaryl triflates (OTf) and nonaflates (ONf) show no difference in reactivity under the optimized conditions, so, both were used depending on precursors availability at the required moment.

With these selected heterobiaryl sulfonates (Figure II.1) in hands, their reactivity under the optimized reaction conditions with olefins **4** and/or **6** was explored (Schemes II.23 and II.25, respectively).



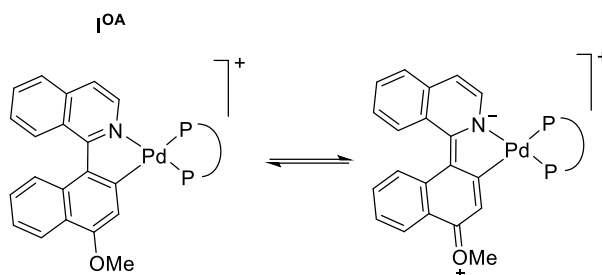
Scheme II.23 – Dynamic kinetic asymmetric Heck reaction using 2,3-dihydrofuran **4**. Heterobiaryls scope.

This methodology can be applied to the alkenylation of a variety of heterobiaryl sulfonates in very high selectivities. Quinazoline derivative **5c** showed similar results than the model substrate. However, phthalazine analogue **5d** was less reactive, possibly due to electronic effects caused by the two contiguous nitrogen atoms. The results obtained with the model substrate were even improved by the picoline derivative, obtaining complete reactivity and selectivity towards **5e**.

Heterobiaryl nonaflate **3f** is a more challenging substrate for the undesired push-pull effect conjugation with the OMe substituent at the cationic $\text{I}^{\text{O}^{\text{A}}}$, and it is based on two main factors. First, the partial double bond character and shorter bond length at the axis are expected to slow down the required atropisomerization event (Scheme II.24).¹¹⁶ Second, as

¹¹⁶ Gómez-Gallego, M.; Martín-Ortiz, M.; Sierra, M. A. *Eur. J. Org. Chem.* **2011**, 32, 6502.

a consequence of the higher electron density, and therefore, basicity of the isoquinoline N atom, the dissociation of the N–Pd bond is also more challenging.



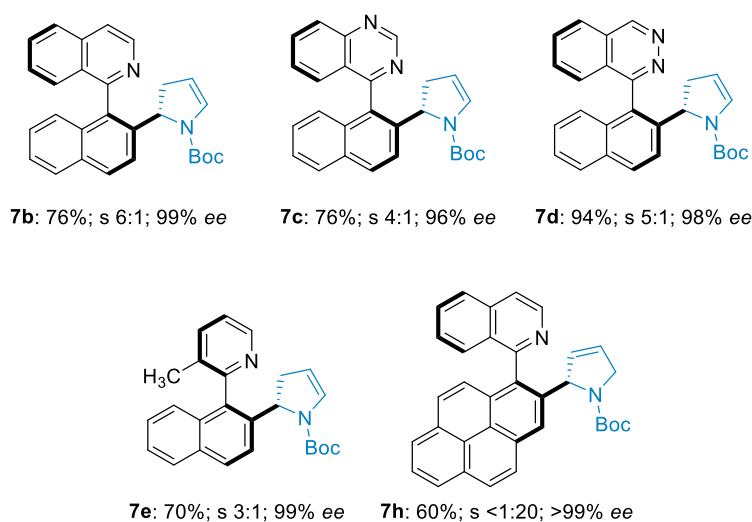
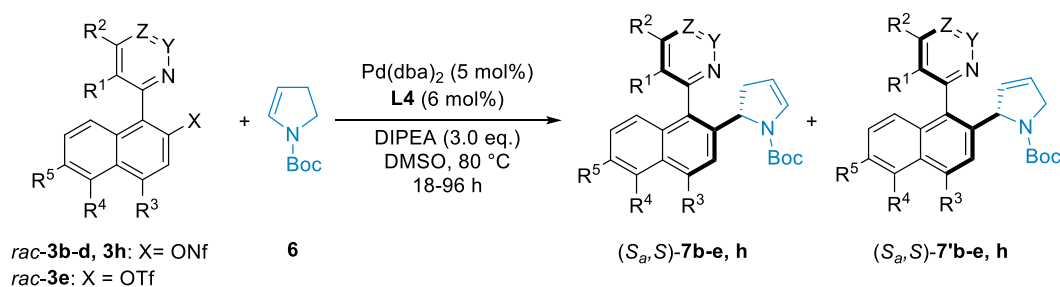
Scheme II.24 – Push-pull effect observed on **3f I^{OA}**.

Indeed, **3f** was not a suitable substrate in previous DYKAT-based strategies developed in our group,^{25b,117} with the exception of the asymmetric alkylation reaction.^{25c} To our delight, the dynamic kinetic asymmetric Heck reaction allowed the isolation of the corresponding product in moderate yields and excellent enantiomeric excess.

Different substitution on the naphthalene ring were also tolerated by this methodology, thus, **5g** and **5h** were obtained in moderate to good yields, and excellent selectivities. Remarkably, **3i** (Figure II.1) displayed no reactivity towards the expected product; instead, ¹H-NMR analysis of the reaction crude showed only starting material and dehalogenation product **1b(H)**.

Besides, the scope of heterobiaryl sulfonates with *N*-Boc-dihydropyrrole **6** was also studied in parallel (Scheme II.25). In general, the dynamic kinetic asymmetric Heck reactions using **6** were less regioselective than those with **4**, albeit nearly perfect enantioselectivities were achieved in all cases. As a striking exception, the pyrenyl **7'h** isomer was formed exclusively, although again with an excellent diastereo- and enantioselectivity. As a possible explanation, the high steric hindrance of the pyrenyl group may prevent reinsertion of the non-isomerized product.

¹¹⁷ Ramírez-López, P.; Ros, A.; Romero-Arenas, A.; Iglesias-Sigüenza, J.; Fernández, R.; Lassaletta, J. M. *J. Am. Chem. Soc.* **2016**, *138*, 12053.



Scheme II.25 – Dynamic kinetic asymmetric Heck reaction using *N*-Boc-2,3-dihydropyrrole **6**. Heterobiaryls scope.

Importantly, the synthesis of **5b** and **7b** was scaled up to 1.8 and 1.5 mmol, respectively, and could also be performed with a lower catalyst loading (2 mol % Pd(dba)₂ and 2.4 mol % (*R*)-DM-BINAP) to obtain the products with similar results (**5b**: 81% yield, s > 20:1, dr >20:1, 97% ee; **5b**: 60% yield, s 6:1, dr >20:1, 99% ee). Indeed, from these scale-up experiments, the absolute configuration of the two main products formed in the reaction were determined, since both **5b** and the minor isomer **7'b** could be crystallized and their structures analysed by X-Ray diffraction techniques (Figure II.2).

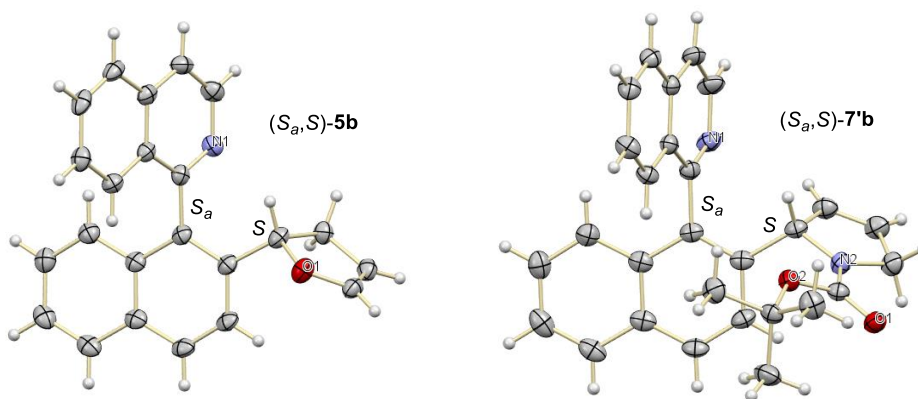


Figure II.2 – X-ray structures of (S_a,S) -**5b** and (S_a,S) -**7'b**. Thermal ellipsoids drawn for 50% probability.

Remarkably, as observed in the above X-ray structures, both regioisomers present the same configuration at the stereogenic centre. These data indicate that in our case there is no kinetic resolution associated to the isomerization of the olefin, as observed by other authors.^{89,118} A similar trend has been previously reported for asymmetric Heck reactions using 3,3'-disubstituted DM-BINAP ligands.¹¹⁹ Additionally, the same absolute configuration was observed when an hemilabile ligand as BINAP(O) was used in the arylation of 2,3-dihydrofuran with either phenyltriflate or phenyliodide.^{91a}

II.3.4. Dynamic kinetic asymmetric Heck reaction with acyclic alkenes

Subsequently, the scope of this new catalytic transformation was investigated with respect to acyclic olefins. As electron rich olefins are needed, butyl vinyl ether **8** was selected as an appropriate candidate for such purpose. It has to be considered that, with terminal alkenes, two different linear or branched products can be obtained depending on how they coordinate to the palladium complex. Previous studies have shown that cationic reaction pathways for the Heck reaction with terminal alkenes presents high preference for the internal arylation, leading mainly to the branched product.^{108a} So, this trend is expected to be maintained in our system, since the combination of the poor coordinating ability of

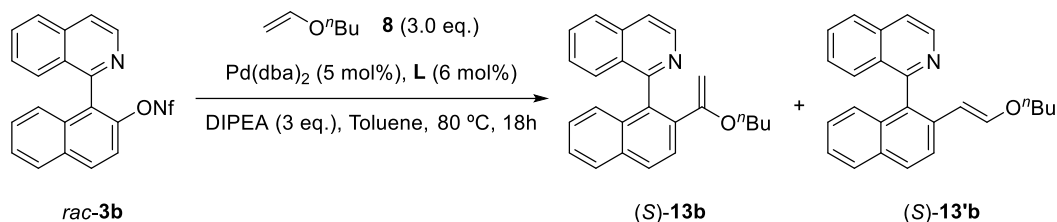
¹¹⁸(a) Ozawa, F.; Kubo, A.; Matsumoto, Y.; Hayashi, T.; Nishioka, E.; Yanagi, K.; Moriguchi, K. *Organometallics* **1993**, *12*, 4188. (b) Hii, K. K. M.; Claridge, T. D. W.; Brown, J. M.; Smith, A.; Deeth, R. J. *Helv. Chim. Acta* **2001**, *84*, 3043.

¹¹⁹ Rankic, D. A.; Lucciola, D.; Keay, B. A. *Tetrahedron Lett.* **2010**, *51*, 5724.

triflate counteranion together with the coordination of isoquinoline N, promotes a cationic pathway for the dynamic kinetic asymmetric Heck reaction of heterobiaryl sulfonates.

We first, employed the readily optimized conditions for endocyclic olefins. However, the reaction between *rac*-**3b** and **8** afforded the product **13b** with good but not excellent enantioselectivity (entry 4, Table II.6), and an additional optimization was required, in particular regarding a screening of ligands (Table II.6).

Table II.6 – Ligand screening for the reaction of *rac*-**3b** and butyl vinyl ether **8**.



Entry ^a	Ligand (L)	Conv. (%) ^b	(S)-13:(S)-13'b ^b	ee (%) ^c
1	(<i>R</i>)-BINAP (L1)	>99	>20:1	59
2	(<i>R</i>)-H8-BINAP (L2)	>99	>20:1	35
3	(<i>R</i>)-Tol-BINAP (L3)	>99	>20:1	33
4	(<i>R</i>)-DM-BINAP (L4)	>99	>20:1	83
5	(<i>R</i>)-MeO-BIPHEP (L5)	n.d.	n.d.	51
6	(<i>R</i>)-DM-SEGPHOS (L7)	n.d.	n.d.	73
7	Josiphos SL-J002-1 (L9)	80	>20:1	92
8	(<i>R</i>)- ^t Bu-PHOX (L11)	<5	n.d.	n.d.
9	(<i>R,R</i>)-Me-DUPHOS (L14)	<5	n.d.	n.d.
10	(<i>R</i>)-3,5-Xyl-MeOBIPHEP (L18)	n.d.	n.d.	78
11	(<i>R</i>)-DTBM-SEGPHOS (L19)	<5	n.d.	n.d.
12	Walphos SL-W001-1 (L20)	>99	>20:1	67
13	Josiphos SL-J003-1 (L21)	n.d.	n.d.	34
14	Josiphos SL-J005-1 (L22)	n.d.	n.d.	37
15	Josiphos SL-J009-1 (L23)	n.d.	n.d.	35

16	Josiphos SL-J011-1 (L24)	n.d.	n.d.	81
17	Josiphos SL-J013-1 (L25)	60	>20:1	90
18	Josiphos SL-J216-1 (L26)	n.d.	n.d.	59
19	Josiphos SL-J505-2 (L27)	n.d.	n.d.	82
20^d	Josiphos SL-J002-1 (L9)	95	>20:1	92

^a Reaction performed at 0.1 mmol of *rac*-**3b**. ^b Determined by ¹H-NMR spectroscopy. ^c Determined by chiral HPLC analysis. ^d Reaction allowed for 24h.

As expected, full selectivity towards the branched product was observed with all the ligands screened; no traces of linear product appeared. Although full conversion was obtained with other BINAP analogues, there was no improvement on the enantioselectivity (entries 1-3, Table II.6). Only ferrocenyl-based Josiphos ligands provided better results than (*R*)-DM-BINAP. In particular, **L9** and **L25** allowed us to reach over 90% *ee*, although a slightly lower conversion was observed (entries 7 and 17, Table II.6, respectively). The Josiphos SL-J002-1 (**L9**) ligand showed the best equilibrium between reactivity and selectivity, with a 92% *ee* and 80% conversion, and was then used to explore the scope of this reaction. It was also observed that, under these conditions, longer reaction times (24h instead of 18h) resulted in almost full conversion with no erosion on selectivity. (entry 20, Table II.6).

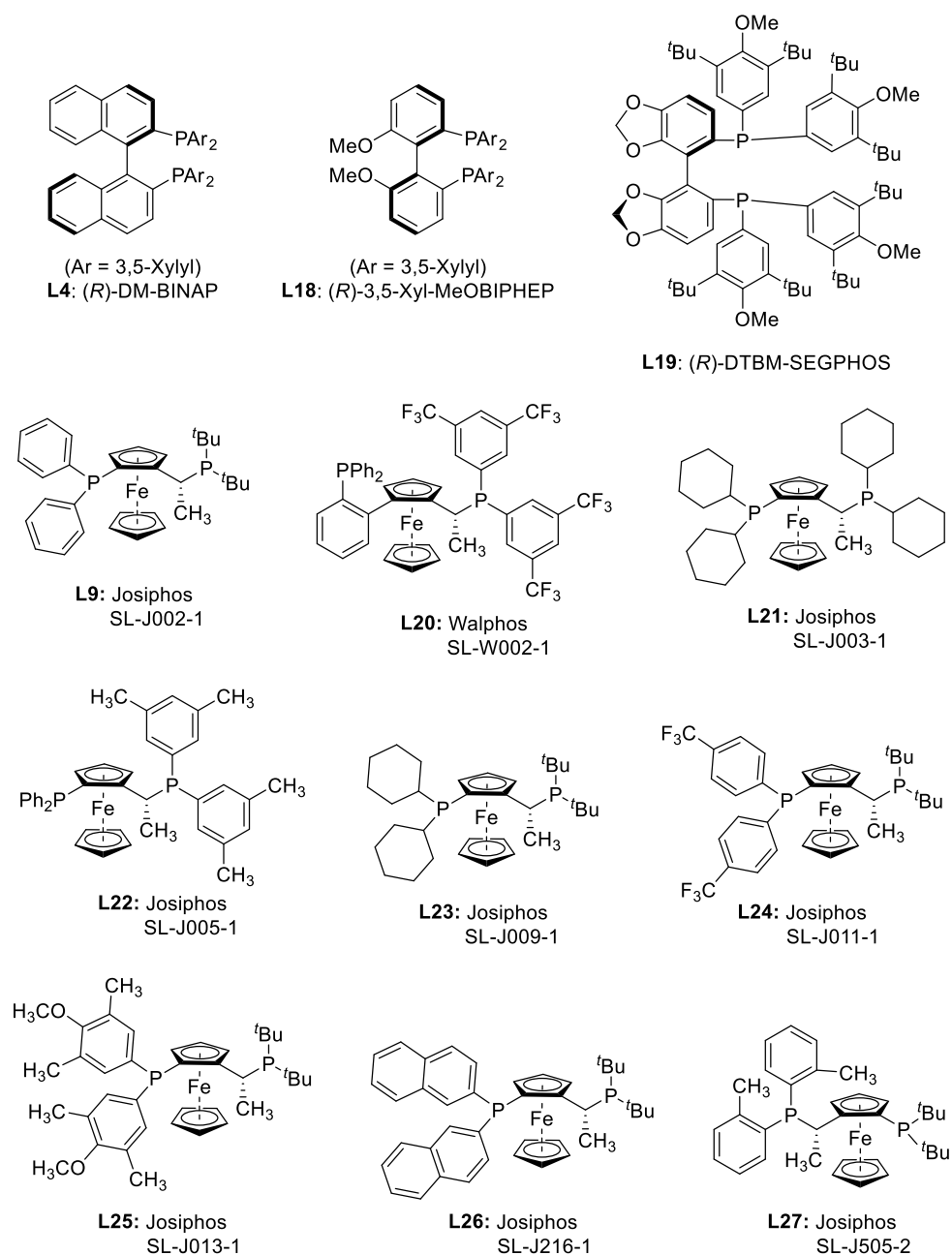
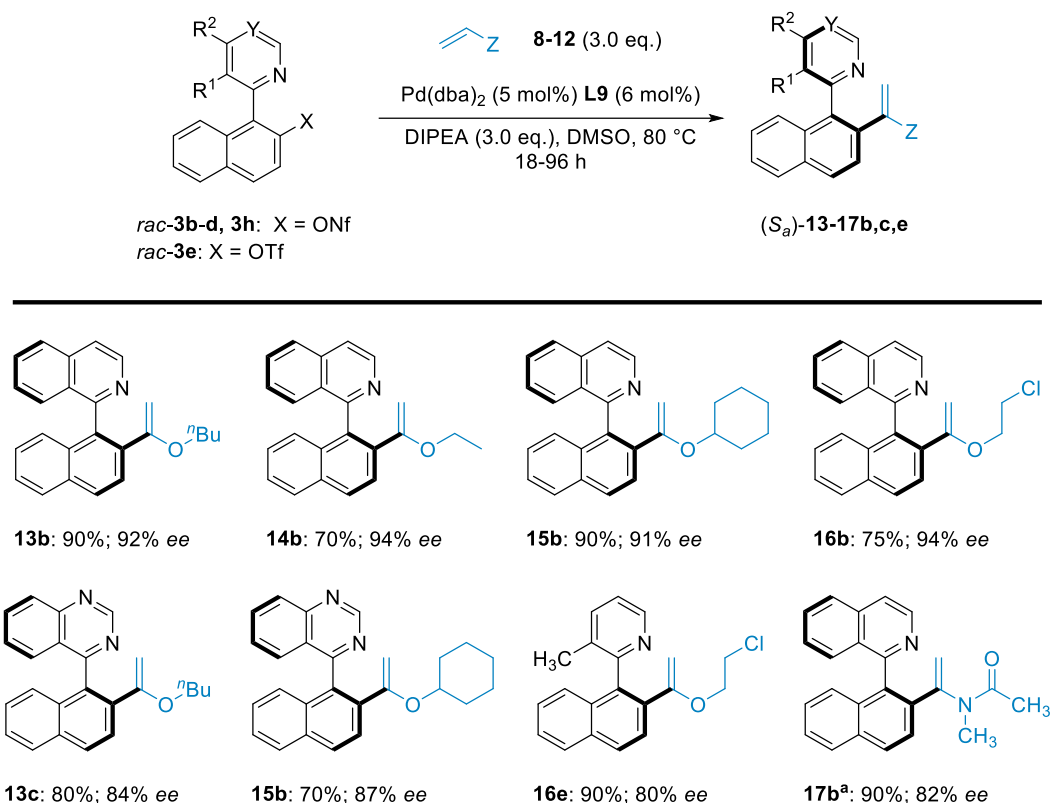


Figure II.3 – Ligands screened for the dynamic kinetic asymmetric Heck reaction between *rac*-**3b** and **8**.

In this case, with acyclic terminal alkenes, the resulting heterobiaryls display only axial chirality; no additional stereocentres are generated. Nonetheless, highly interesting and functionalized axially chiral heterobiaryl structures are also obtained.

With the optimized conditions in hands, the scope of this transformation was explored using vinyl ethers with different alkyl substituents, and *N*-methyl vinyl acetamide (Scheme II.26).



Scheme II.26 – Dynamic kinetic asymmetric Heck reaction: acyclic olefins scope. ^a**L4** was used instead.

The absolute configuration was assigned by analogy to that observed at the stereogenic axis for the reaction with endocyclic olefins. The resulting products could be isolated in good yields and good to excellent enantioselectivities. The best results, were obtained with the model heterobiaryl nonaflate **rac-3b**, with enantiomeric excesses over 90% for all the vinyl ethers employed (**13-16b**). When structural modifications on the heterobiaryl frame were introduced (**13c**, **15b**, **16e**), the selectivities suffered a slightly decrease (80-87% ee), with moderate to good yields in all cases.

Remarkably, the use of vinyl acetamides was limited to *N*-methyl vinyl acetamide: other structural modifications resulted in disappointing results (Figure II.4). Unlike vinyl ethers, ligand **L9** induced no reactivity, and (*R*)-DM-BINAP **L4** was used instead.

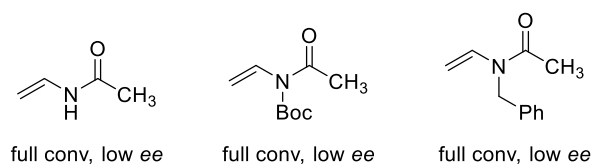


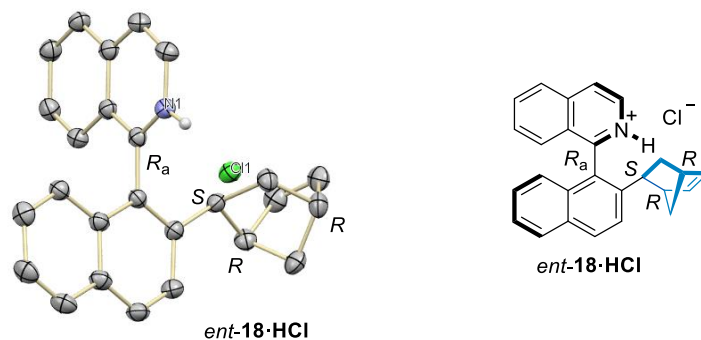
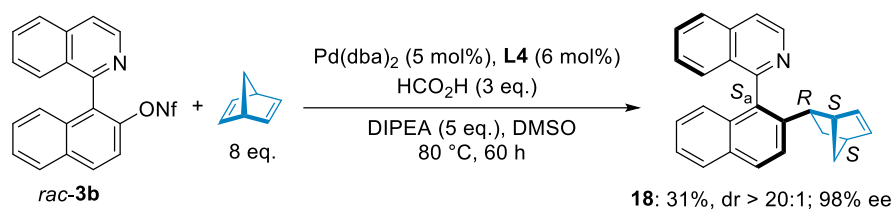
Figure II.4 – Different non-reactive vinyl acetamides studied under optimized conditions.

It can be assumed that *N*-Boc protection of vinyl acetamide decreases the electronic richness of the alkene, preventing its coordination to the Pd(II) centre. Additionally, steric factors may also contribute to the lack of reactivity; as may occur with the *N*-benzyl derivative.

II.3.5. Hydroarylation of 2,5-norbornadiene

Some preliminary experiments also demonstrated that this DYKAT methodology could be extended to the hydroarylation of a bicyclic olefin such as 2,5-norbornadiene.

In fact, the reaction of 2,5-norbornadiene with *rac*-**3b** in the presence of formic acid as hydride source and **L4** as the ligand afforded **18** as a single diastereomer in 98% *ee*, but in moderate yield. Remarkably, no double hydroarylation was observed in this transformation (Scheme II.27). The absolute configuration of product *ent*-**18**·HCl, isolated from a scale-up experiment using (*S*)-DM-BINAP as the ligand, was determined by single-crystal X-ray diffraction analysis, showing an (*R_a,S,R,R*) configuration, as shown in Scheme II.28. Noteworthy, this axis configuration is consistent with the uniform stereochemical outcome observed for the dynamic kinetic asymmetric Heck products **5** or **7**.



Scheme II.27 – Hydroarylation of 2,5-norbornadiene with *rac-3b*. In this case, the reaction was repeated with **L4** enantiomer (*S*)-DM-BINAP in higher scale.

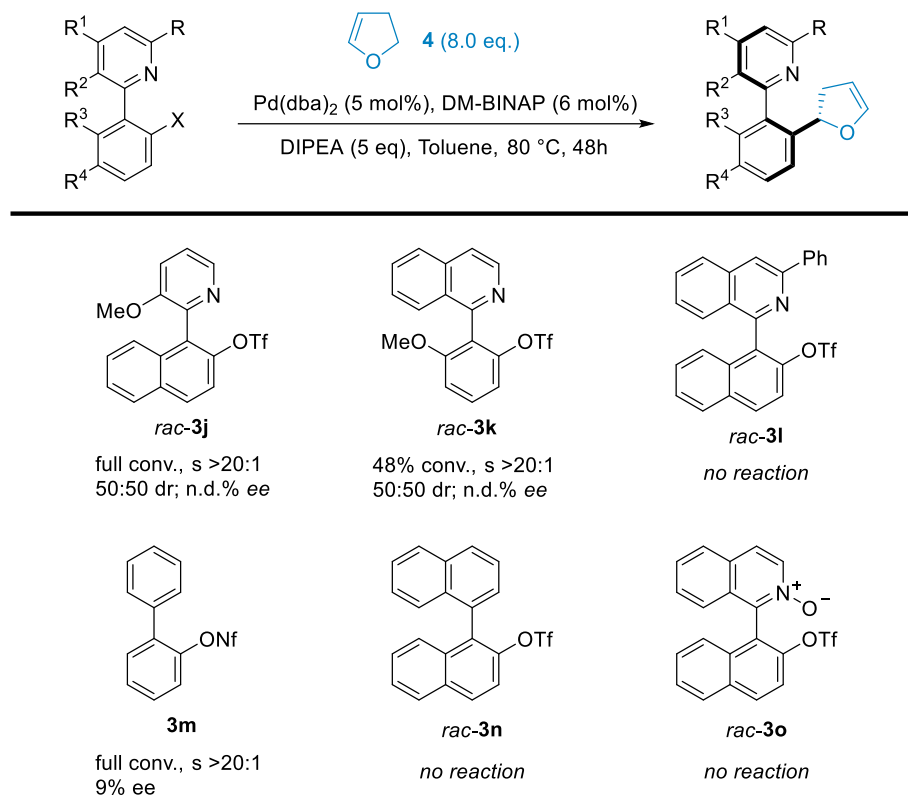
II.3.6. Control experiments

In order to get insight about the reaction mechanism and limitations, some control experiments were performed (Scheme II.28). The first one consisted on the reaction between 2,3-dihydrofuran **4** with triflates *rac-3j* and *rac-3k*, affording the expected Heck product **5j** and **5k**, respectively, with migrated double bond exclusively. However, the resulting products proved to be configurationally labile: after isolation, the pure product appeared as 1:1 mixture of diastereomers. This phenomenon was also previously observed by other authors; changing from alkyl to O-alkyl substituent at the *ortho* position results in a significant decrease of the rotational barrier, and the consequent loss of configurational stability.¹²⁰

Then, the influence of a substitution at the C(α) to isoquinolyl nitrogen atom was also studied. A lack of reactivity was observed when introducing a phenyl group at this

¹²⁰ Min, C.; Lin, Y.; Seidel, D. *Angew. Chem. Int. Ed.* **2017**, *56*, 15353.

position (*rac*-**3l**). A possible explanation arises from the steric hindrance of the aryl ring that prevents the coordination of the nitrogen and further oxidative addition.

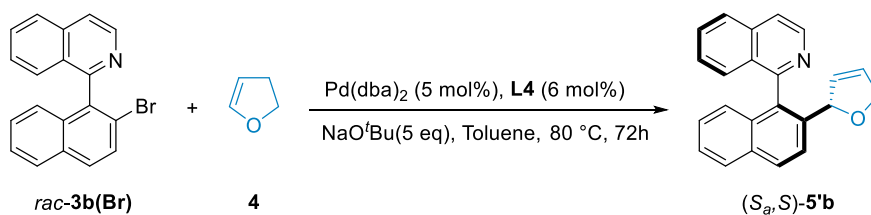


Scheme II.28 – Control experiments.

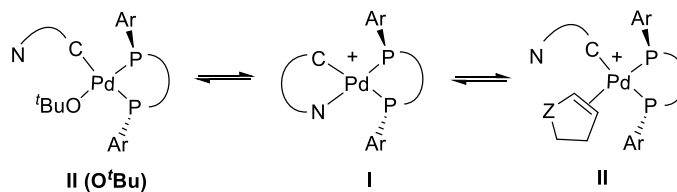
The reaction with biphenyl nonaflate **3m** was also studied, leading to the expected Heck product in high selectivity but a negligible 9% *ee*. The result with this simpler system highlights the importance of a synergistic effect between the chiral ligand and the heterobiaryl moiety during the stereocontrolling step of the reaction. Moreover, no coupling product was formed in the reaction with the more sterically demanding heterobiaryl triflate analogue *rac*-**3n**, showing that the coordinating isoquinolyl N atom is required to assist the oxidative addition step. A similar situation appears with *N*-oxide *rac*-**3o**, where the isoquinolyl N is blocked for coordination (and therefore assistance for the oxidative addition can only be provided by the oxygen) indicating that the formation of a

five membered cationic palladacycle is also essential to reactivity, and the six membered palladacycle is not a valid alternative.

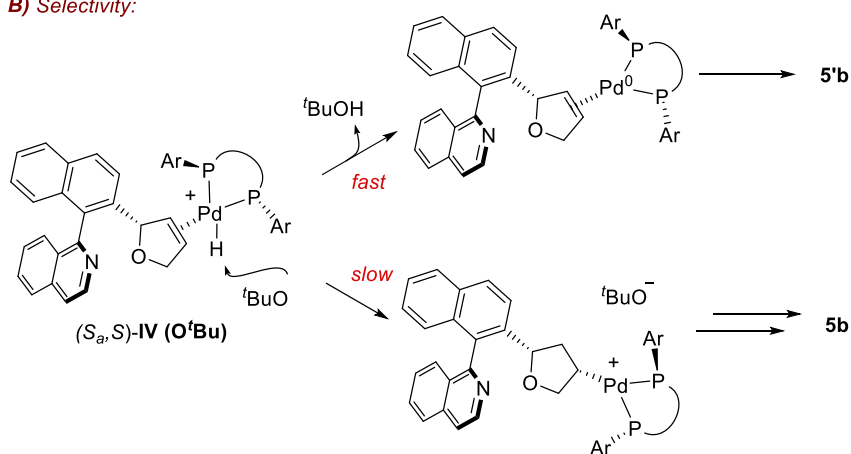
Finally, a very interesting result was obtained when 1-(2-bromonaphthalen-1-yl)isoquinoline *rac*-**3b(Br)** was used as the starting material, in combination with NaO^tBu as base. The non-isomerized product **5'b** was exclusively formed in 93% ee. It is assumed that a Br→O^tBu ligand exchange occurred, triggered by precipitation of NaBr, insoluble in toluene.¹¹⁷ Hence, the main difference with the reaction from **3b** is the higher basicity and coordinating ability of O^tBu counteranion compared to OTf. The lower reactivity observed could be then explained by the lower concentration of the reactive intermediate **II**, in equilibrium with the unproductive neutral species **II(O^tBu)** since it is not easy for the neutral olefin to displace this counteranion (Scheme II.29A). The exclusive formation of **5'b** could be attributed to a fast deprotonation of the intermediate (*S_aS*)-**IV(O^tBu)** by the base with respect to the reinsertion of Pd (Scheme II.29B).



A) Reactivity:



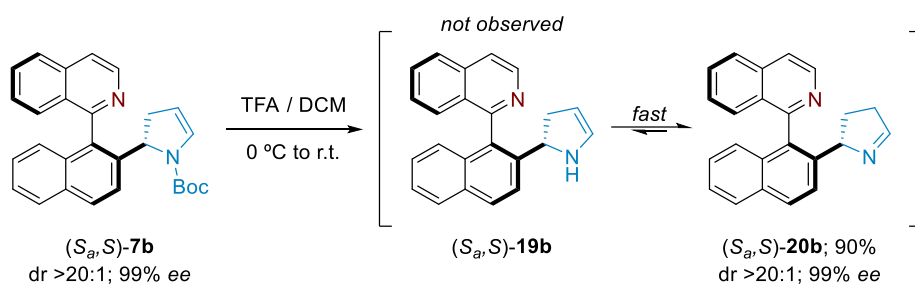
B) Selectivity:



Scheme II.29 – Control experiment performed between *rac*-3b(Br) and 4.

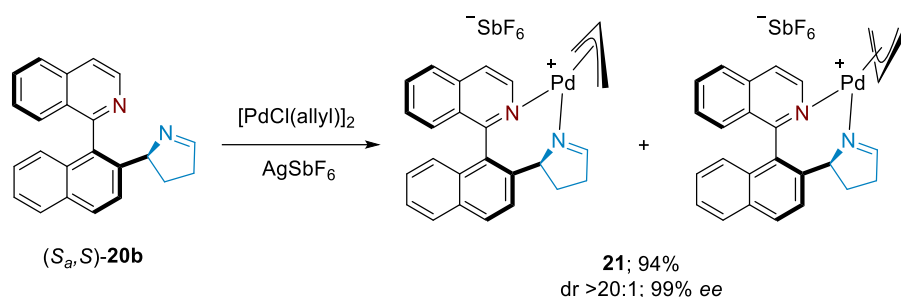
II.3.7. Representative transformations

Compound (*S_a*,*S*)-7b was chosen to illustrate the synthetic utility of the products synthesized through this methodology. The most direct transformation with this compound is the deprotection of the *N*-Boc group. Treatment with TFA in dichloromethane afforded exclusively the imine product (*S_a*,*S*)-20b presumably formed from enamine (*S_a*,*S*)-19b after a rapid enamine-imine equilibrium (Scheme II.30).



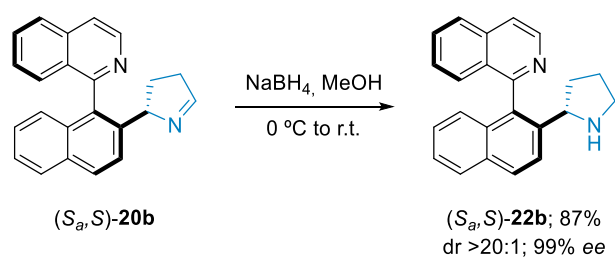
Scheme II.30 – N-Boc deprotection of asymmetric Heck reaction product $(S_a,S)\text{-7b}$.

This cyclic imine could be seen as a N,N ligand by itself. Moreover, it was employed in combination with $[\text{PdCl}(\text{allyl})]_2$ and AgSbF_6 for the synthesis of the chiral Pd complex **21**, in which the two possible conformations of the allyl ligand could be observed by NMR (Scheme II.31).



Scheme II.31 – Synthesis of $[\text{Pd}(\text{allyl})(S_a,S)\text{-20b}]$ complex **21**.

Additionally, reduction of the imine $(S_a,S)\text{-20b}$ with NaBH_4 , afforded a bifunctional pyrrolidine derivative $(S_a,S)\text{-22b}$ with an appealing structural frame for its use in asymmetric organocatalysis as a proline-type bifunctional organocatalysts (Scheme II.32).



Scheme II.32 – Reduction of imine $(S_a,S)\text{-20b}$ for the synthesis of proline-type bifunctional organocatalyst.

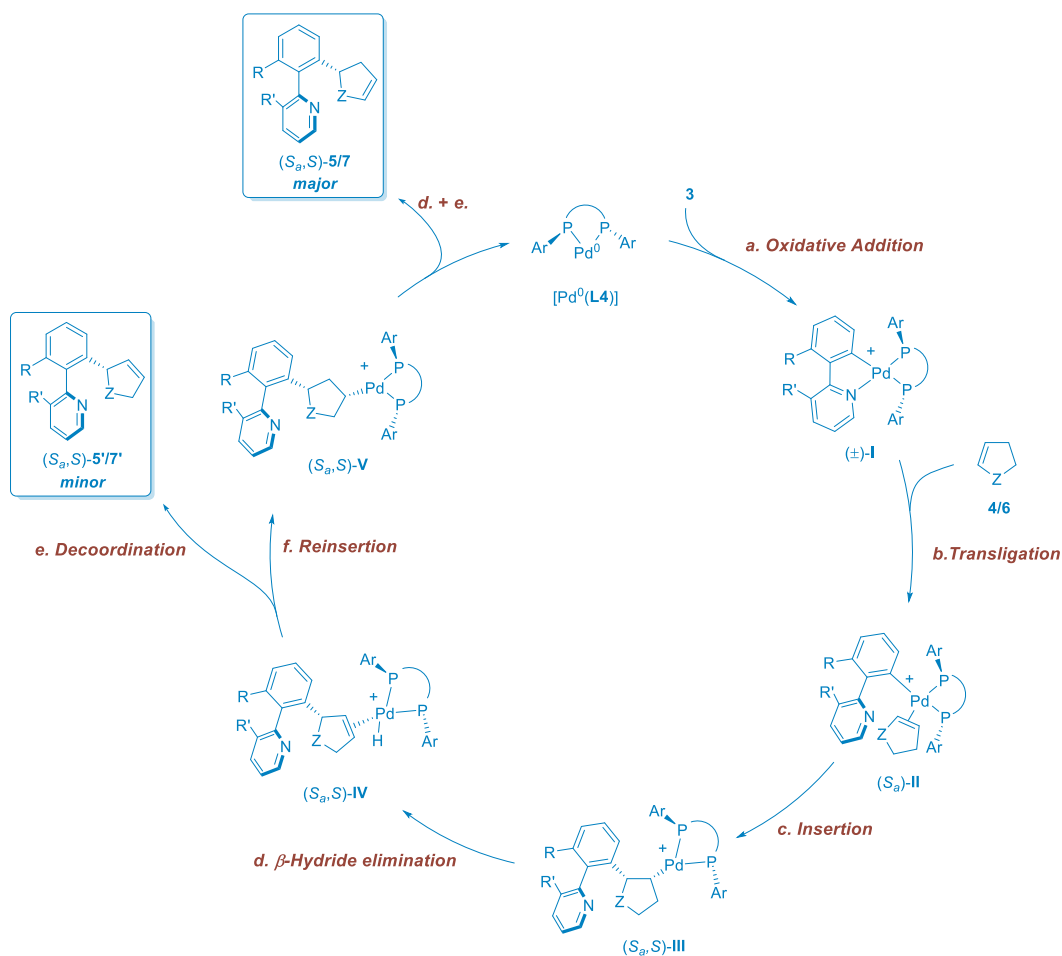
Importantly, no epimerization was observed during any of these transformations, and highly functionalized heterobiaryls with both central and axial chirality with potential uses as ligands or catalysts have been obtained.

II.3.8. Mechanistic study

Later on, DFT calculations were carried out by Professor Enrique Gómez Bengoa from University of Pais Vasco (UPV-EHU) in order to gain a deeper insight into the mechanism and the origin of the high enantio- and diastereoselectivities observe in this reaction.

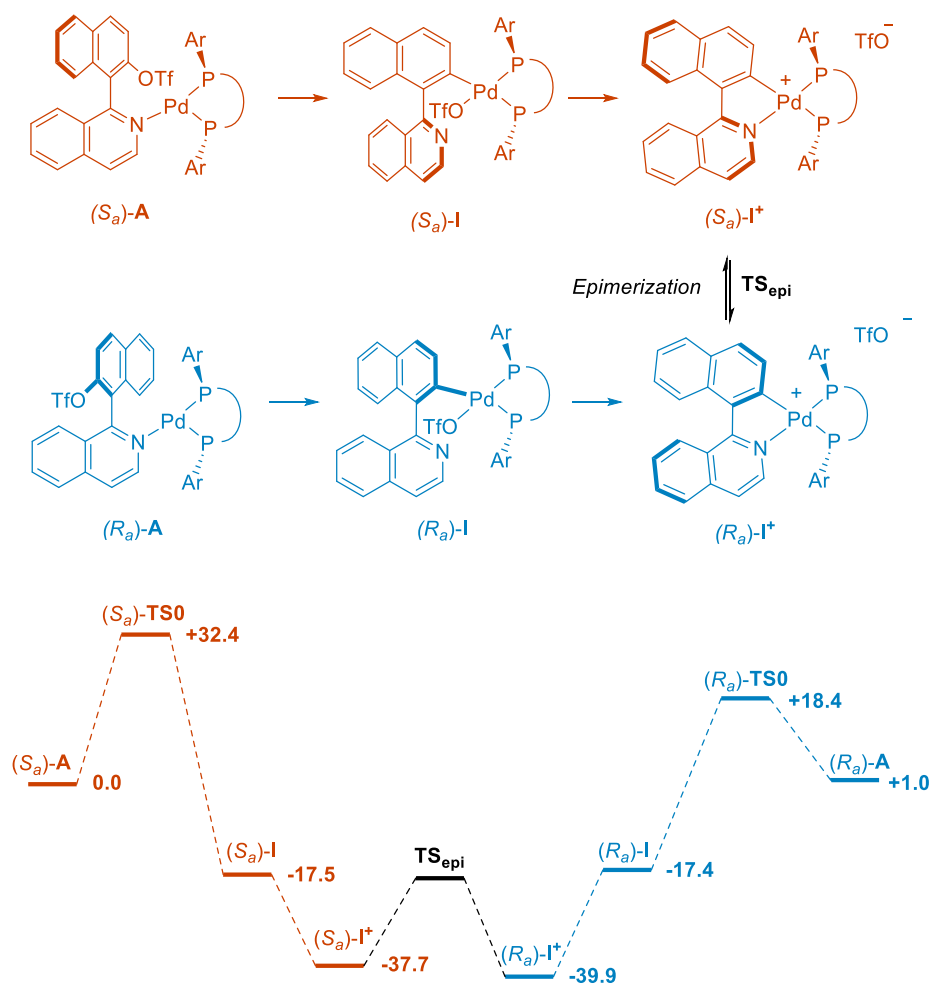
We first assumed a fundamental catalytic cycle as the one described in **II.2.1.**, consisting on: [a] oxidative addition of sulfonate substrates **3** to Pd(0) source providing cationic intermediate (\rightarrow **I**), [b] transligation, or alkene coordination (\rightarrow **II**), [c] migratory insertion of this alkene to Pd^{II}-C bond (\rightarrow **III**), [d] double bond reinstallation by β -hydride elimination (\rightarrow **IV**), [e] palladium decooordination leading to final minor products **5'** or [f] reinsertion (\rightarrow **V**) and a second β -hydride elimination (\rightarrow **VI**), to afford double bond migration products **5** after Pd decooordination (Scheme II.33).¹²¹

¹²¹ For a theoretical study of the asymmetric Heck reaction using P,N-ligands see: Henriksen, S. T.; Norrby, P.-O.; Kaukoranta, P.; Andersson, P. G. *J. Am. Chem. Soc.* **2008**, *130*, 10414.



Scheme II.33 – Fundamental catalytic cycle. Depicted for the formation of (S_a,S) -5/7 and (S_a,S) -5'/7'.

The model reaction between *rac*-**3b** and **4** using ligand **L4** under the optimal conditions was chosen to perform the computational studies. As mentioned above, this reaction can lead to eight possible isomeric products by combination of the different configurations of the stereogenic axis and centre, and the final position of the double bond (see Scheme II.18).

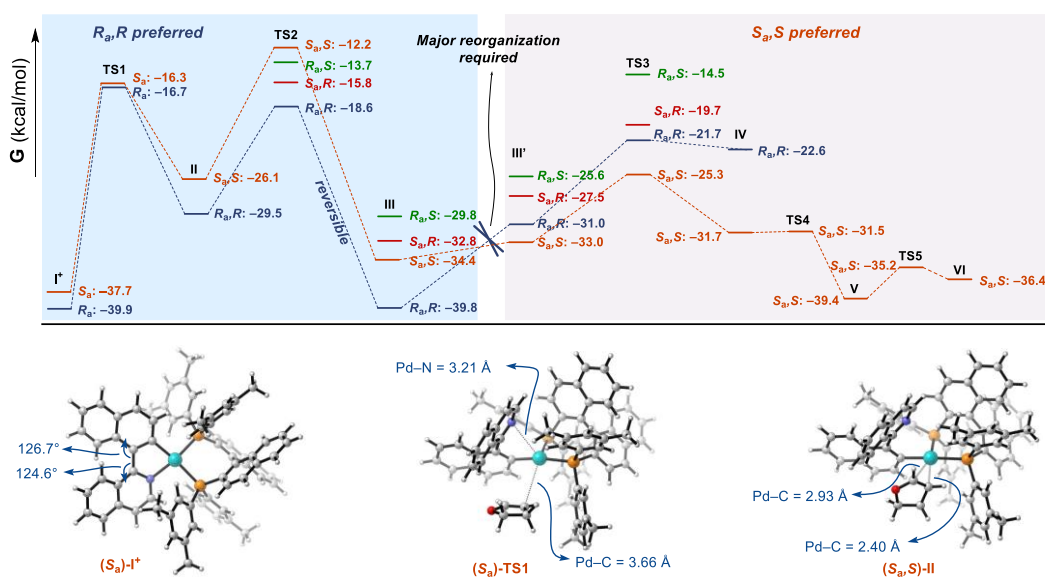


Scheme II.34 – Computed energies for the atropisomerization process.

The DFT studies started from diastereomeric complexes (*S_a*)-**A** (considered $G = 0$) and (*R_a*)-**A** ($\Delta G = +1.0$ kcal/mol) formed after coordination of isoquinolyl nitrogen from both substrate enantiomers **3b** to $[\text{Pd}^0(\text{L4})]$ catalyst (Scheme II.34). Transition states (*R_a*)-**TS0** and (*S_a*)-**TS0** for the oxidative addition step were located for both atropisomers at $\Delta G^\ddagger = 18.4$ and 32.4 kcal/mol, respectively, leading to intermediates (*S_a*)-**I** and (*R_a*)-**I** of similar energies ($\Delta G = -17.5$ and -17.4 kcal/mol). The displacement of the triflate by the isoquinoline N atom to form cationic intermediates (*S_a*)-**I**⁺ and (*R_a*)-**I**⁺ provides an additional stabilization of 20.2 and 22.5 kcal/mol, respectively. It is necessary that these diastereomeric Pd(II) intermediates interconvert into each other in a fast equilibrium for

the dynamic kinetic transformation to take place. Subsequently, the later steps must present different activation energies for the diverse diastereomeric transition states. In fact, a low barrier for this epimerization was computed (**TS_{epi}**: $\Delta G^\ddagger = +21.0$ kcal/mol), showing the affordability of the rotation around the stereogenic axis at this point.

As was anticipated, the coordination of dihydrofuran **4** to form intermediates **II** in the next step requires decooordination of the isoquinolyl N and rotation of the biaryl group above or below the coordination plane; thus, fixing the configuration of the stereogenic axis. Surprisingly, calculations indicate that this ligand exchange process is concerted, which means that in the located transition states **TS1**, the dihydrofuran molecule is moving into the coordination sphere of palladium as the same time as the isoquinoline is rotating away from the metal centre. In (*S_a*)-**TS1**, the Pd–N and Pd–alkene distances are 3.2 and 3.7 Å respectively. The high activation barrier for this process can be attributed to the crowded environment in which the ligands are moving (i.e. $\Delta G^\ddagger = 23.2$ kcal/mol for (*R_a*)-**TS1**) (Figure II.5).



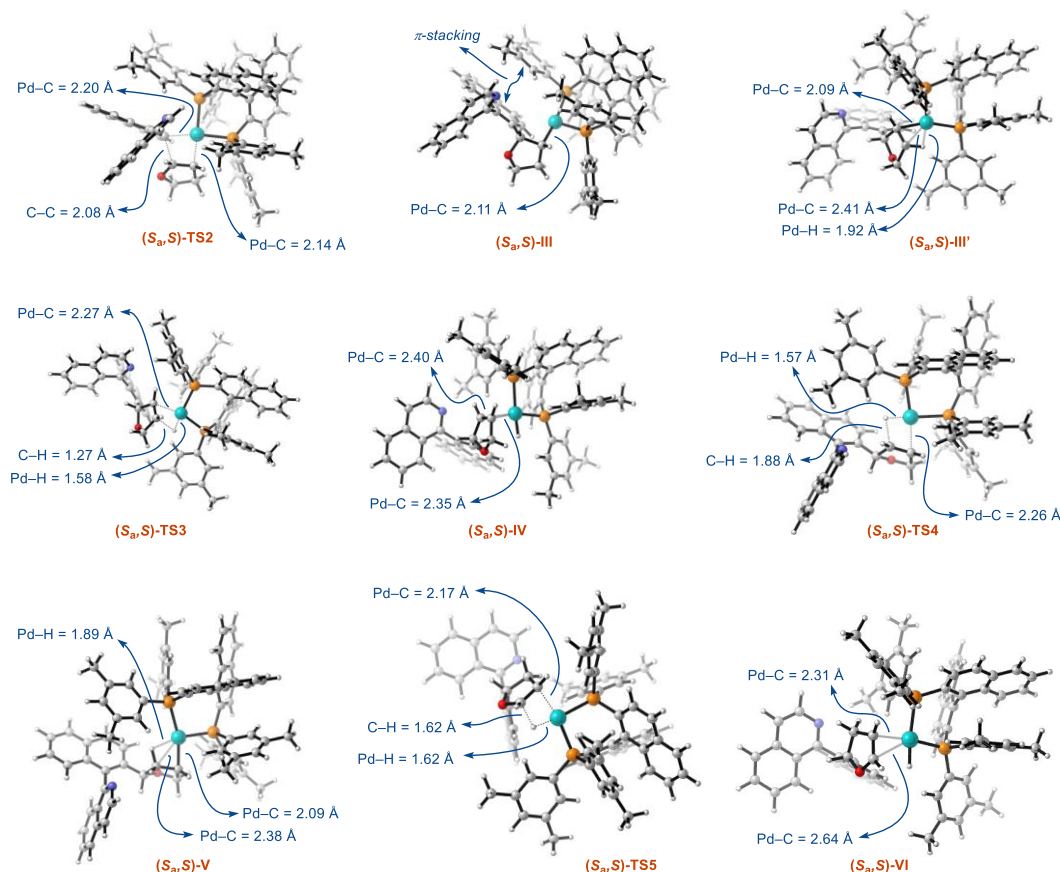


Figure II.5 – Computed energies for key intermediates and transition states performed at the M06/def2tzvpp//B3LYP/6-31G(d,p) (Pd,SDD) (IEFPCM,toluene) level. Selected 3D structures are illustrated using CYLview.¹²²

In the next step, alkene insertion into the C(Aryl)–Pd bond, four different transition states (**TS2**) were located for the four forming diastereomers: the two orientations for the isoquinoline ring, and the two possible alkene coordination modes, above or below the coordination plane in each case. Noteworthy, some of them present relatively low activation energies, with a minimum of $\Delta G^\ddagger = 10.9$ kcal/mol for (*R_aR*)-**TS2**, with an energy value actually lower than that of the previous step, (*R_a*)-**TS1**. In contrast, the highest activation energy ($\Delta G^\ddagger = 13.9$ kcal/mol) corresponds to (*S_aS*)-**TS2**, which is in contrast with the experimental results, since *S_aS* is always obtained as the major stereoisomer, with

¹²² Legault, C. Y. *CYLview*, 1.0b; Université de Sherbrooke: Sherbrooke, Canada, 2009; <http://www.cylview.org>

high levels of selectivity (in some cases, the only isomer observed). This fact suggests that **TS2** might not be the rate determining nor the stereocontrolling step, which should therefore be located at a later stage in the catalytic cycle.

The reaction evolves through **TS3** to reinstall the alkene functionality after a β -hydride elimination. It was also found that this step presents an important activation barrier, especially due to the high stability of the insertion intermediate **III**. Interestingly, the isomer preference reverses at this point, and (*S*,*S*)-**TS3** becomes the most favoured diastereomer ($\Delta G^{\ddagger}_{I \rightarrow TS3} = 12.4$ kcal/mol), in agreement with the experimental results. The corresponding diastereomeric transition states (*R*,*S*)-**TS3** or (*S*,*R*)-**TS3** are very high in energy ($\Delta G^{\ddagger}_{I \rightarrow TS3} = 25.4$ and 18.0 kcal/mol, respectively), while (*R*,*R*)-**TS3** has an activation barrier of $\Delta G^{\ddagger}_{I \rightarrow TS3} = 18.2$ kcal/mol, consistent values for the high levels of diastereoselectivity observed. Therefore, **TS3** becomes a solid candidate to be the stereodetermining step of the reaction. This proposal requires reversibility of **TS2** step, and indeed, the barrier for the reverse process from (*R*,*R*)-**III** to (*R*,*R*)-**TS2** shows an affordable energy value of 21.4 kcal/mol. On the other hand, after inspection of the structure of the elimination transition states (**TS3**) it becomes evident that they cannot be directly accessed from the previous **III** intermediates. A large reorganization of the biaryl moiety must take place to prepare the system for the β -hydride elimination step. Furthermore, a second intermediate structures **III'** were located, presenting an agostic interaction of Pd with the adjacent C–H bond from the alkene, immediately preceding the β -hydride elimination. IRC calculations starting from **TS2** and **TS3** respectively, were also performed in order to confirm the participation of intermediates **III** and **III'** in the mechanism. Unfortunately, suitable transition state(s) for the conversion of intermediates **III** into **III'** were not possible to find, but looking closely at their structures, a comparative analysis reveals that it is required a major reorganization in a sterically very crowded environment. Moreover, this reorganization appears to be particularly complex for the (*R*,*R*) isomer. For instance, the required the change in the $P_{syn}-Pd-C3_{(furan)}-C4_{(furan)}$ dihedral angle in these species is illustrative: from (*R*,*R*)-**III** to (*R*,*R*)-**III'** this angle moves from 66.6° to 150.5°, while the same rotation in the (*S*,*S*) pairs is significantly shorter

(from -93.0° to -144.0° ; Figure II.6). Furthermore, a potential energy surface scan (a mathematical function that gives the energy of a molecule as a function of its geometry¹²³) was performed for the variation of the dihedral angle in (S_a,S) -**III** from 93° to 144° without any remarkable limitation, while the angle in (R_a,R) -**III** presents a restricted rotation at the interval between 67° and 110° due to the steric collision between the isoquinoline and the aryl phosphine moieties at that point; therefore, the rotation to 150.0° would not be easily affordable. To complete this rotation, the phosphines moieties have to move largely aside with the significant energetic cost associated.

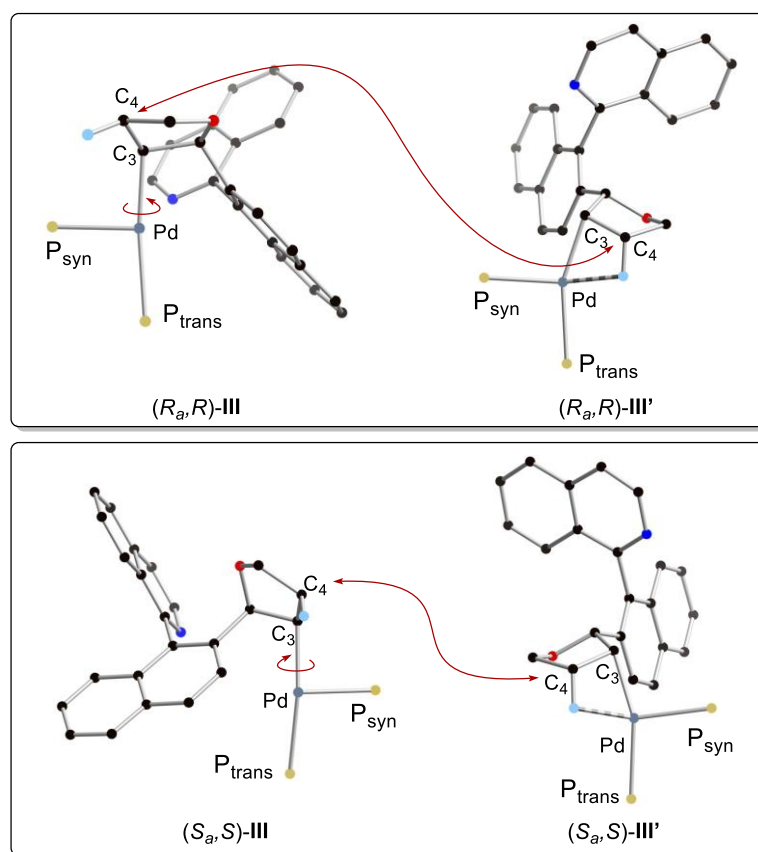


Figure II.6 – Comparison of intermediates **III** and **III'** in (S_a,S) and (R_a,R) series. Ligands omitted for clarity.

¹²³ Lewars E.G. (Ed). (2011). *The Concept of the Potential Energy Surface*. In: *Computational Chemistry*. Dordrecht: Springer.

From this point forward, intermediates **IV** can evolve to either the minor detected products **5'** by decoordination or, after reinsertion [\rightarrow **V** via **TS4**] and second β -hydride elimination [\rightarrow **VI** via **TS5**], the major (or unique, in some cases) products **5**. The activation energies for these last steps are very low ($\Delta G^\ddagger = 0.2$ and 4.2 kcal/mol for (S_a,S) -**TS4** and (S_a,S) -**TS5**, respectively) and, therefore, they would not have any relevant influence on the stereochemical outcome of the reaction.

The main conclusion that could be drawn from this mechanistic discussion is that the combination of the reversibility at **TS2**, together with a large energy difference between the isomeric **TS3** transition states and the difficulties for the reorganization from **III** to **III'** can explain the preferential formation of the (S_a,S) -**5/7** isomers. This analysis provides an unprecedented mechanistic profile that appears to be governed by the heterobiaryl moiety. In sharp contrast, the migratory insertion is responsible for the stereochemical outcome of the reaction in simpler systems and, in this cases, the asymmetric Heck reaction using (R) -BINAP or (R) -DM-BINAP ligands results in the formation of major products with the R configuration in low to moderate enantiomeric excesses.

II.4 Conclusions.

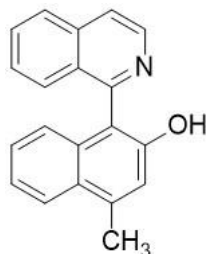
To summarize this chapter, we have developed a novel methodology for the synthesis of functionalized heterobiaryls bearing both central and axial chirality based on a dynamic kinetic asymmetric Heck reaction. The resulting products were obtained with excellent yields and regio-, diastereo- and enantioselectivities. Furthermore, the versatility of these enantioenriched products has been demonstrated through some transformations that allowed us to obtain highly interesting structures such as a N,N-ligand (*S_aS*)-**20b** or a novel class of bifunctional proline-type organocatalyst (*S_aS*)-**22b** with no precedents in literature. Importantly, no erosion on the enantiopurity was observed during any of these transformations.

Additionally, it can be concluded that the previously described DYKAT approach for the synthesis of axially chiral heterobiaryls, can be extended, by selecting the proper transformation, to the simultaneous generation of central and axial chirality elements in heterobiaryl skeletons.

II.5. Experimental Section.

II.5.1. Synthesis of alcohols precursors to nonaflates substrates.

Synthesis of 1-(Isoquinolin-1-yl)-4-methylnaphthalen-2-ol



Following the described procedure for borylation of 1-(4-methylnaphthalen-1-yl)isoquinoline (933 mg, 3.47 mmol),¹¹³ without further purification of the resulting product, the reaction crude was dissolved in THF (50 mL) and treated with a 1:1 mixture of H₂O₂ (30%)/NaOH (20 mL, 2M aq.). After stirring for 30 min at room temperature, the reaction mixture was diluted with CH₂Cl₂ (5 mL) and washed with NH₄Cl (aq.). The organic layer was dried over MgSO₄, filtered, concentrated, and the residue was purified by flash chromatography on silica gel (1:1 EtOAc/*n*-hex) to give the desired product (950 mg, 96%) as a yellowish amorphous solid.

¹H-NMR (400 MHz, CDCl₃/MeOD): δ 8.58 (d, *J* = 5.7 Hz, 1H), 7.94 (d, *J* = 8.3 Hz, 1H), 7.89 (d, *J* = 8.2 Hz, 1H), 7.74 (d, *J* = 5.7 Hz, 1H), 7.66 (t, *J* = 7.4 Hz, 1H), 7.55 (d, *J* = 8.4 Hz, 1H), 7.36 (t, *J* = 7.9 Hz, 1H), 7.29 (t, *J* = 8.3 Hz, 1H), 7.17 (t, *J* = 7.9 Hz, 1H), 7.08 (s, 1H), 6.98 (t, *J* = 8.2 Hz, 1H), 2.88 (br s, 1H), 2.66 (s, 3H).

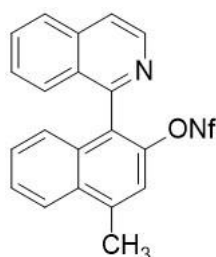
¹³C-NMR (100 MHz, CDCl₃/MeOD): δ 157.9, 152.1, 141.6, 137.4, 136.7, 133.7, 130.7, 128.6, 128.0, 127.8, 127.4, 126.8, 126.2, 125.1, 124.1, 122.9, 120.7, 119.2, 116.0, 19.4.

HRMS (ESI) calculated for C₂₀H₁₆NO (M + H⁺) 286.1226. Found 286.1224.

II.5.2. General procedure for the synthesis of nonaflates **3g** and **3h**.

Following a described procedure,¹²⁴ over a suspension of alcohol precursor (1.0 eq.) and K₂CO₃ (1.5 eq.) in dry acetonitrile (0.5 M), perfluorobutanesulfonyl fluoride (90%, 1.2 eq.) was added in one portion, and the resulting mixture was vigorously stirred for 24 h. After completion (TLC monitoring), the reaction mixture was filtered through a pad of celite, the solvent was removed in vacuum, and the residue was purified by flash column chromatography over silica gel.

Synthesis of 1-(Isoquinolin-1-yl)-4-methylnaphthalen-2-yl-1-nonaflate. **3g**



Following the general procedure from the alcohol precursor, purification afforded **3g** (1.33 g, 70%) as a yellow amorphous solid.

¹H-NMR (400 MHz, CDCl₃): δ 8.75 (d, *J* = 5.7 Hz, 1H), 8.13 (d, *J* = 8.5 Hz, 1H), 7.95 (d, *J* = 8.3 Hz, 1H), 7.82 (d, *J* = 5.7 Hz, 1H), 7.70 (t, *J* = 8.1 Hz, 1H), 7.59 (t, *J* = 8.1 Hz, 1H), 7.45–7.37 (m, 4H), 7.27 (d, *J* = 8.1 Hz, 1H), 2.86 (s, 3H).

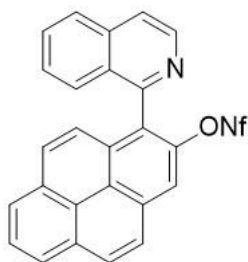
¹³C-NMR (100 MHz, CDCl₃): δ 154.2, 144.5, 142.5, 138.8, 136.3, 133.2, 131.8, 130.5, 128.6, 127.6, 127.5, 127.4, 127.2, 127.0, 126.9, 124.5, 121.1, 119.9, 19.8, (C from nonaflate group not observed).

¹⁹F-NMR (377 MHz, CDCl₃): δ -80.74 (t, *J* = 9.7 Hz), -110.20 – -110.52 (m), -121.03 – -121.38 (m), -125.82 – -126.37 (m).

HRMS (ESI) calculated for C₂₄H₁₅F₉NO₃S (M + H⁺) 568.0623. Found 568.0613.

¹²⁴ Shekhar, S.; Dunn, T. B.; Kotecki, B. J.; Montavon, D. K.; Cullen, S. C., *J Org Chem*, **2011**, *76*, 4552.

Synthesis of 1-(Isoquinolin-1-yl)pyren-2-yl-1-nonaflate. **3h**



Following the procedure for the synthesis of 1-(Isoquinolin-1-yl)-4-methylnaphthalen-2-ol, starting from 1-(pyren-1-yl)isoquinoline^{Error! Marcador no definido.} (830 mg, 2.52 mmol), without isolation of the resulting alcohol, the residue was subjected to the described general procedure for the synthesis of nonaflates to afford **3h** (285 mg, 18%) as a yellowish amorphous solid.

¹H-NMR (400 MHz, CDCl₃): δ 8.83 (d, *J* = 5.7 Hz, 1H), 8.33 (d, *J* = 7.5 Hz, 1H), 8.29 (s, 1H), 8.27 (d, *J* = 7.6 Hz, 1H), 8.24 (d, *J* = 7.6 Hz, 1H), 8.19 (d, *J* = 9.0 Hz, 1H), 8.10 (t, *J* = 7.6 Hz, 1H), 8.0 (d, *J* = 9.0 Hz, 2H), 7.89 (d, *J* = 5.7 Hz, 1H), 7.75–7.71 (m, 1H), 7.49 (d, *J* = 9.2 Hz, 1H), 7.42 (d, *J* = 3.6 Hz, 2H).

¹³C-NMR (100 MHz, CDCl₃) δ 154.6, 145.3, 142.7, 136.4, 132.8, 132.1, 131.1, 130.6, 130.5, 129.7, 129.6, 128.9, 127.7, 127.1, 127.0, 126.9, 126.7, 126.6, 126.6, 126.4, 124.8, 124.0, 123.8, 121.2, 116.5, (C from nonaflate group not observed).

¹⁹F-NMR (377 MHz, CDCl₃): δ -76.49 – -88.67 (m), -107.89 – -113.04 (m), -120.07 – -122.48 (m), -124.94 – -128.75 (m).

HRMS (ESI) calculated for C₂₉H₁₅F₉NO₃S (M + H⁺) 628.0623. Found 628.0615.

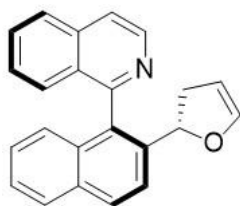
II.5.3. General procedure for the Dynamic Kinetic Asymmetric Heck Reaction

A flame-dried Schlenk tube was charged with the corresponding heterobiaryl sulfonate *rac*-**3b-i** (0.1 mmol), Pd(dba)₂ (5 mol%, 2.9 mg) and ligand **L4** or **L9** (6 mol%). After three cycles of vacuum-argon, anhydrous solvent (0.5 mL) was added and the resulting mixture was stirred for 20 min at room temperature. Then Et₃N (0.3-0.5 mmol) and the corresponding olefin (8 eq. of **4**, 5 eq. of **6** or 3 eq. of **8-12**) were sequentially added

and the resulting mixture was stirred at 80 °C for 18-96 hours. The reaction crude was allowed to reach room temperature, then brine (5 mL) was added and the resulting mixture was extracted with EtOAc (4 × 3 mL). The collected organic phases were dried over anhydrous Na₂SO₄, filtered, concentrated, and the residue was purified by column chromatography on silica gel using different CH₂Cl₂/EtOAc and Toluene/EtOAc mixtures.

Note: The racemic products were prepared by heating at 80 °C a mixture of the corresponding starting heterobiaryl sulfonate (1.0 eq.), DIPEA (3.0 eq.) and olefin (5.0-8.0 eq.) in 1 mL of solvent, using (±)-BINAP (12 mol%)/Pd(dba)₂ (10 mol%) as catalyst. Then reaction mixture was subjected to the same work-up than described for the asymmetric version, and both isomeric products were separated from reaction crude by preparative TLC prior to HPLC analysis.

Synthesis of (S)-1-{2-[(S)-2,3-Dihydrofuran-2-yl]naphthalen-1-yl}isoquinoline. **5b**



Following the general procedure from **3b** and **4**, after 18 h and further purification by flash chromatography (CH₂Cl₂→25:1 CH₂Cl₂/EtOAc) afforded **5b** (29 mg, 90%) as a light-yellow solid. The pure product was crystallized by slow diffusion of *n*-pentane into a solution of the product in DCM to give pale yellow prisms suitable for X-Ray analysis.

$[\alpha]_D^{20} -4.7$ (*c* 0.51, CHCl₃) for 97% *ee*.

¹H-NMR (400 MHz, CDCl₃): δ 8.71 (d, *J* = 5.7 Hz, 1H), 8.05 (d, *J* = 8.7 Hz, 1H), 7.93 (t, *J* = 7.7 Hz, 2H), 7.82 (d, *J* = 8.7 Hz, 1H), 7.78 (dd, *J* = 5.8 and 0.8 Hz, 1H), 7.69 (ddd, *J* = 8.2, 6.7 and 1.3 Hz, 1H), 7.49 (dd, *J* = 8.5 and 1.1 Hz, 1H), 7.47–7.42 (m, 1H), 7.42–7.38 (m, 1H), 7.25 (td, *J* = 7.6, 6.8 and 1.3 Hz, 1H), 7.01 (dd, *J* = 8.6 and 1.1 Hz, 1H), 6.38 (d, *J* = 2.6 Hz, 1H), 5.02 (t, *J* = 10.0 Hz, 1H), 4.90 (q, *J* = 2.6 Hz, -1H), 3.04–2.29 (m, 2H).

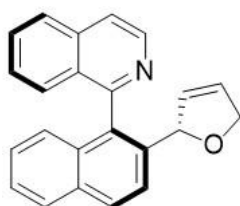
^{13}C -NMR (100 MHz, CDCl_3) δ 159.3, 145.3, 142.5, 139.3, 136.2, 133.3, 133.0, 132.3, 130.6, 130.0, 128.5, 128.0, 127.8, 127.3, 126.9, 126.5, 126.2, 125.9, 123.0, 120.4, 99.6, 80.3, 38.4.

HRMS (ESI) calculated for $\text{C}_{23}\text{H}_{18}\text{NO}$ ($\text{M} + \text{H}^+$) 324.1383. Found 324.1381.

HPLC (AD-H column, 85:15 *n*-hex/IPA, 30 °C, 1.0 mL/min): t_{R} 7.32 min (minor) and 9.56 min (major).

M. p. 68-70 °C.

Synthesis of (S)-1-{2-[(S)-2,5-Dihydrofuran-2-yl]naphthalen-1-yl}isoquinoline. 5'b



Following the general procedure from **3b(Br)**¹²⁵ and **4**, with NaO^tBu instead of DIPEA, after 72 h and further purification by flash chromatography ($\text{CH}_2\text{Cl}_2 \rightarrow 25:1 \text{CH}_2\text{Cl}_2/\text{EtOAc}$) afforded **5'b** (6.5 mg, 20%) as a light-yellow amorphous solid.

$[\alpha]_{\text{D}}^{20} -80.8$ (*c* 0.08, CHCl_3) for 93% *ee*.

^1H -NMR (400 MHz, CDCl_3): δ 8.75 (d, $J = 5.8$ Hz, 1H), 8.06 (d, $J = 8.6$ Hz, 1H), 8.00 (d, $J = 8.2$ Hz, 1H), 7.94 (d, $J = 8.2$ Hz, 1H), 7.88 (d, $J = 5.9$ Hz, 1H), 7.77 (t, $J = 7.6$ Hz, 1H), 7.67 (d, $J = 8.5$ Hz, 1H), 7.57 (d, $J = 8.4$ Hz, 1H), 7.47 (td, $J = 7.7$ and 3.1 Hz, 2H), 7.28 (dd, $J = 8.5$ and 7.0 Hz, 1H), 6.97 (d, $J = 8.5$ Hz, 1H), 6.12 – 6.02 (m, 1H), 5.96 (dt, $J = 6.3$ and 1.9 Hz, 1H), 5.40 (td, $J = 4.2$ and 2.0 Hz, 1H), 4.92 (ddt, $J = 12.9$, 6.3 and 2.0 Hz, 1H), 4.64 (ddt, $J = 12.9$, 4.2 and 1.9 Hz, 1H).

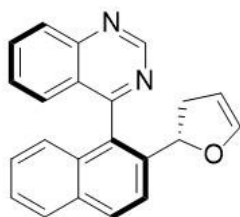
¹²⁵ Thaler, T.; Geittner, F.; Knochel, P. *Synlett*, **2007**, 17, 2655.

^{13}C -NMR (100 MHz, CDCl_3) δ 159.0, 140.7, 138.9, 136.6, 133.0, 132.3, 131.5, 130.8, 129.8, 128.5, 128.3, 128.1, 127.8, 126.9, 126.6, 126.0, 125.9, 125.9, 124.2, 121.0, 85.6, 77.3, 76.4.

HRMS (ESI) calculated for $\text{C}_{23}\text{H}_{18}\text{NO}$ ($\text{M} + \text{H}^+$) 324.1383. Found 324.1380.

HPLC (IA column, 85:15 *n*-hex/IPA, 30 °C, 1.0 mL/min): t_{R} 6.52 min (minor) and 7.54 min (major).

Synthesis of (S)-4-{2-[(S)-2,3-Dihydrofuran-2-yl]naphthalen-1-yl}quinazoline. 5c



Following the general procedure from **3c** and **4**, after 48 h and further purification by flash chromatography ($\text{CH}_2\text{Cl}_2 \rightarrow 20:1 \text{ CH}_2\text{Cl}_2/\text{EtOAc}$) afforded **5c** (30 mg, 92%) as a yellow amorphous solid.

$[\alpha]_{\text{D}}^{20} +8.2$ (*c* 0.61, CHCl_3) for 94% *ee*.

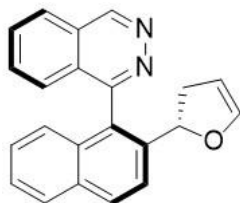
^1H -NMR (400 MHz, CDCl_3) δ 9.51 (s, 1H), 8.18 (dd, $J = 8.6$ and 1.0 Hz, 1H), 8.08 (d, $J = 8.7$ Hz, 1H), 7.94 (d, $J = 8.4$ Hz, 2H), 7.82 (d, $J = 8.7$ Hz, 1H), 7.48 (ddd, $J = 7.9$, 4.6 and 1.2 Hz, 3H), 7.30 (ddd, $J = 8.3$, 6.9 and 1.2 Hz, 1H), 7.00 (dd, $J = 8.6$ and 1.2 Hz, 1H), 6.37 (q, $J = 2.5$ Hz, 1H), 5.01 (dd, $J = 10.7$ and 9.1 Hz, 1H), 4.92 (q, $J = 2.6$ Hz, 1H), 2.84 (ddt, $J = 15.6$, 10.7 and 2.4 Hz, 1H), 2.72 (ddt, $J = 15.7$, 9.1 and 2.4 Hz, 1H)

^{13}C -NMR (100 MHz, CDCl_3): δ 168.5, 154.9, 150.4, 145.3, 139.2, 134.5, 132.9, 131.5, 130.8, 130.4, 128.8, 128.4, 128.2, 127.0, 127.0, 126.2, 125.6, 125.2, 123.0, 99.6, 80.0, 38.6.

HRMS (ESI) calculated for $\text{C}_{22}\text{H}_{17}\text{N}_2\text{O}$ ($\text{M} + \text{H}^+$) 325.1335. Found 325.1332.

HPLC (AD-H column, 90:10 *n*-hex/IPA, 30 °C, 0.7 mL/min): t_{R} 16.25 min (major) and 17.61 min (minor).

Synthesis of (S)-1-{2-[(S)-2,3-Dihydrofuran-2-yl]naphthalen-1-yl}phthalazine. **5d**



Following the general procedure from **3d** and **4**, after 72 h and further purification by flash chromatography ($\text{CH}_2\text{Cl}_2 \rightarrow 10:1 \text{ CH}_2\text{Cl}_2/\text{EtOAc}$) afforded **5d** (17 mg, 52%) as a beige amorphous solid.

$[\alpha]_D^{20} +3.4$ (c 0.28, CHCl_3) for 90% *ee*.

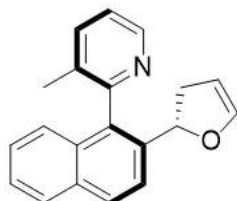
$^1\text{H-NMR}$ (400 MHz, CDCl_3): δ 9.67 (s, 1H), 8.10 (d, $J = 8.7$ Hz, 1H), 8.09 (dt, $J = 8.2$ and 1.0 Hz, 1H), 7.94 (d, $J = 7.9$ Hz, 1H), 7.92 (ddd, $J = 8.2$, 7.0 and 1.1 Hz, 1H), 7.84 (d, $J = 8.7$ Hz, 1H), 7.73 (ddd, $J = 8.2$, 7.0 and 1.1 Hz, 1H), 7.50–7.45 (m, 1H), 7.47–7.43 (m, 1H), 7.31–7.25 (m, 1H), 7.01 (dd, $J = 8.5$ and 1.0 Hz, 1H), 6.36 (q, $J = 2.4$ Hz, 1H), 5.00 (dd, $J = 10.7$ and 9.2 Hz, 1H), 4.93 (q, $J = 2.6$ Hz, 1H), 2.89 (ddt, $J = 15.6$, 10.7 and 2.4 Hz, 1H), 2.78 (ddt, $J = 15.9$, 9.1 and 2.4 Hz, 1H).

$^{13}\text{C-NMR}$ (100 MHz, CDCl_3): δ 159.2, 151.1, 145.1, 140.0, 133.2, 132.9, 132.9, 132.2, 130.3, 129.8, 128.2, 127.1, 126.8, 126.5, 126.4, 126.2, 126.1, 125.9, 123.1, 99.9, 80.2, 38.5.

HRMS (ESI) calculated for $\text{C}_{22}\text{H}_{17}\text{N}_2\text{O}$ ($\text{M} + \text{H}^+$) 325.1335. Found 325.1334.

HPLC (AD-H column, 85:15 *n*-hex/IPA, 30 °C, 1 mL/min): t_R 18.18 min (minor) and 24.54 min (major).

Synthesis of (S)-2-{2-[(S)-2,3-Dihydrofuran-2-yl]naphthalen-1-yl}-3-methylpyridine. **5e**



Following the general procedure from **3e** and **4**, after 24 h and further purification by flash chromatography (CH₂Cl₂→10:1 CH₂Cl₂/EtOAc) afforded **5e** (28.5 mg, 99%) as a beige amorphous solid.

$[\alpha]_D^{20}$ -4.9 (*c* 0.35, CHCl₃) for >99% *ee*.

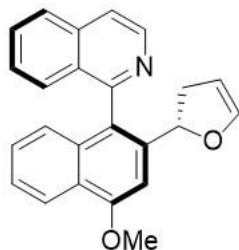
¹H-NMR (400 MHz, CDCl₃) δ 8.62 (dd, *J* = 4.9 and 1.7 Hz, 1H), 7.97 (d, *J* = 8.7 Hz, 1H), 7.92–7.86 (m, 1H), 7.74 (d, *J* = 8.7 Hz, 1H), 7.72–7.66 (m, 1H), 7.46 (ddd, *J* = 8.2, 6.8 and 1.2 Hz, 1H), 7.36 (ddd, *J* = 8.3, 6.8 and 1.4 Hz, 1H), 7.32 (dd, *J* = 7.7 and 4.8 Hz, 1H), 7.14 (dd, *J* = 8.4 and 1.0 Hz, 1H), 6.44 (q, *J* = 2.6 Hz, 1H), 5.13 (dd, *J* = 10.7 and 9.2 Hz, 1H), 4.95 (q, *J* = 2.6 Hz, 1H), 2.83 (ddt, *J* = 15.5, 10.7 and 2.4 Hz, 1H), 2.71 (ddt, *J* = 15.7, 9.2 and 2.4 Hz, 1H), 2.03 (s, 3H).

¹³C-NMR (100 MHz, CDCl₃): δ 157.2, 147.3, 145.3, 137.9, 137.8, 134.8, 133.2, 133.1, 131.3, 129.1, 128.1, 126.5, 125.8, 125.5, 123.1, 122.7, 99.7, 80.3, 38.2, 18.9.

HRMS (ESI) calculated for C₂₀H₁₈NO (M + H⁺) 288.1383. Found 288.1385.

HPLC (IB column, 98:2 *n*-hex/IPA, 30 °C, 1 mL/min): *t_R* 8.43 min (minor) and 8.92 min (major).

Synthesis of (S)-1-{2-[(S)-2,3-Dihydrofuran-2-yl]-4-methoxynaphthalen-1-yl}isoquinoline. **5f**



Following the general procedure from **3f** and **4**, after 96 h and further purification by flash chromatography (CH₂Cl₂→25:1 CH₂Cl₂/EtOAc) afforded **5f** (19 mg, 53%) as a beige amorphous solid.

$[\alpha]_D^{20}$ -34.4 (*c* 0.17, CHCl₃) for 99% *ee*.

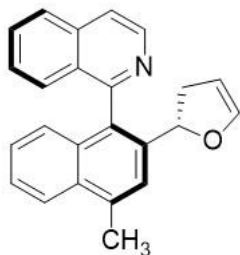
¹H-NMR (400 MHz, CDCl₃): δ 8.70 (d, *J* = 5.7 Hz, 1H), 8.34 (ddd, *J* = 8.4, 1.4 and 0.7 Hz, 1H), 7.92 (dt, *J* = 8.3, 1.0 Hz, 1H), 7.75 (dd, *J* = 5.8 and 0.9 Hz, 1H), 7.68 (ddd, *J* = 8.2, 6.8 and 1.3 Hz, 1H), 7.53 (dd, *J* = 8.5 and 1.1 Hz, 1H), 7.45–7.41 (m, 1H), 7.41–7.38 (m, 1H), 7.28–7.24 (m, 1H), 7.12 (s, 1H), 6.95 (ddd, *J* = 8.5, 1.2 and 0.7 Hz, 1H), 6.40 (q, *J* = 2.3 Hz, 1H), 5.01 (t, *J* = 10.1 Hz, 1H), 4.92–4.90 (m, 1H), 4.12 (s, 3H), 2.76 (q, *J* = 2.4 Hz, 1H), 2.73 (q, *J* = 2.3 Hz, 1H).

¹³C-NMR (100 MHz, CDCl₃) δ 159.5, 156.5, 145.2, 142.5, 139.6, 136.3, 133.6, 130.5, 128.8, 127.7, 127.4, 127.0, 126.8, 125.9, 125.3, 125.2, 122.0, 120.3, 100.3, 99.8, 80.7, 55.7, 38.4.

HRMS (ESI) calculated for C₂₄H₂₀NO₂ (M + H⁺) 354.1489. Found 354.1487.

HPLC (AD-H column, 85:15 *n*-hex/IPA, 30 °C, 1.0 mL/min): *t*_R 8.28 min (minor) and 11.99 min (major).

Synthesis of (S)-1-{2-[(S)-2,3-Dihydrofuran-2-yl]-4-methylnaphthalen-1-yl}isoquinoline. **5g**



Following the general procedure from **3g** and **4**, after 48 h and further purification by flash chromatography ($\text{CH}_2\text{Cl}_2 \rightarrow 10:1 \text{ CH}_2\text{Cl}_2/\text{EtOAc}$) afforded **5g** (28 mg, 84%) as a beige amorphous solid.

$[\alpha]_D^{20} -8.3$ (c 0.37, CHCl_3) for >99% *ee*.

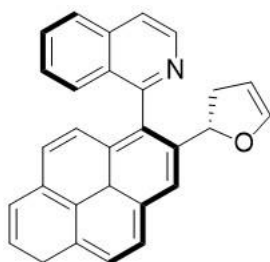
$^1\text{H-NMR}$ (400 MHz, CDCl_3) δ 8.70 (d, $J = 5.7$ Hz, 1H), 8.07 (d, $J = 8.4$ Hz, 1H), 7.93 (d, $J = 8.2$ Hz, 1H), 7.76 (d, $J = 5.7$ Hz, 1H), 7.68 (t, $J = 7.9$ Hz, 1H), 7.64 (s, 1H), 7.51–7.46 (m, 2H), 7.39 (t, $J = 7.6$ Hz, 1H), 7.26 (t, $J = 8.4$ Hz, 1H), 7.02 (d, $J = 8.4$ Hz, 1H), 6.38 (q, $J = 2.5$ Hz, 1H), 5.50 (t, $J = 10.0$ Hz, 1H), 4.90 (q, $J = 2.5$ Hz, 1H), 2.82 (s, 3H), 2.77–2.72 (m, 2H).

$^{13}\text{C-NMR}$ (100 MHz, CDCl_3): δ 159.5, 145.2, 142.4, 138.7, 136.2, 136.0, 132.4, 132.2, 131.7, 130.5, 128.6, 127.7, 127.4, 126.8, 126.1, 125.7, 124.2, 123.4, 120.3, 99.6, 80.3, 38.3, 19.8.

HRMS (ESI) calculated for $\text{C}_{24}\text{H}_{20}\text{NO}$ ($\text{M} + \text{H}^+$) 338.1539. Found 338.1535.

HPLC (AD-H column, 90:10 *n*-hex/IPA, 30 °C, 1 mL/min): t_R 11.27 min (major, single peak observed).

Synthesis of (S)-1-{2-[(S)-2,3-Dihydrofuran-2-yl]pyren-1-yl}isoquinoline. **5h**



Following the general procedure from **3h** and **4**, after 48 h and further purification by flash chromatography (CH₂Cl₂→25:1 CH₂Cl₂/EtOAc) afforded **5h** (26.4 mg, 66%) as a light yellow amorphous solid.

$[\alpha]_D^{20} +116.4$ (*c* 0.19, CHCl₃) for 98% *ee*.

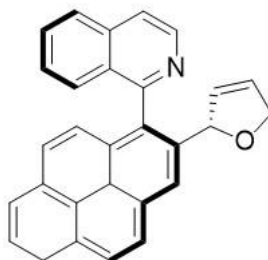
¹H-NMR (400 MHz, CDCl₃): δ 8.82 (d, *J* = 5.7 Hz, 1H), 8.57 (s, 1H), 8.25 (d, *J* = 7.6 Hz, 1H), 8.23 (d, 9.0 Hz, 1H), 8.18 (d, 9.2 Hz, 1H), 8.15 (d, *J* = 7.0 Hz, 1H), 8.04 (d, *J* = 7.6 Hz, 1H), 8.00 (d, *J* = 8.3 Hz, 1H), 7.90 (d, *J* = 9.2 Hz, 1H), 7.87 (d, *J* = 5.7 Hz, 1H), 7.73 (ddd, *J* = 8.2, 6.2, 1.7 Hz, 1H), 7.44–7.37 (m, 2H), 7.32 (d, *J* = 9.2 Hz, 1H), 6.54 (q, *J* = 2.4 Hz, 1H), 5.30 (t, *J* = 9.9 Hz, 1H), 4.97 (q, *J* = 2.6 Hz, 1H), 2.87 (t, *J* = 2.4 Hz, 1H), 2.85 (t, *J* = 2.4 Hz, 1H).

¹³C-NMR (100 MHz, CDCl₃) δ 159.5, 145.2, 142.5, 140.0, 136.2, 131.9, 131.3, 131.2, 130.7, 130.6, 129.9, 128.7, 128.0, 127.9, 127.8, 127.6, 127.3, 126.9, 126.0, 125.4, 125.2, 125.1, 124.5, 124.1, 121.4, 120.5, 99.5, 80.7, 39.2.

HRMS (ESI) calculated for C₂₉H₂₀NO (M + H⁺) 398.1539. Found 398.1532.

HPLC (AD-H column, 90:10 *n*-hex/IPA, 30 °C, 1.0 mL/min): *t*_R 14.73 min (major) and 19.70 min (minor).

Synthesis of (S)-1-{2-[(S)-2,5-Dihydrofuran-2-yl]pyren-1-yl}isoquinoline. **5'h**



Following the general procedure from **3h** and **4**, after 48 h and further purification by flash chromatography (CH₂Cl₂→25:1 CH₂Cl₂/EtOAc) afforded **5'h** (5 mg, 13%) as a light yellow amorphous solid.

$[\alpha]_D^{20} +41.9$ (*c* 0.14, CHCl₃) for 91% *ee*.

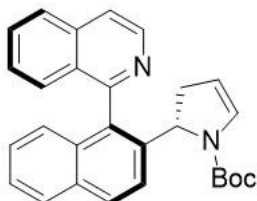
¹H-NMR (400 MHz, CDCl₃): δ 8.80 (d, *J* = 5.8 Hz, 1H), 8.40 (s, 1H), 8.22 (d, *J* = 7.5 Hz, 1H), 8.16 (d, *J* = 9.1 Hz, 1H), 8.13 (d, *J* = 9.0 Hz, 1H), 8.12 (d, *J* = 7.6 Hz, 1H), 8.02–7.98 (m, 2H), 7.89 (d, *J* = 5.8 Hz, 1H), 7.86 (d, *J* = 9.2 Hz, 1H), 7.74 (t, *J* = 6.8 Hz, 1H), 7.42–7.36 (m, 2H), 7.23 (d, *J* = 9.2 Hz, 1H), 6.14 (br s, 1H), 5.95 (d, *J* = 4.5 Hz, 1H), 5.62 (br s, 1H), 5.05 (dd, *J* = 12.6, 5.5 Hz, 1H), 4.71 (d, *J* = 12.6 Hz, 1H).

¹³C-NMR (100 MHz, CDCl₃) δ 159.7, 142.4, 139.3, 136.2, 131.8, 131.5, 131.4, 131.3, 130.7, 130.6, 129.9, 128.9, 127.9, 127.8, 127.8, 127.6, 127.5, 126.8, 126.0, 125.4, 125.2, 125.1, 124.5, 124.2, 122.8, 120.5, 86.0, 76.4.

HRMS (ESI) calculated for C₂₉H₂₀NO (M + H⁺) 398.1539. Found 398.1532.

HPLC (IA column, 90:10 *n*-hex/IPA, 30 °C, 1.0 mL/min): *t*_R 11.02 min (major) and 15.99 min (minor).

Synthesis of *N*-Boc protected (S)-1-{2-[(S)-2,3-dihydro-1*H*-pyrrol-2-yl]naphthalen-1-yl}isoquinoline. **7b**



Following the general procedure from **3b** and **6**, after 36 h and further purification by flash chromatography (CH₂Cl₂→25:1 CH₂Cl₂/EtOAc) afforded **7b** (32 mg, 76%) as a light yellow amorphous solid. NMR spectra showed a *ca.* 3:2 mixture of Boc rotamers when the experiment was recorded at 298K.

$[\alpha]_D^{20} -19.18$ (*c* 0.50, CHCl₃) for 99% *ee*.

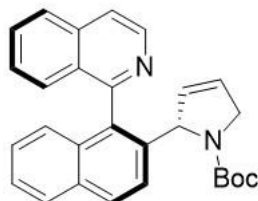
¹H-NMR (400 MHz, CDCl₃): δ 8.72 (br s, 1H), 7.98 (d, *J* = 8.8 Hz, 1H), 7.95–7.90 (m, 2.4H), 7.78–7.76 (m, 1H), 7.71 (t, *J* = 7.2 Hz, 1H), 7.57 (br s, 0.6H), 7.52 (d, *J* = 8.6 Hz, 1H), 7.41 (br s, 2H), 7.22 (br s, 1H), 6.97–6.90 (m, 1H), 6.77 (br s, 0.6H), 6.61 (br s, 0.4H), 4.88 (br s, 1H), 4.77 (br s, 1H), 2.82–2.76 (m, 1.6H), 2.67 (br s, 0.4H), 1.40 (s, 3.6H), 1.26 (s, 5.4H).

¹³C-NMR (100 MHz, CDCl₃) δ 159.3, 142.6 (br s), 142.4 (br s), 140.6 (br s), 136.3, 132.9, 132.6 (br s), 130.5 (br s), 130.1 (br s), 129.1 (br s), 128.9 (br s), 127.9, 127.4 (br s), 126.9 (br s), 126.3, 125.7, 125.3, 122.1 (br s), 121.8 (br s), 120.3, 106.4 (br s), 105.6 (br s), 80.5 (br s), 58.7 (br s), 41.6 (br s), 28.4.

HRMS (ESI) calculated for C₂₈H₂₇N₂O₂ (M + H⁺) 423.2067. Found 423.2064.

HPLC (AD-H column, 85:15 *n*-hex/IPA, 30 °C, 1.0 mL/min): *t*_R 4.63 min (minor) and 5.48 min (major).

Synthesis of *N*-Boc protected (S)-1-{2-[(S)-2,5-dihydro-1*H*-pyrrol-2-yl]naphthalen-1-yl}isoquinoline. **7'b**



Following the general procedure from **3b** and **6**, after 36 h and further purification by flash chromatography (CH₂Cl₂→25:1 CH₂Cl₂/EtOAc) afforded **7'b** (8 mg, 18%) as a light yellow solid. NMR spectra showed a *ca.* 7:3 mixture of Boc rotamers when the experiment was recorded at 298K. The pure product was crystallized by slow diffusion of *n*-pentane into a solution of the product in DCM to give pale yellow prisms suitable for X-Ray analysis.

$[\alpha]_D^{20}$ -205.1 (*c* 0.47, CHCl₃) for 99% *ee*.

¹H-NMR (400 MHz, CDCl₃): δ 8.78 (d, *J* = 5.7 Hz, 0.7H), 8.74 (d, *J* = 5.7 Hz, 0.3H), 7.96 (ddt, *J* = 27.2, 18.9, 8.6 Hz, 3.4H), 7.82 (d, *J* = 5.7 Hz, 0.7H), 7.79 (d, *J* = 5.7 Hz, 0.3H), 7.78 – 7.68 (m, 1H), 7.61 (d, *J* = 8.4 Hz, 0.7H), 7.56 (d, *J* = 8.7 Hz, 0.7H), 7.54 – 7.47 (m, 0.4H), 7.45 (ddd, *J* = 8.1, 6.8, 1.1 Hz, 0.8H), 7.43 – 7.34 (m, 1H), 7.29 – 7.18 (m, 1H), 6.97 (d, *J* = 8.5 Hz, 0.7H), 6.90 (d, *J* = 8.5 Hz, 0.3H), 6.07 (dq, *J* = 6.6, 2.2 Hz, 0.7H), 6.02 – 5.90 (m, 0.3H), 5.73 – 5.67 (m, 1H), 5.24 (br s, 0.3H), 5.17 (dt, *J* = 5.3, 2.4 Hz, 0.7H), 4.50 – 4.15 (m, 2H), 1.45 (s, 2H), 1.29 (s, 7H).

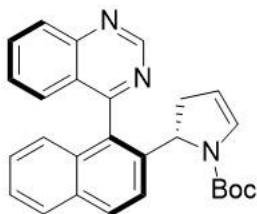
¹³C-NMR (100 MHz, CDCl₃) δ 159.7, 154.3, 142.6, 138.7, 136.3, 132.8, 132.7, 132.5, 132.3, 131.9, 130.8, 130.5, 129.4, 129.2, 128.8, 128.2, 128.1, 127.9, 127.7, 127.4, 127.0, 126.4, 125.7, 125.5, 125.4, 123.7, 123.4, 122.8, 120.5, 80.0, 79.2, 66.6, 54.6, 29.7, 28.6.

HRMS (ESI) calculated for C₂₈H₂₇N₂O₂ (M + H⁺) 423.2067. Found 423.2067.

HPLC (IA column, 98:2 *n*-hex/IPA, 30 °C, 1.0 mL/min): *t_R* 12.45 min (minor) and 15.45 min (major).

M.p. 152-157 °C.

Synthesis of *N*-Boc protected (S)-4-{2-[(S)-2,3-dihydro-1*H*-pyrrol-2-yl]naphthalen-1-yl}quinazoline. **7c**



Following the general procedure from **3c** and **6**, after 48 h and further purification by flash chromatography (CH₂Cl₂→25:1 CH₂Cl₂/EtOAc) afforded **7c** (32 mg, 76%) as a light yellow amorphous solid. NMR spectra showed a *ca.* 1:1 mixture of Boc rotamers when the experiment was recorded at 298K.

$[\alpha]_D^{20} +6.13$ (*c* 0.30, CHCl₃) for 96% *ee*.

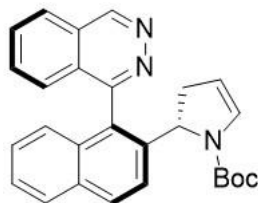
¹H-NMR (400 MHz, CDCl₃): δ 9.53–9.49 (br s, 1H), 8.21–8.18 (br s, 1H), 8.01 (d, *J* = 9.0 Hz, 1H), 7.97–7.88 (br s, 2H), 7.81 (br s, 0.5H), 7.54 (d, *J* = 8.5 Hz, 1H), 7.52–7.36 (br s, 2.5H), 7.28–7.23 (m, 1H), 6.96–6.90 (m, 1H), 6.77 (br s, 0.5H), 6.59 (br s, 0.5H), 4.90–4.85 (m, 1H), 4.74 (br s, 1H), 2.96–2.85 (m, 1H), 2.77–2.59 (m, 1H), 1.39 (s, 4.5H), 1.21 (s, 4.5H).

¹³C-NMR (100 MHz, CDCl₃) δ 168.9, 154.9 (br s), 154.7, 150.7, 150.4, 140.7 (br s), 140.2 (br s), 134.4 (br s), 134.3, 134.0, 133.6, 132.4 (br s), 132.0, 131.4, 130.3 (br s), 130.1 (br s), 129.9, 129.8 (br s), 128.9 (br s), 128.8, 128.4, 128.1 (br s), 127.8, 127.7, 127.3 (br s), 126.8, 126.7, 126.3, 125.6, 125.4, 125.3, 125.0, 124.8, 122.1 (br s), 121.9 (br s), 106.1 (br s), 105.5 (br s), 80.5 (br s), 80.1 (br s), 58.5 (br s), 58.2 (br s), 41.9, 39.7, 28.3.

HRMS (ESI) calculated for C₂₇H₂₆N₃O₂ (M + H⁺) 424.2020. Found 424.2014.

HPLC (AD-H column, 85:15 *n*-hex/IPA, 30 °C, 1.0 mL/min): *t_R* 4.72 min (minor) and 5.87 min (major).

Synthesis of *N*-Boc protected (S)-1-{2-[(S)-2,3-dihydro-1*H*-pyrrol-2-yl]naphthalen-1-yl}phthalazine. **5d**



Following the general procedure from **3d** and **6**, after 60 h and further purification by flash chromatography (CH₂Cl₂→10:1 CH₂Cl₂/EtOAc) afforded **7d** (34 mg, 80%) as a yellowish amorphous solid. The product was isolated as a mixture of **7d/7'd**. NMR spectra showed a *ca.* 3:2 mixture of Boc rotamers when the experiment was recorded at 298K.

$[\alpha]_D^{20}$ -2.3 (*c* 0.69, CHCl₃) for 98% *ee*.

¹H-NMR (400 MHz, CDCl₃): δ 9.66 (s, 1H), 8.11–8.02 (m, 2H), 7.98–7.91 (m, 2H), 7.78 (br s, 1H), 7.73–7.64 (m, 0.6H), 7.56 (d, *J* = 8.6 Hz, 1H), 7.55–7.48 (m, 0.4H), 7.43 (br s, 1H), 7.24 (br s, 1H), 6.96–6.87 (m, 1H), 6.76 (br s, 0.4H), 6.61 (br s, 0.6H), 4.91–4.88 (m, 1H), 4.70 (br s, 1H), 2.97–2.70 (m, 2H), 1.38 (s, 5.4H), 1.20 (s, 3.6H).

¹³C-NMR (100 MHz, CDCl₃) δ 159.7 (br s), 151.0, 141.5 (br s), 141.1 (br s), 133.6, 132.8, 132.8, 132.6, 132.5, 132.4, 130.2-129.6 (br s), 128.3, 128.0 (br s), 127.7 (br s), 126.6-126.4 (br s), 126.1, 125.9 (br s), 125.6, 125.5, 125.4, 125.2, 122.9, 122.2 (br s), 121.9 (br s), 106.5 (br s), 105.8 (br s), 80.4 (br s), 80.0 (br s), 58.3 (br s), 41.9 (br s), 39.7 (br s), 28.3.

HRMS (ESI) calculated for C₂₇H₂₆N₃O₂ (M + H⁺) 424.2020. Found 424.2011.

HPLC (AD-H column, 85:15 *n*-hex/IPA, 30 °C, 1.0 mL/min): *t*_R 7.68 min (minor) and 13.40 min (major).

Synthesis of *N*-Boc protected (*S*)-2-{2-[(*S*)-2,3-dihydro-1*H*-pyrrol-2-yl]naphthalen-1-yl}-3-methylpyridine. **7e**



Following the general procedure from **3e** and **6**, after 48 h and further purification by flash chromatography (CH₂Cl₂→10:1 CH₂Cl₂/EtOAc) afforded **7e** (26 mg, 70%) as a light yellow amorphous solid. NMR spectra showed a *ca.* 3:2 mixture of Boc rotamers when the experiment was recorded at 298K.

$[\alpha]_D^{20} -17.1$ (*c* 0.86, CHCl₃) for 99% *ee*.

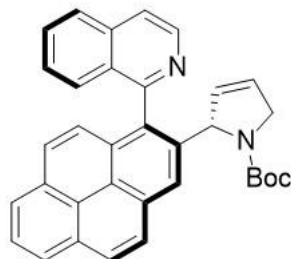
¹H NMR (400 MHz, CDCl₃): δ 8.61 (br s, 1H), 7.89 (d, *J* = 8.6 Hz, 1H), 7.86 (m, 1H), 7.69 (d, *J* = 7.6 Hz, 1H), 7.44 (d, *J* = 8.6 Hz, 1H), 7.41 (m, 1H), 7.33–7.27 (m, 2H), 7.10 (d, *J* = 8.4 Hz, 1H), 6.79 (br s, 0.4H), 6.65 (br s, 0.6H), 4.88 (br s, 1H), 4.80 (br s, 1H), 2.88–2.54 (m, 2H), 2.18 (br s, 3H), 1.41 (s, 5.4H), 1.26 (s, 2.6H).

¹³C NMR (100 MHz, CDCl₃) δ 158.4, 157.6 (br s), 151.1 (br s), 147.3–146.9, 146.9, 139.3, 138.2, 137.8, 137.8, 137.7, 134.1 (br s), 133.6, 132.7, 132.4, 131.9 (br s), 131.7 (br s), 131.3, 130.3 (br s), 128.9, 128.8, 128.3, 128.3, 128.2, 128.0, 126.3, 126.3, 126.2, 125.7, 125.3, 125.3, 125.2, 125.0, 122.5 (br s), 122.4, 121.8 (br s), 106.3 (br s), 105.8 (br s), 80.7 (br s), 79.9 (br s), 58.7, (br s), 58.0 (br s), 39.6 (br s), 28.5, 28.4, 19.2, 18.9.

HRMS (ESI) calcd for C₂₅H₂₇N₂O₂ (M + H⁺) 387.2067. Found 387.2062.

HPLC (AD-H column, 90:10 *n*-hex/IPA, 30 °C, 1.0 mL/min): *t*_R 4.52 min (minor) and 5.10 min (major).

Synthesis of *N*-Boc protected (*S*)-1-{2-[(*S*)-2,5-dihydro-1*H*-pyrrol-2-yl]pyren-1-yl}isoquinoline. 7'h



Following the general procedure from **3h** and **6**, after 48 h and further purification by flash chromatography (CH₂Cl₂→25:1 CH₂Cl₂/EtOAc) afforded **7'h** (29.8 mg, 60%) as a light yellow amorphous solid. NMR spectra showed a *ca* 3:1 mixture of Boc rotamers when the experiment was recorded at 298K. Data for the major rotamer are given.

$[\alpha]_D^{20}$ -27.6 (*c* 0.26 CHCl₃) for >99% *ee*.

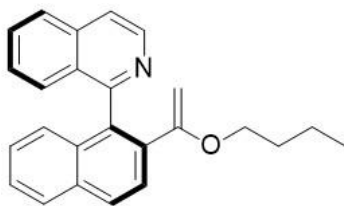
¹H NMR (400 MHz, CDCl₃, 298K): δ 8.82 (d, *J* = 5.7 Hz, 1H), 8.23–8.18 (m, 2H), 8.16–8.08 (m, 3H), 8.01–7.97 (m, 2H), 7.85 (d, *J* = 13.2 Hz, 1H), 7.84 (d, *J* = 8.7 Hz, 1H), 7.72 (t, *J* = 7.6 Hz, 1H), 7.48 (d, *J* = 8.3 Hz, 1H), 7.32 (t, *J* = 7.6 Hz, 1H), 7.20 (d, *J* = 9.2 Hz, 1H), 6.19 (d, *J* = 5.9 Hz, 1H), 5.70 (d, *J* = 6.1 Hz, 1H), 5.36 (br s, 1H), 4.55 (dd, *J* = 15.6 and 5.2 Hz, 1H), 4.39 (dd, *J* = 15.6 and 1.6 Hz, 1H), 1.18 (s, 9H).

¹³C NMR (100 MHz, CDCl₃) δ 159.6, 154.4, 142.5, 139.1, 136.3, 132.7, 131.8, 131.2, 130.6, 130.8, 130.3, 128.5, 128.0, 127.9, 127.5, 127.4, 127.0, 125.4, 125.2, 124.9, 124.7, 124.5, 123.8, 123.2, 121.2, 120.7, 79.9, 66.8, 54.6, 28.5.

HRMS (ESI) calculated for C₃₄H₂₉N₂O₂ (M + H⁺) 497.2214. Found 497.2224.

HPLC (IA column, 90:10 *n*-hex/IPA, 30 °C, 1.0 mL/min): *t*_R 6.86 min (minor) and 10.08 min (major).

Synthesis of (S)-1-[2-(1-Butoxyvinyl)naphthalen-1-yl]isoquinoline. **13b**



Following the general procedure from **3b** and **8**, after 18 h and further purification by flash chromatography (15:1 Toluene/EtOAc + 3% Et₃N) afforded **13b** (31 mg, 90%) as a light yellow amorphous solid.

$[\alpha]_D^{20}$ -27.0 (*c* 0.65, CHCl₃) for 92% *ee*.

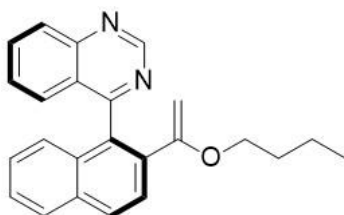
¹H-NMR (400 MHz, CDCl₃) δ 8.68 (d, *J* = 5.7 Hz, 1H), 7.99 (dd, *J* = 8.6, 0.9 Hz, 1H), 7.92 (ddt, *J* = 8.2, 6.2, 0.9 Hz, 2H), 7.77 (d, *J* = 8.6 Hz, 1H), 7.74 (d, *J* = 5.8 Hz, 1H), 7.67 (ddd, *J* = 8.2, 6.8, 1.2 Hz, 1H), 7.54 (dq, *J* = 8.5, 1.0 Hz, 1H), 7.46 (ddd, *J* = 8.1, 6.7, 1.2 Hz, 1H), 7.37 (ddd, *J* = 8.3, 6.8, 1.2 Hz, 1H), 7.28 (ddd, *J* = 8.3, 6.7, 1.3 Hz, 1H), 7.16 (dd, *J* = 8.6, 1.1 Hz, 1H), 4.28 (d, *J* = 2.4 Hz, 1H), 4.05 (d, *J* = 2.4 Hz, 1H), 3.31 – 3.23 (m, 1H), 3.23 – 3.15 (m, 1H), 1.06 – 0.76 (m, 4H), 0.68 (t, *J* = 7.1 Hz, 3H).

¹³C-NMR (100 MHz, CDCl₃) δ 161.1, 160.7, 142.1, 135.9, 135.2, 134.3, 133.5, 132.7, 129.9, 128.9, 128.5, 127.9, 127.8, 126.8, 126.6, 126.5, 126.4, 126.4, 126.0, 119.6, 87.0, 67.2, 30.3, 19.0, 13.7.

HRMS (ESI) calculated for C₂₅H₂₄NO (*M* + H⁺) 354.1852. Found 354.1848.

HPLC (IA column, 90:10 *n*-hex/IPA, 30 °C, 1.0 mL/min): *t*_R 6.15 min (minor) and 7.12 min (major).

Synthesis of (S)-4-[2-(1-Butoxyvinyl)naphthalen-1-yl]quinazoline. **13c**



Following the general procedure from **3c** and **8**, after 18 h and further purification by flash chromatography (15:1 Toluene/EtOAc + 3% Et₃N) afforded **13c** (27.2 mg, 80%) as a light yellow amorphous solid.

$[\alpha]_D^{20}$ -20.2 (*c* 0.40, CHCl₃) for 84% *ee*.

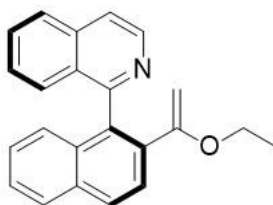
¹H-NMR (400 MHz, CDCl₃) δ 9.45 (s, 1H), 8.19 – 8.12 (m, 1H), 8.05 – 8.01 (m, 1H), 7.95 (d, *J* = 8.0 Hz, 1H), 7.91 (ddd, *J* = 8.4, 6.8, 1.5 Hz, 1H), 7.78 (d, *J* = 8.6 Hz, 1H), 7.56 – 7.53 (m, 1H), 7.50 (ddd, *J* = 8.1, 6.8, 1.2 Hz, 1H), 7.45 (ddd, *J* = 8.2, 6.8, 1.2 Hz, 1H), 7.33 (ddd, *J* = 8.3, 6.8, 1.3 Hz, 1H), 7.17 (dd, *J* = 8.5, 1.0 Hz, 1H), 4.41 (d, *J* = 2.6 Hz, 1H), 4.12 (d, *J* = 2.6 Hz, 1H), 3.22 (t, *J* = 6.2 Hz, 2H), 0.97 – 0.82 (m, 4H), 0.67 (t, *J* = 7.1 Hz, 3H).

¹³C-NMR (100 MHz, CDCl₃) δ 170.0, 160.6, 154.7, 149.9, 135.0, 133.7, 133.4, 131.8, 131.5, 129.4, 128.4, 128.1, 127.4, 127.4, 126.9, 126.3, 126.2, 126.0, 125.6, 87.5, 67.3, 30.1, 18.9, 13.6.

HRMS (ESI) calculated for C₂₄H₂₃N₂O (M + H⁺) 355.1805. Found 355.1809.

HPLC (AS-H column, 98:2 *n*-hex/IPA, 30 °C, 1.0 mL/min): *t*_R 10.53 min (major) and 12.92 min (minor).

Synthesis of (*S*)-1-[2-(1-Ethoxyvinyl)naphthalen-1-yl]isoquinoline. **14b**



Following the general procedure from **3b** and **9**, after 24 h and further purification by flash chromatography (15:1 Toluene/EtOAc + 3% Et₃N) afforded 27 mg of a 6:1 mixture of **14b** (70%) and naphthylisoquinoline as a light yellow amorphous solid

$[\alpha]_D^{20}$ -27.1 (*c* 0.25, CHCl₃) for 94% *ee*.

¹H-NMR (400 MHz, CDCl₃) δ 8.68 (d, *J* = 5.7 Hz, 1H), 7.99 (dd, *J* = 8.7, 0.8 Hz, 1H), 7.92 (dd, *J* = 8.3, 6.7 Hz, 2H), 7.77 (d, *J* = 8.5 Hz, 1H), 7.74 (dd, *J* = 5.7, 0.9 Hz, 1H), 7.67 (ddd,

$J = 8.2, 6.8, 1.2$ Hz, 1H), 7.53 (d, $J = 1.0$ Hz, 1H), 7.47 (ddd, $J = 8.1, 6.7, 1.2$ Hz, 1H), 7.38 (ddd, $J = 8.4, 6.8, 1.2$ Hz, 1H), 7.32 – 7.26 (m, 1H), 7.17 (dd, $J = 8.5, 1.0$ Hz, 1H), 4.30 (d, $J = 2.4$ Hz, 1H), 4.05 (d, $J = 2.4$ Hz, 1H), 3.34 – 3.18 (m, 2H), 0.54 (t, $J = 7.0$ Hz, 3H).

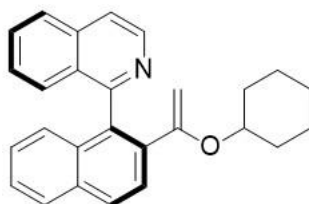
^{13}C NMR (100 MHz, CDCl_3) δ 160.9, 160.7, 142.1, 135.9, 135.0, 134.3, 133.5, 132.7, 129.9, 128.9, 128.5, 127.9, 127.8, 126.8, 126.6, 126.5, 126.4, 126.3, 126.0, 119.6, 87.0, 62.8, 13.4.

HRMS (ESI) calculated for $\text{C}_{23}\text{H}_{20}\text{NO}$ ($\text{M} + \text{H}^+$) 326.1539. Found 326.1541.

HPLC (IA column, 95:5 *n*-hex/IPA, 30 °C, 1.0 mL/min): t_{R} 9.86 min (minor) and 11.15 min (major).

Synthesis of (*S*)-1-{2-[1-(Cyclohexyloxy)vinyl]naphthalen-1-yl}isoquinoline.

15b



Following the general procedure from **3b** and **10**, after 24 h and further purification by flash chromatography (15:1 Toluene/EtOAc + 3% Et_3N) afforded **15b** (35 mg, 90%) as a light yellow amorphous solid.

$[\alpha]_{\text{D}}^{20} -9.3$ (c 0.43, CHCl_3) for 91% *ee*.

^1H -NMR (400 MHz, CDCl_3) δ 8.68 (d, $J = 5.7$ Hz, 1H), 7.99 (d, $J = 8.6$ Hz, 1H), 7.93 (d, $J = 5.4$ Hz, 1H), 7.91 (d, $J = 5.6$ Hz, 1H), 7.76 (d, $J = 8.7$ Hz, 1H), 7.74 (d, $J = 4.9$ Hz, 1H), 7.66 (ddd, $J = 8.2, 6.8, 1.2$ Hz, 1H), 7.54 (d, $J = 8.4$ Hz, 1H), 7.46 (ddd, $J = 8.1, 6.8, 1.2$ Hz, 1H), 7.43 – 7.34 (m, 1H), 7.29 – 7.25 (m, 1H), 7.13 (d, $J = 8.5$ Hz, 1H), 4.27 (d, $J = 2.3$ Hz, 1H), 4.04 (d, $J = 2.3$ Hz, 1H), 3.62 (tt, $J = 9.1, 3.4$ Hz, 1H), 1.48 (dd, $J = 9.1, 3.2$ Hz, 1H), 1.47 – 1.33 (m, 2H), 1.15 – 1.04 (m, 2H), 1.04 – 0.95 (m, 1H), 0.96 – 0.81 (m, 2H), 0.73 – 0.59 (m, 1H), 0.56 – 0.44 (m, 1H).

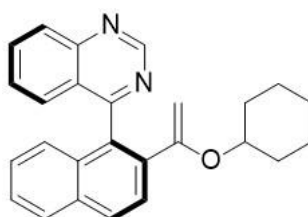
^{13}C -NMR (100 MHz, CDCl_3) δ 160.7, 158.8, 142.1, 136.0, 135.6, 134.3, 133.4, 132.7, 129.9, 129.0, 128.4, 127.9, 127.8, 126.8, 126.6, 126.6, 126.4, 126.4, 125.9, 120.0, 87.7, 74.2, 30.6, 30.3, 25.6, 23.8, 23.7.

HRMS (ESI) calculated for $\text{C}_{27}\text{H}_{26}\text{NO}$ ($\text{M} + \text{H}^+$) 380.2009. Found 380.2005.

HPLC (IA column, 90:10 *n*-hex/IPA, 30 °C, 1.0 mL/min): t_{R} 6.67 min (minor) and 7.48 min (major).

Synthesis of (S)-4-{2-[1-(Cyclohexyloxy)vinyl]naphthalen-1-yl}quinazoline.

15c



Following the general procedure from **3c** and **10**, after 24 h and further purification by flash chromatography (15:1 Toluene/EtOAc + 3% Et_3N) afforded **15c** (26.6 mg, 70%) as a light yellow amorphous solid.

$[\alpha]_{\text{D}}^{20}$ -19.6 (c 0.44, CHCl_3) for 87% *ee*.

^1H -NMR (400 MHz, CDCl_3) δ 9.46 (s, 1H), 8.15 (d, $J = 8.5$ Hz, 1H), 8.02 (d, $J = 8.6$ Hz, 1H), 7.94 (d, $J = 8.3$ Hz, 1H), 7.90 (t, $J = 7.6$ Hz, 1H), 7.77 (d, $J = 8.6$ Hz, 1H), 7.55 (d, $J = 8.3$ Hz, 1H), 7.47 (dt, $J = 16.1, 7.6$ Hz, 2H), 7.35 – 7.29 (m, 1H), 7.14 (d, $J = 8.5$ Hz, 1H), 4.40 (d, $J = 2.5$ Hz, 1H), 4.10 (d, $J = 2.6$ Hz, 1H), 3.61 (tt, $J = 9.2, 3.6$ Hz, 1H), 1.46 – 1.35 (m, 3H), 1.15 – 0.83 (m, 5H), 0.58 – 0.37 (m, 2H).

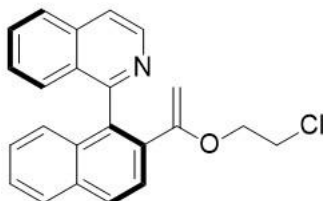
^{13}C -NMR (100 MHz, CDCl_3). δ 170.0, 158.4, 154.6, 150.0, 135.4, 133.7, 133.3, 131.8, 131.4, 129.3, 128.3, 128.1, 127.5, 127.4, 126.9, 126.4, 126.7, 125.9, 125.8, 87.8, 74.5, 30.4, 30.2, 25.4, 23.8, 23.7.

HRMS (ESI) calculated for $\text{C}_{26}\text{H}_{25}\text{N}_2\text{O}$ ($\text{M} + \text{H}^+$) 381.1961. Found 381.1958.

HPLC (AD-H column, 85:15 *n*-hex/IPA, 30 °C, 1.0 mL/min): t_{R} 7.61 min (minor) and 8.22 min (major).

Synthesis of (S)-1-{2-[1-(2-Chloroethoxy)vinyl]naphthalen-1-yl}isoquinoline.

16b



Following the general procedure from **3b** and **11**, after 18 h and further purification by flash chromatography (15:1 Toluene/EtOAc + 3% Et₃N) afforded **16b** (27 mg, 75%) as a yellowish amorphous solid.

$[\alpha]_D^{20}$ -23.6 (*c* 0.68, CHCl₃) for 94% *ee*.

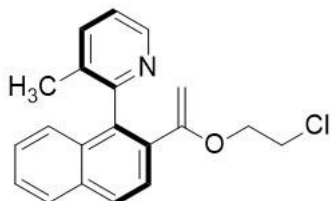
¹H-NMR (400 MHz, CDCl₃) δ 8.69 (d, *J* = 5.8 Hz, 1H), 8.01 (d, *J* = 8.5 Hz, 1H), 7.94 (d, *J* = 8.3 Hz, 2H), 7.77 (d, *J* = 8.6 Hz, 1H), 7.76 (dd, *J* = 5.7, 0.9 Hz, 1H), 7.70 (ddd, *J* = 8.2, 6.8, 1.2 Hz, 1H), 7.54 (dd, *J* = 8.4, 1.1 Hz, 1H), 7.48 (ddd, *J* = 8.1, 6.8, 1.2 Hz, 1H), 7.40 (ddd, *J* = 8.3, 6.8, 1.2 Hz, 1H), 7.30 (ddd, *J* = 8.3, 6.8, 1.3 Hz, 1H), 7.18 – 7.13 (m, 1H), 4.35 (d, *J* = 2.9 Hz, 1H), 4.08 (d, *J* = 2.9 Hz, 1H), 3.55 (dt, *J* = 10.2, 6.5 Hz, 1H), 3.47 (ddd, *J* = 10.2, 6.5, 5.6 Hz, 1H), 2.97 (ddd, *J* = 11.1, 6.5, 5.6 Hz, 1H), 2.84 (dt, *J* = 11.2, 6.5 Hz, 1H).

¹³C-NMR (125 MHz, CDCl₃) δ 160.6, 160.1, 142.1, 135.9, 134.5, 134.2, 133.6, 132.6, 130.2, 128.8, 128.7, 127.9, 127.7, 127.1, 126.6, 126.6, 126.5, 126.2, 126.2, 119.8, 88.3, 67.2, 40.6.

HRMS (ESI) calculated for C₂₃H₁₉NOCl (M + H⁺) 360.1150. Found 360.1146.

HPLC (IA column, 90:10 *n*-hex/IPA, 30 °C, 1.0 mL/min): *t*_R 8.08 min (minor) and 9.56 min (major).

Synthesis of (S)-2-{2-[1-(2-Chloroethoxy)vinyl]naphthalen-1-yl}-3-methylpyridine. **16e**



Following the general procedure from **3e** and **11**, after 18 h and further purification by flash chromatography (15:1 Toluene/EtOAc + 3% Et₃N) afforded **16e** (29 mg, 90%) as a yellowish amorphous solid.

$[\alpha]_D^{20} +1.84$ (*c* 0.52, CHCl₃) for 80% *ee*.

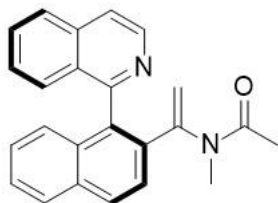
¹H-NMR (400 MHz, CDCl₃) δ 8.59 (d, *J* = 4.5 Hz, 1H), 7.91 (t, *J* = 7.3 Hz, 2H), 7.70 (d, *J* = 8.6 Hz, 1H), 7.64 (d, *J* = 7.6 Hz, 1H), 7.49 (t, *J* = 7.5 Hz, 1H), 7.38 (t, *J* = 7.6 Hz, 1H), 7.33 – 7.25 (m, 1H), 7.22 (d, *J* = 8.5 Hz, 1H), 4.32 (d, *J* = 2.8 Hz, 1H), 4.21 (d, *J* = 2.8 Hz, 1H), 3.84 (dt, *J* = 10.3, 6.4 Hz, 1H), 3.76 (dt, *J* = 10.7, 5.7 Hz, 1H), 3.45 (dt, *J* = 11.4, 5.7 Hz, 1H), 3.32 (dt, *J* = 10.9, 6.4 Hz, 1H), 2.04 (s, 3H).

¹³C-NMR (100 MHz, CDCl₃) δ 160.3, 158.4, 146.5, 137.3, 135.7, 133.6, 133.4, 133.1, 131.7, 128.1, 128.0, 126.6, 126.4, 126.2, 125.9, 122.2, 88.0, 67.5, 41.2, 19.0.

HRMS (ESI) calculated for C₂₀H₁₉NOCl (M + H⁺) 324.1150. Found 324.1147. Found 324.1381.

HPLC (AD-H column, 85:15 *n*-hex/IPA, 30 °C, 1.0 mL/min): *t*_R 5.69 min (major) and 6.15 min (minor).

Synthesis of (S)-N-{1-[1-(Isoquinolin-1-yl)naphthalen-2-yl]vinyl}-N-methylacetamide. **17b**



Following the general procedure from **3b** and **12**, after 48 h and further purification by flash chromatography (3:1 Toluene/EtOAc + 3% Et₃N) afforded **17b** (31.7 mg, 90%) as a yellowish amorphous solid.

$[\alpha]_D^{20} -14.7$ (*c* 0.70, CHCl₃) for 82% *ee*.

¹H-NMR (500 MHz, CDCl₃) δ 8.71 (d, *J* = 5.7 Hz, 1H), 8.06 (d, *J* = 8.7 Hz, 1H), 7.96 (d, *J* = 8.3 Hz, 2H), 7.78 (d, *J* = 5.8 Hz, 1H), 7.74 – 7.67 (m, 1H), 7.63 (d, *J* = 8.6 Hz, 1H), 7.52 (t, *J* = 7.6 Hz, 1H), 7.42 (d, *J* = 4.1 Hz, 2H), 7.32 (t, *J* = 7.8 Hz, 1H), 7.08 (d, *J* = 8.6 Hz, 1H), 5.16 (s, 1H), 4.92 (s, 1H), 2.58 (s, 3H), 1.63 (s, 3H).

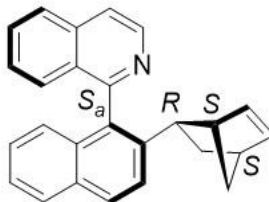
¹³C-NMR (100 MHz, CDCl₃) 170.5, 159.2, 148.7, 142.6, 136.2, 134.9, 134.2, 133.5, 132.9, 130.5, 129.3, 128.4, 128.0, 127.5, 127.2, 127.1, 127.1, 126.7, 126.5, 126.5, 120.4, 114.7, 34.8, 21.8.

HRMS (ESI) calculated for C₂₄H₂₁N₂O (M + H⁺) 497.2224. Found 353.1648. Found 353.1645.

HPLC (AD-H column, 85:15 *n*-hex/IPA, 30 °C, 1.0 mL/min): *t*_R 12.64 min (major) and 14.48 min (minor).

II.5.4. Hydroarylation of 2,5-norbornadiene

Synthesis of (*S*)-1-{2-[(1*S*,2*R*,4*S*)-Bicyclo[2.2.1]hept-5-en-2-yl]naphthalen-1-yl}isoquinoline. **18**



Following the general procedure for the Dynamic Kinetic Asymmetric Heck Reaction from **3b** (0.1 mmol) and 2,5-norbornadiene (8.0 eq.) in presence of formic acid (3.0 eq.), purification by flash chromatography (25:1 Toluene/EtOAc) afforded **18** (10.7 mg, 31%) as a light yellow amorphous solid.

$[\alpha]_D^{20} -32.8$ (*c* 0.49, CHCl₃) for 98% *ee*.

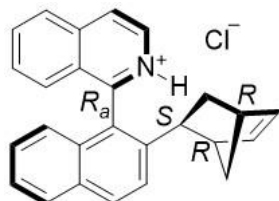
¹H-NMR (400 MHz, CDCl₃) δ 8.73 (d, *J* = 5.7 Hz, 1H), 8.00 (d, *J* = 8.7 Hz, 1H), 7.96 (d, *J* = 8.3 Hz, 1H), 7.91 (d, *J* = 8.2 Hz, 1H), 7.77 (d, *J* = 5.8 Hz, 1H), 7.72 (d, *J* = 8.5 Hz, 2H), 7.48 – 7.37 (m, 3H), 7.23 (ddd, *J* = 8.3, 6.8, 1.3 Hz, 1H), 6.92 (d, *J* = 8.5 Hz, 1H), 5.89 (dd, *J* = 5.7, 2.9 Hz, 1H), 5.69 (dd, *J* = 5.7, 3.2 Hz, 1H), 2.87 (d, *J* = 14.3 Hz, 2H), 2.28 (dd, *J* = 9.0, 5.0 Hz, 1H), 1.84 (d, *J* = 8.4 Hz, 1H), 1.77 (dt, *J* = 12.2, 4.4 Hz, 1H), 1.48 (d, *J* = 8.6 Hz, 1H), 1.16 (ddd, *J* = 11.7, 9.1, 2.5 Hz, 1H).

¹³C-NMR (100 MHz, CDCl₃) δ 160.7, 142.6, 142.1, 137.1, 136.1, 135.5, 132.9, 131.8, 130.2, 128.6, 128.5, 127.7, 127.3, 127.2, 126.9, 126.1, 125.7, 125.0, 123.9, 120.0, 47.2, 46.7, 42.1, 41.2, 35.0.

HRMS (ESI) calculated for C₂₆H₂₂N (M + H⁺) 348.1747. Found 348.1741.

HPLC (IA column, 95:5 *n*-hex/IPA, 30 °C, 1.0 mL/min): *t*_R 9.48 min (minor) and 10.93 min (major).

Synthesis of (*R*)-1-{2-[(1*R*,2*S*,4*R*)-Bicyclo[2.2.1]hept-5-en-2-yl]naphthalen-1-yl}isoquinoline hydrochloride. *ent*-18**·HCl**



Over a solution of *ent*-**18** (10 mg, 0.029 mmol) in the minimum amount of diethyl ether, one drop of hydrochloric acid 37% was added. Further filtration afforded *ent*-**18**·HCl (10.7 mg, 31%) as a white solid. Crystallization by slow diffusion of *n*-pentane into a solution of the product in DCM afforded pale yellow prisms suitable for X-Ray analysis.

$[\alpha]_D^{20} +109.1$ (*c* 0.49, CHCl₃) for 98% *ee*.

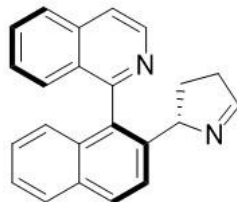
¹H-NMR (400 MHz, CDCl₃) δ 8.89 (s, 1H), 8.30 (d, *J* = 29.3 Hz, 2H), 8.21 – 8.04 (m, 2H), 7.96 (d, *J* = 7.8 Hz, 1H), 7.76 (d, *J* = 8.7 Hz, 2H), 7.65 (d, *J* = 8.3 Hz, 1H), 7.47 (d, *J* = 7.3 Hz, 1H), 7.31 (s, 1H), 6.76 – 6.58 (m, 1H), 5.94 (dd, *J* = 5.7, 2.8 Hz, 1H), 5.72 (dd, *J* = 5.7, 2.9 Hz, 1H), 2.99 (s, 1H), 2.90 (s, 1H), 2.01 – 2.14 (m, 2H), 1.85 (d, *J* = 8.6 Hz, 1H), 1.53 (d, *J* = 8.6 Hz, 1H), 1.31 – 1.17 (m, 1H).

¹³C-NMR (100 MHz, CDCl₃) δ 157.3, 144.3, 138.6, 138.1, 136.6, 136.1, 132.8, 132.2, 132.0, 131.6, 131.2, 129.2, 128.5, 128.2, 128.1, 127.9, 126.1, 125.7, 124.7, 124.3, 123.7, 47.1, 46.9, 42.4, 42.1, 35.4.

M.p. 72-75 °C.

II.5.5. Representative transformations from 7b.

Synthesis of (*S,S*)-1-{2-[(*S*)-3,4-Dihydro-2H-pyrrol-2-yl]naphthalen-1-yl}isoquinoline. 20b



Over a cooled (0 °C) solution of **7b** (0.1 mmol) in CH₂Cl₂ (0.5 mL) trifluoroacetic acid (0.25 mL) was added dropwise. Then solution was allowed to warm to r.t., and stirred for 30 min. The reaction mixture was neutralized with NaHCO₃ sat. solution and extracted with CH₂Cl₂. After purification by flash chromatography (12:1 CH₂Cl₂/EtOAc), **20b** (29 mg, 90%) was afforded as a light yellow amorphous solid. A single product was observed by ¹H-NMR of the reaction crude; hence epimerization did not occur.

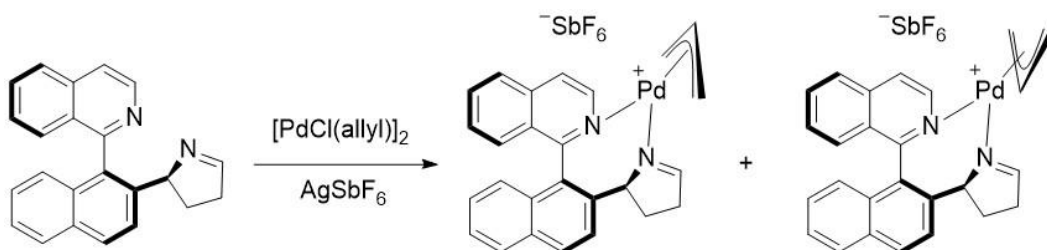
$[\alpha]_D^{20} -10.1$ (*c* 0.52, CHCl₃) for 99% *ee*.

¹H-NMR (400 MHz, CDCl₃): δ 8.73 (d, *J* = 5.1 Hz, 1H), 7.99 (d, *J* = 8.6 Hz, 1H), 7.92 (d, *J* = 9.2 Hz, 1H), 7.89 (d, *J* = 9.3 Hz, 1H), 7.78–7.76 (m, 2H), 7.67 (t, *J* = 7.2 Hz, 1H), 7.61 (d, *J* = 8.4 Hz, 1H), 7.43–7.39 (m, 3H), 7.24 (t, *J* = 7.2 Hz, 1H), 7.00 (d, *J* = 8.4 Hz, 1H), 4.57 (t, *J* = 8.2 Hz, 1H), 2.70 (dd, *J* = 18.0 and 10.2 Hz, 1H), 2.37 (m, 1H), 2.11 (m, 1H), 1.71 (m, 1H).

¹³C-NMR (100 MHz, CDCl₃) δ 168.2, 159.9, 142.4, 140.3, 136.1, 133.7, 132.6, 132.5, 130.5, 129.2, 128.5, 127.9, 127.8, 127.4, 126.7, 126.2, 126.0, 125.4, 123.6, 120.2, 73.8, 37.6, 31.0.

HRMS (ESI) calculated for C₂₃H₁₉N₂ (M + H⁺) 323.1543. Found 324.1539.

Synthesis of the Pd-20b complex. 21



Over a dried Schlenk tube containing a solution of $[\text{Pd(allyl)Cl}]_2$ (0.025 mmol, 9.1 mg) in anhydrous-deoxygenated DCM (1 mL), a solution of **20b** (0.05 mmol, 16.1 mg) in anhydrous-deoxygenated DCM (1 mL) was added dropwise. The resulting mixture was stirred at rt for 1 hour, and then a solution of AgSbF_6 (0.05 mmol, 17.2 mg) in dry THF (0.5 mL) was added. The reaction was stirred 3 hours in dark, filtered through celite and concentrated to dryness to afford **21** (33 mg, 94%) as a pale amorphous solid. NMR spectra showed a *ca* 1:1 mixture of rotamers around the Pd-allyl bond when the experiment was recorded at 298K.

$[\alpha]_D^{20} -7.1$ (*c* 0.25, CHCl_3) for 99% *ee*.

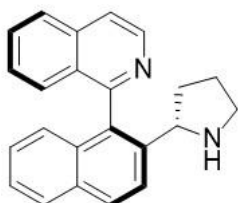
$^1\text{H-NMR}$ (400 MHz, CDCl_3): δ 8.88 (d, $J = 6.1$ Hz, 0.5H), 8.52 (d, $J = 6.1$ Hz, 0.5H), 8.16 (d, $J = 8.4$ Hz, 0.5H), 8.10-7.96 (m, 4H), 7.80 (t, $J = 7.1$ Hz, 0.5H), 7.79 (t, $J = 7.6$ Hz, 0.5H), 7.71 (d, $J = 8.4$ Hz, 0.5H), 7.65 (s, 0.5H), 7.59 (d, $J = 8.5$ Hz, 0.5H), 7.55-7.50 (m, 1H), 7.48-7.40 (m, 1H), 7.28-7.20 (m, 1H), 7.12 (d, $J = 8.5$ Hz, 0.5H), 7.03 (d, $J = 8.5$ Hz, 0.5H), 6.64 (d, $J = 8.6$ Hz, 0.5H), 6.53 (d, $J = 8.6$ Hz, 0.5H), 5.66 (m, 0.5H), 5.30 (br s, 0.5H), 5.12 (br s, 0.5H), 4.94 (m, 0.5H), 4.08 (d, $J = 12.2$ Hz, 0.5H), 4.07 (d, $J = 12.8$ Hz, 0.5H), 4.00 (t, $J = 7.2$ Hz, 1H), 3.23 (d, $J = 12.6$ Hz, 1H), 2.59 (m, 1H), 2.52 (d, $J = 12.2$ Hz, 0.5H), 2.43 (m, 1H), 2.32 (d, $J = 12.8$ Hz, 0.5H), 2.22 (m, 1H), 1.12 (m, 1H).

$^{13}\text{C-NMR}$ (100 MHz, CDCl_3) δ 175.4, 175.4, 160.0, 159.7, 142.8, 142.6, 136.8, 136.4, 136.2, 136.1, 132.9, 132.8, 132.8, 132.6, 132.6, 132.4, 131.0, 130.6, 129.7, 129.7, 129.5, 129.4, 128.4, 128.4, 128.3, 128.2, 127.7, 127.6, 127.4, 127.2, 127.1, 127.0, 126.8, 125.2, 124.0, 124.0, 117.1, 116.5, 78.7, 78.5, 61.5, 60.3, 59.8, 59.0, 38.0, 37.8, 31.1, 31.0.

$^{19}\text{F NMR}$ (377 MHz, CDCl_3): δ -107.2.

HRMS (ESI) calculated for $C_{26}H_{23}N_2Pd$ ($M^+ - SbF_6$) 469.0896. Found 469.0893.

Synthesis of (S)-1-{2-[(S)-Pyrrolidin-2-yl]naphthalen-1-yl}isoquinoline. **22b**



To a cooled (0 °C) solution of **20b** (0.1 mmol) in MeOH (1 mL), NaBH₄ (2.0 eq.) was added. Then solution was allowed to warm to rt, and stirred for 30 min. Then H₂O (1 mL) was added and the resulting mixture was extracted with CH₂Cl₂. After purification by flash chromatography (8:1 CH₂Cl₂/EtOAc), **22b** (28 mg, 87%) was afforded as a light yellow amorphous solid. A single product was observed by ¹H-NMR of the reaction crude; hence epimerization did not occur.

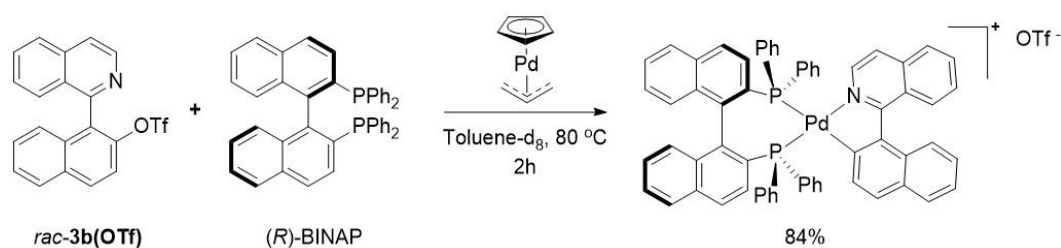
$[\alpha]_D^{20}$ -26.1 (*c* 0.49, CHCl₃) for 99% *ee*.

¹H-NMR (400 MHz, CDCl₃): δ 8.70 (d, *J* = 5.8 Hz, 1H), 8.00 (d, *J* = 8.7 Hz, 1H), 7.94 (d, *J* = 8.2 Hz, 1H), 7.89–7.86 (m, 2H), 7.78 (d, *J* = 5.7 Hz, 1H), 7.69 (ddd, *J* = 8.2, 6.6 and 1.4 Hz, 1H), 7.45–7.36 (m, 3H), 7.21 (ddd, *J* = 8.4, 6.7 and 1.3 Hz, 1H), 6.90 (d, *J* = 8.9 Hz, 1H), 3.83 (t, *J* = 7.6 Hz, 1H), 3.51 (br s, 1H), 3.12 (dt, *J* = 9.8 and 6.8 Hz, 1H), 2.88 (m, 1H), 2.04 (m, 1H), 1.82 (m, 1H), 1.74–1.60 (m, 2H).

¹³C-NMR (100 MHz, CDCl₃) δ 159.9, 142.3, 139.7, 136.2, 134.1, 132.7, 132.5, 130.6, 129.4, 128.7, 127.9, 127.8, 127.2, 127.0, 126.3, 125.9, 125.6, 124.7, 120.4, 60.3, 47.0, 34.2, 25.6.

HRMS (ESI) calculated for $C_{23}H_{21}N_2$ ($M + H^+$) 325.1699. Found 325.1695.

II.5.6. Isolation of the Oxidative Addition Intermediate $\text{I}^{\text{O}}_{\text{A-L1}}(\text{OTf}^-)$.



A flame-dried and deoxygenated Schlenk tube was charged with (R)-BINAP (0.1 mmol, 62 mg) and 1-(isoquinolin-1-yl)naphthalene-2-yl triflate *rac*-**3b**(OTf) (0.1 mmol, 40 mg). After three cycles of vacuum- N_2 , $[\text{Pd}(\text{Cp})(\text{allyl})]$ (0.1 mmol, 21 mg) and dry and deuterated toluene (2 mL) were added. The reaction mixture was stirred for 2h at 80 °C and a yellow precipitated was formed. The solid was filtered and washed with cold toluene to afford $\text{I}^{\text{O}}_{\text{A-L1}}(\text{OTf}^-)$ (95 mg, 84%) as a yellow solid. Crystallization by slow diffusion of *n*-pentane into a solution of THF gave pale yellow needles suitable for X-Ray analysis. Triflate counteranions are extremely disordered and cannot be modeled, even with restraints. The SQUEEZE routine of the PLATON software has therefore been used to cancel out the effects of those anions. The unmodified SQUEEZE map contains 260 electrons per unit cell which is suitable with 4 triflate anions.

$[\alpha]_{\text{D}}^{20} = +351.4$ (c 0.31, CHCl_3).

$^1\text{H-NMR}$ (400 MHz, CD_2Cl_2) δ 8.14 (br s, 2H), 8.04 (d, $J = 8.7$ Hz, 1H), 8.00 (br s, 1H), 7.96 – 7.87 (m, 2H), 7.74 (d, $J = 8.2$ Hz, 1H), 7.70 – 7.49 (m, 12H), 7.49 – 7.37 (m, 6H), 7.36 – 7.10 (m, 10H), 7.05 – 6.92 (m, 3H), 6.86 – 6.72 (m, 4H), 6.68 (d, $J = 8.6$ Hz, 1H), 6.56 (br s, 1H).

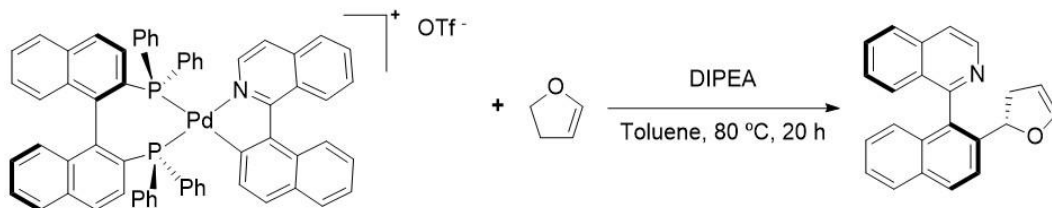
$^{13}\text{C-NMR}$ (100 MHz, CD_2Cl_2) δ 169.7 (d, $J_{\text{C,P}} = 3.8$ Hz), 168.2 (dd, $J_{\text{C,P}} = 118.7, 10.5$ Hz), 143.6, 142.7 (d, $J_{\text{C,P}} = 6.3$ Hz), 139.3 (d, $J_{\text{C,P}} = 3.8$ Hz), 139.2 (d, $J_{\text{C,P}} = 4.3$ Hz), 138.9 (d, $J_{\text{C,P}} = 1.5$ Hz), 138.9 (d, $J_{\text{C,P}} = 13.1$ Hz), 137.6, 137.4, 137.2, 135.7 (d, $J_{\text{C,P}} = 12.5$ Hz), 134.7, 134.6, 134.1 (d, $J_{\text{C,P}} = 9.9$ Hz), 133.7, 133.6, 132.9, 132.8, 132.7, 132.6, 132.0 (d, $J_{\text{C,P}} = 11.3$ Hz), 131.9 (d, $J_{\text{C,P}} = 3.8$ Hz), 131.3, 131.2, 130.8, 130.3, 130.2, 129.7, 129.6, 129.5, 129.2, 129.1, 129.0, 128.9, 128.7, 128.5, 128.4, 128.3, 128.2, 128.2, 128.1, 128.0,

127.9, 127.8, 127.7, 127.6, 127.3, 127.3, 127.2, 127.1, 127.0, 127.0, 126.9, 126.2, 126.2, 125.8, 125.5, 123.2, 122.8, 122.2, 121.6, 121.1 (q, $J_{C,F} = 321$ Hz), 120.6.

^{31}P NMR (202 MHz, CD_2Cl_2) δ 40.9 (d, $J = 47.4$ Hz), 16.1 (d, $J = 47.4$ Hz).

HRMS (ESI) calculated for $\text{C}_{63}\text{H}_{44}\text{NP}_2\text{Pd}$ (M^+) 982.1978. Found 982.1993.

II.5.7. Reaction of Oxidative Addition Intermediate $\text{I}^{\text{OA}}_{\text{Li}}(\text{OTf}^-)$ with 2,3-dihydrofuran **4**.



To a flame-dried Schlenk tube, $\text{I}^{\text{OA}}_{\text{Li}}(\text{OTf}^-)$ (25 mg, 0.022 mmol) was added and dissolved in anhydrous toluene. Then DIPEA (5 eq.) and **4** (8 eq.) were subsequently added and heated at 80 °C for 20 h. The reaction crude was allowed to reach room temperature, water (5 mL) was added and the resulting mixture was extracted with EtOAc (4×3 mL). The organic layer was dried over anhydrous Na_2SO_4 , filtered, concentrated, and the residue was purified by flash column chromatography on silica gel ($\text{CH}_2\text{Cl}_2 \rightarrow 25:1 \text{ CH}_2\text{Cl}_2/\text{EtOAc}$) affording **5b** (6 mg, 82% yield, 77% *ee*) as a light-yellow solid. The spectroscopy and physical data matched those obtained with **5b** afforded by following the general procedure for the Dynamic Kinetic Asymmetric Heck Reaction.

CHAPTER III

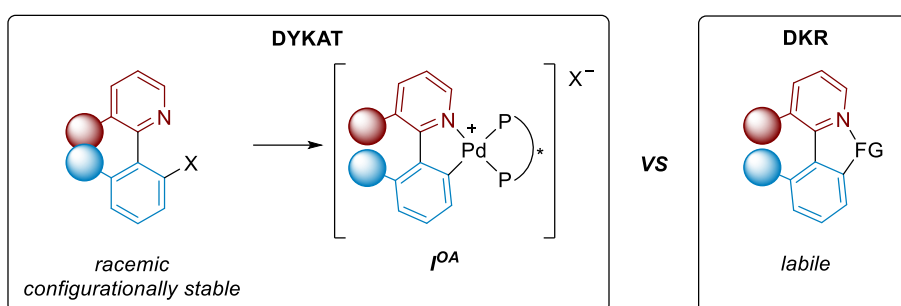
*Dynamic Kinetic Resolution of
Heterobiaryl Ketones by Zinc-Catalyzed
Asymmetric Hydrosilylation*

Angewandte Chemie International Edition **2018**, 57, 3777.

III. Dynamic Kinetic Resolution of Heterobiaryl Ketones by Zinc-catalyzed Asymmetric Hydrosilylation

III.1. Introduction

This chapter describes an unprecedented strategy for the atroposelective synthesis of heterobiaryls which consists on a dynamic kinetic resolution (DKR). In chapter II, the methodology was based on a DYKAT strategy and, therefore, racemic and configurationally stable heterobiaryl starting materials were employed. In this case, however, the substrate needs to be configurationally labile in order to make possible a DKR (Scheme III.1).



Scheme III.1 – Atropisomerization through 5-membered cyclic TS or intermediates in DYKAT and DKR strategies for the asymmetric synthesis of heterobiaryls. FG = Lewis acidic functional group.

Taking advantage of the nucleophilic character of the isoquinolyl nitrogen, we envisioned that the introduction of a Lewis acidic (electrophilic) functionality FG in the *ortho* position of the lower aromatic unit would result in a Lewis acid-base interaction with the nitrogen from the heteroaromatic counterpart (Scheme III.1). As a working hypothesis, we anticipated that a relatively fast racemization should be facilitated through the formation of a five-membered intermediate or transition state: as in the DYKAT case, this geometry produces the widening of the angles involved in the stereochemical stability of the stereogenic axis. In this scenario, any asymmetric transformation that destroys the Lewis acid character of such functional group FG should short out the interaction, thereby providing configurational stability and eventually resulting in a preferred atropisomeric

form. In other words, such transformation would constitute a dynamic kinetic atroposelective resolution.

A similar behaviour to that proposed above was also observed during previous investigations by our research group on the N-directed borylation of (hetero)arenes.¹²⁶ In this work, the authors suggest a similar interaction between a isoquinoly/pyridyl nitrogen atom and the boron atom of a boryl group in a co-planar conformation of both aromatic and heteroaromatic rings, which compromises the configurational stability of the stereogenic axis. Noteworthy, the internal ‘ate’ complex in this type of products was the most stable product when there is no strong inhibition to co-planarity, while it is postulated as an intermediate in more crowded systems (Scheme III.2).

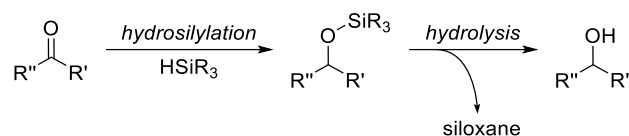


Scheme III.2 – N-directed asymmetric borylation of (hetero)arenes developed by our group.

Despite their modest Lewis acidity, formyl/acyl derivatives are appealing candidates considering the number of possible transformations (quaternizations) that would result in the loss of its Lewis acid character of the carbonyl group with concomitant stabilization of the stereogenic axis. A good transformation to eliminate the electrophilic character of this carbonyl would consist on an asymmetric catalytic reduction.

Indeed, the reduction of a carbonyl group to the corresponding alcohol represents one of the most important transformations in organic chemistry. In particular, the hydrosilylation reaction provides silyl ethers under mild conditions that can be easily hydrolysed to the corresponding alcohols, and is considered a well-established methodology in Synthesis (Scheme III.3).

¹²⁶ Ros, A.; Estepa, B.; López-Rodríguez, R.; Álvarez, E.; Fernández, R.; Lassaletta, J. M. *Angew. Chem. Int. Ed.* **2011**, *50*, 11724.



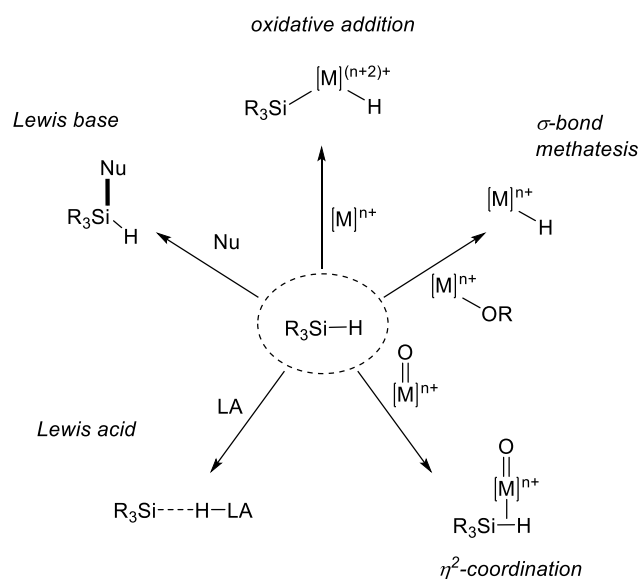
Scheme III.3 – General graph for carbonyl hydrosilylation followed by hydrolysis.

Given the number of catalytic systems available, many of them based in nonprecious metals,¹²⁷ the hydrosilylation of ketones was the first option to explore the stated hypothesis. One of the main benefits of the hydrosilylation procedure compared to other carbonyl reduction methods are the mild conditions usually required together with the use of silane as hydride donors, which are chemically stable, cheap and easy to handle. In these silanes, the Si–H bond has to be activated to make possible the hydride donation, and there are different modes to achieve that purpose including transition metal catalyzed methods, or even metal-free procedures¹²⁸ (Scheme III.4).¹²⁹

¹²⁷ For a revision see: (a) Marciniak, B.; Maciejewski, H.; Pietraszuk, C.; Pawluć, P. In *Hydrosilylation: A Comprehensive Review on Recent Advances*, Marciniak, B., Ed.; Springer: Berlin, **2009**. (b) Li, Y.; Junge, K.; Beller, M. *Zinc-Catalyzed Reductions of Unsaturated Compounds*. In *Zinc Catalysis: Applications in Organic Synthesis*; Enthaler, S.; Wu, X. F., Eds.; Wiley-VCH: Weinheim, **2015**, pp. 14-19. (c) Díez-González, S.; Nolan, S. P. *Org. Prep. Proced. Int.* **2007**, *39*, 523. (d) Marciniak, B. *Coord. Chem. Rev.* **2005**, *249*, 2374.

¹²⁸ Zhou, R.; Goh, Y. Y.; Liu, H.; Tao, H.; Li, L.; Wu, J. *Angew. Chem. Int. Ed.* **2017**, *56*, 16621.

¹²⁹ Rendler, S.; Oestreich, M. *Diverse Modes of Silane Activation for the Hydrosilylation of Carbonyl Compounds*. In *Modern Reduction Methods*, Andersson, P. G.; Munslow, I. M., Eds.; Wiley-VCH, Weinheim, **2008**, pp. 183-207.



Scheme III.4 – Different activation modes for silane reagents.

As mentioned above, the reduction of carbonyls *via* hydrosilylation reaction has been reported using different metals, although most of the reported systems are based on late transition metal complexes, and only scarce attention has been paid to early transition metal complexes, apart from titanium.

The first hydrosilylation of carbonyl compounds was reported by Ojima and co-workers using Wilkinson's catalyst $[RhCl(PPh_3)_3]$ (Scheme III.5A).¹³⁰ Additionally, the pioneering work by Kagan et al.¹³¹ in 1973 on the first asymmetric hydrosilylation of ketones and imines catalyzed by Rh(I)/DIOP complexes (Scheme III.5B) inspired other authors to develop more efficient catalytic systems.¹³² During the first two decades after its discovery, the methodology mainly focused on the use of rhodium, iridium and ruthenium, although, catalytic systems based on iridium and ruthenium have not attracted as much interest compared to rhodium.¹³³ Nonetheless, methods based on ruthenium catalysts have

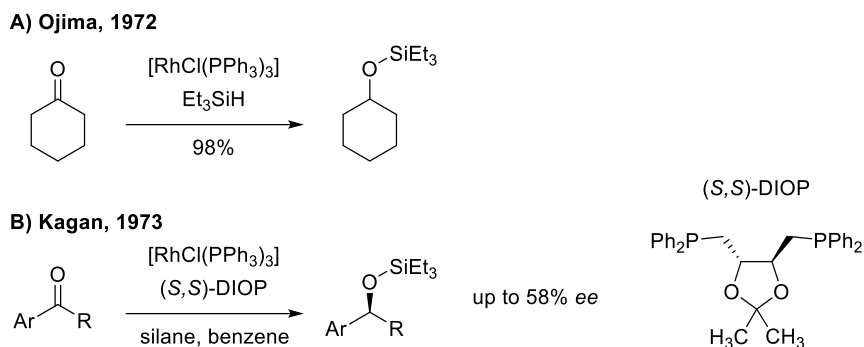
¹³⁰ Ojima, I.; Nihonyan., M.; Nagai, Y. *J. Chem. Soc., Chem. Commun.* **1972**, 938.

¹³¹ Dumont, W.; Poulin, J. C.; Dang, T. P.; Kagan, H. B. *J. Am. Chem. Soc.* **1973**, 95, 8295.

¹³² (a) Riener, K.; Högerl, M. P.; Gigler, P.; Kühn, F. E. *ACS Catal.* **2012**, 2, 613. (b) Duan, W. L.; Shi, M.; Rong, G. B. *Chem. Commun.* **2003**, 23, 2916. (c) Hayashi, T.; Hayashi, C.; Uozumi, Y. *Tetrahedron Asym.* **1995**, 6, 2503.

¹³³ Park, S.; Brookhart, M. *Organometallics* **2010**, 29, 6057.

also been developed, since this metal is more readily available and less expensive than either rhodium or iridium.



Scheme III.5 – First racemic and asymmetric versions of Rh-catalyzed hydrosilylation of ketones.

One of the major breakthroughs in the asymmetric hydrosilylation of ketones occurred in the early 1990's with the discovery of titanocene-based chiral catalysts by the groups of Buchwald,¹³⁴ Halterman,¹³⁵ and Harrod¹³⁶ (Figure III.1).

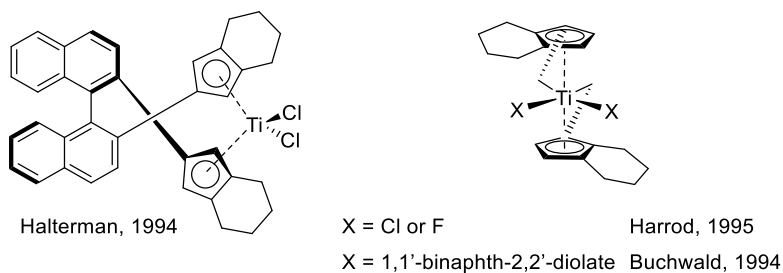


Figure III.1 – Halterman, Buchwald and Harrod's titanocene chiral catalysts for ketone hydrosilylation.

A second important breakthrough in this field took place in 1999, when Mimoun et al. discovered new chiral catalysts based on zinc, where several chiral diamines, diimines, and aminoalcohols were used as ligands in combination with polymethylhydrosiloxane (PMHS) as silylating agent for the reduction of acetophenone

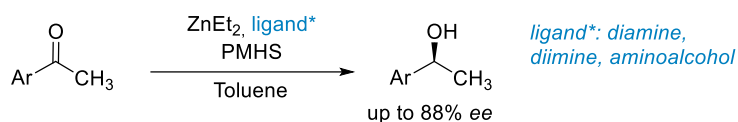
¹³⁴ Carter, M. B.; Schiott, B.; Gutiérrez, A.; Buchwald, S. L. *J. Am. Chem. Soc.* **1994**, *116*, 11667.

¹³⁵ Halterman, R. L.; Ramsey, T. M.; Chen, Z. *J. Org. Chem.* **1994**, *59*, 2642.

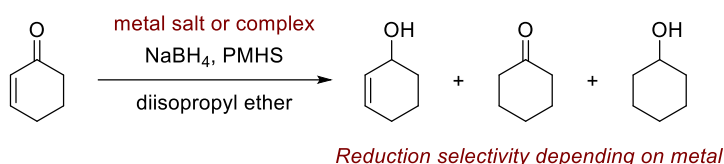
¹³⁶ Harrod, J. F.; Xin, S. *Can. J. Chem.* **1995**, *73*, 999.

derivatives (Scheme III.6A).¹³⁷ Furthermore, a previous work from Mimoun showed that many transition metals (Mn, Co, Fe, Cu, Ni, Pd, Ru, Zr, Cd, and Zn) were able to catalyse the hydrosilylation of ketones with PMHS, using sodium borohydride as activating agent.¹³⁸ Interestingly, experiments carried out on conjugated cyclohexenone showed that Ru, Cu, Ni, and Pd favoured alkene reduction, while the rest of the explored metals provided exclusively ketone reduction product (Scheme III.6B).

A) Mimoun et al., 1999. (ref. 137)



B) Mimoun, 1999. (ref. 138)



Scheme III.6 Mimoun's contribution to transition metal catalyzed asymmetric hydrosilylation of ketones.

In 2004, the groups of Carpentier¹³⁹ and Walsh¹⁴⁰ et al. simultaneously reported some improvement to Mimoun's work with respect to ligands design, in particular by using C2-symmetric 1,2-diaryldiamine ligands. The first was able to increase the enantiomeric excesses to 91%, and also to expand the scope to more functionalized ketones. Meanwhile, Walsh performed a similar study but did not reach enantiomeric purities over 89%. It is worth to mention that both authors showed that PMHS was not the only silylating agent that could be employed under these conditions.

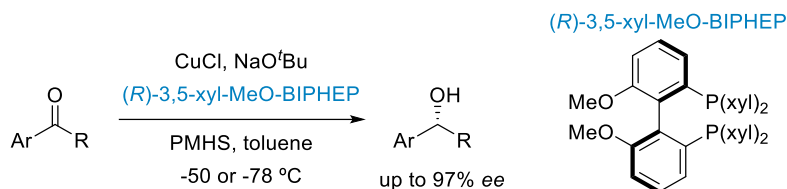
¹³⁷ Mimoun, H.; De Saint Laumer, J. Y.; Giannini, L.; Scopelliti, R.; Floriani, C. *J. Am. Chem. Soc.* **1999**, *121*, 6158.

¹³⁸ Mimoun, H. *J. Org. Chem.* **1999**, *64*, 2582.

¹³⁹ Bette, V.; Mortreux, A.; Savoia, D.; Carpentier, J.-F. *Tetrahedron* **2004**, *60*, 2837.

¹⁴⁰ Mastranzo, V. M.; Quintero, L.; de Parrodi, C. A.; Juaristi, E.; Walsh, P. J. *Tetrahedron* **2004**, *60*, 1781.

Very interesting results were also found by Lipshutz's group when copper catalysis was employed for the asymmetric hydrosilylation of aryl ketones.¹⁴¹ These authors found that combining CuCl with a bisphosphine ligand provided enantiomeric excesses up to 97% (Scheme III.7).



Scheme III.7 – Cu-catalyzed asymmetric hydrosilylation of ketones developed by Lipshutz et al.

More recently, a remarkable method was developed by Beller et al. in 2008, where they demonstrated for the first time that high enantioselectivity (up to 99% *ee*) can be achieved in the Fe-catalyzed hydrosilylation of ketones.¹⁴²

So far, it could be stated that catalysis has changed to meet present social demands of environmentally conscious processes using common metals such as iron, copper, or zinc. Hence, our initial concern has been to employ an inexpensive late transition metal such as zinc,¹⁴³ for the activation of the silane. However, for the heterobiaryl ketones described during this chapter, the presence of the isoquinolyl nitrogen acting as Lewis base has to be considered, since it could also interfere in the activation of Si–H bond. So, the activation mode involved in this transformation is *a priori* not easy to predict.

Regarding to the metal source, the hydrosilylation reaction promoted by inorganic Zn salts is still not well studied, in contrast to the well established application of diethylzinc.¹⁴⁴ In 2009, Nishiyama developed a more sustainable metal source for the asymmetric hydrosilylation by replacing the highly reactive and hazardous dialkyl zinc

¹⁴¹ Lipshutz, B. H.; Noson, K.; Chrisman, W. *J. Am. Chem. Soc.* **2001**, *123*, 12917.

¹⁴² Shaikh, N.; Enthaler, S.; Junge, K.; Beller, M. *Angew. Chem. Int. Ed.* **2008**, *47*, 2497.

¹⁴³ Łowicki, D.; Baś, S.; Mlynarski, J. *Tetrahedron* **2015**, *71*, 1339.

¹⁴⁴ For selected examples catalyzed by ZnEt₂: (a) (b) Ushio, H.; Mikami, K. *Tetrahedron Lett.* **2005**, *46*, 2903. (c) Bette, V.; Mortreux, A.; Lehmann, C. W.; Carpentier, J.-F. *Chem. Commun.* **2003**, *0*, 332.

with a cheaper source such as zinc acetate in combination with chiral diamines.¹⁴⁵ The latter has been consolidated among the optimal ligands for zinc catalyzed asymmetric hydrosilylation of ketones,¹⁴⁶ and they were our first option for this study.

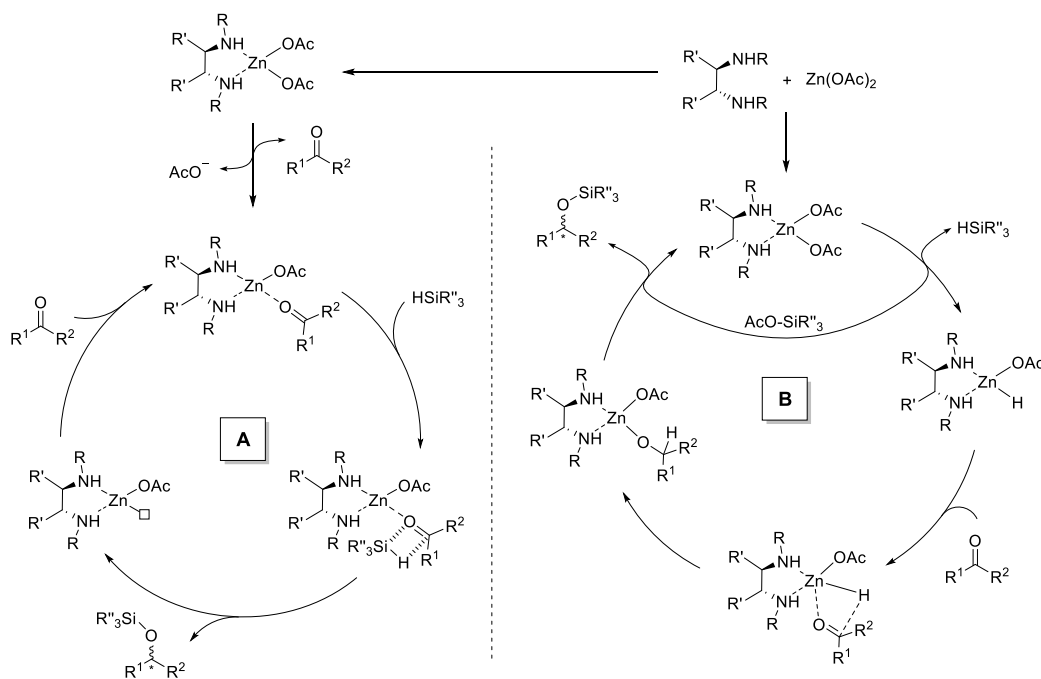
Without considering the complexity of our system, and the possible effect of the isoquinolyl nitrogen atom, different mechanistic proposals have emerged depending on whether the diamine plays the role of a hydride source, or if it behaves just as a spectator ligand. However, some recent mechanistic studies suggest a certain preference for the latter mechanism.¹⁴⁷

Considering this mechanism, two different reaction pathways could be anticipated: a first one involving a Lewis acid activation of the carbonyl by the metal centre, and a second possibility in which Zn-hydride species are responsible for the reduction of the carbonyl group (Scheme III.8).

¹⁴⁵ Inagaki, T.; Yamada, Y.; Phong, L. T.; Furuta, A.; Ito, J. -I.; Nishiyama, H. *Synlett* **2009**, 253.

¹⁴⁶ For selected examples using chiral diamines see: (a) Pang, S.; Peng, J.; Li, J.; Bai, Y.; Xiao, W.; Lai, G. *Chirality* **2013**, 25, 275. (b) Szewczyk, M.; Stanek, F.; Bezlada, A.; Mlynarskia, J. *Adv. Synth. Catal.* **2015**, 357, 3727. (c) Junge, K.; Mçller, K.; Wendt, B.; Das, S.; Gçrdes, D.; Thurow, K.; Beller, M. *Chem. Asian J.* **2012**, 7, 314. (d) Bandini, M.; Melucci, M.; Piccinelli, F.; Sinisi, R.; Tomassi, S.; Umani-Ronchi, A. *Chem. Commun.* **2007**, 43, 4519.

¹⁴⁷ Gajewy, J.; Gawronski, J.; Kwit, M. *Eur. J. Org. Chem.* **2013**, 307.



Scheme III.8 – Proposed mechanisms for the $\text{Zn}(\text{OAc})_2$ -diamine catalyzed hydrosilylation of ketones.

The first reaction pathway (A, on Scheme III.8) initially involves the activation of the carbonyl by the zinc atom acting as a Lewis acid. Then, an heterolytic splitting of Si–H bond is responsible for the reduction of the carbonyl, releasing the resulting alcohol and the catalytically active metal species. On the other hand, in the second reaction pathway (B, on Scheme III.8), a hydride is transferred from the silane to the zinc, generating acetoxy-silane and a Zn–H species. Then, the carbonyl is inserted into this Zn–H bond, and the resulting alkoxide remains bonded to metal centre until it is displaced by a previously formed acetoxy-silane, regenerating the catalytically active species. The desired alkoxy-silane would further be hydrolysed.

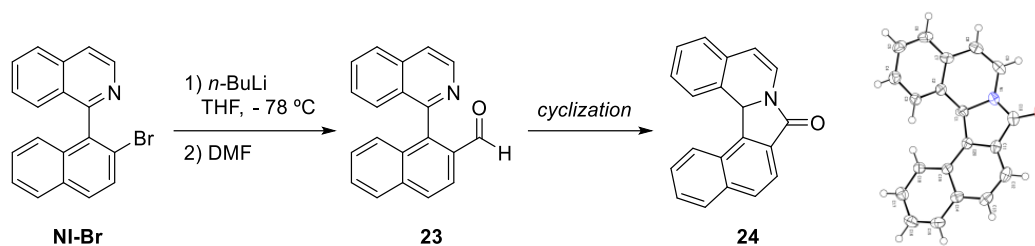
III.2. Results and Discussion.

III.2.1. Substrate design and synthesis.

As a first task prior to develop the strategy, it is necessary to synthesize the starting materials and determine whether our initial hypothesis about the labilization of the substrate

is certain or not. Regarding the carbonyl functionality, there are two main possibilities that can be introduced into the heterobiaryl moiety: aldehyde or ketone.

Initial studies focused on the corresponding aldehyde **23** because its higher electrophilicity and reactivity. Its synthesis was carried out by lithiation of starting naphthylisoquinoline bromide **NI-Br**, employed during the previous studies (see Chapter II), and then trapping with DMF at $-78\text{ }^{\circ}\text{C}$. Unfortunately, the expected product was hardly detected and a rapid cyclization and dearomatization leading to **24** was observed. The structure of **24** was confirmed by single crystal X-ray analysis of a pure sample (Scheme III.9).



Scheme III.9 – Attempt to synthesize the heterobiaryl aldehyde **23**.

Interestingly, while this work was ongoing, the group of Clayden described a biocatalytic reduction of carbonyl-*N*-oxides and they observed the formation of the same product¹⁴⁸ when they tried to synthesize this substrate through Swern oxidation of the parent alcohol. However, the authors solved the problem by oxidation of isoquinolyl nitrogen in order to prevent cyclization and allow for the desired reactivity.

The problem arose from this alternative is that the bonding interaction between the *N*-oxide and the aldehyde carbonyl leads to a six-membered transition state with a high rotational barrier for the atropisomerization that makes it not feasible to perform the DKR. Consequently, the use of heterobiaryls with reduced steric strain was required to make

¹⁴⁸ Staniland, S.; Adams, R. W.; McDouall, J. J. W.; Maffucci, I.; Contini, A.; Grainger, D. M.; Turner, N. J.; Clayden J. *Angew. Chem. Int. Ed.* **2016**, *55*, 10755.

possible the racemization. Specifically, one of the rings from either naphthyl to phenyl or isoquinoline to pyridine was removed (Figure III.2).

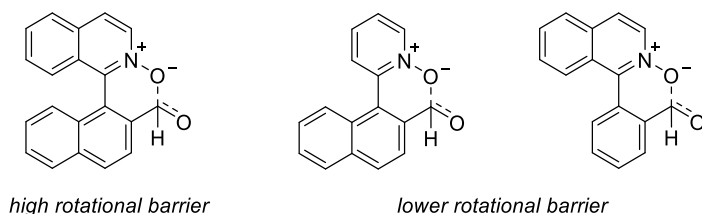
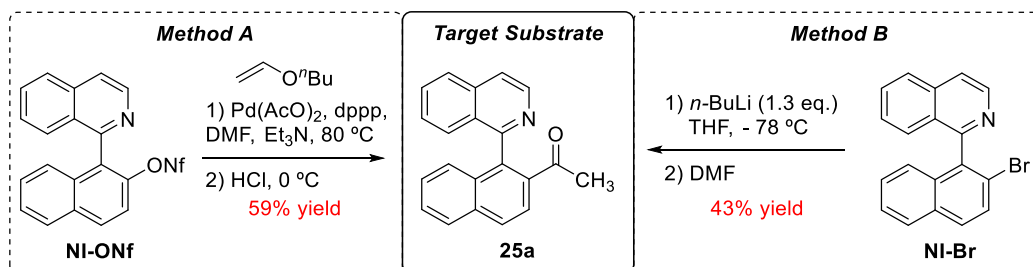


Figure III.2 – Effect of the substitution around the stereogenic axis on the rotational barrier observed by Clayden and co-workers.

In our case, we decided to explore the behaviour of a ketone as the substrate which, although presents a slightly lower electrophilicity than the aldehyde, would generate an additional carbon-based stereocentre. Moreover, it was anticipated that formation of *five-membered* intermediates/transition states would make possible to perform dynamic resolutions with more strained systems than those used by Clayden and co-workers.

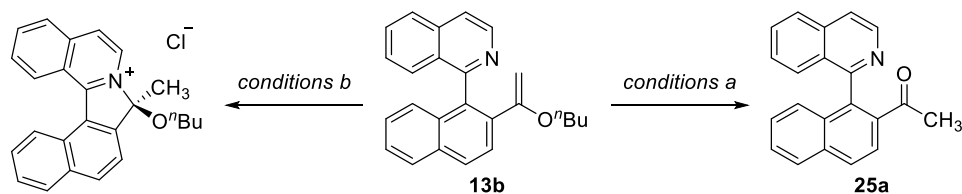
For the synthesis of the target substrates, we considered two possible approaches. Taking advantage of available starting materials used for the dynamic kinetic asymmetric Heck reaction described in previous chapter, either an heterobiaryl sulfonate (Method A) or bromide (Method B) could be used (Scheme III. 10).



Scheme III.10 – Different methods to synthesize the target substrate 25a.

The first approach, Method A, consists on the hydrolysis in acid media of substituted vinyl ether **13b** synthesized through a Pd-catalyzed Heck reaction from **NI-ONf** and butyl vinyl ether. The second, Method B, is based on lithiation and electrophilic trapping of bromide **NI-Br**, the same process showed in Scheme III.9 for the unsuccessful

synthesis of aldehyde **23**. Fortunately, both methods provided the desired product **25a** which proved to be stable and could be isolated in good yields. Interestingly, Method A requires a slow addition of the vinyl ether **13b** over and excess of cooled aqueous HCl solution (*conditions a*); otherwise, if acid is added to the reaction media (*conditions b*), an unexpected intense green-coloured isoquinolynium salt is formed, presumably resulting from nucleophilic attack of isoquinolyl nitrogen to the activated (protonated) vinyl ether (Scheme III.11).

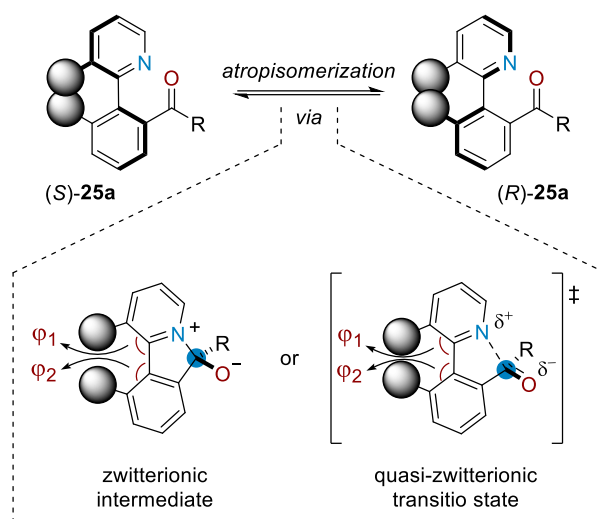


Scheme III.11 – Different products from vinyl ether **13b** hydrolysis with respect to the conditions employed.

III.2.2. Configurational stability analysis of the substrates

The main requirement for the newly synthesized substrates to be suitable for DKR, as mentioned previously, is that they have to be configurationally labile, at least at the reaction temperature, and the analysis of this behaviour is the aim of this section. We have performed this analysis both theoretically and experimentally.

As commented above, our initial hypothesis for the labilization process is that it would proceed through the formation of a five-membered ring *via* a Lewis acid-base interaction between isoquinolyl nitrogen and carbonyl, leading to a zwitterionic intermediate (**zI**) or *quasi*-zwitterionic transition state (**q-zTS**). In this situation, the angles involved in the configurational stability of the stereogenic axis would be widened, facilitating the interconversion between both atropisomers of the heterobiaryl ketone (Scheme III.12).

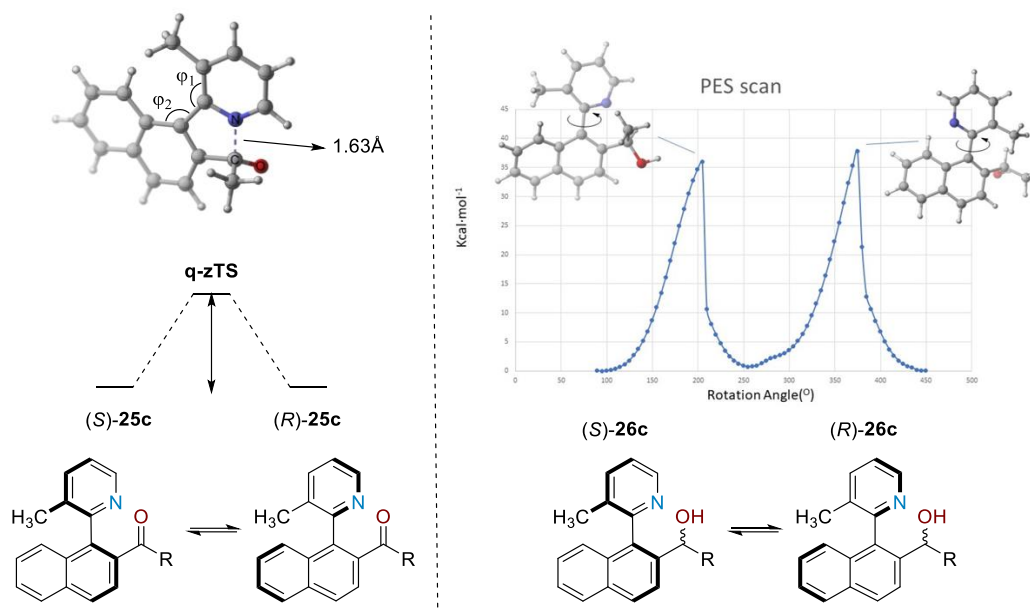


Scheme III.12 – Proposed atropisomerization pathways for heterobiaryl ketone 25a.

III.2.2.1. DFT calculations.

Initially, Professor Joaquín López Serrano, from the University of Sevilla, studied the configurational stability of these heterobiaryl ketones through DFT calculations. To facilitate calculations, the heterobiaryl ketone **25c** derived from picoline moiety and the alcohol resulting from its reduction were employed as model systems.

The calculations showed a significant energetic difference between both rotational barriers. While that of heterobiaryl ketone was located at 22.1 kcal/mol, Relaxed Potential Energy Scan (PES) suggested that the loss of the interaction responsible for the atropisomerization when the ketone is reduced to the secondary alcohol, resulted in a rotational barrier of more than 35 kcal/mol (Scheme III.13).



Scheme III.13 – Calculated rotational barriers for **25c** and **26c**.

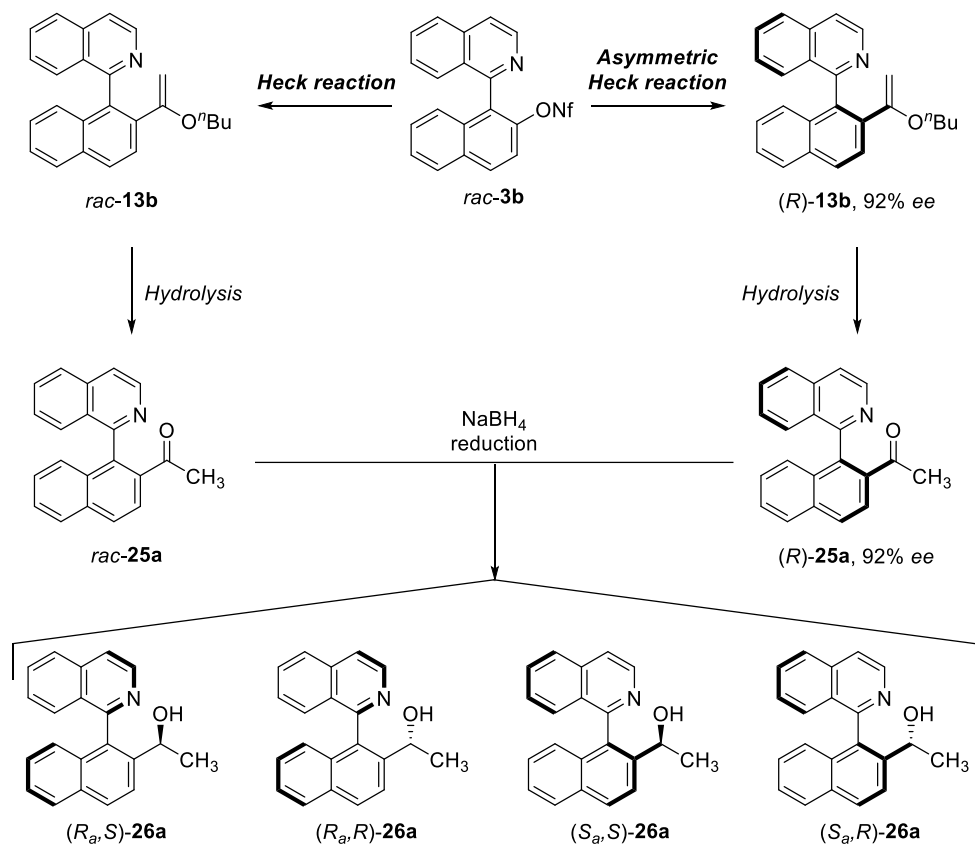
Furthermore, these calculations allowed to obtain a DFT-optimized geometry of the transition state for the isomerization of ketone **25c**. This structure confirmed our initial hypothesis for the atropisomerization pathway, since a distance of 1.63 Å N–C(O)Me showed an interaction and the formation of a *quasi*-zwitterionic transition state indicating the partial formation of a C–N bond. Also remarkable, the angles ϕ_1 and ϕ_2 responsible for the configurational stability of the stereogenic axis are widened to 137.1° and 133.4° respectively.

III.2.2.2. Racemization experiments.

Once this labilization process has been analysed through DFT calculations, showing that these heterobiaryl ketones appear to be configurationally unstable and therefore suitable substrates for DKR, it is also necessary to confirm experimentally what the calculations suggested.

For that purpose, heterobiaryl ketone **25a** was synthesized through the above mentioned Method A (Scheme III.10) and further reduced with NaBH₄. Then, chiral HPLC

analysis of the reaction mixture showed the expected formation of the four possible stereoisomeric alcohols in ca. 1:1:1:1 ratio (Scheme III.14).

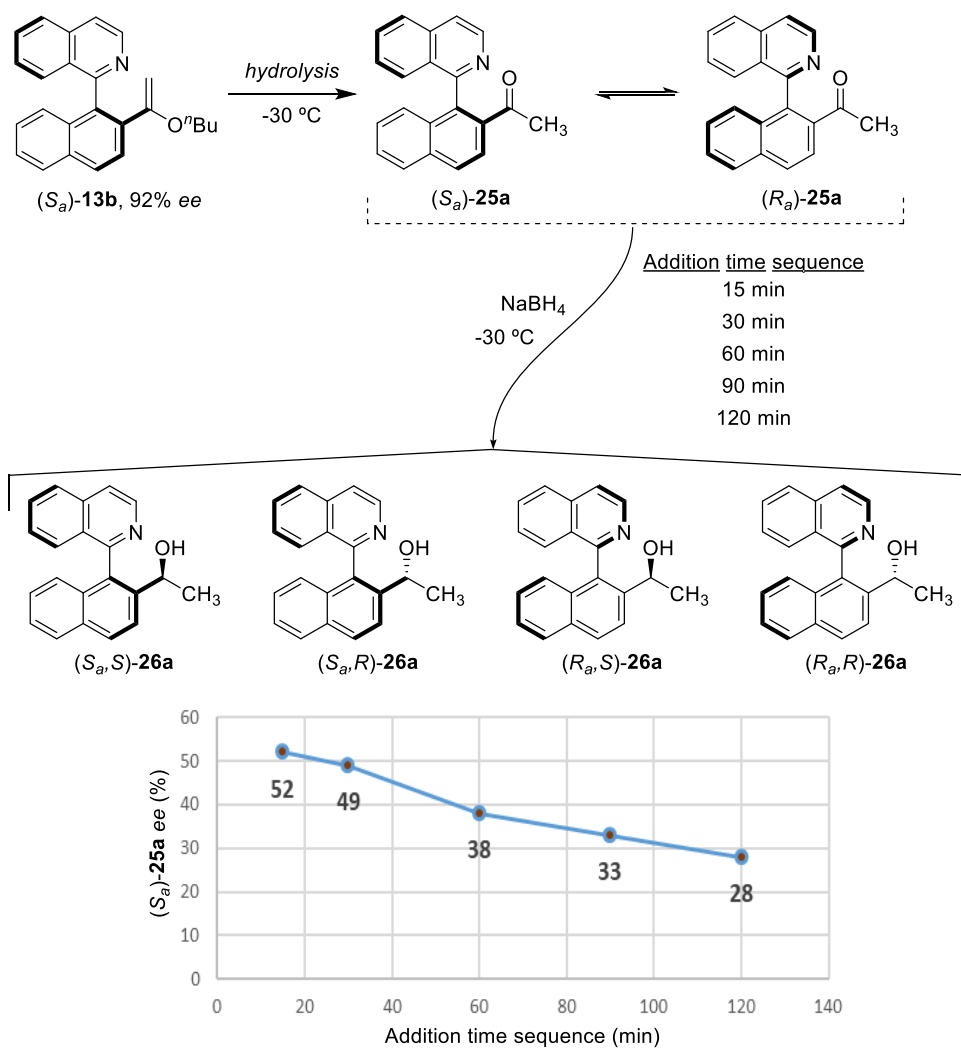


Scheme III.14 – Experiment performed to analyse the racemization event at heterobiaryl ketone 25a.

Remarkably, hydrolysis and further reduction with NaBH₄ of the enantioenriched vinyl ether precursor (*R*)-13b [synthesized through an asymmetric Heck reaction (see Chapter II)], afforded exactly the same mixture as before: the four stereoisomers of the final carbinols in a racemic form. This result clearly shows that there is a complete loss of the enantiomeric purity at (*R*)-25a by a racemization process, which is in agreement with the calculations.

In an attempt to further confirm the configurational instability of these heterobiaryl ketones, a second experiment was carried out, in this case a low temperature racemization analysis. It consisted on Thus, the hydrolysis of the enantioenriched vinyl ether (*R*)-13b

was performed at $-30\text{ }^{\circ}\text{C}$. Then different aliquots were reduced and quenched by adding NaBH_4 at different reaction times and the mixtures were analysed by chiral HPLC (Scheme III.15).



Scheme III.15 – Low temperature racemization experiment.

The aim of this analysis is to measure the ratio between the pair of enantiomers (S_a) -25a and (R_a) -25a along the time at $-30\text{ }^{\circ}\text{C}$ in order to determine if (S_a) -25a is racemizing at low temperature. To correlate them, we measured the ratio between the sum of the two pairs of diastereomers derived from the reduction of each enantiomer of the

starting ketone: (*S,S*)-**26a** + (*S,R*)-**26a** and (*R,S*)-**26a** + (*R,R*)-**26a**. Thus, it was observed a clear decrease on the enantiopurity of (*S*)-**25a** with respect to the time, showing that the racemization process occurs even at low temperature.

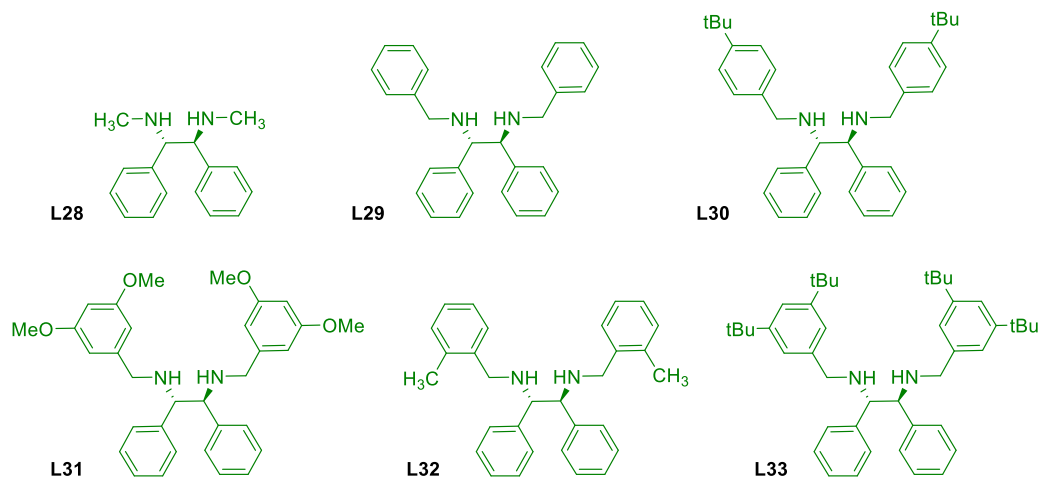
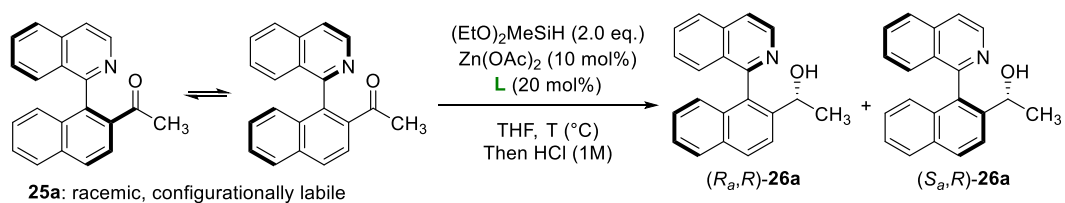
With all these experimental evidences and DFT calculations, the initial hypothesis of the configurational lability of the selected substrate system could be confirmed. The quantitative data, however, must be taken with care, as the racemization must be obviously accelerated by the electrophilic activation of the carbonyl by any protic specie or Lewis acid.

III.2.3. Reaction conditions optimization.

As previously announced, the synthesized heterobiaryl ketones were subjected to zinc catalyzed asymmetric hydrosilylation; and **25a** was chosen as model substrate to find the optimal reaction conditions.

We started screening the reaction conditions for the asymmetric hydrosilylation of **25a** using Zn(OAc)₂, (EtO)₂MeSiH in THF, and using a variety of chiral diamines (Table III.1).

Table III.1 – Ligands screening for asymmetric hydrosilylation of heterobiaryl ketone **25a**.



Entry ^a	L	T (°C)	t (h)	Conv. (%) ^b	d.r. ^b	(R_a,R) - 26a	(S_a,R) - 26a
						ee (%) ^c	ee (%) ^c
1	L28	20	24	>99	1.8:1	40	54
2	L28	0	24	85	1.8:1	59	44
3	L29	20	48	6	4:1	91	41
4	L29	reflux	36	>99	4.5:1	83	52
5	L29	55	36	>99	4.9:1	86	52
6	L30	reflux	36	>99	4.6:1	85	53
7	L31	reflux	36	>99	5:1	85	53
8	L32	reflux	24	>99	4.2:1	91	72
9	L33	reflux	48	>99	4.9:1	98	89
10	L33	20	24	n.r.	n.d.	n.d.	n.d.
11	L33	50	24	12	2.8:1	97	81

12	L33	50	72	55	3:1	98	79
13	L33	55	60	>99	4.4:1	98	83
14 ^d	L33	reflux	36	>99	4.4:1	97	86
15 ^e	L33	reflux	36	>99	5:1	97	90
16 ^{e,f}	L33	reflux	36	>99	4.9:1	74	70
17 ^{e,g}	L33	Reflux	36	n.r.	n.d.	n.d.	n.d.
18 ^{e,h}	L33	Reflux	36	n.r.	n.d.	n.d.	n.d.

^a Reactions performed at 0.1 mmol scale of **25a**. ^b Determined by ¹H-NMR spectroscopy. ^c Determined by chiral HPLC analysis. ^d Zn(OAc)₂ (5 mol%) and **L** (10 mol%). ^e Zn(OAc)₂ (5 mol%) and **L** (6 mol%). ^f Waiting 5 min instead of 1h between the addition of the catalyst, silane and substrate **25a**. ^g PMHS was used as silylating agent. ^h PhMe₂SiH was used as silylating agent.

Interestingly, a first promising result was observed when using (*S,S*)-*N,N'*-dimethyl 1,2-diphenylethylenediamine as ligand (**L28**) at 20 °C, a 2:1 diastereomeric mixture of **26a**, with a 40% *ee* for the major isomer (*R_a,R*)-**26a** (entry 1, Table III.1). A slight increase of the enantiomeric excess was observed at lower temperature, although it remained moderate (entry 2, Table III.1). Fortunately, the easy synthesis and modularity of these diamine ligands¹⁴⁹ facilitated the introduction and analysis of several structural modifications. Surprisingly, changing from methyl to benzyl groups as in **L29** led to a decrease on the reactivity at room temperature (entry 3, Table III.1), but when heated to reflux, full conversion was achieved with 4.5:1 diastereoselectivity and a good 83% *ee* (entry 4, Table III.1). Decreasing temperature to 55 °C, slightly increased diastereoselectivity to 4.9:1 and 86% *ee* for the major diastereomer (entry 5, Table III.1). Ligand **L30** bearing additional *tert*-butyl groups at *para* position of the benzyl groups did not result in any major improvement on either reactivity or selectivities (entry 6, Table III.1). Moreover, **L31** having 3,5-methoxy substitution of benzyl units produced a slight increase in selectivities with full conversion at reflux of THF (entry 7, Table III.1). However, a significant improvement on the enantioselectivity of both major and minor

¹⁴⁹ Kobayashi, S.; Matsubara, R.; Nakamura, Y.; Kitagawa, H.; Sugiura, M. *J. Am. Chem. Soc.* **2003**, *125*, 2507.

diastereomers was achieved after introduction of *ortho*-methyl groups in **L32** (91 and 72% *ee* respectively, entry 8, Table III.1). Finally, the use of **L33** bearing bulky *tert*-butyl substituents in *meta* positions of the benzyl rings, yielded the desired product with excellent conversion and enantioselectivity and a good diastereomeric ratio of 4.9:1 (entry 9, Table III.1). Using **L31**, the reaction at different temperatures from 20 to 55 °C was analysed (entries 10 to 13, Table III.1), however it did not result in any improvement. Importantly, the catalyst loading could be decreased to 5 mol% of Zn(OAc)₂ and 6 mol% of ligand **L33** with no erosion of activity nor selectivity (entry 15, Table III.1).

In an attempt to reduce the time employed to set up the experiments, the reaction was performed by a different addition sequence of the reagents in such way that at the beginning, zinc acetate and the ligand were dissolved in THF and stirred for 1h, then silane was added and stirred for an additional hour, and finally ketone is added to the reaction media. Hence, it was also explored the effect of the intervals in the addition sequence of this reaction by decreasing to 5 minutes instead of 1 hour, but a decrease on the enantioselectivities of both major and minor diastereomers to 74 and 70% *ee* respectively was observed, although the diastereoselectivity remained the same (entry 16, Table III.1).

Remarkable, alternative reducing silane reagents as PMHS and PhMe₂SiH were totally inefficient (entries 17 and 18, Table III.1). A similar behaviour was also observed by Mlynarski and co-workers when screening different silanes in the reduction of aryl ketones.^{146b}

In conclusion, the evaluation of the reaction parameters discussed above allowed to identify the system consisting of Zn(OAc)₂ (5 mol%), **L33** (6 mol%), (EtO)₂MeSiH (2.0 eq.), THF as solvent, at reflux, followed by hydrolysis in aqueous HCl media, as the optimal catalysts and conditions to explore the scope of the reaction.

III.2.4. Reaction scope.

With these optimal conditions in hand, we then moved to explore the dynamic kinetic resolution of different heterobiaryl ketones **25** via a Zn-catalyzed asymmetric hydrosilylation.

A variety of substrates were synthesized introducing structural variations at the heterobiaryl frame in order to examine the robustness of the described methodology (Figure III.3). *Method A* was employed for the synthesis of substrates **25a-c** and **25e-f**. On the other hand, substrates **25d** and **25h** could not be prepared through the same route since the corresponding heterobiaryl sulfonates were not suitable substrates in the Heck reaction, as mentioned in Chapter II, and, therefore, *Method B* was used instead. This route was also employed for the synthesis of the heterobiaryl ketone **25g** since the bromide precursor was available at the laboratory.

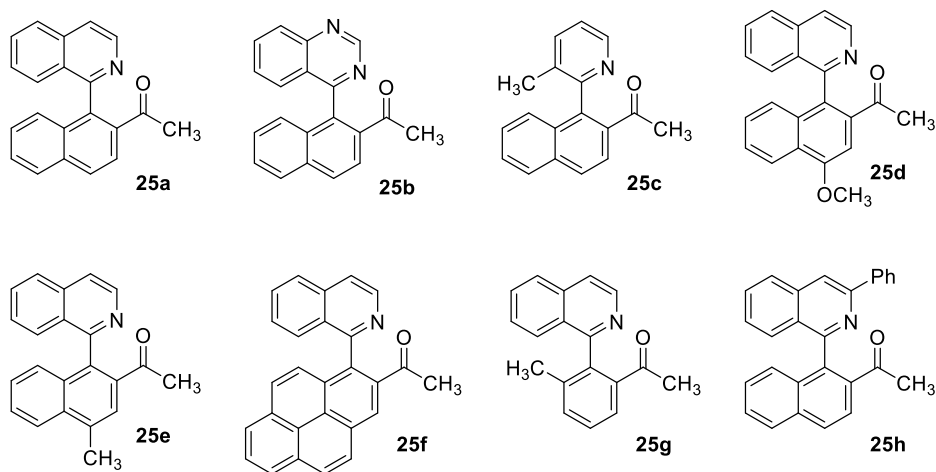
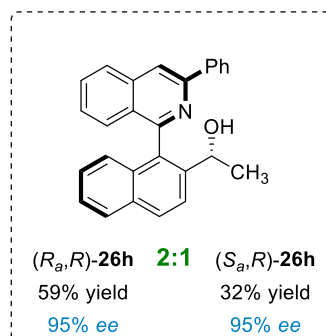
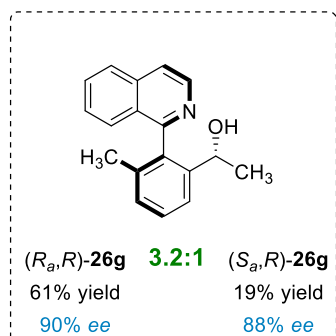
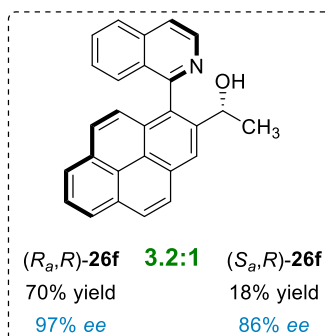
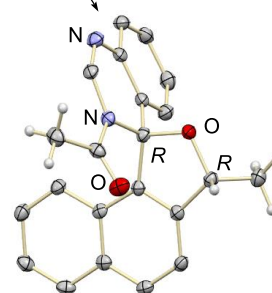
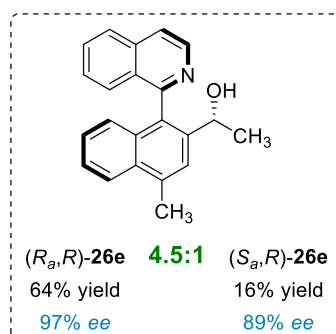
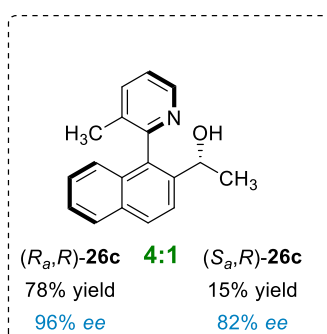
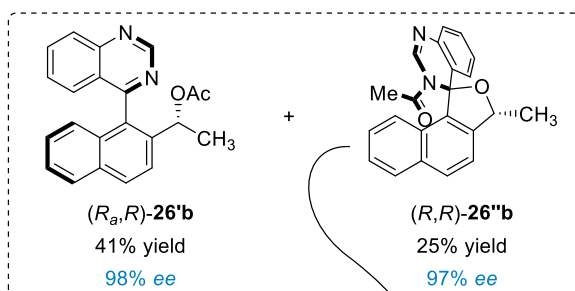
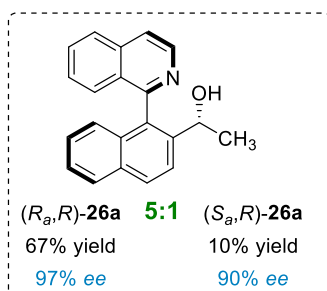
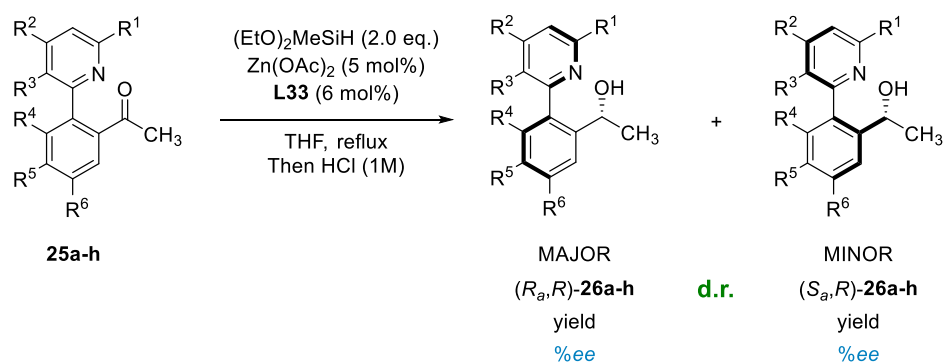


Figure III.3 – Library of heterobiaryl ketones synthesized **25a-h**.

This methodology tolerates variations on the heterobiaryl scaffold, allowing for the synthesis of the corresponding carbinols bearing both central and axial chirality elements (Scheme III.16). In all the cases, the enantioselectivities obtained were excellent, especially for the major diastereomer. Moreover, moderate to good diastereomeric ratios were also

achieved and, importantly, both diastereomers could be easily separated by a simple column chromatography purification.

It is worth to mention the particular case of quinazoline derivative **25b**, yielding the higher diastereoselective ratio from the series (8.5:1). However, the separation of both diastereomers was not possible given the high polarity of the products. To solve the problem, we decided to acetylate the mixture of alcohols directly from the reaction mixture. Surprisingly, treatment with acetic anhydride and 4-dimethylaminopyridine (Ac₂O/DMAP) yielded the acetylated product (*R_a,R*)-**26'b** along with the unexpected spirocyclic derivative (*R,R*)-**26''b**. The latter formally results from an *N*-acetylation and intramolecular 1,2-addition of the hydroxyl group to the azomethine carbon involved in the stereogenic axis, thus dearomatizing the quinazoline moiety in an axial to central chirality transfer process. The absolute configuration of (*R,R*)-**26''b** was determined by single crystal X-ray diffraction analysis.



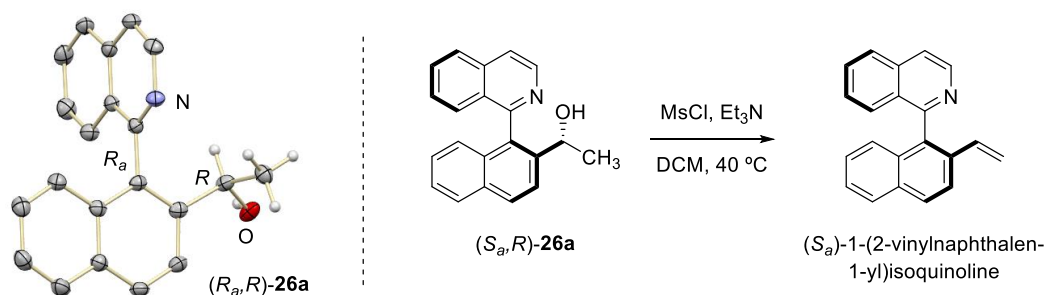
Scheme III.16 – Heterobiaryl scaffolds scope. Only major diastereomer structures are drawn for simplicity.

The carbinol **26c** resulting from the asymmetric hydrosilylation of the 1-(naphthyl)picoline derivative could be obtained in high yield and enantioselectivity (93% overall yield, 96% and 82% *ee* for the major and minor diastereomers, respectively).

The ketone **25e**, bearing a methyl substituent at the 4 position of the naphthalene ring, performed excellently in the transformation to afford both diastereomeric carbinols in 4.5:1 ratio with 97 and 89% *ee* respectively. The more sterically hindered methyl 1-(1-pyrenyl)-isoquinoline derivative **25f** also underwent the asymmetric hydrosilylation in high yield and enantioselectivity. Similar results in terms of diastereoselectivity were obtained for the alcohols **26g**, although the major diastereomer displayed a slightly lower enantioselectivity (90% *ee*) with respect to other major diastereomers. Finally, the substrate bearing a phenyl group at the *ortho* position of the isoquinolyl nitrogen **25h** was well tolerated by this methodology but provided the lower diastereoselectivity value, and the higher enantioselectivity for the minor diastereomer. Unfortunately, heterobiaryl ketone **25d** did not undergo the desired reaction and the starting material was fully recovered.

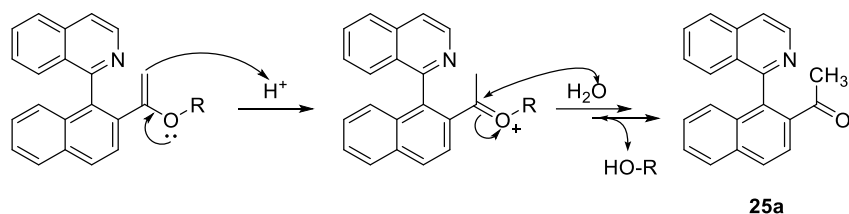
Importantly, the zinc-catalyzed asymmetric hydrosilylation reaction of the model heterobiaryl ketones could also be scaled-up to 1 mmol, affording the carbinol **26a** in higher yield (95%: 77% and 18% of isolated major and minor isomers, respectively), and diastereoselectivity (5.3:1) without compromising the excellent enantioselectivities (97% and 90% *ee* for major and minor isomers, respectively).

The absolute configuration of (*R_a*,*R*)-**26a** was determined after single crystal X-ray analysis, while that of the minor isomer (*S_a*,*R*)-**26a**, was assigned by chemical correlation with the previously described product (*S_a*)-1-(2-vinylnaphthalen-1-yl)isoquinoline,⁶⁶ obtained after treatment of (*S_a*,*R*)-**26a** with mesyl chloride and triethylamine in dichloromethane at 40 °C (Scheme III.17). The absolute configuration of all other products **26** was assigned by analogy.



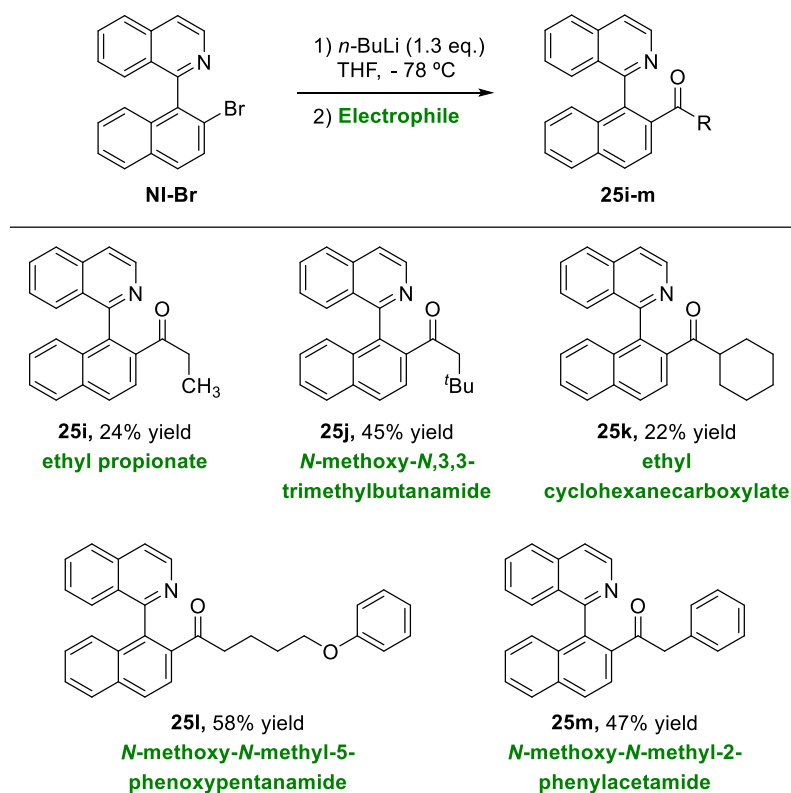
Scheme III.17 – Absolute configuration assignment for (R_a,R) -**26a** and (S_a,R) -**26a**. Thermal ellipsoids drawn for 50% probability.

The next step was to study the influence of ketone substituents different than methyl. The synthesis of these substrates is not affordable through the previously mentioned *Method A* (Scheme III.10), based on the hydrolysis of a vinyl ether precursor, since this route would always provide the corresponding methyl ketone independently of the vinyl ether employed (Scheme III.18).



Scheme III.18 – Mechanism for the hydrolysis of vinyl ether derivatives under acidic conditions.

Therefore, it was necessary to explore different alternatives to obtain these structures. The most direct way, *Method B* (Scheme III.10), consists on performing a lithium-halogen exchange of the **NI-Br** and trapping with acyl transfer reagents different from DMF. Some derivatives that can be employed in this case are esters, amides or aldehydes, among others.



Scheme III.19 – Synthesis of different heterobiaryl ketones through lithiation-electrophilic trapping method.

Thus, this strategy was employed for the synthesis of some heterobiaryl ketones (Scheme III.19), although the yields remained moderate. TLC monitoring showed incomplete reactions even with longer reaction times or higher temperatures. It is also worth to mention that different electrophiles other than those displayed on the above scheme were unsuccessfully examined (Figure III.4).

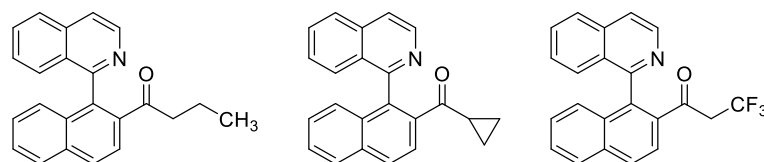
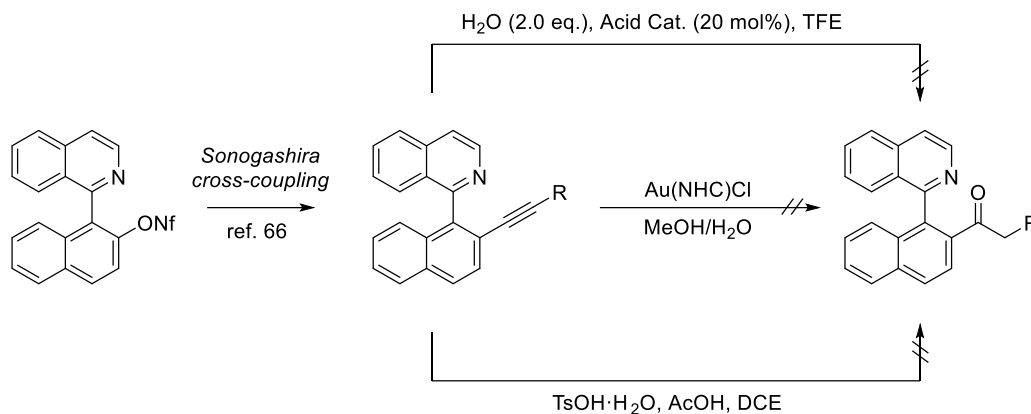


Figure III.4 – Unsuccessful synthesis of other heterobiaryl ketones.

An alternative strategy for the synthesis of these ketones consists on the hydration of internal alkynes prepared through Sonogashira cross-coupling under previously reported

conditions by our research group.⁶⁶ Different methods described for the hydration of alkynes were explored, based on gold catalysis¹⁵⁰ and metal-free procedures.¹⁵¹ Unfortunately, none of them led to the desired product, and only unreacted alkynes were recovered (Scheme III.20).

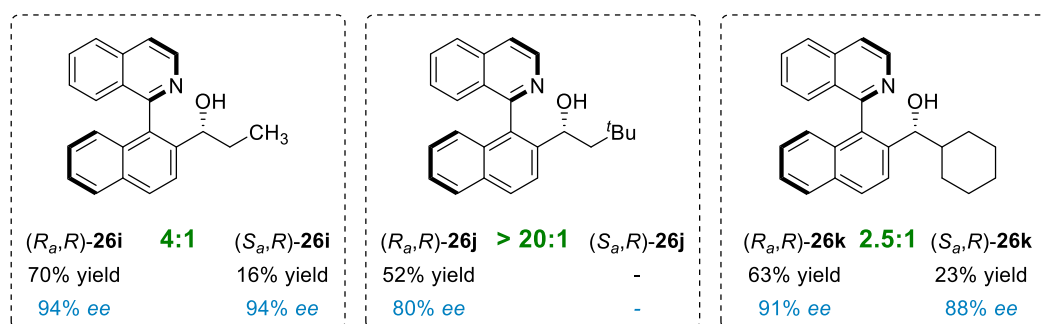
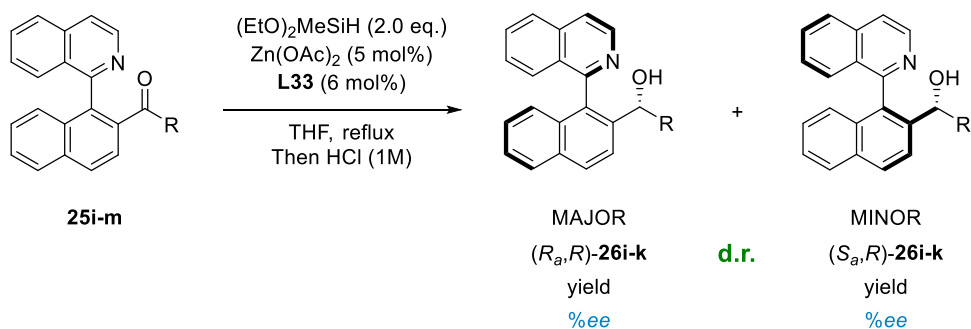


Scheme III.20 – Attempted routes for the synthesis of heterobiaryl ketone through alkyne hydration.

Considering the difficulty for the synthesis of heterobiaryl ketones with substitution different than methyl, the method depicted in Scheme III.19 was selected as the best option. Hence, the substrates subjected to zinc catalyzed asymmetric hydrosilylation in terms of ketones scope would be those synthesized through this method.

¹⁵⁰ (a) Li, F.; Wang, N.; Lu, L.; Zhu, G. *J. Org. Chem.* **2015**, *80*, 3538. (b) Marion, N.; Ramón, R. S.; Nolan, S. P. *J. Am. Chem. Soc.* **2009**, *131*, 448.

¹⁵¹ (a) Liu, W.; Wang, H.; Li, C.-J. *Org. Lett.* **2016**, *18*, 2184. (b) Ye, M.; Wen, Y.; Li, H.; Fu, Y.; Wang, Q. *Tetrahedron Lett.* **2016**, *57*, 4983. (c) Liu, H.; Wei, Y.; Cai, C. *Synlett* **2016**, *27*, A–F.



Scheme III.21 – Aliphatic ketones scope with substitutions different than methyl.

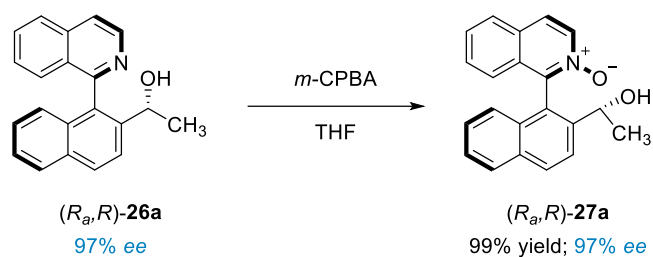
From this scope extension (Scheme III.21), it is clear that this methodology can also be applied to ketones with aliphatic substituents different than methyl. Unfortunately, not all substitutions were allowed, since heterobiaryl ketones **25l** and **25m** (Scheme III.19) did not provide the desired products, and the starting materials were completely recovered. Nonetheless, the asymmetric reduction of heterobiaryl ketones **25i-k** could be satisfactorily performed. It is worth to highlight the result obtained from the reduction of a more sterically demanding ketone **25j**, where a single diastereomer was formed although with a slight decrease on its enantioselectivity. Moreover, the synthesis of **26i** and **26k** displayed similar results than those obtained for the model heterobiaryl ketone **25a**.

So far, the scope of this dynamic kinetic resolution has provided up to eleven different carbinols with high yields, good diastereoselectivities and excellent enantioselectivities.

III.2.4. Representative transformations.

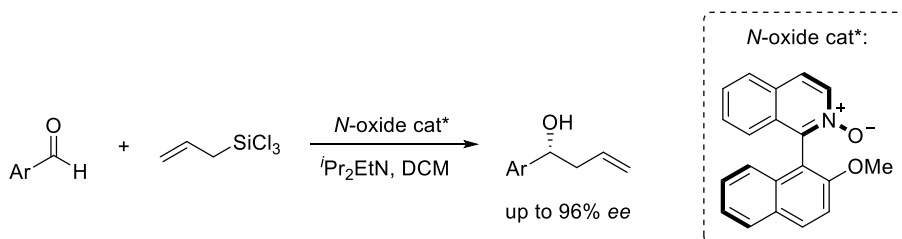
During the previous section, the scope and limitations of the methodology was analyzed. Nonetheless, it is also necessary to show the versatility of the resulting products and their applicability. For this reason, the model heterobiaryl alcohol (*R_a*,*R*)-**26a** was chosen as a platform to carry out a variety of useful derivatizations.

First, the *N*-oxidation of isoquinolyl nitrogen after treatment with *meta*-chloroperbenzoic acid (*m*-CPBA) afforded (*R_a*,*R*)-**27a** in quantitative yield (Scheme III.22).



Scheme III.22 – Isoquinolyl nitrogen oxidation for the synthesis of (*R_a*,*R*)-**27a**.

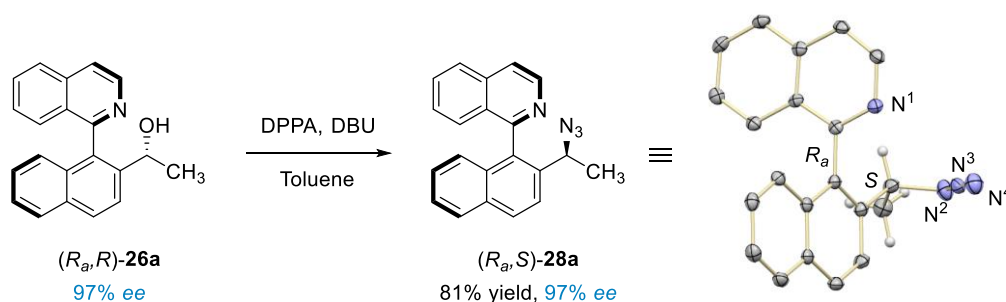
It is worth to mention that the resulting *N*-oxide (*R_a*,*R*)-**27a** could have applications as Lewis base organocatalyst for the Sakurai–Hosomi–Denmark-type asymmetric addition of allylic trichlorosilanes to aldehydes given the structural similarities with the catalyst used by Kočovský (Scheme III.23).¹⁵²



Scheme III.23 – Allylation of aromatic aldehydes developed by the group of Kočovský.

¹⁵² Malkov, A. V., Dufková, L.; Farrugia, L.; Kočovský, P. *Angew. Chem.* **2003**, *115*, 3802.

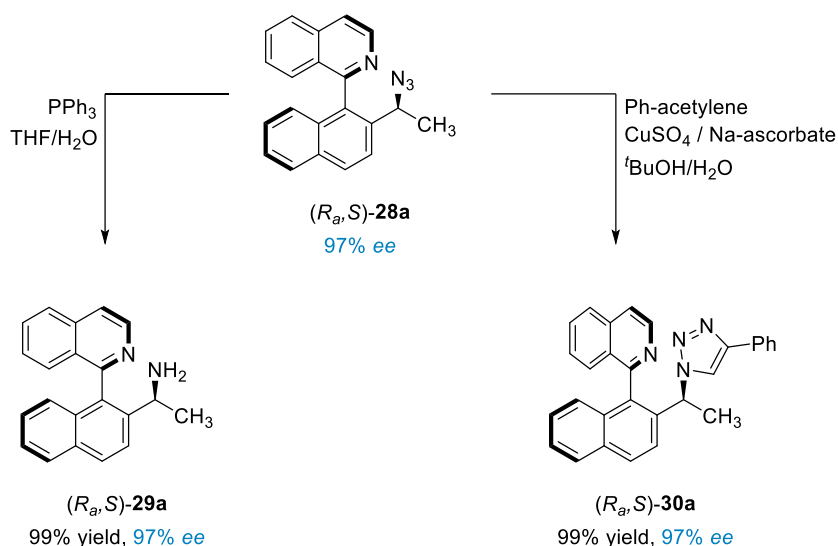
The next transformation was performed over the secondary alcohol. Thus, a variant of the Mitsunobu reaction was carried out on substrate (R_a,R) -**26a** using diphenyl phosphoryl azide (DPPA) in combination with 1,8-diazabicyclo(5.4.0)undec-7-ene (DBU) as base, to achieve the corresponding azide (R_a,S) -**28a** (Scheme III.24).¹⁵³ The single crystal X-ray analysis showed the inversion of the absolute configuration at the stereogenic centre, as expected because of the involved S_N2 mechanism.



Scheme III.24 – Mitsunobu reaction over (R_a,R) -**26a**. Thermal ellipsoids drawn for 50% probability.

This resulting azide (R_a,S) -**28a** shows a very interesting structure that was used for the next two transformations. The first one consisted on the reduction of the azide to the corresponding amine (R_a,S) -**29a** with excellent yield through a Staudinger reduction (Scheme III.25).

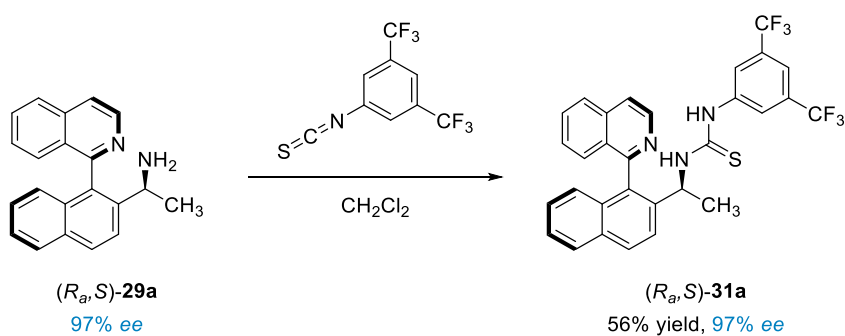
¹⁵³ Thompson, A. S.; Humphrey, G. R.; DeMarco, A. M.; Mathre, D. J.; Grabowski, E. J. *J. Org. Chem.* **1993**, 58, 5886.



*Scheme III.25 – Transformations carried out to azide (*R,S*)-28a.*

The second reaction that was performed on the azide functionality consisted on a copper-catalyzed alkyne-azide cycloaddition (CuAAC), also known as the most paradigmatic example of the “click Chemistry”, providing the 1,2,3-triazole (*R,S*)-**30a** in a quantitative fashion.

Looking at the structure of the amine (*R,S*)-**29a**, its condensation with an iso(thio)cyanate to provide the corresponding (thio)urea could be anticipated. Indeed, a novel class of bifunctional thiourea organocatalyst (*R,S*)-**31a** was easily prepared when employing 1-isothiocyanato-3,5-bis(trifluoromethyl)benzene (Scheme III.26).



*Scheme III.26 – Isothiocyanate condensation to amine (*R,S*)-29a for the synthesis of (*R,S*)-31a.*

However, this thiourea was obtained with moderate yield, a fact that was attributed to the sterically crowded environment around the amino group, hampering the condensation. The product from this reaction presents structural particularities that make it an appealing potential candidate as a bifunctional organocatalyst, and its performance will be evaluated in future projects within our research group.

Summarizing, several functionalized structures have been synthesized using carbinol (*R_a,R*)-**26a**, derived from the Zn-catalyzed asymmetric hydrosilylation, without any erosion on the enantiopurity of the resulting products. Thus, the method provides an accessible route for the synthesis of a variety of ligands and organocatalysts containing both central and axial stereogenic elements.

III.3. Conclusions.

To summarize, along this chapter, an alternative methodology for the simultaneous generation of central and axial chirality elements has been described. In this case, a dynamic kinetic resolution (DKR) of heterobiaryl ketones has been employed together with an atroposelective reduction of these ketones by a Zn-catalyzed asymmetric hydrosilylation reaction we have developed a novel methodology for the synthesis of functionalized. This methodology has allowed for the synthesis of central and axially chiral heterobiaryl carbinols with high diastereo selectivities and excellent enantioselectivities.

Moreover, the resulting products have been efficiently transformed without erosion on the enantiomeric purity, obtaining appealing highly functionalized structures with potential applications as ligands for metal and organocatalysts.

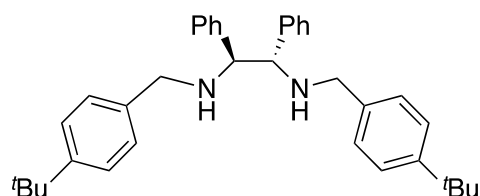
From this strategy, it can be concluded that the atropisomerization event through the formation of five-membered ring transition states can take place efficiently, allowing for the use of more sterically demanding substrates than the previously described in literature.

General procedure for the synthesis of ligands L28-L33

To a suspension of (1*S*,2*S*)-(-)-1,2-diphenylethylenediamine (1.0 eq.) and K₂CO₃ (4.0 eq.) in anhydrous DMF (2 mM) was added a solution of benzylic halide (2.0 eq.) in anhydrous DMF (1 mM). The reaction mixture was kept stirred for 16h at ambient temperature and then quenched by addition of water. The mixture was extracted with EtOAc and washed with water several times and brine. The organic layer was dried over anhydrous MgSO₄. After removal of the drying agent by filtration, the filtrate was concentrated under vacuum. The crude mixture was purified by column chromatography.

Experimental data matched those described in literature for **L28**, **L29** and **L31-L33**.

Synthesis of (1*S*,2*S*)-*N,N'*-Bis[4-(*tert*-butyl)benzyl]-1-phenyl-2-phosphanylethane-1,2-diamine. **L30**



Following the general procedure, using 4-*tert*-butylbenzyl bromide (217 mg, 0.94 mmol). White solid was obtained after column chromatography with *n*-hexane/EtOAc 12:1 (160 mg, 67%).

$[\alpha]_{\text{D}}^{20} +12.7$ (*c* 0.71, CHCl₃).

¹H-NMR (400 MHz, CDCl₃): δ 7.33 (d, *J* = 8.3 Hz, 4H), 7.20-7.14 (m, 10H), 7.07 (dd, *J* = 7.9 and 2.0 Hz, 4H), 3.77 (s, 2H), 3.64 (d, *J* = 13.1 Hz, 2H), 3.52 (d, *J* = 13.1 Hz, 2H), 1.34 (s, 18H).

¹³C-NMR (100 MHz, CDCl₃): δ 149.7, 128.0, 127.9, 127.8, 126.9, 125.2, 68.4, 51.0, 34.4, 31.4.

HRMS (ESI) calculated for C₃₆H₄₅N₂ (M + H⁺) 505.3577. Found 505.3574.

III.4.2. General procedures for the synthesis of heterobiaryl ketones.

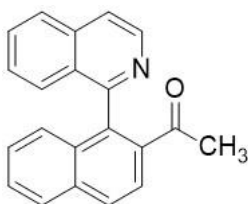
Procedure A: Synthesis via Pd-catalyzed Heck reaction with butyl vinyl ether.

Following a described procedure, a flamed-dried Schlenk tube was charged with the corresponding sulfonate *rac*-**3b-h**, Pd(AcO)₂ (5.6 mg, 0.0025 mmol) and dppp (12 mg, 0.028 mmol). After three cycles of vacuum-argon, DMF (1.5 mL) was added and the resulting mixture was stirred for 20 min at room temperature. Then Et₃N (0.14 mL, 1 mmol) and butyl vinyl ether (0.33 mL, 2.5 mmol) were sequentially added and the resulting mixture was stirred at 80 °C for 72 hours. The reaction crude was allowed to reach room temperature and was slowly added over 10 min to 2M aq. HCl (15 mL) cooled in an ice-water bath. The resulting mixture was stirred for 0.5 h and was poured into CH₂Cl₂ (20 mL). NaHCO₃ was then added until neutrality, the phases separated, and the aqueous layer was extracted with CH₂Cl₂ (3×10 mL). The combined organic layers were dried over anhydrous Na₂SO₄, filtered, concentrated, and the residue was purified by column chromatography on silica gel with *n*-hexane/EtOAc mixtures.

Procedure B: Synthesis via bromide lithiation and electrophilic quenching.

Over a solution of corresponding heterobiaryl bromide (1.0 eq.) in freshly distilled THF (0.05 M) at -80 °C, *n*-BuLi (1.3 eq., 1.6 M in hexane) was added dropwise. After 20 min, the corresponding electrophile (3.0 – 4.0 eq.) was slowly added. The mixture was stirred for 2h, quenched with a saturated aqueous solution of NH₄Cl and allowed to warm to room temperature. The resulting mixture was extracted with EtOAc, the combined organic layers were dried over anhydrous Na₂SO₄, filtered, concentrated, and the residue was purified by column chromatography on silica gel with *n*-hexane/EtOAc mixtures.

Synthesis of 1-[1-(Isoquinolin-1-yl)naphthalen-2-yl]ethan-1-one. **25a**



Following the general procedure **A**, using **3b** (2.28 g, 4.10 mmol) afforded **25a** (723 mg, 59%) as a yellow amorphous solid.

$^1\text{H-NMR}$ (400 MHz, CDCl_3): δ 8.69 (d, $J = 5.7$ Hz, 1H), 8.06 (d, $J = 8.6$ Hz, 1H), 7.98-7.92 (m, 3H), 7.79 (d, $J = 5.7$ Hz, 1H), 7.66 (m, 1H), 7.54 (t, $J = 7.5$ Hz, 1H), 7.38-7.37 (m, 2H), 7.31 (t, $J = 8.0$ Hz, 1H), 7.17 (d, $J = 8.6$ Hz, 1H), 2.13 (s, 3H).

$^{13}\text{C-NMR}$ (100 MHz, CDCl_3): δ 200.8, 159.7, 142.3, 137.0, 136.2, 135.9, 134.8, 132.4, 130.3, 129.0, 128.9, 127.9, 127.7, 127.5, 127.4, 127.0, 127.0, 126.8, 124.9, 120.4, 29.6.

HRMS (ESI) calculated for $\text{C}_{21}\text{H}_{16}\text{NO}$ ($\text{M} + \text{H}^+$) 298.1226. Found 298.1229.

Synthesis of 1-[1-(Quinazolin-4-yl)naphthalen-2-yl]ethan-1-one. **25b**



Following the general procedure **A**, using **3c**¹⁵⁴ (184 mg, 0.5 mmol) afforded **25b** (144 mg, 75%) as a yellow amorphous solid.

$^1\text{H-NMR}$ (400 MHz, CDCl_3): δ 9.41 (s, 1H), 8.16 (d, $J = 8.5$ Hz, 1H), 8.12 (d, $J = 8.7$ Hz, 1H), 8.01 (d, $J = 8.6$ Hz, 1H), 7.97 (d, $J = 8.2$ Hz, 1H), 7.87 (t, $J = 8.1$ Hz, 1H), 7.57 (t, $J = 7.6$ Hz, 1H), 7.40 (t, $J = 7.9$ Hz, 1H), 7.36-7.30 (m, 2H), 7.08 (d, $J = 8.6$ Hz, 1H), 2.46 (s, 3H).

¹⁵⁴ Ramírez-López, P.; Ros, A.; Estepa, B.; Fernández, F.; Fiser, B.; Gómez-Bengoa, E.; Lassaletta, J. M., *ACS Catal.* **2016**, *6*, 3955.

^{13}C -NMR (100 MHz, CDCl_3): δ 199.1, 170.0, 154.7, 149.7, 135.0, 134.8, 134.6, 133.8, 131.7, 129.8, 128.8, 128.2, 128.1, 127.9, 127.6, 127.0, 126.2, 125.5, 124.9, 28.9.

HRMS (ESI) calculated for $\text{C}_{20}\text{H}_{15}\text{N}_2\text{O}$ ($\text{M} + \text{H}^+$) 299.1179. Found 299.1182.

Synthesis of 1-[1-(3-Methylpyridin-2-yl)naphthalen-2-yl]ethan-1-one. **25c**



Following the general procedure **A**, using **3e** (603 mg, 1.16 mmol) afforded **25c** (208 mg, 69%) as a yellow amorphous solid.

^1H -NMR (400 MHz, CDCl_3): δ 8.58 (d, $J = 2.8$ Hz, 1H), 7.96 (d, $J = 8.7$ Hz, 1H), 7.91 (d, $J = 8.3$ Hz, 1H), 7.86 (d, $J = 8.6$ Hz, 1H), 7.66 (d, $J = 7.8$ Hz, 1H), 7.54 (t, $J = 7.8$ Hz, 1H), 7.41 (t, $J = 7.6$ Hz, 1H), 7.32 (t, $J = 6.2$ Hz, 1H), 7.25 (d, $J = 9.0$ Hz, 1H), 2.26 (s, 3H), 1.99 (s, 3H).

^{13}C -NMR (100 MHz, CDCl_3): δ 201.6, 157.5, 146.9, 137.9, 137.5, 135.5, 134.9, 133.6, 131.5, 128.6, 128.1, 127.7, 127.2, 126.7, 124.8, 122.9, 29.9, 18.9.

HRMS (ESI) calculated for $\text{C}_{18}\text{H}_{16}\text{NO}$ ($\text{M} + \text{H}^+$) 262.1226. Found 262.1225.

Synthesis of 1-[1-(isoquinolin-1-yl)-4-methylnaphthalen-2-yl]ethan-1-one. **25e**



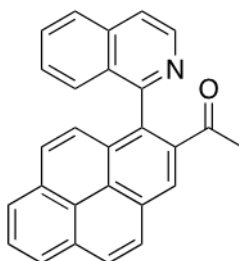
Following the general procedure **A**, using **3g** (284 mg, 0.5 mmol) afforded **25e** (145 mg, 93%) as a yellow amorphous solid.

$^1\text{H-NMR}$ (400 MHz, CDCl_3): δ 8.69 (d, $J = 5.7$ Hz, 1H), 8.11 (d, $J = 8.4$ Hz, 1H), 7.92 (d, $J = 8.4$ Hz, 1H), 7.81 (s, 1H), 7.78 (d, $J = 5.7$ Hz, 1H), 7.66 (t, $J = 7.1$ Hz, 1H), 7.58 (t, $J = 7.6$ Hz, 1H), 7.40-7.28 (m, 3H), 7.20 (d, $J = 8.8$ Hz, 1H), 2.85 (s, 3H), 2.08 (s, 3H).

$^{13}\text{C-NMR}$ (100 MHz, CDCl_3): δ 201.1, 159.9, 142.3, 135.9, 135.9, 135.6, 135.2, 134.0, 132.5, 130.2, 129.1, 128.1, 127.5, 127.5, 126.9, 126.9, 126.6, 125.4, 124.1, 120.4, 29.7, 19.7.

HRMS (ESI) calculated for $\text{C}_{22}\text{H}_{18}\text{NO}$ ($\text{M} + \text{H}^+$) 312.1383. Found 312.1386.

Synthesis of 1-[1-(Isoquinolin-1-yl)pyren-2-yl]ethan-1-one. **25f**.



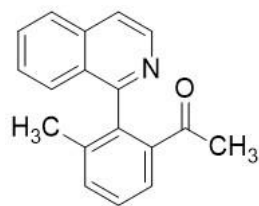
Following the general procedure **A**, using **3h** (284 mg, 0.45 mmol) afforded **25f** (125 mg, 76%) as a yellow amorphous solid.

$^1\text{H-NMR}$ (400 MHz, CDCl_3): δ 8.74 (d, $J = 5.8$ Hz, 1H), 7.70 (s, 1H), 8.27 (d, $J = 7.7$ Hz, 1H), 8.22 (s, 2H), 8.16 (d, $J = 7.5$ Hz, 1H), 8.07 (t, $J = 7.6$ Hz, 1H), 7.98 (d, $J = 8.3$ Hz, 1H), 7.90 (d, $J = 9.2$ Hz, 1H), 7.84 (d, $J = 5.8$ Hz, 1H), 7.69 (m, 1H), 7.40 (d, $J = 9.2$ Hz, 1H), 7.36-7.35 (m, 2H), 2.40 (s, 3H).

$^{13}\text{C-NMR}$ (100 MHz, CDCl_3): δ 201.2, 160.3, 142.2, 136.7, 136.0, 132.6, 131.8, 131.1, 130.5, 130.3, 129.3, 128.7, 128.6, 127.6, 127.5, 127.1, 127.1, 127.0, 126.2, 125.9, 125.7, 125.5, 125.1, 124.1, 120.5, 29.5.

HRMS (ESI) calcd. for $\text{C}_{27}\text{H}_{18}\text{NO}$ ($\text{M} + \text{H}^+$) 372.1383. Found 372.1383.

Synthesis of 1-[2-(Isoquinolin-1-yl)-3-methylphenyl]ethan-1-one. **25g**



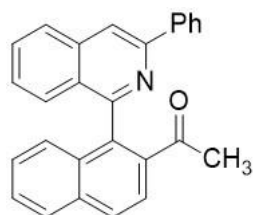
Following the general procedure **B**, using **3i(Br)**¹⁵⁵ (191 mg, 0.64 mmol), and *N,N*-dimethylacetamide (180 μ L, 1.92 mmol) afforded **25g** (109 mg, 58%) as a yellow amorphous solid.

¹H-NMR (400 MHz, CDCl₃): δ 8.56 (d, *J* = 5.7 Hz, 1H), 7.86 (d, *J* = 8.2 Hz, 1H), 7.73 (dd, *J* = 6.7 and 2.3 Hz, 1H), 7.66-7.62 (m, 2H), 7.49-7.41 (m, 4H), 2.14 (s, 3H), 1.93 (s, 3H).

¹³C-NMR (100 MHz, CDCl₃): δ 200.3, 160.8, 142.1, 139.0, 137.9, 137.8, 135.8, 133.7, 130.0, 128.3, 127.9, 127.4, 127.0, 126.7, 126.3, 119.9, 28.9 19.7.

HRMS (ESI) calculated for C₁₈H₁₆NO (*M* + H⁺) 262.1226. Found 262.1227.

Synthesis of 1-[1-(3-Phenylisoquinolin-1-yl)naphthalen-2-yl]ethan-1-one. **25h**



Following the general procedure **A**, using **3i** (315 mg, 0.5 mmol) afforded **25h** (109 mg, 58%) as a yellow amorphous solid.

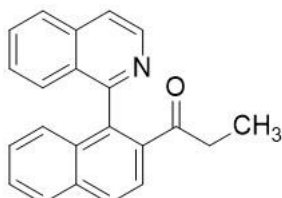
¹H-NMR (400 MHz, CDCl₃): δ 8.23 (s, 1H), 8.19-8.17 (m, 2H), 8.09 (d, *J* = 8.6 Hz, 1H), 8.00-7.97 (m, 3H), 7.67 (ddd, *J* = 8.1, 6.5 and 1.5 Hz, 1H), 7.55 (m, 1H), 7.51-7.47 (m, 2H), 7.42-7.33 (m, 5H), 2.09 (s, 3H).

¹⁵⁵ Ramírez-López, P.; Ros, A.; Romero-Arenas, A.; Iglesias-Sigüenza, J.; Fernández, R.; Lassaletta, J. M., *J. Am. Chem. Soc.* **2016**, *138*, 12053.

^{13}C -NMR (100 MHz, CDCl_3): δ 201.4, 159.2, 150.6, 139.3, 137.1, 137.0, 136.8, 134.8, 132.4, 130.4, 128.9, 128.7, 128.5, 128.0, 128.0, 127.6, 127.4, 127.3, 127.1, 127.0, 126.8, 124.8, 116.5, 29.9.

HRMS (ESI) calculated for $\text{C}_{27}\text{H}_{20}\text{NO}$ ($\text{M} + \text{H}^+$) 374.1539. Found 374.1539.

Synthesis of 1-[1-(Isoquinolin-1-yl)naphthalen-2-yl]propan-1-one. **25i**



Following the general procedure **B**, using **3b(Br)**; Error! Marcador no definido. (167 mg, 0.5 mmol) and ethyl propionate (253 μL , 2 mmol) afforded **25i** (37 mg, 24%) as a yellow amorphous solid.

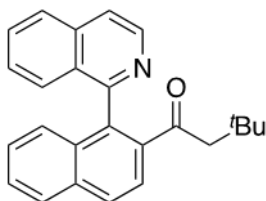
^1H -NMR (400 MHz, CDCl_3): δ 8.66 (d, $J = 5.7$ Hz, 1H), 8.06 (d, $J = 8.6$ Hz, 1H), 7.95 (d, $J = 7.4$ Hz, 1H), 7.93 (d, $J = 8.2$ Hz, 1H), 7.92 (d, $J = 8.6$ Hz, 1H), 7.78 (d, $J = 5.7$ Hz, 1H), 7.67 (m, 1H), 7.53 (ddd, $J = 8.1$, 6.8 and 1.2 Hz, 1H), 7.38 (d, $J = 3.7$ Hz, 2H), 7.31 (ddd, $J = 10.2$, 6.8 and 1.3 Hz, 1H), 2.66 (m, 1H), 2.50 (m, 1H), 0.89 (d, $J = 7.2$ Hz, 3H).

^{13}C -NMR (100 MHz, CDCl_3): δ 204.1, 159.8, 142.1, 136.5, 135.9, 134.6, 132.5, 130.4, 129.1, 128.9, 128.0, 127.5, 127.4, 127.1, 127.0, 127.0, 124.5, 120.5, 35.0, 8.2.

HRMS (ESI) calculated for $\text{C}_{22}\text{H}_{18}\text{NO}^+$ ($\text{M} + \text{H}^+$) 312.1383. Found 312.1380.

Synthesis of 1-[1-(isoquinolin-1-yl)naphthalen-2-yl]-3,3-dimethylbutan-1-one. **25j**

25j



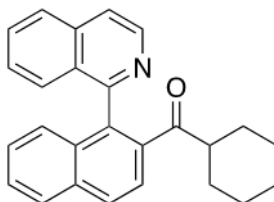
Following the general procedure **B**, using **3b(Br)**; Error! Marcador no definido. (167 mg, 0.5 mmol) and *N*-methoxy-*N*-3,3-trimethylbutanamide (318 mg, 2 mmol) afforded **25j** (76 mg, 45%) as a yellow amorphous solid.

¹H-NMR (400 MHz, CDCl₃): δ 8.66 (d, *J* = 5.8 Hz, 1H), 8.05 (d, *J* = 8.6 Hz, 1H), 7.95 (d, *J* = 8.2 Hz, 1H), 7.93 (d, *J* = 8.5 Hz, 1H), 7.81 (d, *J* = 9.1 Hz, 1H), 7.79 (d, *J* = 7.4 Hz, 1H), 7.70 (m, 1H), 7.52 (t, *J* = 7.7 Hz, 1H), 7.43-7.37 (m, 2H), 7.32 (t, *J* = 7.9 Hz, 1H), 7.19 (d, *J* = 8.7 Hz, 1H), 2.17 (s, 2H), 0.80 (s, 9H).

¹³C-NMR (100 MHz, CDCl₃): δ 204.5, 159.5, 139.1, 136.0, 134.4, 132.3, 130.5, 129.1, 128.0, 127.6, 127.4, 127.2, 127.0, 124.4, 120.6, 53.7, 31.3, 29.6.

HRMS (ESI) calculated for C₂₅H₂₄NO (M + H⁺) 354.1852. Found 354.1854.

Synthesis of Cyclohexyl[1-(isoquinolin-1-yl)naphthalen-2-yl]methanone. **25k**



Following the general procedure **B**, using **3b(Br)** (167 mg, 0.5 mmol) and ethyl cyclohexanecarboxylate (312 mg, 2 mmol) afforded **25k** (40 mg, 22%) as a yellow amorphous solid.

¹H-NMR (400 MHz, CDCl₃): δ 8.68 (d, *J* = 5.7 Hz, 1H), 8.05 (d, *J* = 8.5 Hz, 1H), 7.95 (d, *J* = 8.5 Hz, 1H), 7.92 (d, *J* = 8.5 Hz, 1H), 7.79 (d, *J* = 8.6 Hz, 1H), 7.77 (d, *J* = 5.7 Hz, 1H), 7.67 (ddd, *J* = 8.2, 6.4 and 1.6 Hz, 1H), 7.52 (ddd, *J* = 8.2, 6.7 and 1.2 Hz, 1H), 7.43-7.36 (m, 2H), 7.32 (ddd, *J* = 8.2, 6.7 and 1.3 Hz, 1H), 7.23 (d, *J* = 8.5 Hz, 1H), 2.44 (m, 1H), 1.71-1.61 (m, 2H), 1.59-1.49 (m, 2H), 1.29 (m, 1H), 1.21-1.09 (m, 2H), 1.08-0.99 (m, 2H), 0.87 (m, 1H).

¹³C-NMR (100 MHz, CDCl₃): δ 208.1, 159.4, 142.1, 137.5, 135.9, 134.4, 132.3, 130.3, 129.0, 128.9, 128.0, 127.5, 127.3, 127.3, 127.1, 127.0, 126.9, 124.5, 120.4, 49.1, 28.9, 28.5, 25.7, 25.6, 25.6.

HRMS (ESI) calculated for C₂₆H₂₄NO (M + H⁺) 366.1852. Found 366.1845.

III.4.3. General procedure for the Zn-catalyzed asymmetric hydrosilylation of heterobiaryl ketones.

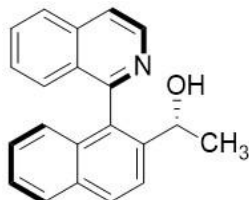
To a flame-dried Schlenk tube, zinc acetate (0.92 mg, 0.005 mmol, 5 mol%) and **L33** (3.7 mg, 0.006 mmol, 6 mol%) were dissolved in freshly distilled THF (0.4 mL) and stirred for 1 h at room temperature under N₂ atmosphere. Then (EtO)₂MeSiH (32 μL, 0.2 mmol, 2.0 eq.) was added and the reaction mixture was stirred for an additional hour. Finally, heterobiaryl ketone **25** (0.1 mmol, 1.0 eq.) was added and the resulting mixture was stirred at 70 °C for 36 h. The reaction crude was allowed to reach room temperature, 1M aq. HCl (0.5 mL) was added and the resulting mixture was stirred for *ca.* 1 h. CH₂Cl₂ (2 mL) was added, the mixture was neutralized with saturated aqueous solution of NaHCO₃, the phases separated, and the aqueous layer extracted 3 times with CH₂Cl₂. The combined organic layers were dried over anhydrous Na₂SO₄, filtered and concentrated under reduced pressure. The residue was purified by flash chromatography (6:1 CH₂Cl₂/EtOAc) affording the resulting carbinols **26**.

Note. Racemic products were prepared as follows: To a solution of ketone 25 in MeOH cooled with an ice-water bath, sodium borohydride (2.0 eq.) was added in portions and the resulting mixture was allowed to warm to room temperature. After complete disappearance of the starting material by TLC, the reaction mixture was quenched by careful addition of saturated aqueous solution of NH₄Cl and the resulting mixture was extracted with EtOAc. The combined organic layers were dried over anhydrous Na₂SO₄, filtered, concentrated. Diastereomers were separated from reaction crude by preparative TLC prior to HPLC analysis.

Yields and characterization data for each isomer of **26** are as follows.

Synthesis of 1-[1-(Isoquinolin-1-yl)naphthalen-2-yl]ethan-1-ol. **26a**

Following the general procedure using heterobiaryl ketone **25a** (30 mg, 0.1 mmol), purification by flash chromatography (6:1 CH₂Cl₂/EtOAc) afforded both diastereomers characterized separately:



(*R,R*)-**26a** (20 mg, 67%).

$[\alpha]_D^{20}$ -312.0 (*c* 0.48, CHCl₃) for 97% *ee*.

¹H-NMR (400 MHz, CDCl₃): δ 8.70 (dd, *J* = 5.8 and 1.6 Hz, 1H), 8.03 (dd, *J* = 8.7 and 3.2 Hz, 1H), 7.95 (d, *J* = 8.3 Hz, 1H), 7.91 (d, *J* = 8.2 Hz, 1H), 7.85 (dd, *J* = 8.6 and 2.8 Hz, 1H), 7.78 (d, *J* = 5.8 Hz, 1H), 7.70 (m, 1H), 7.45–7.36 (m, 3H), 7.24 (t, *J* = 7.1 Hz, 1H), 6.96 (d, *J* = 8.4 Hz, 1H), 4.49 (m, 1H), 2.15 (br s, 1H), 1.37 (d, *J* = 6.5 Hz, 3H).

¹³C-NMR (100 MHz, CDCl₃) δ 159.5, 142.4, 141.7, 136.2, 132.9, 132.4, 130.6, 129.4, 128.6, 128.0, 127.7, 127.0, 127.0, 126.4, 126.1, 125.7, 123.4, 120.4, 68.2, 24.7.

HRMS (ESI) calculated for C₂₁H₁₈NO (M + H⁺) 300.1383. Found 300.1385.

HPLC (AS-H column, *n*-hex/IPA 85:15, T= 30°C, F= 1.0 mL/min): *t*_R 5.98 min (major) and 13.19 min (minor).

M. p. 175-177 °C.



(*S,R*)-**26a** (3 mg, 10%).

$[\alpha]_D^{20}$ +153.5 (*c* 0.51, CHCl₃) for 90% *ee*.

$^1\text{H-NMR}$ (400 MHz, CDCl_3): δ 8.65 (d, $J = 5.8$ Hz, 1H), 8.00 (d, $J = 8.6$ Hz, 1H), 7.96 (d, $J = 8.3$ Hz, 1H), 7.91 (d, $J = 8.2$ Hz, 1H), 7.85 (d, $J = 8.6$ Hz, 1H), 7.81 (d, $J = 5.8$ Hz, 1H), 7.71 (ddd, $J = 8.2, 6.3$ and 1.8 Hz, 1H), 7.44 (ddd, $J = 8.1, 6.8$ and 1.2 Hz, 1H), 7.41–7.34 (m, 2H), 7.23 (ddd, $J = 8.4, 6.8$ and 1.3 Hz, 1H), 6.92 (dd, $J = 8.5$ and 0.8 Hz, 1H), 4.47 (q, $J = 6.5$ Hz, 1H), 3.59 (br s, 1H), 1.36 (d, $J = 6.5$ Hz, 3H).

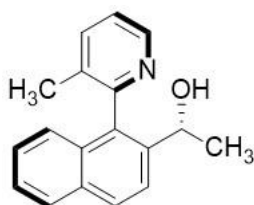
$^{13}\text{C-NMR}$ (100 MHz, CDCl_3) δ 159.5, 141.9, 141.8, 136.2, 133.5, 132.7, 132.3, 130.8, 129.6, 128.8, 128.1, 127.7, 127.7, 127.1, 126.4, 126.1, 125.7, 123.2, 120.8, 66.3, 21.8.

HRMS (ESI) calculated for $\text{C}_{21}\text{H}_{18}\text{NO}$ ($\text{M} + \text{H}^+$) 300.1383. Found 300.1385.

HPLC (AS-H column, *n*-hex/IPA 85:15, $T = 30^\circ\text{C}$, $F = 1.0$ mL/min): t_{R} 4.54 min (minor) and 5.11 min (major).

Synthesis of 1-[3-(Methylpyridin-2-yl)naphthalen-2-yl]ethan-1-ol. **26c**

Following the general procedure using heterobiaryl ketone **25c** (52 mg, 0.2 mmol), Purification by flash chromatography (6:1 $\text{CH}_2\text{Cl}_2/\text{EtOAc}$) afforded both diastereomers characterized separately:



(*R,R*)-**26c** (41 mg, 78%).

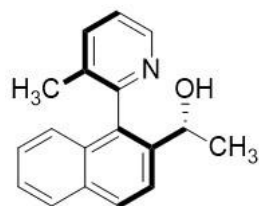
$[\alpha]_{\text{D}}^{20} +5.1$ (c 0.32, CHCl_3) for 96% *ee*.

$^1\text{H-NMR}$ (400 MHz, CDCl_3): δ 8.58 (dd, $J = 4.8$ and 1.6 Hz, 1H), 7.92 (d, $J = 8.6$ Hz, 1H), 7.85 (d, $J = 8.1$ Hz, 1H), 7.72 (d, $J = 8.6$ Hz, 1H), 7.66 (d, $J = 7.7$ Hz, 1H), 7.43 (ddd, $J = 8.0, 6.8$ and 1.2 Hz, 1H), 7.34–7.28 (m, 2H), 7.07 (d, $J = 8.4$ Hz, 1H), 4.55 (q, $J = 6.5$ Hz, 1H), 2.54 (br s, 1H), 1.97 (s, 3H), 1.34 (d, $J = 6.5$ Hz, 3H).

$^{13}\text{C-NMR}$ (100 MHz, CDCl_3) δ 157.2, 147.0, 140.4, 137.8, 134.0, 133.0, 132.9, 131.4, 128.9, 128.0, 126.4, 125.6, 125.2, 123.4, 122.6, 68.3, 24.7, 18.9.

HRMS (ESI) calculated for $\text{C}_{18}\text{H}_{18}\text{NO}$ ($\text{M} + \text{H}^+$) 264.1383. Found 264.1385.

HPLC (AS-H column, *n*-hex/IPA 90:10, T= 30°C, F= 1.0 mL/min): t_R 6.14 min (major) and 7.32 min (minor).



(*S,R*)-**26c** (8 mg, 15%).

$[\alpha]_D^{20} +44.0$ (*c* 0.39, CHCl₃) for 82% *ee*.

¹H-NMR (400 MHz, CDCl₃): δ 8.59 (dd, *J* = 4.9 and 1.0 Hz, 1H), 7.95 (d, *J* = 8.6 Hz, 1H), 7.89 (d, *J* = 8.2 Hz, 1H), 7.80 (d, *J* = 8.6 Hz, 1H), 7.77 (d, *J* = 7.8 Hz, 1H), 7.46 (ddd, *J* = 8.0, 6.8 and 1.2 Hz, 1H), 7.39 (dd, *J* = 7.8 and 5.0 Hz, 1H), 7.36 (ddd, *J* = 8.2, 6.8 and 1.3 Hz, 1H), 7.10 (d, *J* = 8.5 Hz, 1H), 4.54 (q, *J* = 6.5 Hz, 1H), 4.05 (br s, 1H), 2.00 (s, 3H), 1.46 (d, *J* = 6.5 Hz, 3H).

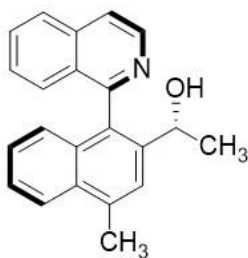
¹³C-NMR (100 MHz, CDCl₃) δ 156.5, 146.1, 140.9, 139.0, 134.3, 133.9, 132.8, 131.0, 129.4, 128.4, 126.7, 125.8, 125.0, 123.3, 123.2, 66.2, 21.6, 18.9.

HRMS (ESI) calculated for C₁₈H₁₈NO (*M* + H⁺) 264.1383. Found 264.1385.

HPLC (AS-H column, *n*-hex/IPA 90:10, T= 30°C, F= 1.0 mL/min): t_R 4.43 min (minor) and 4.90 min (major).

Synthesis of 1-[1-(Isoquinolin-1-yl)-4-methylnaphthalen-2-yl]ethan-1-ol. **26e**

Following the general procedure using heterobiaryl ketone **25e** (62 mg, 0.2 mmol), purification by flash chromatography (6:1 CH₂Cl₂/EtOAc) afforded both diastereomers characterized separately:



(*R,R*)-**26e** (40.4 mg, 64%).

$[\alpha]_D^{20} +4.7$ (*c* 0.50, CHCl₃) for 97% *ee*.

¹H-NMR (400 MHz, CDCl₃): δ 8.69 (d, *J* = 5.8 Hz, 1H), 8.06 (d, *J* = 8.2 Hz, 1H), 7.93 (d, *J* = 8.2 Hz, 1H), 7.76 (d, *J* = 5.8 Hz, 1H), 7.69 (s, 1H), 7.67 (ddd, *J* = 8.1, 6.6 and 1.0 Hz, 1H), 7.49–7.44 (m, 2H), 7.36 (t, *J* = 7.6 Hz, 1H), 7.24 (ddd, *J* = 8.2, 6.8 and 1.2 Hz, 1H), 6.99 (d, *J* = 8.4 Hz, 1H), 4.44 (q, *J* = 6.4 Hz, 1H), 2.82 (s, 3H), 2.16 (br s, 1H), 1.35 (d, *J* = 6.4 Hz, 3H).

¹³C-NMR (100 MHz, CDCl₃) δ 159.8, 142.4, 141.1, 136.2, 135.8, 132.6, 132.1, 131.2, 130.4, 128.8, 127.6, 127.1, 126.9, 126.7, 126.0, 125.5, 124.1, 124.0, 120.2, 68.3, 24.6, 19.8.

HRMS (ESI) calculated for C₂₂H₂₀NO (*M* + H⁺) 314.1539. Found 314.1540.

HPLC (AS-H column, *n*-hex/IPA 85:15, T= 30°C, F= 1.0 mL/min): *t*_R 4.86 min (major) and 9.68 min (minor).



(*S,R*)-**26e** (10 mg, 16%).

$[\alpha]_D^{20} +44.6$ (*c* 0.63, CHCl₃) for 89% *ee*.

¹H-NMR (400 MHz, CDCl₃): δ 8.65 (d, *J* = 5.8 Hz, 1H), 8.07 (d, *J* = 8.4 Hz, 1H), 7.95 (d, *J* = 8.2 Hz, 1H), 7.78 (d, *J* = 5.8 Hz, 1H), 7.71–7.68 (m, 2H), 7.48 (ddd, *J* = 8.2, 6.8 and

1.2 Hz, 1H), 7.37 (d, $J = 3.4$ Hz, 2H), 7.23 (ddd, $J = 8.2, 6.7$ and 1.2 Hz, 1H), 6.95 (d, $J = 8.4$ Hz, 1H), 4.44 (q, $J = 6.5$ Hz, 1H), 3.68 (br s, 1H), 2.82 (s, 3H), 1.38 (d, $J = 6.5$ Hz, 3H).

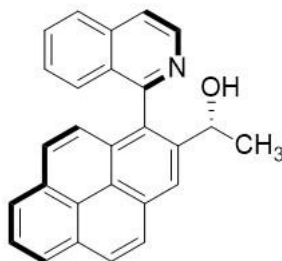
^{13}C -NMR (100 MHz, CDCl_3) δ 160.0, 142.1, 141.2, 136.2, 135.9, 132.5, 132.4, 132.0, 130.6, 129.0, 127.9, 127.6, 127.0, 126.9, 126.1, 125.6, 124.3, 123.9, 120.7, 66.4, 21.6, 19.9.

HRMS (ESI) calcd. for $\text{C}_{22}\text{H}_{20}\text{NO}$ ($\text{M} + \text{H}^+$) 314.1539. Found 314.1541.

HPLC (IA column, *n*-hex/IPA 90:10, $T = 30^\circ\text{C}$, $F = 1.0$ mL/min): t_{R} 7.70 min (minor) and 8.63 min (major).

Synthesis of 1-[1-(Isoquinolin-1-yl)pyren-2-yl]ethan-1-ol. **26f**

Following the general procedure using heterobiaryl ketone **25fg** (56 mg, 0.15 mmol), Purification by flash chromatography (6:1 $\text{CH}_2\text{Cl}_2/\text{EtOAc}$) afforded both diastereomers characterized separately:



(*R,R*)-**26f** (39 mg, 70%).

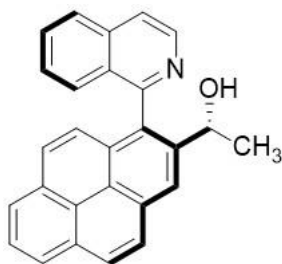
$[\alpha]_{\text{D}}^{20} -284.9$ (c 0.49, CHCl_3) for 97% *ee*.

^1H -NMR (400 MHz, CDCl_3): δ 8.76 (d, $J = 5.7$ Hz, 1H), 8.53 (s, 1H), 8.21 (d, $J = 7.6$ Hz, 1H), 8.13-8.09 (m, 3H), 7.99 (t, $J = 7.6$ Hz, 1H), 7.97 (d, $J = 8.3$ Hz, 1H), 7.84 (s, 1H), 7.82 (d, $J = 3.5$ Hz, 1H), 7.67 (ddd, $J = 8.2, 6.2,$ and 1.6 Hz, 1H), 7.34-7.27 (m, 2H), 7.23 (d, $J = 9.2$ Hz, 1H), 4.76 (q, $J = 6.4$ Hz, 1H), 2.66 (br s, 1H), 1.45 (d, $J = 6.5$ Hz, 3H).

^{13}C -NMR (100 MHz, CDCl_3) δ 159.8, 142.4, 142.3, 136.2, 131.8, 131.2, 131.1, 130.6, 130.5, 130.0, 128.9, 127.9, 127.9, 127.7, 127.5, 127.2, 127.0, 126.0, 125.4, 125.2, 125.1, 124.2, 124.0, 120.5, 69.0, 25.5.

HRMS (ESI) calculated for $\text{C}_{27}\text{H}_{20}\text{NO}$ ($\text{M} + \text{H}^+$) 374.1539. Found 374.1539.

HPLC (AS-H column, *n*-hex/IPA 85:15, T= 30°C, F= 1.0 mL/mi): t_R 6.59 min (major) and 13.67 min (minor).



(*S,R*)-**26f** (10 mg, 18%).

$[\alpha]_D^{20} +50.2$ (*c* 0.88, CHCl₃) for 86% *ee*.

¹H-NMR (400 MHz, CDCl₃): δ 8.74 (d, *J* = 5.8 Hz, 1H), 8.50 (s, 1H), 8.18 (d, *J* = 7.6 Hz, 1H), 8.12 (d, *J* = 7.6 Hz, 1H), 8.05-7.99 (m, 4H), 7.86 (d, *J* = 5.8 Hz, 1H), 7.82 (d, *J* = 9.2 Hz, 1H), 7.72 (ddd, *J* = 8.2, 6.7 and 1.3 Hz, 1H), 7.33 (ddd, *J* = 8.5, 6.9 and 1.2 Hz, 1H), 7.28 (d, *J* = 8.1 Hz, 1H), 7.18 (d, *J* = 9.2 Hz, 1H), 4.77 (q, *J* = 6.5 Hz, 1H), 1.53 (d, *J* = 6.5 Hz, 3H).

¹³C-NMR (100 MHz, CDCl₃) δ 159.9, 142.2, 141.8, 136.3, 131.8, 131.3, 130.8, 130.6, 129.9, 129.1, 127.9, 127.9, 127.8, 127.5, 127.1, 126.0, 125.6, 125.2, 125.2, 124.4, 123.8, 121.8, 120.9, 66.5, 21.9.

HRMS (ESI) calculated for C₂₇H₂₀NO (M + H⁺) 374.1539. Found 374.1542.

HPLC (AS-H column, *n*-hex/IPA 95:5, T= 30°C, F= 1.0 mL/min): t_R 9.68 min (minor) and 11.34 min (major).

Synthesis of 1-[2-(Isoquinolin-1-yl)-3-methylphenyl]ethan-1-ol. **26g**

Following the general procedure using heterobiaryl ketone **25g** (52 mg, 0.2 mmol), Purification by flash chromatography (6:1 CH₂Cl₂/EtOAc) afforded both diastereomers characterized separately:



(*R,R*)-**26g** (32 mg, 61%).

$[\alpha]_D^{20} +11.9$ (*c* 0.49, CHCl₃) for 90% *ee*.

¹H-NMR (400 MHz, CDCl₃): δ 8.60 (d, *J* = 5.8 Hz, 1H), 7.90 (d, *J* = 8.2 Hz, 1H), 7.71–7.68 (m, 2H), 7.54 (d, *J* = 8.0 Hz, 1H), 7.52 (d, *J* = 7.3 Hz, 1H), 7.46 (t, *J* = 7.3 Hz, 1H), 7.41 (t, *J* = 7.6 Hz, 1H), 7.24 (d, *J* = 7.5 Hz, 1H), 4.27 (q, *J* = 6.4 Hz), 2.43 (br s, 1H), 1.86 (s, 3H), 1.21 (d, *J* = 6.4 Hz, 3H).

¹³C-NMR (100 MHz, CDCl₃) δ 160.4, 144.4, 142.0, 136.4, 136.2, 135.8, 130.5, 129.1, 128.9, 127.7, 127.7, 127.0, 126.6, 123.2, 120.1, 68.3, 24.8, 19.8.

HRMS (ESI) calculated for C₂₃H₁₈NO (*M* + H⁺) 264.1383. Found 264.1385.

HPLC (AS-H column, *n*-hex/IPA 85:15, T= 30°C, F= 1.0 mL/min): *t*_R 4.66 min (major) and 9.39 min (minor).



(*S,R*)-**26g** (10 mg, 19%).

$[\alpha]_D^{20} +31.8$ (*c* 0.63, CHCl₃) for 88% *ee*.

¹H-NMR (400 MHz, CDCl₃): δ 8.59 (d, *J* = 5.8 Hz, 1H), 7.93 (d, *J* = 8.2 Hz, 1H), 7.75 (d, *J* = 5.8 Hz, 1H), 7.73 (ddd, *J* = 8.1, 6.0 and 1.9 Hz, 1H), 7.57–7.50 (m, 3H), 7.45 (t, *J* = 7.6 Hz, 1H), 7.26 (d, *J* = 7.7 Hz, 1H), 4.24 (q, *J* = 6.5 Hz), 3.34 (br s, 1H), 1.86 (s, 3H), 1.32 (d, *J* = 6.5 Hz, 3H).

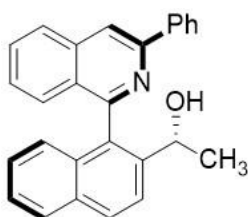
¹³C-NMR (100 MHz, CDCl₃) δ 160.5, 144.1, 141.2, 136.7, 136.5, 136.4, 130.9, 129.3, 129.1, 127.9, 127.8, 127.2, 127.2, 122.9, 120.7, 66.1, 21.1, 20.1

HRMS (ESI) calculated for C₂₃H₁₈NO (M + H⁺) 264.1383. Found 264.1385.

HPLC (AS-H column, *n*-hex/IPA 99:1, T= 30°C, F= 1.0 mL/min): t_R 16.38 min (minor) and 18.32 min (major).

Synthesis of 1-[1-(3-Phenylisoquinolin-1-yl)naphthalen-2-yl]ethan-1-ol. **26h**

Following the general procedure using heterobiaryl ketone **25h** (37 mg, 0.1 mmol), Purification by flash chromatography (6:1 CH₂Cl₂/EtOAc) afforded both diastereomers characterized separately:



(*R,R*)-**26h**(22mg, 59%).

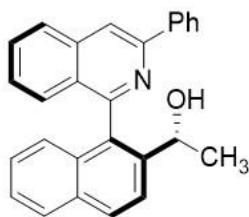
[α]_D²⁰ +19.6 (*c* 0.49, CHCl₃) for 95% *ee*.

¹H-NMR (400 MHz, CDCl₃): δ 8.22 (d, *J* = 0.5 Hz, 1H), 8.20-8.17 (m, 2H), 8.07 (d, *J* = 8.7 Hz, 1H), 8.00 (d, *J* = 8.3 Hz, 1H), 7.93 (d, *J* = 8.3 Hz, 1H), 7.91 (d, *J* = 8.6 Hz, 1H), 7.68 (ddd, *J* = 8.2, 6.6 and 1.4 Hz, 1H), 7.50–7.38 (m, 5H), 7.34 (ddd, *J* = 8.5, 6.6 and 1.2 Hz, 1H), 7.24 (ddd, *J* = 8.3, 6.8 and 1.3 Hz, 1H), 7.08 (dd, *J* = 8.4 and 0.8 Hz, 1H), 4.49 (q, *J* = 6.4 Hz, 1H), 2.04 (br s, 1H), 1.45 d, *J* = 6.4 Hz, 3H).

¹³C-NMR (100 MHz, CDCl₃) δ 159.3, 150.5, 141.8, 139.4, 137.1, 133.3, 132.9, 132.5, 130.6, 129.4, 128.8, 128.6, 128.0, 127.7, 127.5, 127.4, 127.1, 127.1, 126.4, 126.4, 125.8, 123.5, 116.2, 68.4, 25.1.

HRMS (ESI) calculated for C₂₇H₂₂NO (M + H⁺) 376.1696. Found 376.1697.

HPLC (IA column, *n*-hex/IPA 85:15, T= 30°C, F= 1.0 mL/min): t_R 6.55 min (minor) and 9.73 min (major).



(*S,R*)-**26h** (12 mg, 32%).

$[\alpha]_D^{20} +46.2$ (*c* 0.74, CHCl₃) for 95% *ee*.

¹H-NMR (400 MHz, CDCl₃): δ 8.23 (s, 1H), 8.14-8.11 (m, 2H), 8.07 (d, *J* = 8.7 Hz, 1H), 8.01 (d, *J* = 8.3 Hz, 1H), 7.94 (d, *J* = 8.3 Hz, 1H), 7.89 (d, *J* = 8.7 Hz, 1H), 7.70 (ddd, *J* = 8.2, 5.2 and 2.9 Hz, 1H), 7.48–7.43 (m, 3H), 7.41–7.35 (m, 3H), 7.24 (ddd, *J* = 8.3, 6.8 and 1.4 Hz, 1H), 7.05 (dd, *J* = 8.5 and 0.8 Hz, 1H), 4.58 (q, *J* = 6.5 Hz, 1H), 3.81 (br s, 1H), 1.46 d, *J* = 6.5 Hz, 3H).

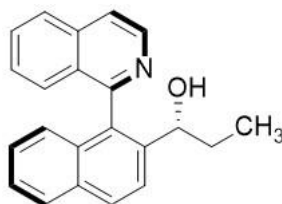
¹³C-NMR (100 MHz, CDCl₃) δ 159.5, 150.5, 141.4, 138.9, 137.1, 132.8, 132.5, 130.8, 129.5, 128.8, 128.7, 128.1, 127.8, 127.8, 127.5, 127.4, 127.0, 127.0, 126.5, 126.4, 125.8, 123.0, 116.7, 66.4, 20.8.

HRMS (ESI) calculated for C₂₇H₂₂NO (*M* + H⁺) 376.1696. Found 376.1698.

HPLC (IA column, *n*-hex/IPA 85:15, T= 30°C, F= 1.0 mL/min): t_R 6.65 min (major) and 8.73 min (minor).

Synthesis of 1-[1-(Isoquinolin-1-yl)naphthalen-2-yl]propan-1-ol. **26i**

Following the general procedure using heterobiaryl ketone **25i** (31 mg, 0.1 mmol), Purification by flash chromatography (6:1 CH₂Cl₂/EtOAc) afforded both diastereomers characterized separately:



(*R,R*)-**26i** (22 mg, 70%).

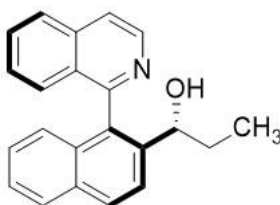
$[\alpha]^{20}_{\text{D}}$ $[\alpha]^{20}_{\text{D}}$ +8.8 (*c* 0.33, CHCl_3) for 94% *ee*.

$^1\text{H-NMR}$ (400 MHz, CDCl_3): δ 8.72 (d, $J = 5.8$ Hz, 1H), 8.07 (d, $J = 8.6$ Hz, 1H), 8.03 (d, $J = 8.3$ Hz, 1H), 7.95 (d, $J = 8.2$ Hz, 1H), 7.90 (d, $J = 6.0$ Hz, 1H), 7.79 (t, $J = 8.4$ Hz, 2H), 7.56–7.41 (m, 3H), 7.29–7.24 (m, 1H), 6.92 (d, $J = 8.5$ Hz, 1H), 4.35 (t, $J = 6.9$ Hz, 1H), 1.74–1.58 (m, 2H), 0.80 (t, $J = 7.4$ Hz, 3H).

$^{13}\text{C-NMR}$ (100 MHz, CDCl_3): δ 159.4, 141.4, 140.1, 140.0, 136.7, 132.8, 132.6, 131.6, 129.8, 128.7, 128.3, 128.1, 127.6, 127.2, 126.7, 125.9, 125.8, 124.5, 121.2, 74.4, 31.2, 10.5.

HRMS (ESI) calculated for $\text{C}_{22}\text{H}_{20}\text{NO}$ ($\text{M} + \text{H}^+$) 314.1539. Found 314.1539.

HPLC (AS-H column, *n*-hex/IPA 85:15, $T = 30^\circ\text{C}$, $F = 1.0$ mL/min): t_{R} 5.44 min (major) and 6.97 min (minor).



(*S,R*)-**26i** (5 mg, 16%).

$[\alpha]^{20}_{\text{D}}$ +11.7 (*c* 0.10, CHCl_3) for 94% *ee*.

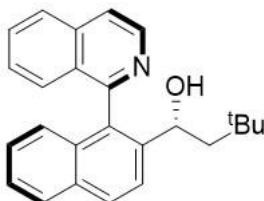
$^1\text{H-NMR}$ (400 MHz, CDCl_3): δ 8.68 (d, $J = 5.7$ Hz, 1H), 8.06 (d, $J = 8.6$ Hz, 1H), 8.02 (d, $J = 8.3$ Hz, 1H), 7.93 (d, $J = 8.6$ Hz, 1H), 7.91 (d, $J = 5.7$ Hz, 1H), 7.85 (d, $J = 8.7$ Hz, 1H), 7.78 (m, 1H), 7.47–7.43 (m, 3H), 7.23 (ddd, $J = 8.2, 6.8$ and 1.3 Hz, 1H), 6.88 (d, $J = 8.4$ Hz, 1H), 4.16 (t, $J = 7.0$ Hz, 1H), 1.75 (m, 1H), 0.63 (d, $J = 7.4$ Hz, 3H).

$^{13}\text{C-NMR}$ (100 MHz, CDCl_3) δ 159.3, 141.2, 140.7, 140.6, 136.5, 132.7, 132.2, 131.5, 129.9, 128.8, 128.2, 128.0, 127.1, 126.5, 126.0, 125.9, 123.8, 121.3, 72.1, 28.4, 10.5.

HRMS (ESI) calculated for $\text{C}_{22}\text{H}_{20}\text{NO}$ ($\text{M} + \text{H}^+$) 314.1539. Found 314.1540.

HPLC (AS-H column, *n*-hex/IPA 85:15, $T = 30^\circ\text{C}$, $F = 1.0$ mL/min): t_{R} 4.23 min (minor) and 4.58 min (major).

Synthesis of (*R*)-1-{1-[(*R*)-Isoquinolin-1-yl]naphthalen-2-yl}-3,3-dimethylbutan-1-ol. **26j**



Following the general procedure using heterobiaryl ketone **25j** (36 mg, 0.1 mmol), Purification by flash chromatography (6:1 CH₂Cl₂/EtOAc) afforded **26j** as single diastereomer (d.r. >20:1, 19 mg, 52%).

$[\alpha]_D^{20} +50.1$ (*c* 0.50, CHCl₃) for 80% *ee*.

¹H-NMR (400 MHz, CDCl₃): δ 8.69 (d, *J* = 5.7 Hz, 1H), 7.96 (d, *J* = 8.2 Hz, 1H), 7.92 (d, *J* = 8.6 Hz, 2H), 7.82 (d, *J* = 8.6 Hz, 1H), 7.79 (d, *J* = 5.8 Hz, 1H), 7.71 (dd, *J* = 8.2, 6.6 Hz, 1H), 7.51 – 7.43 (m, 1H), 7.40 (t, *J* = 7.6 Hz, 1H), 7.34 (d, *J* = 8.5 Hz, 1H), 7.26 (dd, *J* = 8.2, 6.6 Hz, 1H), 6.99 (d, *J* = 8.5 Hz, 1H), 4.53 – 4.46 (m, 1H), 3.76 (br s, 1H), 1.76 (dd, *J* = 14.4, 9.1 Hz, 1H), 1.30 (dd, *J* = 13.7, 2.3 Hz, 1H), 0.47 (s, 9H).

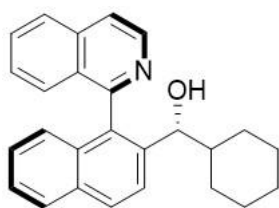
¹³C-NMR (100 MHz, CDCl₃) δ 159.6, 142.9, 142.1, 136.2, 132.5, 132.4, 132.2, 130.6, 129.3, 128.8, 128.0, 127.8, 127.4, 127.0, 126.3, 126.1, 125.5, 124.0, 120.5, 67.9, 50.2, 30.1, 29.5.

HRMS (ESI) calculated for C₂₅H₂₆NO (*M* + H⁺) 356.2009. Found 356.2008.

HPLC (IA column, *n*-hex/IPA 95:5, T= 30°C, F= 1.0 mL/min.): t_R 14.20 min (major) and 16.30 min (minor).

Synthesis of Cyclohexyl[1-(isoquinolin-1-yl)naphthalen-2-yl]methanol. **26k**

Following the general procedure using heterobiaryl ketone **25k** (37 mg, 0.1 mmol), Purification by flash chromatography (6:1 CH₂Cl₂/EtOAc) afforded both diastereomers characterized separately:



(*R_a*,*R*)-**26k** (23 mg, 63%).

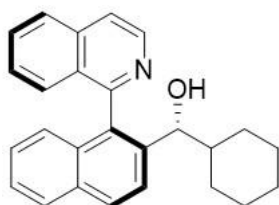
$[\alpha]_D^{20}$ -54.9 (*c* 0.90, CHCl₃) for 91% *ee*.

¹H-NMR (400 MHz, CDCl₃): δ 8.66 (d, *J* = 5.8 Hz, 1H), 8.02 (d, *J* = 8.6 Hz, 1H), 7.98 (d, *J* = 8.3 Hz, 1H), 7.91 (d, *J* = 8.1 Hz, 1H), 7.82 (d, *J* = 5.8 Hz, 1H), 7.81 (d, *J* = 8.6 Hz, 1H), 7.74 (ddd, *J* = 8.1, 6.2 and 1.8 Hz, 1H), 7.44–7.38 (m, 3H), 7.21 (t, *J* = 8.2 Hz, 1H), 6.88 (d, *J* = 8.4 Hz, 1H), 3.87 (d, *J* = 9.2 Hz, 1H), 3.65 (br s, 1H), 2.08 (d, *J* = 12.8 Hz, 1H), 1.85 (q, *J* = 8.1 Hz, 1H), 1.62 (d, *J* = 13.4 Hz, 1H), 1.51 (d, *J* = 12.8 Hz, 1H), 1.41 (d, *J* = 13.1 Hz, 1H), 1.23-1.01 (m, 3H), 0.93-0.82 (m, 1H), 0.69 (qd, *J* = 12.8 and 3.3 Hz, 1H), 0.29 (qd, *J* = 12.4 and 3.5 Hz, 1H).

¹³C-NMR (100 MHz, CDCl₃) δ 159.5, 141.5, 140.6, 136.3, 134.6, 132.6, 132.3, 131.0, 129.6, 128.9, 128.2, 128.1, 127.6, 127.0, 126.4, 126.1, 125.8, 124.4, 120.9, 75.4, 41.8, 29.5, 29.5, 26.2, 25.9, 25.7.

HRMS (ESI) calculated for C₂₆H₂₆NO (M + H⁺) 368.2009. Found 368.2009.

HPLC (IB column, *n*-hex/IPA 90:10, T= 30°C, F= 1.0 mL/min): *t_R* 5.38 min (minor) and 5.79 min (major).



(*S_a*,*R*)-**26k** (8.5 mg, 23%).

$[\alpha]_D^{20}$ +21.8 (*c* 0.30, CHCl₃) for 88% *ee*.

¹H-NMR (400 MHz, CDCl₃): δ 8.71 (d, *J* = 5.8 Hz, 1H), 8.03 (d, *J* = 8.6 Hz, 1H), 7.98 (d, *J* = 8.2 Hz, 1H), 7.91 (d, *J* = 8.4 Hz, 1H), 7.85 (d, *J* = 5.8 Hz, 1H), 7.74 (t, *J* = 7.2 Hz, 1H), 7.70 (d, *J* = 8.7 Hz, 1H), 7.47–7.40 (m, 3H), 7.24 (ddd, *J* = 8.3, 6.7 and 1.3 Hz, 1H), 6.95

(d, $J = 8.6$ Hz, 1H), 4.01 (d, $J = 8.4$ Hz, 1H), 1.90 (d, $J = 12.7$ Hz, 1H), 1.61 (br s, 1H), 1.50 (m, 2H), 1.35 (m, 1H), 1.18 (d, $J = 10.1$ Hz, 1H), 1.00 (t, $J = 9.5$ Hz, 1H), 0.95-0.75 (m, 4H).

^{13}C NMR (100 MHz, CDCl_3) δ 159.6, 141.2, 140.2, 136.4, 132.8, 132.6, 131.0, 129.3, 128.8, 128.0, 127.8, 127.2, 127.1, 126.5, 126.0, 125.8, 125.2, 120.7, 77.8, 44.0, 29.8, 29.2, 26.2, 25.9, 25.8.

HRMS (ESI) calculated for $\text{C}_{26}\text{H}_{26}\text{NO}$ ($\text{M} + \text{H}^+$) 368.2009. Found 368.2009.

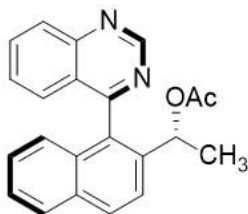
HPLC (AS-H column, *n*-hex/IPA 85:15, $T = 30^\circ\text{C}$, $F = 1.0$ mL/min): t_{R} 5.00 min (major) and 6.13 min (minor).

III.3.3. Acetylation of more polar carbinol **3e**.

To a flame-dried Schlenk tube, zinc acetate (1.8 mg, 0.01 mmol, 5 mol%) and **L33** (7.4 mg, 0.012 mmol, 6 mol%) were dissolved in freshly distilled THF (0.8 mL) and stirred for 1 h at room temperature under N_2 atmosphere. Then $(\text{EtO})_2\text{MeSiH}$ (64 μL , 0.4 mmol, 2 eq.) was added and the reaction mixture was stirred for an additional hour. Finally, heterobiaryl ketone **25b** (0.2 mmol, 1.0 eq.) was added and the resulting mixture was stirred at 70°C for 36 h. The reaction crude was allowed to reach room temperature, 1M aq. HCl (1 mL) was added and the resulting mixture was stirred for *ca.* 1 h. CH_2Cl_2 (10 mL) was added, the mixture was neutralized with saturated NaHCO_3 , the phases separated, and the aqueous layer extracted 3 times with CH_2Cl_2 . The combined organic layers were dried over anhydrous Na_2SO_4 , filtered and concentrated to a final volume of 1-2 mL. Acetic anhydride (28 μL , 0.3 mmol) and *N,N*-dimethylaminopyridine (5 mg, 0.04 mmol) were then added and after stirring at room temperature for 1h, the reaction mixture was diluted with water and extracted 3 times with CH_2Cl_2 . The combined organic layers were dried over anhydrous Na_2SO_4 and the solvent was evaporated in vacuo. Purification by flash chromatography (6:1 $\text{CH}_2\text{Cl}_2/\text{EtOAc}$) afforded:

Synthesis of (1*R*)-1-{1-[(*R*)-Quinazolin-4-yl]naphthalen-2-yl}ethyl acetate 3'e.

26'b



(*R,R*)-26'b (28 mg, 41%).

$[\alpha]_{\text{D}}^{20} -29.7$ (*c* 0.44, CHCl₃) for 98% *ee*.

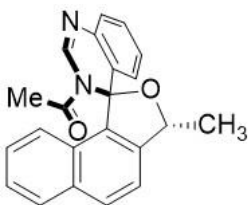
¹H-NMR (400 MHz, CDCl₃): δ 9.51 (s, 1H), 8.18 (d, *J* = 8.5 Hz, 1H), 8.06 (d, *J* = 8.7 Hz, 1H), 7.95–7.91 (m, 2H), 7.75 (d, *J* = 8.7 Hz, 1H), 7.52–7.45 (m, 3H), 7.28 (ddd, *J* = 8.4, 6.8 and 1.3 Hz, 1H), 6.92 (dd, *J* = 8.5 and 0.8 Hz, 1H), 5.37 (q, *J* = 6.6 Hz), 1.89 (s, 3H), 1.56 (d, *J* = 6.6 Hz, 3H).

¹³C-NMR (100 MHz, CDCl₃) δ 169.7, 168.2, 154.8, 150.4, 138.2, 134.5, 132.7, 131.5, 131.3, 130.1, 128.5, 128.1, 127.8, 127.7, 127.0, 126.2, 125.6, 125.1, 122.5, 70.4, 22.2, 20.9.

HRMS (ESI) calculated for C₂₂H₁₉N₂O₂ (M + H⁺) 343.1441. Found 343.1443.

HPLC (IA column, *n*-hex/IPA 85:15, T= 30°C, F= 1.0 mL/min): t_R 5.38 min (major) and 6.34 min (minor).

Synthesis of 1-[(1*R*,3*R*)-3-Methyl-3*H*,3'*H*-spiro[naphtho(1,2-*c*)furan-1,4'-quinazolin]-3'-yl]ethan-1-one. (*R,R*)-26''b



(*R,R*)-3''e: (17 mg, 25%).

$[\alpha]_{\text{D}}^{20} -115.5$ (*c* 0.37, CHCl₃) for 97% *ee*.

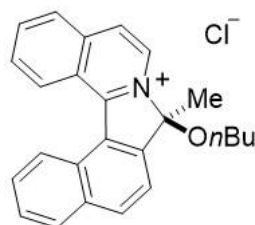
$^1\text{H-NMR}$ (400 MHz, CDCl_3): δ 8.20 (s, 1H), 7.94 (d, $J = 8.4$ Hz, 1H), 7.88 (d, $J = 8.2$ Hz, 1H), 7.47 (d, $J = 7.2$ Hz, 1H), 7.41 (d, $J = 8.4$ Hz, 1H), 7.38 (ddd, $J = 8.1, 6.8$ and 1.1 Hz, 1H), 7.34–7.25 (m, 2H), 7.15 (d, $J = 8.3$ Hz, 1H), 7.02 (ddd, $J = 8.5, 7.4$ and 1.2 Hz, 1H), 6.75 (dd, $J = 7.9$ and 1.4 Hz, 1H), 5.76 (q, $J = 6.7$ Hz), 2.24 (s, 3H), 1.70 (d, $J = 6.7$ Hz, 3H).

$^{13}\text{C-NMR}$ (100 MHz, CDCl_3) δ 170.5, 142.6, 141.6, 137.8, 133.9, 133.3, 130.7, 129.6, 129.0, 128.3, 127.8, 127.4, 127.3, 126.9, 126.0, 125.5, 122.6, 117.9, 95.6, 82.6, 24.2, 21.1.

HRMS (ESI) calcd. for $\text{C}_{22}\text{H}_{19}\text{N}_2\text{O}_2$ ($\text{M} + \text{H}^+$) 343.1441. Found 343.1443.

HPLC (IA column, *n*-hex/IPA 85:15, $T = 30^\circ\text{C}$, $F = 1.0$ mL/min): t_{R} 14.51 min (major) and 24.42 min (minor).

Synthesis of 8-Butoxy-8-methyl-8H-benzo[6,7]isoindolo[1,2-a]isoquinolin-7-ium chloride.



Following the described procedure, a flame-dried Schlenk tube was charged with triflate **3b** (1.26 mmol), $\text{Pd}(\text{OAc})_2$ (8.1 mg, 0.036 mmol) and dppp (15.7 mg, 0.038 mmol). After three cycles of vacuum-argon, DMF (3 mL) was added and the resulting mixture was stirred for 20 min at room temperature. Then Et_3N (0.35 mL, 2.52 mmol) and butyl vinyl ether (0.39 mL, 3.78 mmol) were sequentially added and the resulting mixture was stirred at 80°C for 72 hours. Then, 2M aq. HCl (15 mL) were added over 10 min to the reaction crude at room temperature. The resulting mixture was stirred for 0.5 h and was poured into CH_2Cl_2 (20 mL). NaHCO_3 was then added until neutrality, the phases separated, and the aqueous layer was extracted with CH_2Cl_2 (3×10 mL). The combined organic layers were dried over anhydrous Na_2SO_4 , filtered, concentrated, and the residue was purified by

column chromatography (EtOAc/MeOH 5:1) to afford the product as a yellow solid (343 mg, 70%).

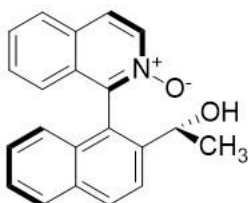
$^1\text{H-NMR}$ (400 MHz, CD_3OD): δ 9.18 (d, $J = 8.7$ Hz, 1H), 8.97 (d, $J = 6.5$ Hz, 1H), 8.76 (d, $J = 8.5$ Hz, 1H), 8.56 (dd, $J = 13.9, 7.5$ Hz, 2H), 8.46 (d, $J = 8.1$ Hz, 1H), 8.32 (q, $J = 9.1, 8.2$ Hz, 2H), 8.19 (d, $J = 8.1$ Hz, 1H), 8.01 (d, $J = 8.2$ Hz, 1H), 7.94 (t, $J = 7.5$ Hz, 1H), 7.87 (d, $J = 7.6$ Hz, 1H), 3.07 (d, $J = 9.4$ Hz, 1H), 2.78 (d, $J = 8.7$ Hz, 2H), 2.19 (s, 3H), 1.57 – 1.45 (m, 2H), 1.44 – 1.32 (m, 2H), 0.84 (t, $J = 7.5$ Hz, 3H).

$^{13}\text{C-NMR}$ (100 MHz, CD_3OD) δ 154.3, 145.1, 141.1, 137.2, 136.5, 136.1, 130.3, 129.9, 129.6, 129.0, 128.5, 128.3, 127.9, 127.8, 127.0, 125.6, 124.8, 123.7, 119.3, 103.4, 65.4, 30.9, 25.3, 18.7, 12.6.

HRMS (ESI) calcd. for $\text{C}_{25}\text{H}_{24}\text{NO}$ ($\text{M} + \text{H}^+$) 354.1852. Found 354.1848.

III.4.4. Representative transformations from 26a.

Synthesis of (*R*)-1-{2-[(*R*)-1-Hydroxyethyl]naphthalen-1-yl}isoquinoline 2-oxide. (*R_a*,*R*)-27a



Over a cooled ($0\text{ }^\circ\text{C}$) solution of (*R_a*,*R*)-26a (30 mg, 0.1 mmol) in THF (5 mL), m-CPBA (77%; 45 mg, 0.2 mmol,) was added in portions. The resulting mixture was warmed to rt and stirred for 3 hours. Then, CH_2Cl_2 (5 mL) was added and the mixture was washed once with saturated aqueous NaHCO_3 . The organic layer was dried over anhydrous Na_2SO_4 , filtered, concentrated, and the resulting residue was purified by flash chromatography ($\text{CH}_2\text{Cl}_2 \rightarrow 5:1$ EtOAc/MeOH) to afford (*R_a*,*R*)-27a (100 mg, 94%) as a white foam.

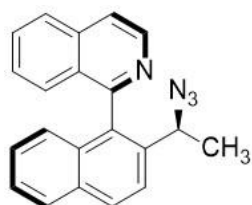
$[\alpha]_{\text{D}}^{20} -12.0$ (c 0.25, CHCl_3) for 97% *ee*.

$^1\text{H-NMR}$ (400 MHz, CDCl_3) δ 8.43 (d, $J = 7.1$ Hz, 1H), 8.08 (d, $J = 8.6$ Hz, 1H), 7.96 (d, $J = 4.2$ Hz, 1H), 7.93 (d, $J = 4.4$ Hz, 1H), 7.89 (d, $J = 7.2$ Hz, 1H), 7.72 (d, $J = 8.6$ Hz, 1H), 7.64 (t, $J = 7.6$ Hz, 1H), 7.48 (t, $J = 7.2$ Hz, 1H), 7.43 (t, $J = 7.7$ Hz, 1H), 7.35 – 7.26 (m, 1H), 7.13 (d, $J = 8.5$ Hz, 1H), 6.92 (d, $J = 8.5$ Hz, 1H), 4.85 (q, $J = 6.6$ Hz, 1H), 1.32 (d, $J = 6.6$ Hz, 3H).

$^{13}\text{C-NMR}$ (400 MHz, CDCl_3) δ 146.4, 143.5, 137.1, 133.2, 131.6, 130.6, 130.3, 129.7, 129.4, 130.0, 128.5, 127.3, 127.1, 126.2, 125.7, 125.0, 124.7, 124.1, 124.1, 70.0, 24.4.

HRMS (ESI) calculated for $\text{C}_{21}\text{H}_{17}\text{NO}_2$ ($\text{M} + \text{H}^+$) 316.1338 Found 316.1330.

Synthesis of (*R*)-1-{2-[(*S*)-1-Azidoethyl]naphthalen-1-yl}isoquinoline. (*R_a,S*)-28a****



To a solution of (*R_a,R*)-**26a** (90 mg, 0.3 mmol) and DPPA (96 μL , 0.45 mmol) in toluene (1.5 mL) at 0 °C was added DBU (75 μL , 0.51 mmol) via syringe. The mixture was stirred at 0 °C for 1 h and then at 60 °C for 48 h. After that time ethyl acetate (10 mL) was added and the mixture was washed with water, brine, dried over anhydrous Na_2SO_4 , filtrated and concentrated *in vacuo*. Purification by flash chromatography ($\text{CH}_2\text{Cl}_2 \rightarrow 25:1$ $\text{CH}_2\text{Cl}_2/\text{EtOAc}$) afforded (*R_a,S*)-**28a** (79 mg, 81%) as a light yellow solid.

$[\alpha]_{\text{D}}^{20} +37.8$ (c 0.51, CHCl_3) for 97% *ee*.

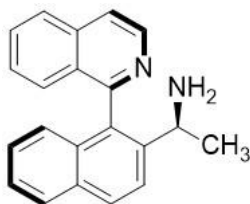
$^1\text{H-NMR}$ (400 MHz, CDCl_3): δ 8.79 (d, $J = 5.7$ Hz, 1H), 8.07 (d, $J = 8.7$ Hz, 1H), 7.97 (d, $J = 8.3$ Hz, 1H), 7.93 (d, $J = 8.3$ Hz, 1H), 7.81 (d, $J = 5.7$ Hz, 1H), 7.75 (d, $J = 10.9$ Hz, 1H), 7.70 (t, $J = 7.4$ Hz, 1H), 7.46 (t, $J = 7.4$ Hz, 1H), 7.39 (t, $J = 8.0$ Hz, 1H), 7.32 (d, $J = 8.5$ Hz, 1H), 7.26 (t, $J = 7.0$ Hz, 1H), 6.97 (d, $J = 8.5$ Hz, 1H), 4.39 (q, $J = 6.8$ Hz, 1H), 1.27 (d, $J = 6.8$ Hz, 3H).

^{13}C -NMR (100 MHz, CDCl_3) δ 158.8, 142.8, 137.5, 136.1, 134.6, 132.8, 132.3, 130.5, 129.6, 128.9, 127.9, 127.6, 127.1, 127.0, 126.7, 126.4, 126.1, 123.4, 120.4, 57.9, 21.7.

HRMS (ESI) calculated for $\text{C}_{21}\text{H}_{17}\text{N}_4$ ($\text{M} + \text{H}^+$) 325.1448. Found 325.1440.

M. p. 154-157°C.

**Synthesis of (*R*)-1-{1-[(*S*)-Isoquinolin-1-yl]naphthalen-2-yl}ethan-1-amine.
(*R_a,S*)-29a**



Triphenylphosphine (118 mg, 0.45 mmol) was added portionwise to a stirred solution of (*R_a,S*)-**28a** (49 mg, 0.15 mmol) in THF (0.3 mL). After 5 min, H_2O (54 μL , 3 mmol) was added and the resultant mixture was heated at 50 °C for 48 h. The reaction mixture was then allowed to cool to rt and concentrated *in vacuo*. Purification by flash chromatography (9:1 EtOAc/MeOH) afforded (*R_a,S*)-**29a** (52 mg, 99%) as a light yellow solid.

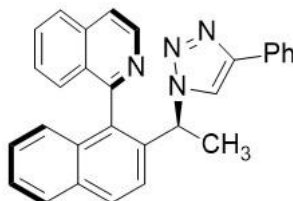
$[\alpha]_{\text{D}}^{20} -13.7$ (*c* 0.69, CHCl_3) for 97% *ee*.

^1H -NMR (400 MHz, CDCl_3): δ 8.69 (d, $J = 5.8$ Hz, 1H), 7.94 (d, $J = 8.3$ Hz, 1H), 7.93 (d, $J = 8.7$ Hz, 1H), 7.88 (d, $J = 8.2$ Hz, 1H), 7.79 (d, $J = 8.4$ Hz, 1H), 7.77 (d, $J = 5.8$ Hz, 1H), 7.68 (ddd, $J = 8.2, 6.1$ and 1.9 Hz, 1H), 7.42 (ddd, $J = 8.1, 6.8$ and 1.2 Hz, 1H), 7.38–7.32 (m, 2H), 7.22 (ddd, $J = 8.3, 6.8$ and 1.3 Hz, 1H), 6.90 (d, $J = 8.4$ Hz, 1H), 3.74 (q, $J = 6.6$ Hz, 1H), 3.46 (br s, 2H), 1.29 (d, $J = 6.6$ Hz, 3H).

^{13}C -NMR (100 MHz, CDCl_3) δ 159.8, 142.5, 142.0, 136.1, 133.8, 132.5, 132.5, 130.5, 129.5, 128.8, 127.9, 127.5, 127.3, 127.0, 126.4, 126.1, 125.6, 123.0, 120.4, 47.8, 22.8.

HRMS (ESI) calculated for $\text{C}_{21}\text{H}_{19}\text{N}_2$ ($\text{M} + \text{H}^+$) 299.1543. Found 299.1546.

Synthesis of (*R*)-1-{2-[(*S*)-1-(4-Phenyl-1*H*-1,2,3-triazol-1-yl)ethyl]naphthalen-1-yl}isoquinoline. (*R_aS*)-30a



To a mixture of (*R_aS*)-**28a** (33 mg, 0.1 mmol) and phenylacetylene (15 mg, 16 μ L, 0.15 mmol) in *t*-BuOH (3 mL) and water (240 μ L), a solution of CuSO₄·5H₂O (0.1 M in water, 100 μ L, 0.01 mmol) and (*L*)-sodium ascorbate (0.1 M in water, 200 μ L, 0.02 mmol) were then sequentially added. The resulting mixture was stirred at 35 °C for 5 h. The reaction mixture was allowed to reach room temperature, washed with a saturated aqueous solution of NH₃, and extracted with DCM (3× 5 mL). The combined organic phase was dried over anhydrous Na₂SO₄, filtered, concentrated to dryness, and the crude product was purified by column chromatography (CH₂Cl₂→3:1 CH₂Cl₂/EtOAc) affording (*R_aS*)-**30a** (44 mg, 99%) as a white solid.

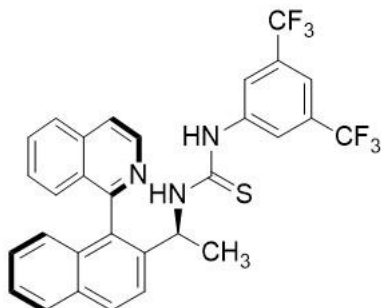
$[\alpha]_D^{20} +470.5$ (*c* 0.47, CHCl₃) for 97% *ee*.

¹H-NMR (400 MHz, CDCl₃): δ 8.79 (d, *J* = 5.7 Hz, 1H), 8.00 (d, *J* = 8.8 Hz, 1H), 7.99 (d, *J* = 8.3 Hz, 1H), 7.92 (s, 1H), 7.91 (d, *J* = 7.6 Hz, 1H), 7.86 (d, *J* = 5.7 Hz, 1H), 7.80-7.77 (m, 2H), 7.74 (ddd, *J* = 8.2, 6.2 and 1.9 Hz, 1H), 7.60 (d, *J* = 8.8 Hz, 1H), 7.50-7.43 (m, 3H), 7.34 (t, *J* = 7.2 Hz, 2H), 7.32-7.25 (m, 2H), 7.01 (d, *J* = 8.5 Hz, 1H), 5.30 (q, *J* = 7.0 Hz, 1H), 1.93 (d, *J* = 7.0 Hz, 3H).

¹³C-NMR (100 MHz, CDCl₃) δ 158.7, 147.6, 142.5, 136.9, 136.2, 134.4, 133.0, 132.2, 130.9, 130.7, 130.2, 128.9, 128.6, 128.1, 128.0, 127.8, 127.2, 127.0, 126.9, 126.5, 126.3, 125.6, 123.2, 121.0, 120.6, 57.4, 20.5.

HRMS (ESI) calculated for C₂₉H₂₃N₄ (*M* + H⁺) 427.1917. Found 427.1917.

Synthesis of 1-[3,5-Bis(trifluoromethyl)phenyl]-3-[(*S*)-1-[1-((*R*)-isoquinolin-1-yl)naphthalen-2-yl]ethyl]urea. (*R_a,S*)-31a



Amine (*R_a,S*)-**29a** (30 mg, 0.1 mmol) was added to a solution of 3,5-bis(trifluoromethyl)phenyl isothiocyanate (18 μ L, 27 mg, 0.1 mmol) in CH_2Cl_2 (200 μ L). The resulting mixture was stirred for 3 h at rt. The solvent was removed under reduced pressure and the product was purified by flash column chromatography (4:1 *n*-hexane/EtOAc) to afford (*R_a,S*)-**31a** (29 mg, 90%) as a light yellow solid.

$[\alpha]_{\text{D}}^{20} +380.5$ (*c* 0.51, CHCl_3) for 97% *ee*.

$^1\text{H-NMR}$ (400 MHz, CDCl_3): δ 10.53 (s, 1H), 8.45 (d, $J = 5.8$ Hz, 1H), 8.19 (br s, 2H), 8.08 (d, $J = 8.7$ Hz, 1H), 8.01 (d, $J = 8.3$ Hz, 1H), 7.93 (d, $J = 8.2$ Hz, 1H), 7.87 (d, $J = 5.8$ Hz, 1H), 7.79 (d, $J = 8.7$ Hz, 1H), 7.77 (ddd, $J = 8.2, 6.7$ and 1.4 Hz, 1H), 7.61 (br s, 1H), 7.50 (ddd, $J = 8.1, 6.8$ and 1.2 Hz, 1H), 7.47–7.38 (m, 3H), 7.29 (ddd, $J = 8.4, 6.9$ and 1.3 Hz, 1H), 6.95 (d, $J = 8.5$ Hz, 1H), 4.62 (m, 1H), 1.35 (d, $J = 6.7$ Hz, 3H).

$^{13}\text{C-NMR}$ (100 MHz, CDCl_3) δ 179.6, 159.0, 141.3 (d, $J_{\text{C,F}} = 2$ Hz), 137.9, 136.6, 132.8, 132.8, 131.8, 131.4, 131.4, 131.2 (d, $J_{\text{C,F}} = 100$ Hz), 131.0, 130.9, 129.0, 128.4, 128.3, 127.3, 127.3, 127.1, 126.5, 126.1, 125.0 (br s), 123.3, 123.2 (q, $J_{\text{C,F}} = 271$ Hz), 121.8, 118.4 (br s), 50.4, 23.6.

$^{19}\text{F-NMR}$ (376 MHz, CDCl_3) δ -62.9.

HRMS (ESI) calculated for $\text{C}_{30}\text{H}_{22}\text{F}_6\text{N}_3\text{O}$ ($\text{M} + \text{H}^+$) 570.1433. Found 570.1437.

CHAPTER IV

*Catalytic Asymmetric Synthesis of
Axially Chiral Diamines by
Reductive Amination and DKR*

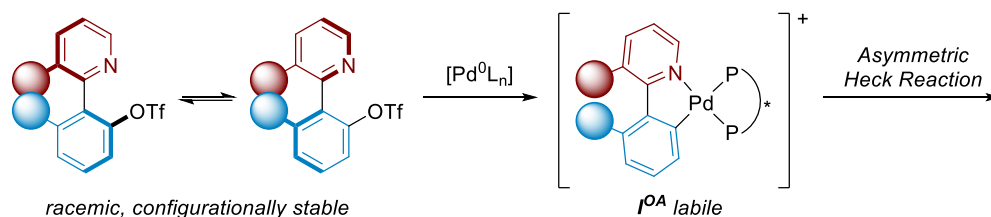
Unpublished Results.

IV. Catalytic Asymmetric synthesis of Axially Chiral Diamines by Reductive Amination and DKR

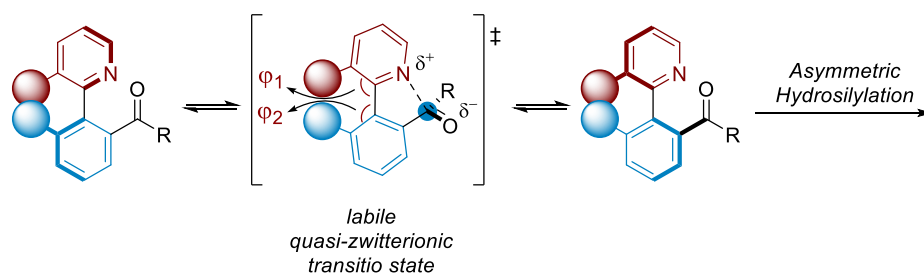
IV.1. Introduction

In Chapter I, different methods for the dynamization of stereogenic axis in already existing biaryl structures have been described. Most of the given examples exploit the formation of a (metalla)cycle in which the angles around the stereogenic axis are widened, thus compromising its configurational stability. These (metalla)cycles consist on five or six-membered rings. It has been seen that these processes can proceed with or without the need of a catalyst, depending on whether we have a DYKAT or DKR process, respectively. Throughout the previous two chapters, novel strategies for the resolution of heterobiaryls that have taken advantage of these two processes have been developed and, in particular, both of them proceed through the formation of five-membered rings which are particularly efficient in the labilization of the stereogenic axis (Scheme IV.1).

• **Chapter II:** DYKAT approach



• **Chapter III:** DKR approach



Scheme IV.1 – Strategies for the dynamization of stereogenic axes developed in Chapters II and III.

However, as previously discussed, when a six-membered ring is involved, it might be necessary to decrease the steric congestion around the stereogenic axis in order to facilitate the interconversion between the two atropisomers, since the widening of the angles involved in the configurational stability is lower than when five-membered rings are formed. Indeed, the biocatalytic resolution of biaryl *N*-oxide aldehydes reported by Clayden and co-workers (an example also discussed in Chapter I) requires the use of less hindered systems to achieve the DKR through a six-membered ring formed from the interaction between *N*-oxide and the aldehyde functionality (Figure IV.1).⁶⁰

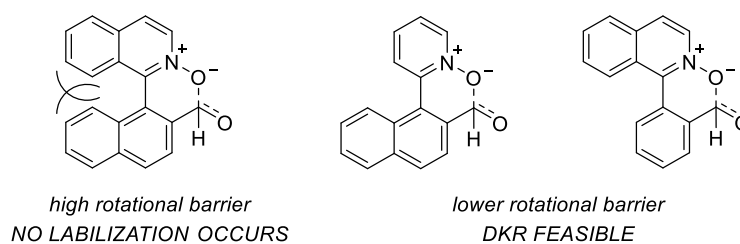
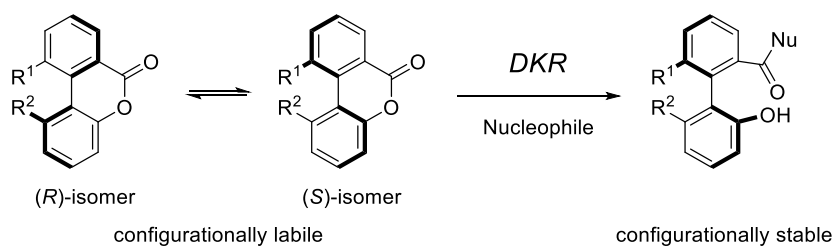


Figure IV.1 – Clayden’s heterobiaryl atropisomerization mode to perform DKR.

Another strategy for the labilization of a stereogenic axis through a six-membered ring, also mentioned at Chapter I, occurs in Bringmann’s lactones ring opening.^{47,51} These systems present two main differences with respect to Clayden’s example: on one hand, Bringmann’s lactones are based on biaryl structures compared to Clayden’s heterobiaryls; and on the other hand, a covalent bond is responsible for the labilization of the axis in Bringmann’s lactone, while a simple bonding interaction plays the same role in Clayden’s system (Scheme IV.2).



Scheme IV.2 – Lactone strategy involving a dynamic kinetic resolution.

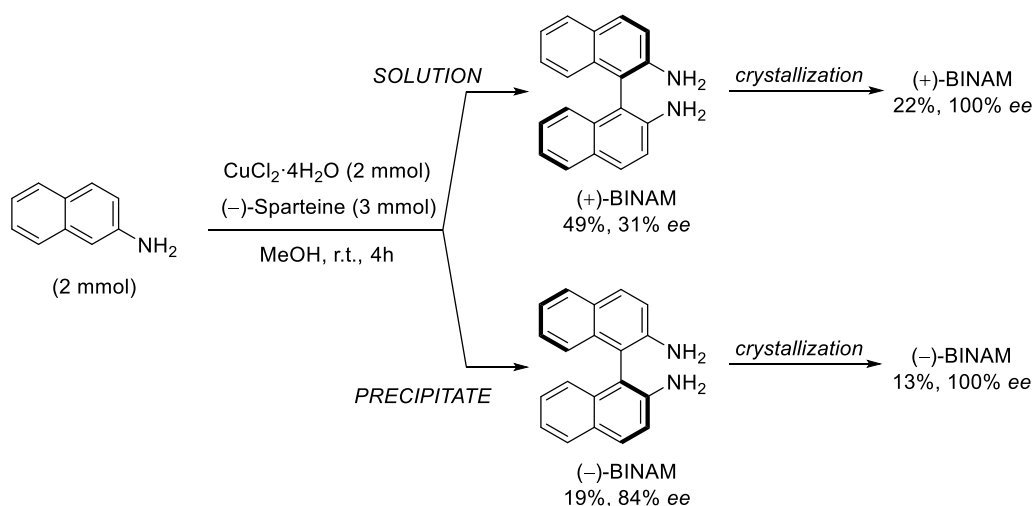
It has been previously discussed that the strategy developed by Bringmann has been widely applied for the synthesis of axially chiral biaryls through a nucleophilic attack to the carbonyl centre, and subsequent cleavage of the lactone bridge to establish the axial configuration in the resulting biaryl products, now configurationally stable.

This strategy has been established as an efficient catalytic approach for the synthesis of axially chiral diols and amino-alcohols in excellent yields and enantioselectivities but, surprisingly, it has never been employed for the synthesis of related and more interesting axially chiral diamines. Indeed, a literature survey reveals that there is only a handful of catalytic asymmetric methods to prepare such compounds.

IV.1.1. Synthesis of axially chiral diamines, homologues of BINAM.

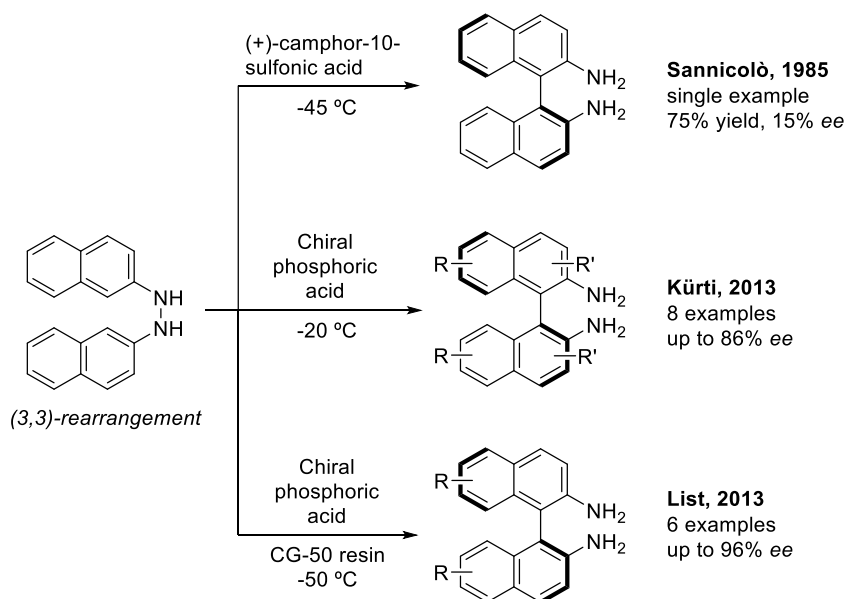
Remarkably, there is only one precedent for the synthesis of BINAM based on the direct asymmetric formation of the stereogenic axis. The method was described in 1992 and consists of a copper mediated asymmetric coupling of two aromatic fragments. In this case, it was possible to isolate both isomers of the coupling product by a simple fractional crystallization, although, enantiomeric excesses and yields were moderate. On the other hand, both isomers could be crystallized to obtain enantiopure BINAM (Scheme IV.3).¹⁵⁶

¹⁵⁶ Smrčina, M.; Lorenc, M.; Hanuš, V.; Sedmera, P.; Kočovský, P. *J. Org. Chem.* **1992**, *57*, 1917.



Scheme IV.3 – Asymmetric coupling for the synthesis of BINAM.

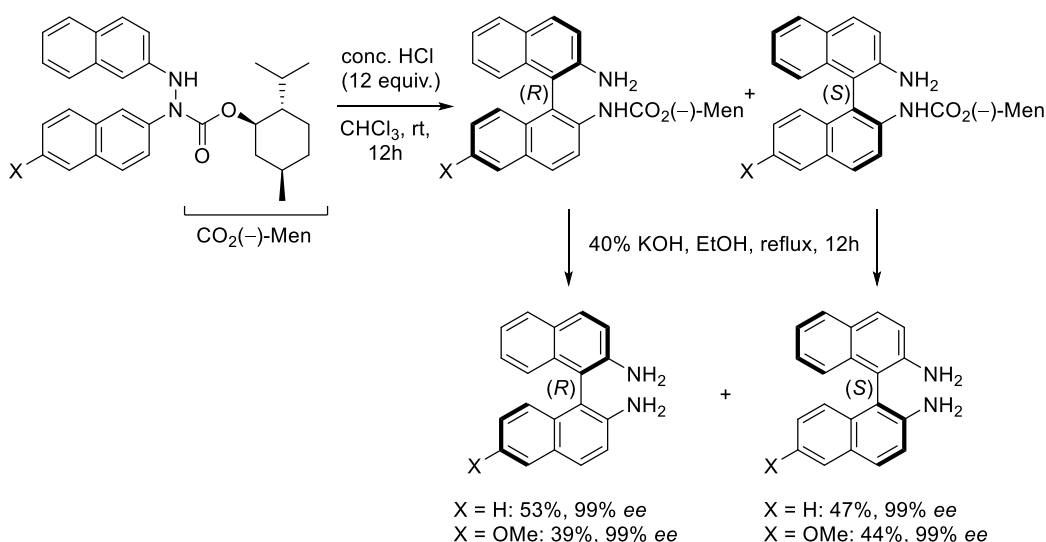
As mentioned, this is the only example of an asymmetric intermolecular coupling for the synthesis of BINAM or its derivatives. However, there is an alternative strategy to synthesize these structures, based on the acid-catalyzed atroposelective (3,3)-rearrangement (aza-Cope) of 1,2-di(naphthalen-2-yl)hydrazine, also known as benzidine rearrangement, to yield diaminobiaryls (Scheme IV.4).



Scheme IV.4 – Synthesis of BINAM derivatives through atroposelective (3,3)-rearrangement reaction.

The first example of this method was reported in 1985 by Sannicolò, who used (+)-camphor-10-sulphonic acid as the catalyst to afford the BINAM product in a negligible 15% ee.¹⁵⁷ Although this class of rearrangement has been studied with other purposes, it was not until 2013 that two independent reports by the groups of Kürti¹⁵⁸ and List¹⁵⁹ appeared, expanding the scope of this methodology for the synthesis of other BINAM derivatives with much higher enantiomeric excesses (Scheme IV.4).

Just one year later, Chen and Zhang reported a diastereoselective (3,3)-benzidine rearrangement of 1,2-di(naphthalen-2-yl)hydrazine substituted at one nitrogen atom by (-)-menthyl formate. In this way, the non-selective rearrangement leads to the two diastereomers of the *N*-substituted BINAM derivatives that, after separation and hydrolysis in basic conditions, provides the enantiomerically pure free BINAM derivatives (Scheme IV.5).¹⁶⁰



Scheme IV.5 – Diastereoselective (3,3)-rearrangement reaction for the synthesis of BINAM derivatives.

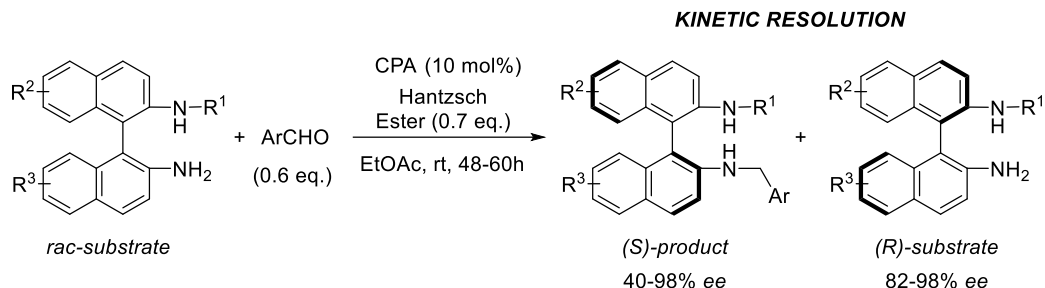
¹⁵⁷ Sannicolò, F. *Tetrahedron Lett.* **1985**, 26, 119.

¹⁵⁸ Li, G.-Q.; Gao, H.; Keene, C.; Devonas, M.; Ess, D. H.; Kürti, L. *J. Am. Chem. Soc.* **2013**, 135, 7414.

¹⁵⁹ De, C. K.; Pescioli, F.; List, B. *Angew. Chem. Int. Ed.* **2013**, 52, 9293.

¹⁶⁰ Li, B.; Zhang, S.; Chen, W. *Tetrahedron: Asymmetry* **2014**, 25, 1002

Alternatively, Tan and co-workers, developed an efficient strategy for the kinetic resolution of axially chiral BINAM derivatives. The method involves a cascade process catalyzed by a chiral phosphoric acid (CPA), consisting of imine formation and ensuing transfer hydrogenation (Scheme IV.6).¹⁶¹



Scheme IV.6 – Kinetic resolution strategy developed by Tan et al.

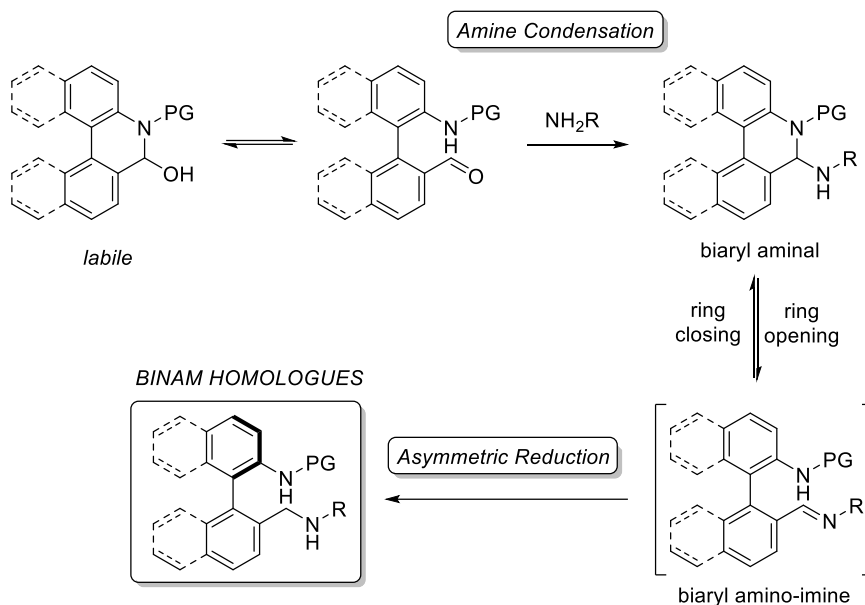
Taking into account the few existing catalytic asymmetric methods to synthesize axially chiral diamine derivatives, the development of more reliable and straightforward approaches to optically pure homologues of BINAM is expected to greatly expand the number of applications of this type of axially chiral derivatives in asymmetric catalysis.

In this context, we considered that a dynamization strategy based on the formation of cyclic intermediates or transition states would be a suitable strategy to cover this need. Therefore, a suitable design requires the introduction in biaryl scaffolds of functional groups able to interact to each other, forming cyclic intermediates for the labilization of the axis and able to be transformed in a catalytic asymmetric way into the desired amine functionalities.

We know, from the work developed by Akiyama,⁵⁶ that biaryl *N,O*-acetals from an imine and an alcohol are able to labilize the stereogenic axis. On this basis, we questioned whether related biaryl amins could behave in a similar way. If it is the case, since an equilibrium with the open form (imine) can be also assumed, then the desired diamine

¹⁶¹ Cheng, D.-J.; Yan, L.; Tian, S.-K.; Wu, M.-Y.; Wang, L.-X.; Fan, Z.-L.; Zheng, S.-C.; Liu, Y.; Tan, B. *Angew. Chem. Int. Ed.* **2014**, *53*, 3684.

targets could be easily accessed by asymmetric transfer hydrogenation of the imine functionality *via* DKR (Scheme IV.7).



Scheme IV.7 – Concept for the proposed strategy.

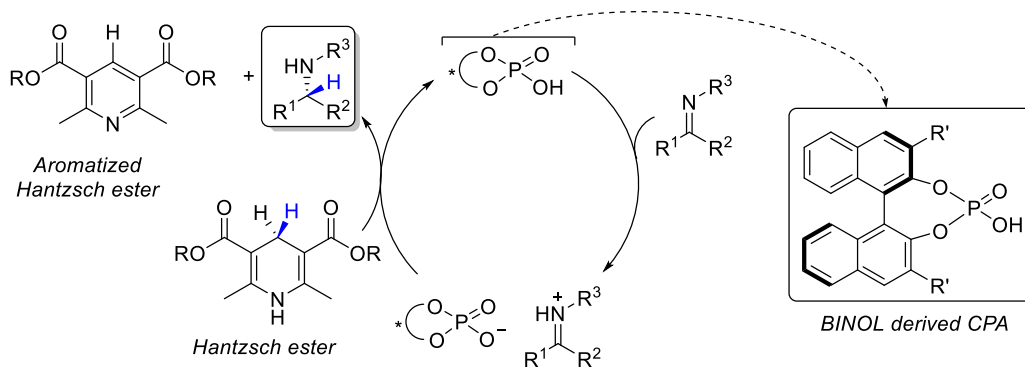
The key step in this approach would be the ring opening-closing event between biaryl amination and amino-imine structures. If the two atropisomers of the biaryl imine are able to rapidly interconvert into each other through the biaryl amination, then the dynamic kinetic resolution would be feasible. Nevertheless, it would also be necessary to select a proper atroposelective reduction method in order to obtain the enantioenriched axially chiral diamines with high selectivity, and a good option could be to perform an asymmetric transfer hydrogenation of the imine functionality.

IV.1.2. Asymmetric Transfer Hydrogenation of imines.

The asymmetric transfer hydrogenation (ATH) methodology for the enantioselective reduction of imines (or ketones) represents a mild and appealing alternative to classical hydrogenation procedures that involve the use of hydrogen gas and its subsequent hazards. This methodology represents a way of transforming imines and

carbonyls (the actual precursor of imines) into chiral amines, and two general approaches have been developed: (i) organocatalytic ATH, and (ii) metal-catalyzed ATH.¹⁶²

With respect to the first approach, most of the organocatalyzed ATH of imines use a chiral phosphoric acid (CPA) derived from BINOL as the catalyst and the Hantzsch ester as the hydrogen donor.



Scheme IV.8 – Catalytic cycle proposed by Rueping and co-workers for CPA catalyzed ATH.

The group of Rueping proposed a general mechanism for the ATH of imines under these conditions that involves a first activation of the imine by CPA generating an iminium ion, followed by a hydrogen transfer from the Hantzsch ester with the regeneration of the catalyst (Scheme 8). The driving force of this catalytic cycle comprises the aromatization of Hantzsch ester into the corresponding pyridine.¹⁶³

On the other hand, the metal-catalyzed ATH approach has mainly been developed using ruthenium¹⁶⁴, rhodium¹⁶⁵ and even iron¹⁶⁶ or iridium¹⁶⁷ complexes, in combination with 1,2-aminoalcohols or 1,2-diamines as the chiral ligands. The first efficient ATH of

¹⁶² Foubelo, F.; Yus, M. *Chem. Rec.* **2015**, *15*, 907.

¹⁶³ Rueping, M.; Sugiono, E.; Schoepke, F. R. *Synlett* **2010**, 852.

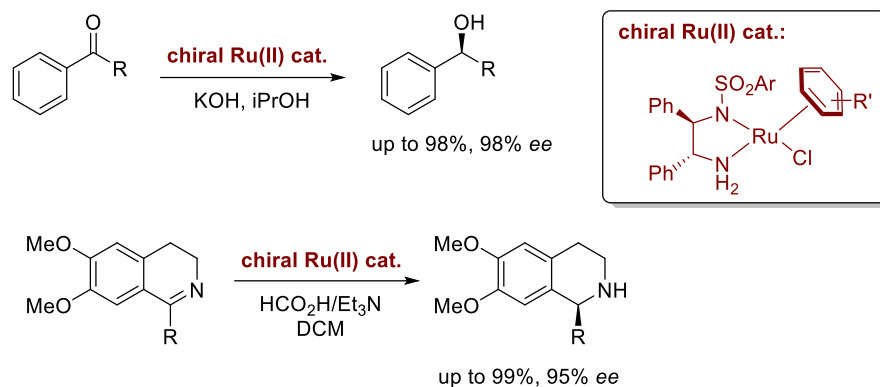
¹⁶⁴ CITAS

¹⁶⁵ (a) Mao, J.; Baker, D. C.; *Org. Lett.*, **1999**, *1*, 841. (b) Kang, S.; Han, J.; Lee, E. S.; Choi, E. B.; Lee, H.-K. *Org. Lett.* **2010**, *12*, 4184.

¹⁶⁶ Mikhailine, A. A.; Maishan, M. I.; Morris R. H. *Org. Lett.* **2012**, *14*, 4638.

¹⁶⁷ Pan, H.-J.; Zhang, y.; Shan, C.; Yu, Z.; Lan, Y.; Zhao, Y. *Angew. Chem. Int. Ed.* **2016**, *55*, 9615.

prochiral ketones¹⁶⁸ and imines¹⁶⁹ was reported by Noyori in 1995 and 1996, respectively, using chiral Ru(II)-TsDPEN and η^6 -aromatic ligand, as catalyst (Scheme IV.9).



Scheme IV.9 – Noyori's first reports in ATH of ketones and imines.

These achievements by Noyori constituted a breakthrough for the asymmetric transfer hydrogenation of imines, and since then, ruthenium(II) complexes with chiral 1,2-diphenylethylenediamine and η^6 -arene ligands, and their structural variations, have become the most employed catalytic systems, with many reports being focused on its application as a convenient and efficient catalyst for the ATH of imines,¹⁷⁰ even in aqueous media.¹⁷¹

Given the importance of the Ru(II)/TsDPEN catalyzed ATH reaction, the role of each component of this catalytic system in the outcome of the reaction and its mechanism has been studied in detail. It was Noyori itself the first who reported a mechanistic

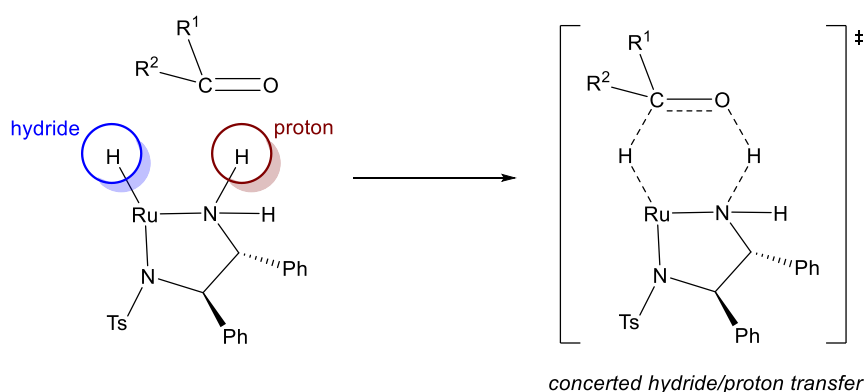
¹⁶⁸ (a) Hashiguchi, S.; Fujii, A.; Takehara, J.; Ikariya, T.; Noyori, R. *J. Am. Chem. Soc.* **1995**, *117*, 7562. (b) Uematsu, N.; Fujii, A.; Hashiguchi, S.; Ikariya, T.; Noyori, R. *J. Am. Chem. Soc.* **1996**, *118*, 2521.

¹⁶⁹ Uematsu, N.; Fujii, A.; Hashiguchi, S.; Ikariya, T.; Noyori, R. *J. Am. Chem. Soc.* **1996**, *118*, 4916.

¹⁷⁰ For some selected examples of Ru(II)/TsDPEN catalyzed ATH of imines, see: (a) Williams, G. D.; Pike, R. A.; Wade, C. E.; Wills, M. *Org. Lett.* **2003**, *5*, 4227 (b) Kadyrov, R.; Riermeier, T.; *Angew. Chem. Int. Ed.* **2003**, *42*, 5472. (c) Ros, A.; Magriz, A.; Dietrich, H.; Ford, M.; Fernández, R.; Lassaletta, J. M. *Adv. Synth. Catal.* **2005**, *347*, 1917. (d) Přeč, J.; Václavík, J.; Šot, P.; Pecháček, J.; Vilhanová, B.; Januščák, J.; Syslová, K.; Pažout, R.; Maixner, J.; Zápál, J.; Kuzma, M.; Kačer, P. *Catalysis Communications*, **2013**, *36*, 67. (e) Wu, Z.; Perez, M.; Scalone, M.; Ayad, T.; Ratovelomanana-Vidal, V. *Angew. Chem. Int. Ed.* **2013**, *52*, 4925.

¹⁷¹ Wu, J.; Wang, F.; Ma, Y.; Cui, X.; Cun, L.; Zhu, J.; Deng, J.; Yu, B. *Chem. Commun.*, **2006**, 1766.

perspective for the asymmetric transfer hydrogenation of carbonyl compounds.¹⁷² Studies on the corresponding reaction involving imines are more limited, and for a time it was assumed that both functionalities follow the same mechanistic profile. Noyori showed that for the reduction of ketones, the hydridic Ru–H and protic N–H were simultaneously delivered to the C=O bond involving a six-membered cyclic transition state in the outer coordination sphere of ruthenium (Scheme IV.10).



Scheme IV.10 – Six-membered cyclic TS proposed by Noyori for the ATH of ketones.

However, it has been shown that for imines the same reaction pathway is not applicable. In fact, the reaction with imines does not proceed without the presence of a slightly acidic media. It has been proposed that this acid media facilitates the pre-activation of the imine by protonation and formation of iminium ion, which would later enter into the catalytic cycle and a hydride from Ru–H species would be transferred to the azomethine carbon of the protonated imine;¹⁷³ thus, suggesting an ionic mechanism for this reaction (Scheme IV.12).

There are some research groups that have shed some light on the mechanism involved in the ATH of imines, although it is still not completely understood.¹⁷⁴ A relevant

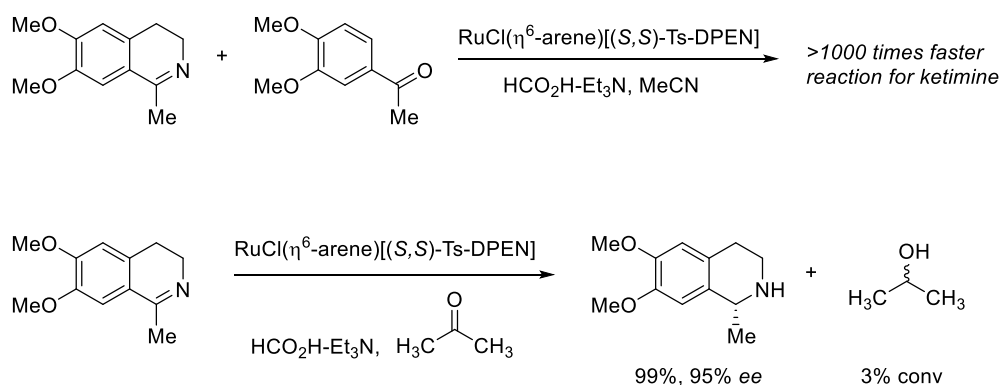
¹⁷² Noyori, R.; Yamakawa, M.; Hashiguchi, S. *J. Org. Chem.* **2001**, *66*, 7931.

¹⁷³ Shende, V. S.; Deshpande, S. H.; Shingote, S. K.; Joseph, A.; Kelkar, A. A. *Org. Lett.* **2015**, *17*, 2878.

¹⁷⁴ For selected studies on the ionic mechanism for imines ATH, see: (a) Åberg, J. B.; Samec, J. S. M.; Bäckvall, J.-E. *Chem. Commun.*, **2006**, 2771. (b) Martins, J. E. D.; Clarkson, G. J.; Wills, M. *Org. Lett.* **2009**, *11*, 847. (c) Soni, R.; Cheung, F. K.; Clarkson, G. C.; Martins, J. E. D.; Graham,

work developed by Kačer and co-workers focused on a DFT computational study to investigate the ionic mechanism pathway.¹⁷⁵ This study revealed that the structures of six-membered cyclic transition states (see Scheme IV.10) and subsequent concerted proton/hydride transfer were not involved for the reduction of imines due to the following reasons: (i) the opposite enantiomer to that observed experimentally are predicted; (ii) the imine could not be protonated, which is necessary for the reaction to proceed, and (iii) the single point energy between the favoured and disfavoured transition states is so high (43.2 kJ/mol) that the reaction would proceed with absolute enantiocontrol, which is not the case.

Furthermore, Noyori pointed out that, although the Ru(II)/TsDPEN system catalyses the reduction of ketones in formic acid-triethylamine mixture, the same reaction for imines is much faster. Even competitive experiments were performed, revealing that a ketimine can be >1000 times more reactive than the analogous ketone. Moreover, the same ketimine could be reduced even in acetone, providing the desired amine in 99% yield and 95% *ee*, while just a 3% of 2-propanol from acetone reduction was observed (Scheme IV.11).^{169,176} These experiments show the exquisite functional group selectivity displayed by the ATH of imines under Noyori's conditions.



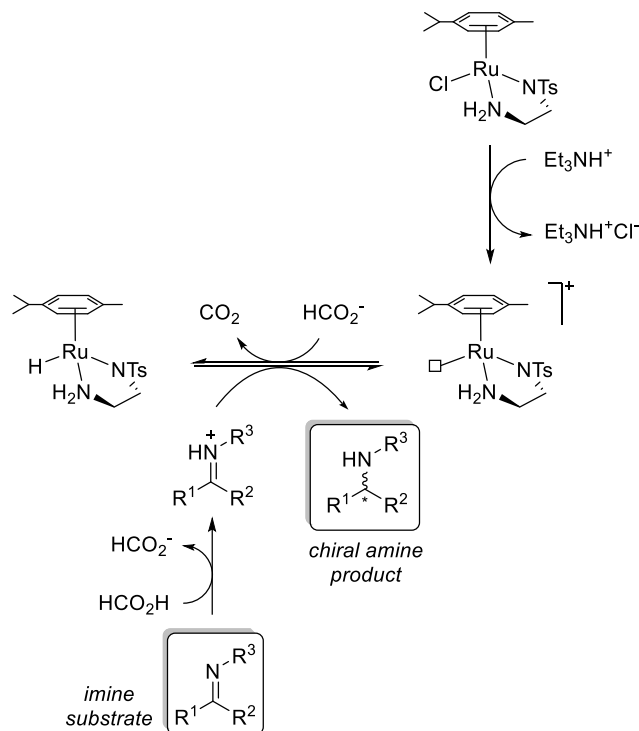
Scheme IV.11 – Competitive experiments to show chemoselectivity of ATH under these conditions.

M. A.; Wills, M. *Org. Biomol. Chem.* **2011**, 9, 3290. (d) Šot, P.; Vilhanová, B.; Pecháček, J.; Václavík, J.; Zápál, J.; Kuzma, M.; Kačer, P. *Tetrahedron: Asymmetry* **2014**, 25, 1346.

¹⁷⁵ Václavík, J.; Kuzma, M.; Přech, J.; Kačer, P. *Organometallics*, **2011**, 30, 4822.

¹⁷⁶ Noyori, R.; Hashiguchi, S. *Acc. Chem. Res.* **1997**, 30, 97.

Considering the aspects so far described for the asymmetric transfer hydrogenation of imines, it could be proposed a mechanism similar to that depicted below (Scheme IV.12).



Scheme IV.12 – Mechanism for the ATH of imines. DPEN substituents are omitted for the sake of clarity.

In this mechanism, as mentioned above, the imine is pre-activated by protonation by the formic acid and ready to enter into the catalytic cycle. Additionally, triethylamine, in the form of triethylammonium because of the acid media, would abstract the chloride from the initial $\text{RuCl}(\eta^6\text{-arene})[\text{Ts-DPEN}]$ complex (in the proposed mechanism, $\eta^6\text{-arene} = p\text{-cymene}$) generating a vacant coordination site. This vacant would be occupied by a hydride from the formate anion in the media, releasing carbon dioxide. Finally, to close the catalytic cycle, Ru-hydride would be transferred to the azomethine carbon of the activated iminium substrate, generating the enantioenriched amine.

In this context, the combination of the “lactone concept” and an asymmetric transfer hydrogenation of imines represents a promising strategy for the synthesis of axially chiral diamines, homologues to BINAM, still an unsolved challenge.

IV.2. Results and discussion

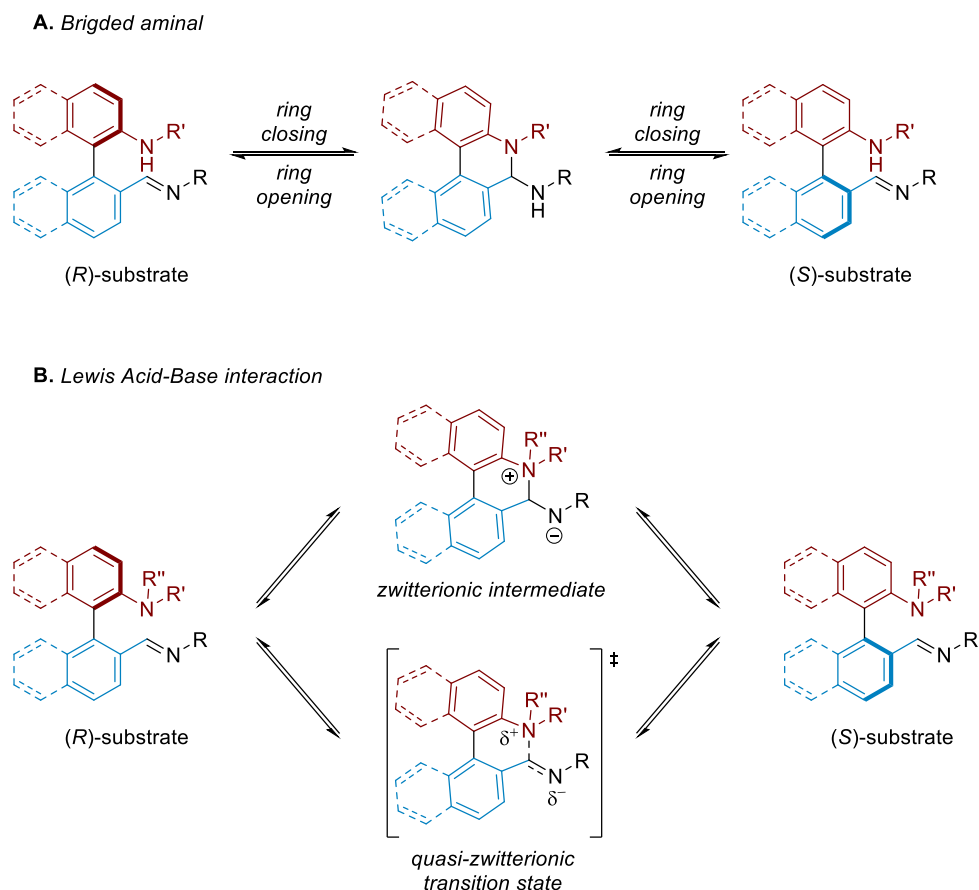
IV.2.1. Substrates design and synthesis.

Based on the previous studies developed by Bringmann,¹⁷⁷ in which tetrasubstituted systems resulted in a slower labilization process at the closed form and the subsequent lower enantioselectivities of the final products, a trisubstituted biaryl system was initially considered. In this situation, we envisaged that a faster racemization event would occur, leading to the desired product in higher enantioselectivity.

Additionally, a very important aspect for the application of the lactone concept to this system is related to the capability of the substrate to racemize in order to make possible the DKR, and therefore, the choice of the proper structure is key to the development of the stated hypothesis. There are two possible types of interaction that would facilitate the interconversion between both atropisomers of the substrate:

- The first one would consist on the formation of a cyclic aminal, analogous to the Akiyama's biaryl *N,O*-acetals. In this situation, it would be necessary an acidic proton at the nitrogen atom, to make possible the formation of the six-membered cyclic aminal. (Scheme IV.13A)
- The second approach consists on a related proposal to that previously described in Chapter III; a Lewis acid-base interaction between a nitrogen atom and, in this case, the azomethine carbon from the imine functionality. The later would provide the labilization either through a zwitterionic intermediate or a quasi-zwitterionic transition state (Scheme IV.13B)

¹⁷⁷ (a) Bringmann, G.; Breuning, M.; Endress, H.; Vitt, D. *Tetrahedron*, **1998**, *54*, 10677. (b) Bringmann, G.; Breuning, M. *Synlett*, **1998**, *6*, 634.

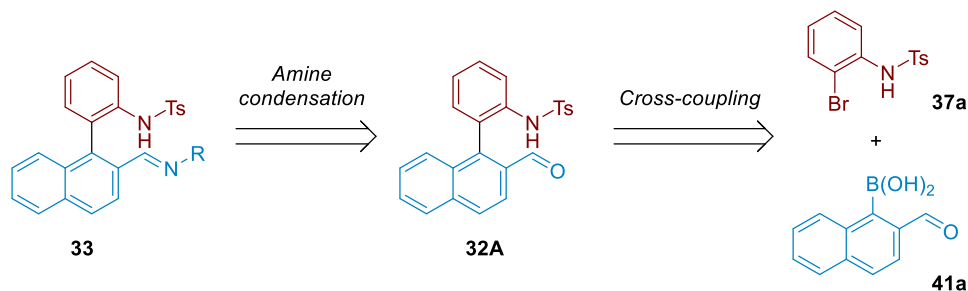


Scheme IV.13 – Alternative labilization modes for imine substrates.

Therefore, two different biaryl imino-amine systems were synthesized in order to determine the optimal labilization pathway. In the first case, an EWG was introduced on the nitrogen atom to increase its acidity in order to promote the formation of a cyclic *N,O*-acetal or an amina. On the other hand, the introduction of a dialkylamino group, where electron donor substituents (i.e. R' and R'' = alkyl...) are employed to increase the Lewis base character of the nitrogen atom, was also accomplished to test the second approach..

The synthesis of both imines from the corresponding aldehydes (or ketones) was considered as the most straightforward method. In turn, these carbonyl compounds could be synthesized by a Suzuki-Miyaura cross-coupling reaction between the two corresponding aromatic counterparts. From preliminary experiments, the optimal approach

is the cross-coupling between (2-formylnaphthalen-1-yl)boronic acid **41a** and *N*-tosyl-2-bromoaniline **37a** (Scheme IV.14).



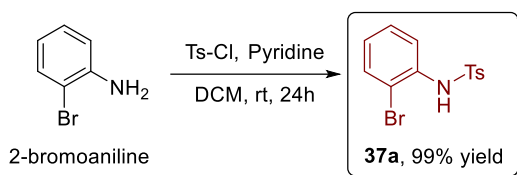
Scheme IV.14 – Retrosynthetic analysis of the desired substrates.

Both coupling fragments were synthesized following described procedures, allowing their synthesis in gram scale. The synthesis of bromide **37a**, was easily carried out by treatment of the inexpensive and commercially available 2-bromoaniline with tosyl chloride and pyridine in dichloromethane.¹⁷⁸ On the other hand, the preparation of boronic acid **41a** needed few more reaction steps, although they proceeded in an efficient manner (Scheme IV.15).¹⁷⁹

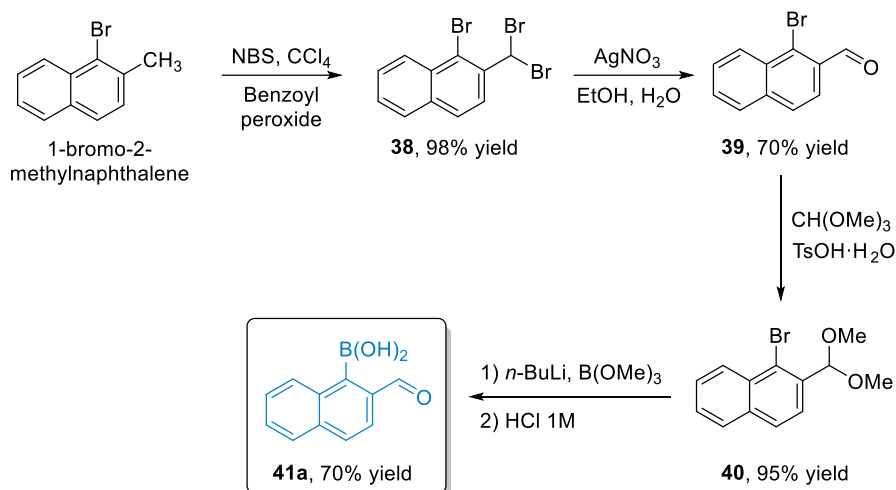
¹⁷⁸ Liwosz, T. W.; Chemler, S. R. *Chem. Eur. J.* **2013**, *19*, 12771.

¹⁷⁹ Referencias para la síntesis de los borónicos

AMINE FRAGMENT



ALDEHYDE FRAGMENT



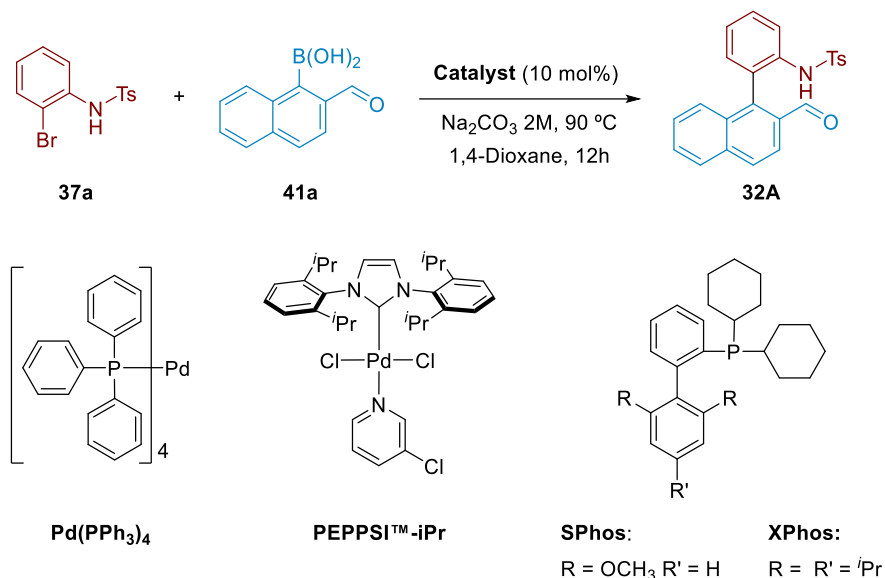
*Scheme IV.15 – Synthetic route for the preparation of bromide **37a** and boronic acid **41a**.*

The next stage consisted on the optimization of the reaction parameters for the cross-coupling between **37a** and **41a**. Initially, different catalysts were explored under standard Suzuki-Miyaura coupling conditions in order to identify the most efficient one (Table IV.1).

The reaction catalyzed by Pd(PPh₃)₄ (entry 1, Table IV.1) was not complete after 12h, affording the coupling product **32A** in 80% conversion. Surprisingly, when the catalyst PEPPSITM-iPr containing a palladium *N*-heterocyclic carbene was employed, the reaction did not take place (entry 2, Table IV.1). Fortunately, the use of electron rich phosphine ligands SPhos or Xphos in combination with Pd₂(dba)₃ allowed us to obtain the desired product in 90% yield and full conversion, respectively (entries 3 and 4, Table IV.1). Furthermore, the reaction catalyzed by Xphos as ligand was carried out in a large scale of 2.0 mmol with a decrease in the catalyst loading to 8 mol%, and the coupling product was

isolated quantitatively (entry 5, Table IV.1). It was also observed that longer reaction times only resulted in a decomposition of the catalyst and the remaining boronic acid.

Table IV.1 – Catalyst optimization for the cross-coupling reaction between **37a** and **41a**.



Entry ^a	Catalyst	Conv. (%) ^b
1	Pd(PPh ₃) ₄	80
2	PEPPSI™- <i>i</i> Pr	n.r.
3	[Pd ₂ (dba) ₃ + SPhos]	90
4	[Pd ₂ (dba) ₃ + XPhos]	>99
5 ^c	[Pd ₂ (dba) ₃ + XPhos]	>99 (98% yield)

^aReaction conditions: 0.1 mmol of bromide, 0.15 mmol of boronic acid, 0.2 mmol of Na₂CO₃ 2M aq. in 0.5 mL of anhydrous solvent. ^b Determined by ¹H-NMR spectroscopy. ^c Reaction set at 2.0 mmol scale, with 8 mol% of catalyst loading.

To our delight, NMR analysis of **32A** showed that the expected equilibrium between open and closed forms, was completely displaced to the cyclic hemiaminal since no aldehyde peak was observed, and a representative signal appears at 6.66 ppm as a singlet, corresponding to the proton at the sp³ carbon of the cyclic hemiaminal. Moreover, when a bidimensional ¹H-¹³C HSQC experiment was performed, it could be observed the

correlation between this singlet and a carbon atom at 80.9 ppm, both displaced to low field because of the influence of the contiguous N and O atoms (Figure IV.2).

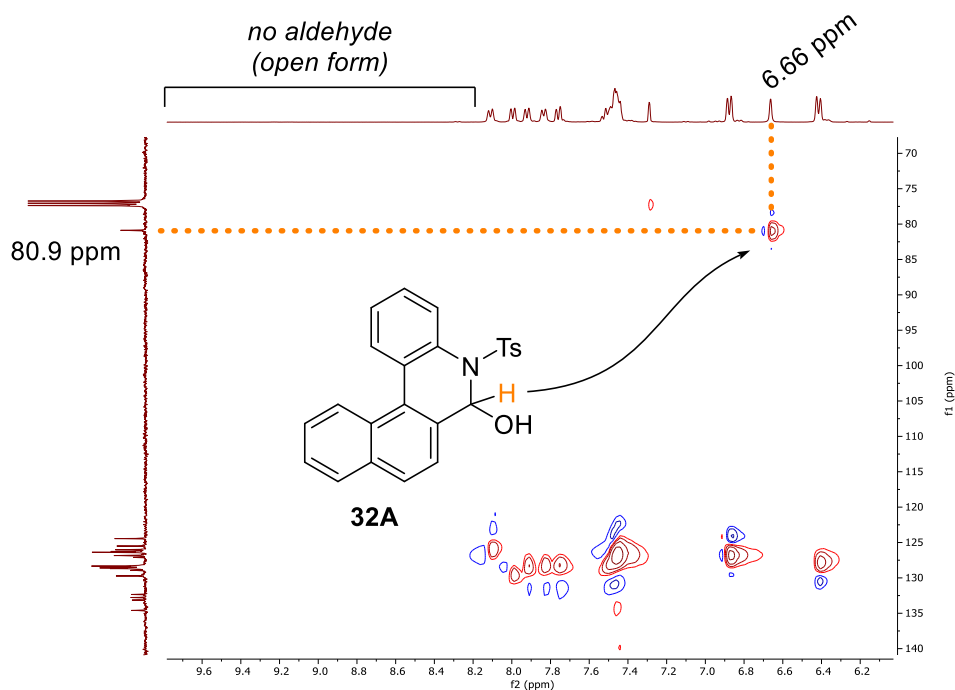


Figure IV.2 – Zoomed-in ^1H - ^{13}C HSQC spectra for **32A**.

Furthermore, it was possible to obtain crystals of **32A** suitable for X-ray diffraction analysis that provided the molecular structure in the solid state, which confirmed our initial hypothesis (Figure IV.3).

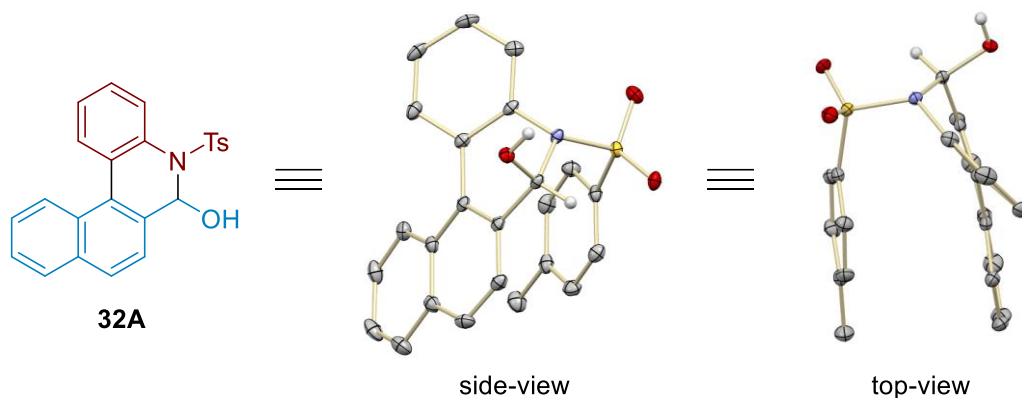
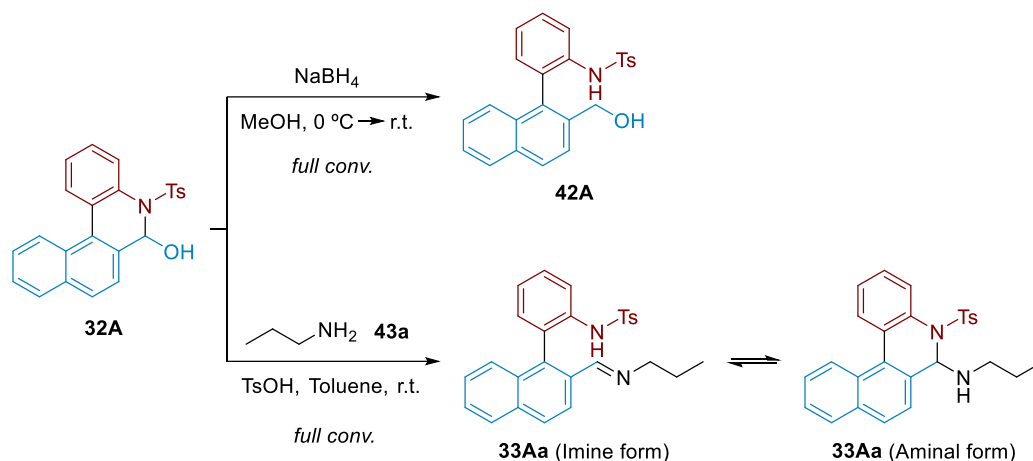


Figure IV.3 – X-ray diffraction structure of **32A**. Hydrogen atoms at sp^2 carbons, and at methyl from tosyl group are omitted for the sake of clarity.

At the top-view image, it can be observed an apparent π -stacking between naphthalene moiety and phenyl from tosyl group that could stabilize the closed hemiaminal structure versus the open form, thus, displacing the equilibrium towards the former. In contrast to what could be expected for the structure of **32A**, the two aromatic rings from biaryl moiety are not in a coplanar disposition, with the six-membered cyclic hemiaminal being slightly distorted.

Considering these observations, the formation of a cyclic hemiaminal that could promote the labilization of the substrate was evinced and, therefore, the initial requisite for a dynamic kinetic resolution was fulfilled. However, our main concern was to confirm if the imine resulting from the condensation of an amine with this aldehyde/hemiaminal, is also labile through a cyclic amination.

Additionally, we needed to determine whether the hemiaminal is in equilibrium with the reactive aldehyde species, or the equilibrium is completely displaced towards the cyclic form. To find this out, two experiments were performed using hemiaminal **32A**: (i) reduction with sodium borohydride, and (ii) condensation with *n*-propylamine. To our delight, the desired alcohol **42A** and imine **33Aa** were obtained in full conversion and short reaction times, confirming that the hemiaminal **32A** is in equilibrium with its open form or that the bridge can therefore be cleaved (Scheme IV.16).



Scheme IV.16 – Proof of reactivity for hemiaminal **32A**.

The $^1\text{H-NMR}$ spectra of **33Aa** showed a singlet at 5.95 ppm, similar to that for the proton at the hemiaminal sp^3 carbon for **32A**, although at a slightly lower chemical shift, indicating a preference for the cyclic aminal form rather than imine structure. This confirmed our initial hypothesis for the labilization through a bridged aminal structure, thus enabling the envisaged dynamic kinetic resolution.

A series of hemiaminals analogous to **32A** were also synthesized in order to explore some structural variations in the reaction scope (Figure IV.4).

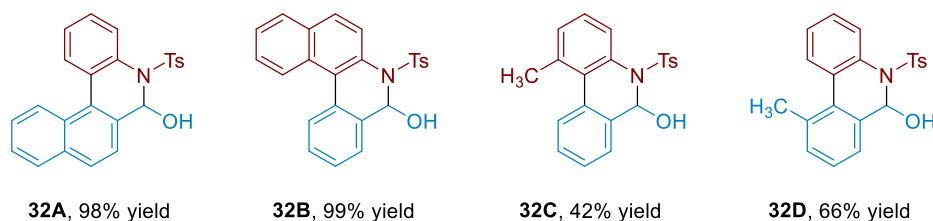
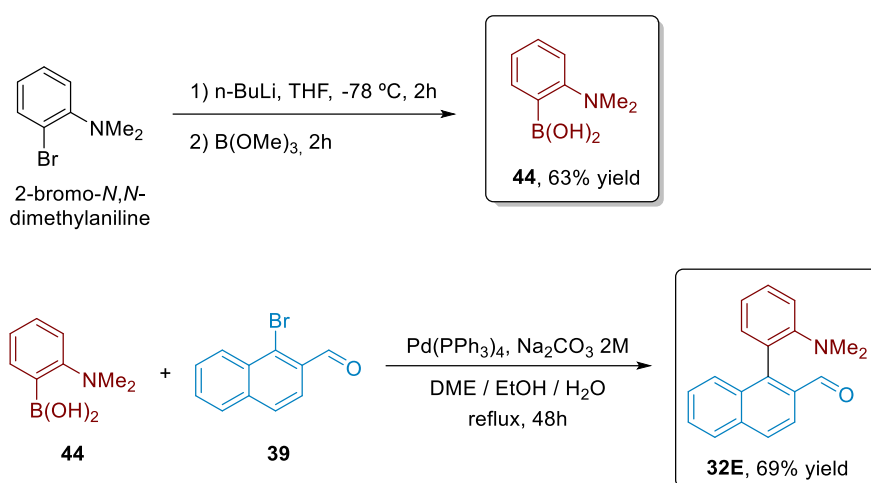


Figure IV.4 – Library of hemiaminal substrates synthesized.

All the substrates synthesized through this methodology present trisubstitution around the stereogenic axis, albeit the synthesis of tetrasubstituted systems (i.e. binaphthyl analogue) were also unsuccessfully attempted.

Concerning the other proposed labilization mode, based on a Lewis acid-base interaction between a nucleophilic nitrogen and an electrophilic imine, the synthesis of the

corresponding substrate was carried out in order to confirm or discard the proposed interaction. In this case, the synthetic route was similar to that followed for the synthesis of **32A**, although the polarity of the coupling partners for the Suzuki-Miyaura reaction were switched. Thus, (2-(dimethylamino)phenyl)boronic acid **44** was prepared from commercially available 2-bromo-*N,N*-dimethylaniline following a described procedure,¹⁸⁰ and 1-bromo-2-naphthaldehyde **39** was readily available as a synthetic intermediate for **32A**, permitting the isolation of **32E** in good yields after the cross-coupling reaction (Scheme IV.17).



Scheme IV.17 – Followed procedure for the synthesis of **32E**.

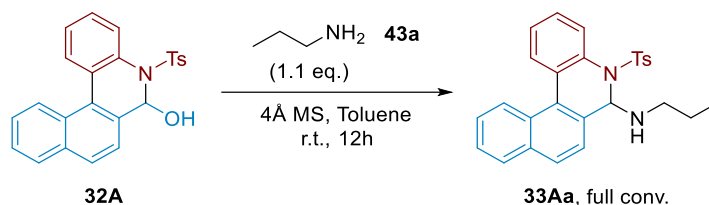
IV.2.2. Optimization of the reaction conditions.

Once we had all the substrates in hands, we decided to perform the synthesis of the desired axially chiral diamines directly from the hemiaminals by a one-pot reductive amination *via* asymmetric transfer hydrogenation in order to reduce the purification steps.

The model system chosen for the optimization of the reaction conditions consists on the asymmetric reductive amination of hemiaminal **32A** with *n*-propylamine **43a**. The first step, condensation of **43a** to **32A** for the formation of imine **33Aa**, did not need to be optimized since it proceeds efficiently under a wide variety of conditions, and those

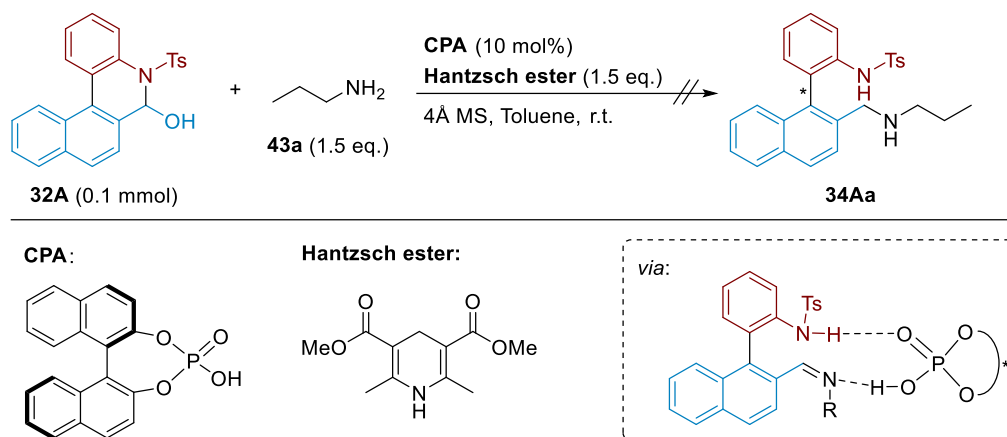
¹⁸⁰ Xu, Z.; Zhang, N.; Wang, T.; Sun, Q.; Wang, Y. US2018/208604, **2018**, A1.

selected were using 4Å molecular sieves in toluene at room temperature for 12h (Scheme IV.18).



Scheme IV.18 – Aldehyde-amine condensation reaction for the synthesis of iminal **33Aa**.

On the other hand, for the asymmetric transfer hydrogenation step, two alternatives were initially considered. The first one consisted on the application of Akiyama's imine ATH conditions using the chiral phosphoric acid derived from (*R*)-BINOL, in combination with Hantzsch ester (diethyl 1,4-dihydro-2,6-dimethyl-3,5-pyridinedicarboxylate), anticipating an activation mode similar to that observed by these authors (Scheme IV.19).

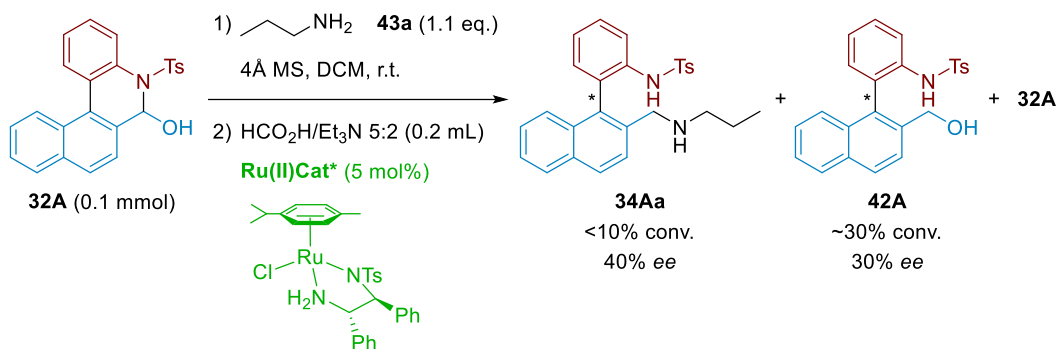


Scheme IV.19 – Asymmetric reductive amination using a CPA in combination with Hantzsch ester.

Unfortunately, the imine **33Aa** remained unreacted and no traces of reduction product **34Aa** was observed under these conditions. This lack of reactivity could be attributed to the very crowded environment around the chiral phosphate/iminium ion pair.

Therefore, we moved to the second alternative for the ATH, that is, the use of a more reactive metal-hydride complex, that should grant the reduction of the imine **33Aa**. Considering the extended use of ruthenium catalysts in combination with chiral diamine

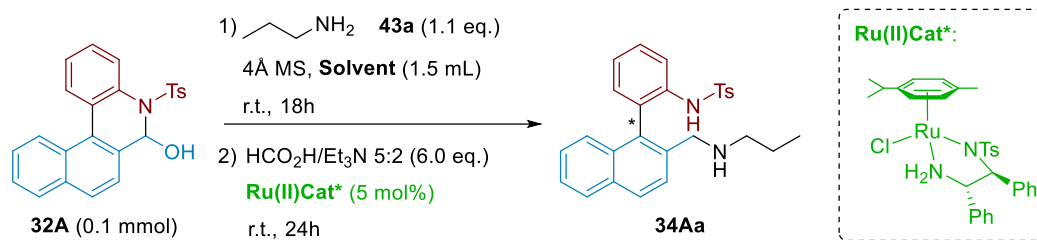
and η^6 -arene ligands, the inexpensive and commercially available $\text{RuCl}(p\text{-cymene})[(S,S)\text{-Ts-DPEN}]$ catalyst together with formic acid/triethylamine 5:2 (molar ratio) azeotropic mixture was chosen to explore this alternative. Initially, we applied the same reaction conditions previously described in our research group for the ATH of α -branched ketimines (Scheme IV.20).^{170c}



Scheme IV.20 – ATH catalyzed by $\text{RuCl}(p\text{-cymene})[(S,S)\text{-Ts-DPEN}]$ and $\text{HCO}_2\text{H}/\text{Et}_3\text{N}$.

Under these conditions the desired amine **34Aa** was formed, although in a negligible conversion (<10%) and 40% of enantiomeric excess. The main products observed were those resulting from imine hydrolysis leading to the starting material **32A** (full conversion from hemiaminal to imine is observed on TLC for the previous step), and its reduction product **42A**, with around 30% conversion and 30% *ee*. This result can be attributed to an excess of the formic acid/triethylamine mixture (from now on, FA/TEA) leading to a more acidic media that results in slower reactions.¹⁷³ Therefore, the amount of FA/TEA was decreased, obtaining a very interesting result when just 40 μL of FA/TEA (6.0 eq.) were added to the imine formed *in situ* in the presence of the catalyst, providing the desired axially chiral diamine **34Aa** with 93% conversion and 94% *ee* (entry 1, Table IV.2). At this point, we next moved to explore the influence of the solvent in the reaction outcome (Table IV.2).

Table IV.2 – Solvent screening for the asymmetric reductive amination of **32A**.

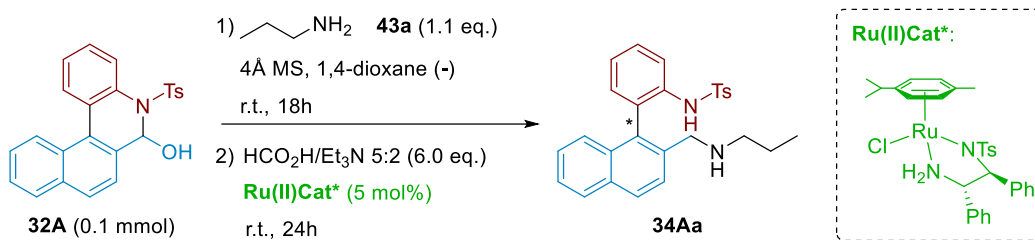


Entry	Solvent	Conv. (%) ^a	ee (%) ^b
1	DCM	93	94
2	Toluene	85	94
3	DCE	64	94
4	DMSO	n.d.	40
5	THF	n.d.	85
6	MeCN	n.d.	73
7	DMF	n.d.	50
8	1,4-Dioxane	91	97

^a Determined by ¹H-NMR spectroscopy. ^b Determined by chiral HPLC analysis.

Changing from dichloromethane to toluene provided similar results in terms of enantioselectivities, although a slight decrease in the reactivity was observed (85% conversion) (entry 2, Table IV.2). A similar but more pronounced effect occurred when dichloromethane was used (entry 3, Table IV.2). The use of more polar solvents as DMSO, THF, acetonitrile or DMF, resulted in a decrease of the enantioselectivities and, therefore, the conversions were not even measured (entries 4-7, Table IV.2). Finally, the use of 1,4-dioxane provided a very high conversion of 91% and an excellent 97% of enantiomeric excess (entry 8, Table IV.2). The solvent employed for the reaction appeared to be an important parameter, with 1,4-dioxane displaying the best results in general terms.

Table IV.3 – Evaluation of the concentration effect.



Entry	1,4-Dioxane (mL)	ee (%)
1	0.5	80
2	1.0	92
3	1.5	97
4	2.0	97

^a Determined by chiral HPLC analysis.

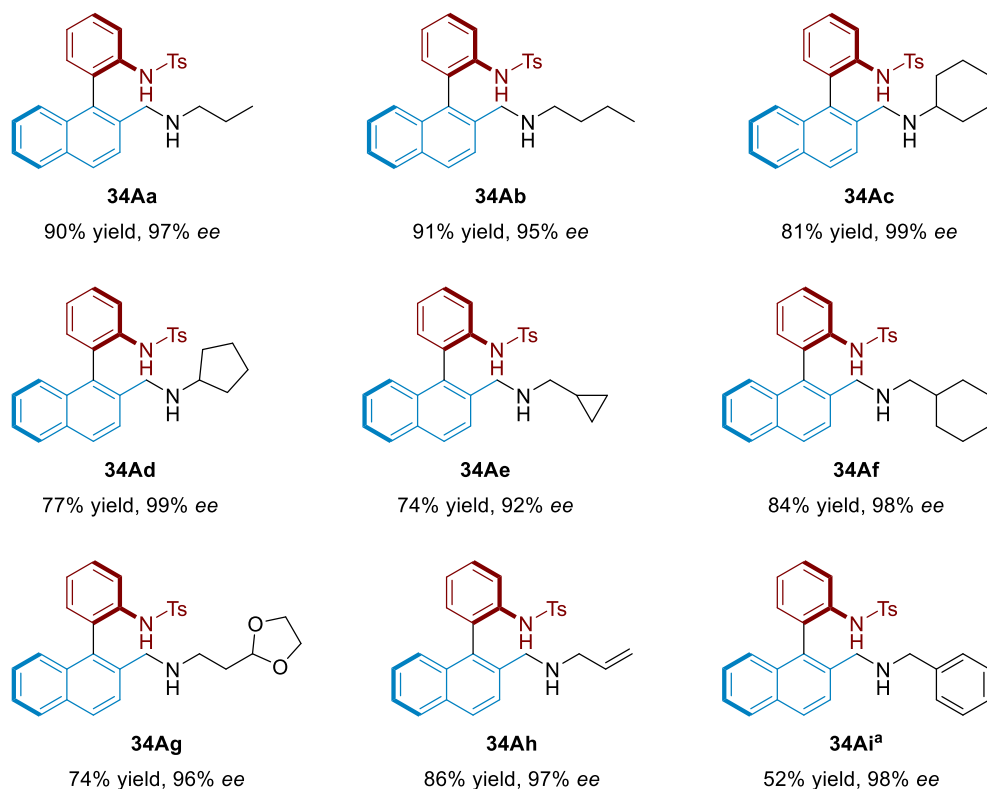
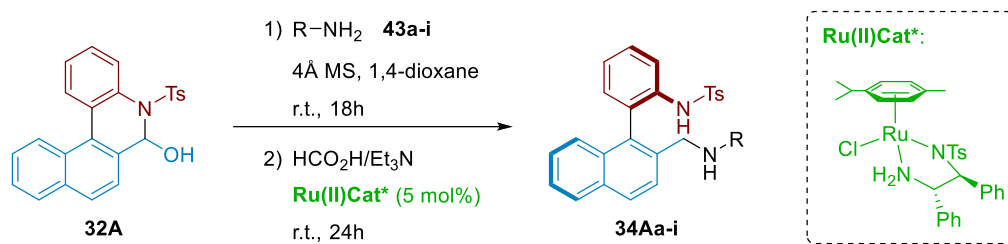
Interestingly, the enantioselectivity of the reaction was highly dependent of the concentration of the reaction media (Table IV.3). Increasing the concentration led to a decrease of the enantiomeric excess of the diamine **34Aa** to 92% or 80% when the amount of 1,4-dioxane employed was 1.0 or 0.5 mL, respectively (entries 2 and 1, Table IV.3). Nonetheless, when the reaction was more diluted, using 2.0 mL (entry 4, Table IV.3) the enantiomeric excess was not affected compared to the values for 1.5 mL (entry 3, Table IV.3).

Therefore, the optimal conditions for the asymmetric reductive amination of **32A** were fixed as follows: *n*-propylamine **43a** (1.1 eq.) in 1,4-dioxane (1.5 mL), and further addition of FA/TEA 5:2 (6.0 eq.) and the commercially available RuCl(*p*-cymene)[(S,S)-Ts-DPEN] (5 mol%).

IV.2.3. Reaction scope.

With the optimized conditions in hands, we next moved to explore the scope of amines. Initially, several aliphatic primary amines **43a-i** were employed in combination with **32A**.

From the Scheme IV.21, it can be concluded that the methodology tolerates a wide variety of aliphatic primary amines, leading in all cases to products with excellent enantioselectivities. For instance, the product **34Ab** was obtained with similar results than for the model compound **34Aa**, while exocyclic amines **43c** and **43d** provided excellent selectivity values affording products **34Ac** and **34Ad** in 99% *ee*, in both cases. Additionally, the use of **43e** and **43f** containing a methylene between the amine and the cycloalkyl moiety, led to the desired products in high yield (74% and 84%, respectively) and excellent enantioselectivities (92% and 98%, respectively). This methodology also tolerates the synthesis of the highly functionalised system **34Ag**, containing a protected aldehyde as 1,3-dioxolane, that could be further deprotected, with excellent results (74% yield and 96% *ee*). With the aim of using a removable group to obtain the free axially chiral primary diamine compounds, the reaction was performed with allylamine **43h** and benzylamine **43i**, allowing for the synthesis of the corresponding products **34Ah** and **34Ai** in excellent enantioselectivities, although a lower conversion was observed for the latter, even after a long reaction time.



Scheme IV.21 – Reaction scope for the reductive amination of **32A** with aliphatic primary amines **43a-i**. Reaction conditions: 0.1 mmol of **32A**, 0.11 mmol of amine **43a-i**, 1.5 mL of 1,4-dioxane, 5 mol% of Ru(II)Cat*, and 40 μL of FA/TEA (5:2, molar). ^a ATH step took 5 days.

Additionally, it was possible to determine the absolute configuration of the product **34Aa** by X-ray diffraction analysis, showing an axial *R* configuration for the major enantiomer (Figure IV.5). Hence, the absolute configuration for the rest of reaction products was assigned by analogy.

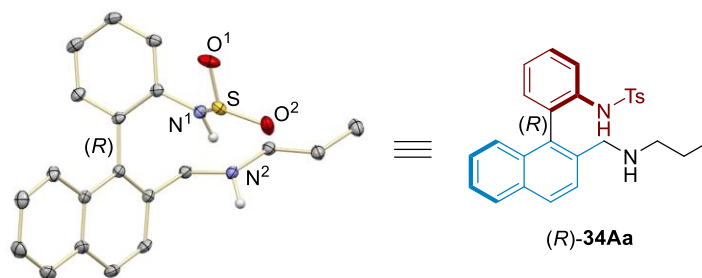
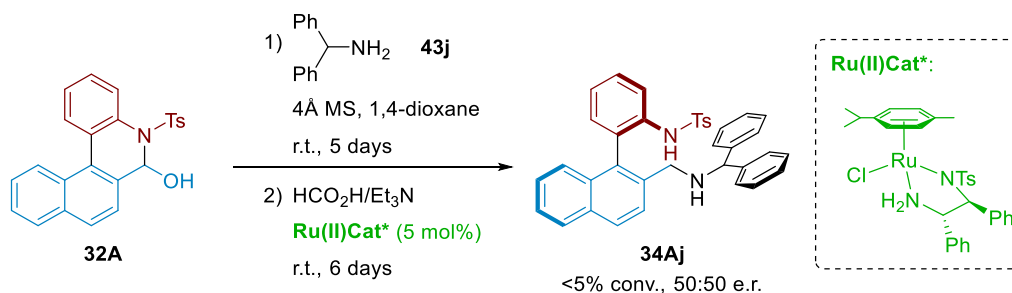


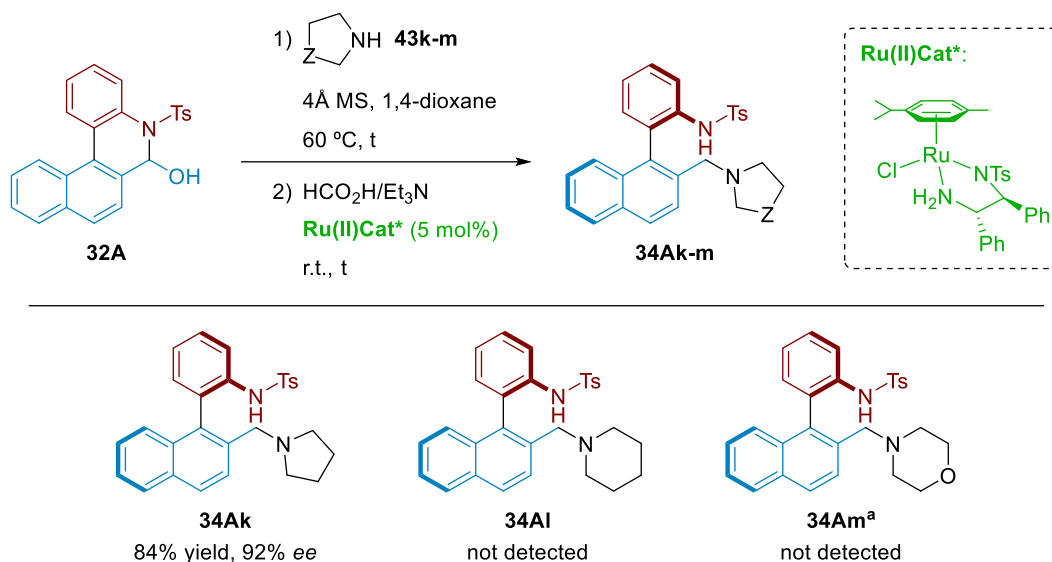
Figure IV.5 – Absolute configuration assignment for (R)-34Aa. C–H bonds and aromatic fragment from tosyl group are omitted for the sake of clarity. Thermal ellipsoids drawn for 50% probability.

Remarkably, the condensation reaction of **32A** with benzhydrylamine **43j** was incomplete after 5 days, and after further addition of FA/TEA and catalyst and additional 6 days of reaction, only traces of the product **32Aj** were observed. Furthermore, these traces were analysed by chiral HPLC showing a racemic mixture of the two enantiomers of **32Aj**, thus, indicating that not only this bulkier amine decreases the reactivity, but may also hamper the formation of the cyclic iminal responsible for the labilization process (Scheme IV.22).



Scheme IV.22 –Asymmetric reductive amination between **32A** and **43j**.

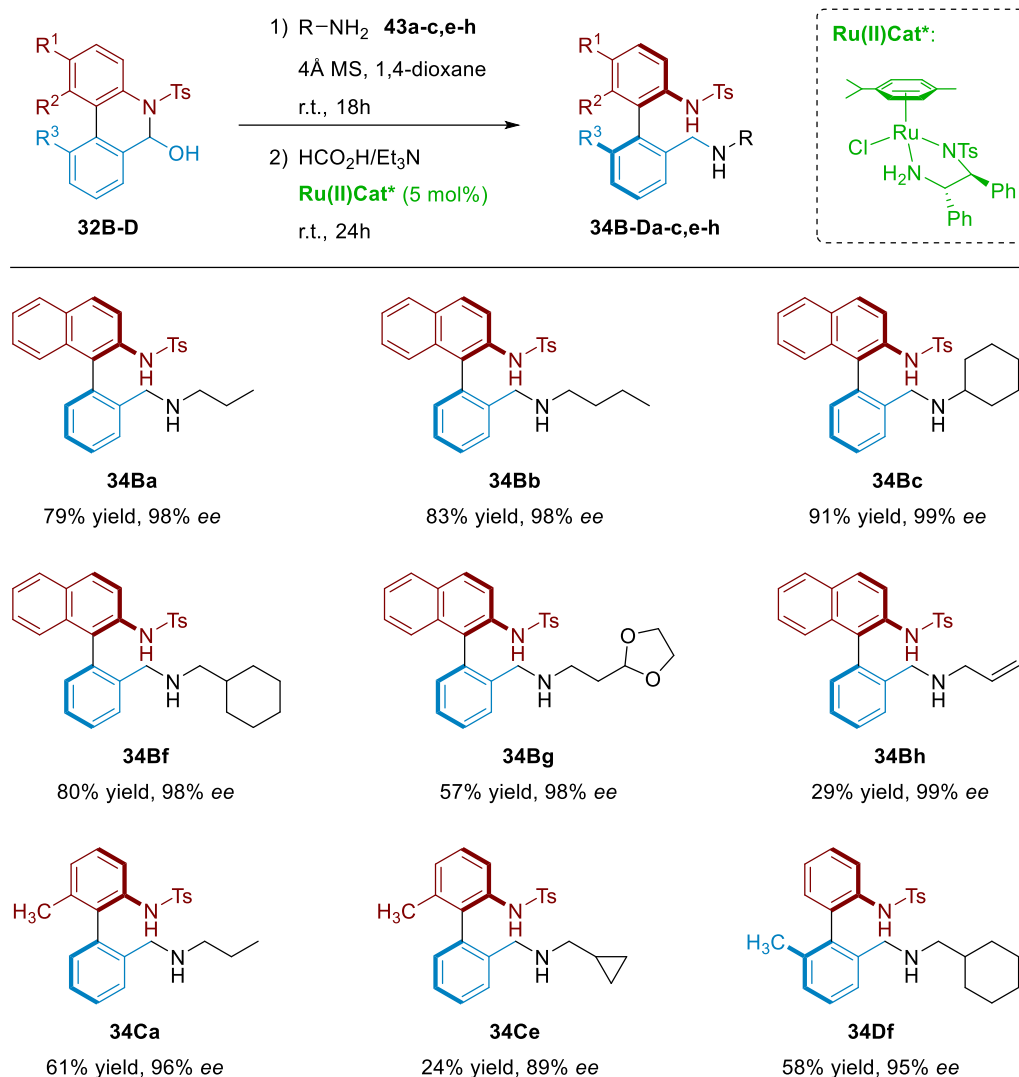
Additionally, this asymmetric reductive amination methodology was extended to cyclic secondary amines **43k-m** (Scheme IV.23). It is important to highlight that, although the bulkiness of the amine negatively affects these reactions, when these amines are used, an iminium specie is formed with much higher electrophilicity than the former carbonyl. We then anticipated that these amines might provide electronic effect that may overcome the steric issues.



Scheme IV.23 – Reaction scope for the reductive amination of **32A** with endocyclic aliphatic amines **43k-m**. Reaction conditions: 0.1 mmol of **32A**, 0.11 mmol of amine **43k-m**, 1.5 mL of 1,4-dioxane, 5 mol% of **Ru(II)Cat***, and 40 μL of FA/TEA (5:2, molar). ^a 5 mol% of *p*-TsOH was added at condensation step.

To our delight, the methodology is suited for the use of pyrrolidine **43k**, affording the desired axially chiral diamine **34Ak** in 84% yield and 92% of enantiomeric excess, after 36 h. It must be mentioned however that it was necessary to heat at 60 °C to facilitate the condensation reaction. Considering this result, we found surprising that when piperidine was used instead, the desired diamine was not detected. In fact, the corresponding imine was completely formed when the condensation reaction was heated to 60 °C (TLC monitoring), but after addition of **Ru(II)Cat*** and FA/TEA, imine hydrolysis followed by aldehyde reduction product **42A** was the only observed product after 6 days at room temperature. The difference in reactivity observed between pyrrolidine and piperidine was attributed to the formation of a more strained system for the former. Furthermore, the reaction of **32A** with morpholine **43m** was also explored. In this case, longer reaction time for both amination and reduction step (3 and 4 days, respectively) was required, and the addition of a 5 mol% of *p*-TsOH (to achieve almost complete condensation) was necessary.

We next explored the scope of the reaction with respect to other biaryl frames **32B-D** (Scheme IV.24).

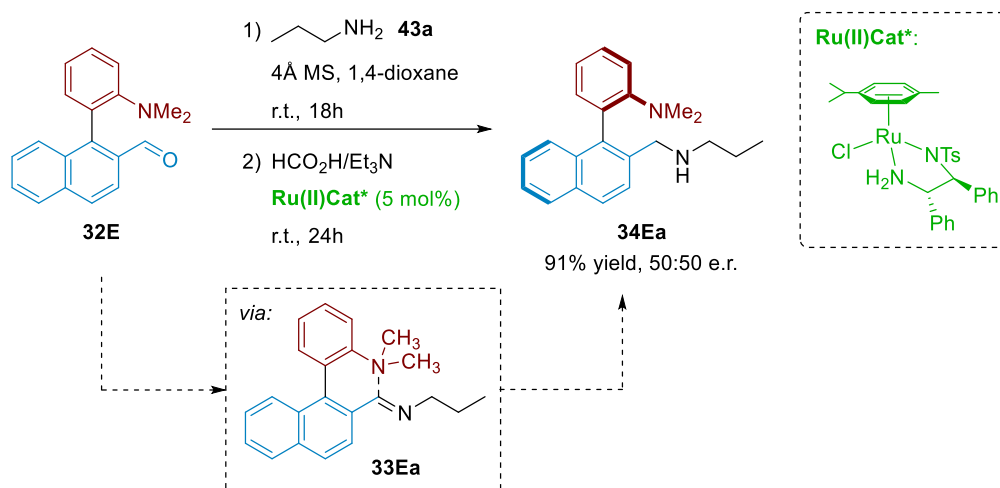


Scheme IV.24 – Reaction scope for the reductive amination of hemiaminals **32B-D** with aliphatic primary amines **43a-c,e-h**. Reaction conditions: 0.1 mmol of **32B-D**, 0.11 mmol of amine, 1.5mL of 1,4-dioxane, 5mol% of **Ru(II)Cat***, and 40μL of FA/TEA (5:2, molar).

This methodology could also be applied when some structural modifications were performed on the biaryl frame. If a naphthyl ring was placed at the *upper fragment* of the biaryl moiety (**32B**) very similar results were observed for the asymmetric reductive

amination of the aminal. For instance, when the reaction was performed with *n*-propylamine **43a**, *n*-butylamine **43b**, cyclohexylamine **43c**, or methylcyclohexylamine **43f**, very high yields and excellent enantioselectivities were achieved in all cases. However, a decrease in reactivity was observed for this system in the reactions with the 1,3-dioxolane derivative **43g** or allylamine **43h**, though the enantiomeric excesses were slightly higher than those shown for **34Ag** or **34Ah**. The use of systems such as **32C** or **32D** resulted in the isolation of the desired products in high enantioselectivity although moderate yields. The case of **34Ce** represents the only example of the series displaying an enantiomeric excess below 90%.

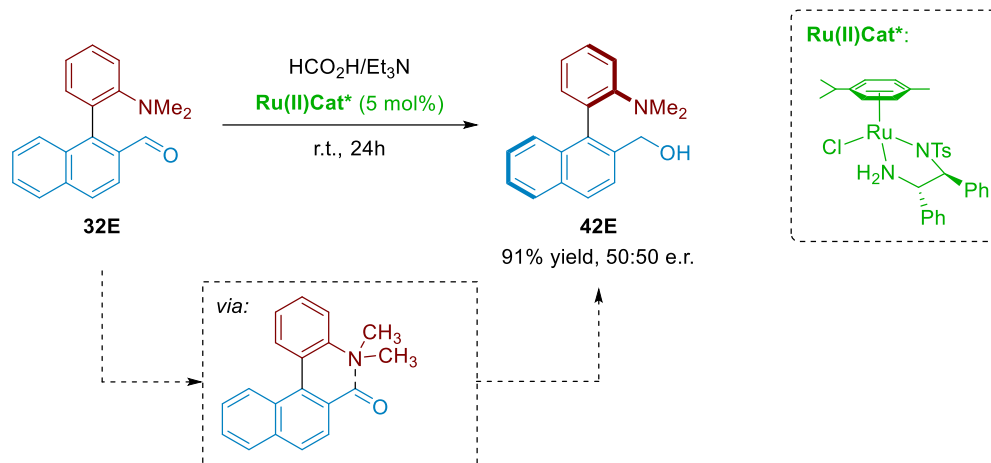
So far, it was confirmed that the labilization event can proceed *via* a cyclic aminal, in an analogous manner than for Akiyam's system. We next focused on the second approach consisting on a labilization through a Lewis acid-base interaction between the nucleophilic nitrogen and the azomethine carbon from the imine group. To address this point, we carried out the reaction between the previously synthesized substrate **32E** and *n*-propylamine **43a** under the already optimized conditions (Scheme IV.25).



Scheme IV.25 – Analysis of the labilization process through Lewis acid-base interaction in imine **33Ea**.

Surprisingly, the product resulting from this reaction (**34Ea**) was obtained as a racemic mixture. A possible explanation is that the Lewis acid-base interaction involving a six-membered intermediate/transition state was not effective enough to reach the

racemization barrier, at least through **33Ea**. It was suggested that using the more electrophilic aldehyde **32E** this labilization process would be more feasible. For that purpose, the direct reduction of the aldehyde substrate **32E** was performed under the optimized conditions for the asymmetric transfer hydrogenation (Scheme IV.26)



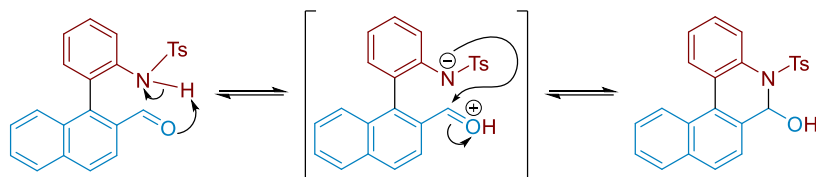
Scheme IV.26 – Analysis of the labilization process via Lewis acid-base interaction at substrate **32E**.

Unexpectedly, the alcohol **42E** resulting from the aldehyde reduction was also isolated again as a racemic mixture. There are *a priori* two possible explanations:

- The presumed interaction between nucleophilic nitrogen and carbonyl is not taking place, possibly due to steric hindrance at the nitrogen.
- The interaction exists, but is not strong enough to force the coplanar conformation that allows the fast interconversion between the two atropisomers.

This result also suggested a plausible mechanism for the labilization event through the formation of the cyclic hemiaminal species in the substrates. This is based on the acidity of the proton at the nitrogen and the protophilicity of the oxygen atom from the aldehyde, promoting an intramolecular proton transfer (prototropy) that provides the activation to form the cyclic hemiaminal (Scheme IV.27). In our particular case, the presence of an electron withdrawing group at the N atom, such as tosyl, proved to be essential to increase

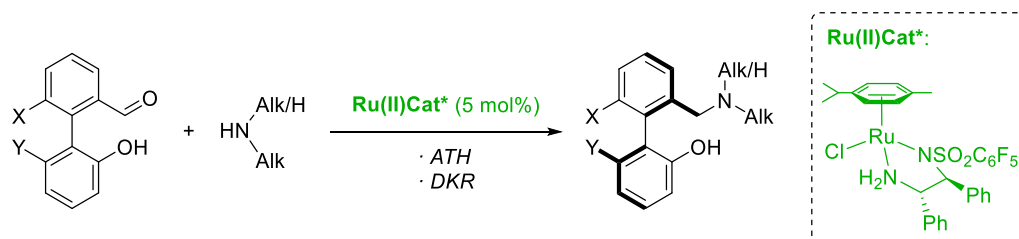
the acidity of the proton involved in the hemiaminal formation, and prevent a possible further conversion to the iminium ion by elimination reaction.



Scheme IV.27 – Proposed mechanism for the formation of cyclic hemiaminal 32A.

In summary, the asymmetric transfer hydrogenation of configurationally unstable amins has emerged as an efficient method for the catalytic enantioselective synthesis of axially chiral diamines of the HOMOBINAM family.

It is worth to mention that, while this work was being developed, Wang and co-workers,¹⁸¹ reported a similar Ru-catalyzed atropo-enantioselective synthesis of biaryl amine-alcohol (Scheme IV.28). However, Wang's system employs the previously described biaryl *N,O*-acetals,⁵⁶ although it also includes substrates presenting tetrasubstitution around the stereogenic axis and a variety of secondary alkyl amines. Furthermore, our system presents the novelty of allowing the synthesis of axially chiral diamines homologues to BINAM, an unresolved challenge in organic synthesis.



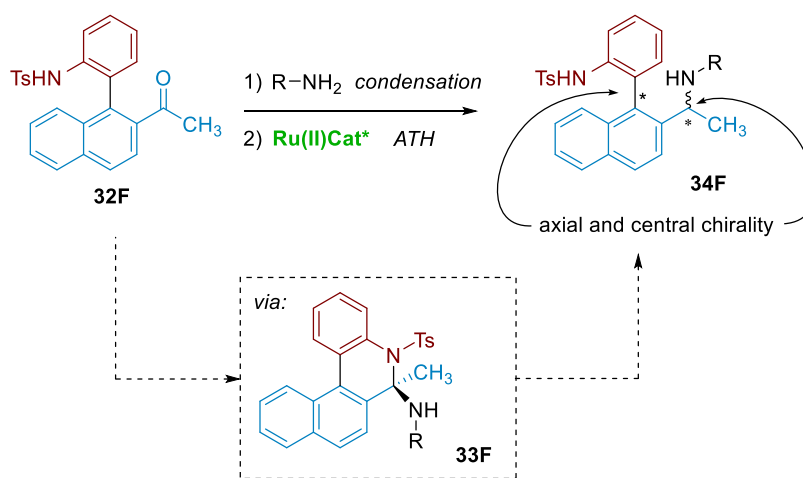
Scheme IV.28 – Wang's Ru-catalyzed asymmetric reductive amination via DKR.

The importance of (hetero)biaryl derivatives containing both axial and central chirality elements was discussed and reviewed along Chapter I, and Chapters II and III show two methodologies that have been developed for the synthesis of novel

¹⁸¹ Guo, D.; Zhang, J.; Zhang, B.; Wang, J. *Org. Lett.* **2018**, *20*, 6284.

representatives of such compounds., In this context, therefore, we wanted to go one step further with this methodology, and determine whether it could be also extended to the synthesis of diamines with the simultaneous generation of central and axial chirality elements.

For that purpose, a structural modification at the substrate was necessary. In particular, the analogue ketone **32F** was synthesized, so that the asymmetric reduction of the iminium intermediate would result in the generation of a stereogenic centre (Scheme IV.29). The first needed was to determine whether the labilization event was still possible in a more crowded environment and with a less electrophilic ketone carbonyl.



Scheme IV.29 – Proposal for method extension to the synthesis of central and axially chiral diamines.

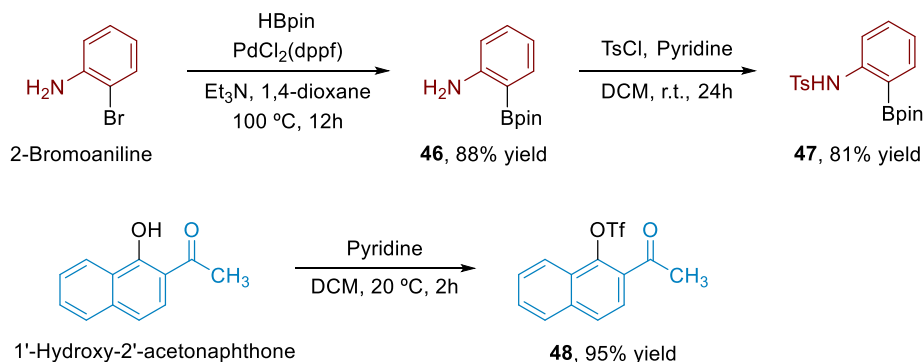
The synthesis of the substrate **32F** was carried out through a similar synthetic procedure than that followed for **32A-E**, with slight modifications of the coupling conditions. Initially, both coupling partners were synthesized according to described procedures, starting from commercially available 2-bromoaniline¹⁸² and 1'-hydroxy-2'-acetonaphthone¹⁸³ (Scheme IV.30A). Then, the cross-coupling reaction between pinacol

¹⁸² Jang, Y. H.; Youn, S. W. *Org. Lett.* **2014**, *16*, 3720.

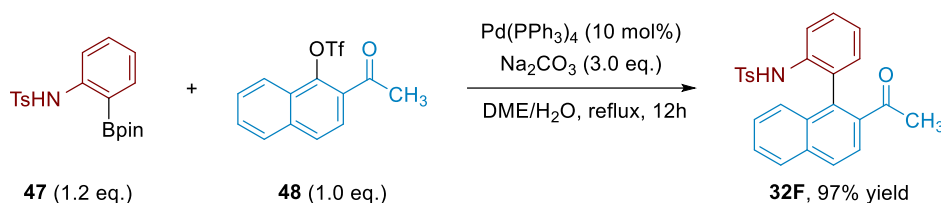
¹⁸³ Penhoat, M.; Levacher, V.; Dupas, G. *J. Org. Chem.* **2003**, *68*, 9517.

borane **47** and triflate **48** was performed under the reaction conditions displayed at Scheme IV.30B, to afford the desired product quantitatively.

A) Synthesis of coupling partners



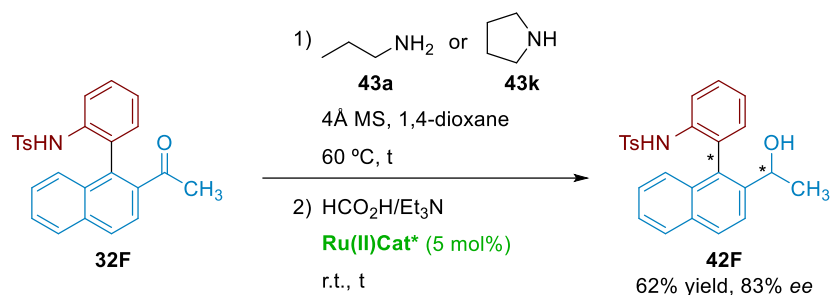
B) Cross-coupling reaction between **48** and **47**



Scheme IV.30 – Synthetic route for accessing biaryl ketone **32F**.

In contrast to substrates **32A-D**, ^1H and ^{13}C -NMR analysis of the coupling product **32F** did not show any traces of the bridged hemiaminal structure. This was attributed to the lower electrophilicity of ketone carbonyl with respect to aldehyde, together with the increase on the steric environment. Thus, a lower labilization rate at the ketone substrate could be expected. However, it could also be argued that, after amine condensation, the generation of an iminium ion provides an increase of electrophilicity enough to allow the dynamic kinetic resolution to proceed.

In order to determine its viability, the reaction between two representative amines (**43a** and **43k**) was performed under the optimal conditions for the asymmetric reductive amination (Scheme IV.31).



Scheme IV.31 – Asymmetric reductive amination protocol performed on biaryl ketone 32F.

Surprisingly, the main reaction product obtained with both amines was the corresponding alcohol from ketone reduction **42F**, and no traces of the desired diamine was observed in any case. It should be noted that, for the reaction with amine **43k**, a catalytic amount of *p*-TsOH was added in order to increase the rate of the condensation reaction. Nonetheless, this is a preliminary result, and this approach has to be further explored as a future prospect. In this regard, it is worth to mention that the methodology described during this Chapter IV is still being studied with the aim of expanding its potential and applicability.

IV.3. Conclusions.

To summarize, in Chapter IV an efficient methodology for the synthesis of axially chiral diamines with high excellent enantioselectivities has been described. This strategy consists on the dynamic kinetic resolution of biaryl cyclic hemiaminal structures by and asymmetric reductive amination *via* Ru-catalyzed transfer hydrogenation. In this case, a fast interconversion between the two atropisomers of the substrate through the formation of cyclic aminal structures is responsible for the high levels of enantioselectivities observed for this reaction.

From this strategy, it can be concluded that an efficient alternative for the unsolved synthesis BINAM homologues has been described. Moreover, as mentioned above, this methodology is currently under investigation in our research group with the aim of expand its high potential.

IV.4. Experimental Section.

IV.4.1. General procedure for the synthesis of *N*-tosyl amines.

The corresponding primary amine (2.0 mmol, 1.0 eq.) was added to a flame-dried Schlenk and dissolved in dry dichloromethane (4.5 mL). Then pyridine (3.0 eq.) and *p*-toluenesulfonyl chloride (1.1 eq.) were subsequently added at room temperature, and reaction mixture was stirred for 24h. Later, reaction was diluted with water and extracted with dichloromethane (x3), and washed with brine. The collected organic phases were dried over anhydrous Na₂SO₄, filtered, concentrated, and the residue was purified by column chromatography on silica gel using different *n*-hex/EtOAc mixtures.

Synthesis of *N*-(1-Bromonaphthalen-2-yl)-4-methylbenzenesulfonamide. **37b**.



Following the general procedure, starting from 1-bromonaphthalen-2-amine (445.8 mg, 2 mmol), afforded **37b** as a white amorphous solid (630 mg, 84%).

¹H-NMR (400 MHz, CDCl₃) δ 8.03 (d, *J* = 8.5 Hz, 1H), 7.90 (d, *J* = 8.9 Hz, 1H), 7.78 (d, *J* = 6.7 Hz, 2H), 7.67 (d, *J* = 7.8 Hz, 2H), 7.54 (t, *J* = 7.8 Hz, 1H), 7.46 (t, *J* = 7.8 Hz, 1H), 7.16 (d, *J* = 8.0 Hz, 2H), 2.32 (s, 3H).

¹³C-NMR (100 MHz, CDCl₃) δ 144.3, 135.9, 133.1, 132.0, 131.9, 129.7, 128.8, 128.2, 128.0, 127.3, 126.9, 126.0, 120.8, 114.2, 21.6.

HRMS (ESI) calcd. for C₁₇H₁₄O₂NBrNaS (M + Na⁺) 397.9821. Found 397.9814.

IV.4.2. Procedures for the cross-coupling reaction for the synthesis of substrates **32A-F**.

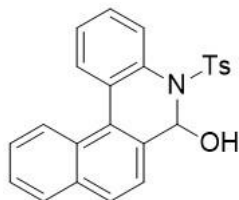
METHOD A: A flame-dried Schlenk tube was charged with Pd₂(dba)₃ (8 mol%), XPhos (10 mol%), bromide (1.0 eq.), boronic acid (1.2 eq.) and anhydrous 1,4-dioxane at room temperature. Finally, 2M aqueous solution of Na₂CO₃ (2.0 eq.) was added, and

reaction mixture was heated to 90 °C for 12-24 h. Then, reaction mixture was cooled to room temperature, brine was added, and the resulting mixture was extracted with EtOAc. The collected organic phases were dried over anhydrous Na₂SO₄, filtered, concentrated, and the residue was purified by column chromatography on silica gel using different *n*-hex/EtOAc mixtures.

METHOD B: A flame-dried Schlenk tube was charged with Pd(PPh₃)₄ (6 mol%), bromide (1.33 eq.), boronic acid (1.0 eq.), DME (10 mM) and EtOH (0.45 mM) at room temperature. Finally, 2M aqueous solution of Na₂CO₃ (2.0 eq.) was added, and reaction mixture was heated to 90 °C for 12-24 h. Then, reaction mixture was cooled to room temperature, brine was added, and the resulting mixture was extracted with EtOAc. The collected organic phases were dried over anhydrous Na₂SO₄, filtered, concentrated, and the residue was purified by column chromatography on silica gel using *n*-hex/EtOAc mixtures.

METHOD C: A flame-dried Schlenk tube was charged with pinacol borane (1.2 eq.), triflate (1.0 eq.), Pd(PPh₃)₄ (10 mol%), Na₂CO₃ 2.0 M aq. (3.0 eq.), and DME (4.5 mM) were heated at reflux for 12 h. After cooling to room temperature, the reaction was quenched by addition of H₂O. The crude mixture was extracted with EtOAc (x3) and the combined organic phases were washed with brine, dried over anhydrous Na₂SO₄, and concentrated *in vacuo*. The residue was purified by column chromatography using *n*-hex/EtOAc mixtures.

Synthesis of 5-Tosyl-5,6-dihydrobenzo[k]phenanthridin-6-ol. **32A**



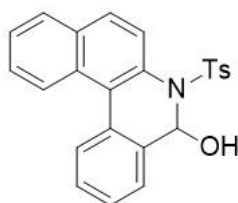
Following the general procedure described for *Method A*, starting from *N*-(2-bromophenyl)-4-methylbenzenesulfonamide **37a** and (2-formylnaphthalen-1-yl)boronic acid **41a**, purification by column chromatography afforded **32A** as a white solid (800 mg, 99%).

$^1\text{H-NMR}$ (400 MHz, CDCl_3) δ 8.08 (d, $J = 8.0$ Hz, 1H), 7.96 (d, $J = 7.9$ Hz, 1H), 7.88 (d, $J = 7.6$ Hz, 1H), 7.80 (d, $J = 7.6$ Hz, 1H), 7.72 (d, $J = 8.3$ Hz, 1H), 7.44 (dt, $J = 13.4, 8.4$ Hz, 5H), 6.84 (d, $J = 7.9$ Hz, 2H), 6.63 (s, 1H), 6.38 (d, $J = 7.9$ Hz, 2H), 3.01 (br s, 1H), 1.64 (s, 3H).

$^{13}\text{C-NMR}$ (100 MHz, CDCl_3) δ 143.2, 134.6, 133.2, 132.8, 132.4, 129.7, 129.0, 128.7, 128.6, 128.6, 128.4, 128.3, 127.1, 126.8, 126.4, 126.3, 126.0, 125.5, 124.5, 80.9, 20.7.

HRMS (ESI) calcd. for $\text{C}_{24}\text{H}_{20}\text{NO}_3\text{S}$ ($\text{M} + \text{H}^+$) 402.1158. Found 402.1156.

Synthesis of 6-Tosyl-5,6-dihydrobenzo[a]phenanthridin-5-ol. **32B**



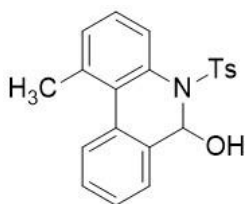
Following the general procedure described for *Method A*, starting from *N*-(1-bromonaphthalen-2-yl)-4-methylbenzenesulfonamide **37b** and (2-formylphenyl)boronic acid **41b**, purification by column chromatography afforded **32B** as a white solid (220 mg, 99%).

$^1\text{H-NMR}$ (400 MHz, CDCl_3) δ 8.45 (t, $J = 4.8$ Hz, 1H), 8.13 (d, $J = 8.9$ Hz, 1H), 7.93 (t, $J = 7.4$ Hz, 2H), 7.65 – 7.32 (m, 6H), 6.98 (d, $J = 8.2$ Hz, 2H), 6.78 – 6.67 (m, 3H), 2.66 (s, 1H), 2.16 (s, 3H).

$^{13}\text{C-NMR}$ (100 MHz, CDCl_3) δ 143.2, 134.8, 133.9, 133.2, 130.6, 129.5, 129.2, 128.9, 128.8, 128.7, 128.4, 128.2, 127.6, 127.3, 126.8, 126.4, 125.9, 125.9, 125.6, 80.3, 21.3.

HRMS (ESI) calcd. for $\text{C}_{24}\text{H}_{20}\text{NO}_3\text{S}$ ($\text{M} + \text{H}^+$) 402.1158. Found 402.1158.

Synthesis of 1-Methyl-5-tosyl-5,6-dihydrophenanthridin-6-ol. 32C



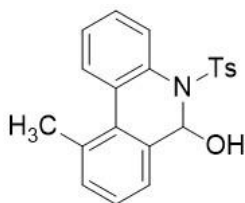
Following the general procedure described for *Method A*, starting from *N*-(2-bromo-3-methylphenyl)-4-methylbenzenesulfonamide **37c**¹⁸⁴ and (2-formylphenyl)boronic acid **41b**, purification by column chromatography afforded **32C** as a white solid (220 mg, 42%).

¹H-NMR (400 MHz, CDCl₃) δ 7.76 (d, *J* = 7.9 Hz, 1H), 7.35 – 7.28 (m, 6H), 7.24 – 7.16 (m, 3H), 6.96 (d, *J* = 7.9 Hz, 2H), 6.74 (d, *J* = 7.9 Hz, 2H), 6.58 (d, *J* = 4.6 Hz, 1H), 2.68 (d, *J* = 4.6 Hz, 1H), 2.56 (s, 3H), 2.18 (s, 3H).

¹³C-NMR (100 MHz, CDCl₃) δ 143.0, 135.0, 134.4, 134.2, 132.9, 130.7, 129.7, 128.6, 128.3, 128.0, 127.9, 127.6, 127.2, 127.1, 126.6, 126.5, 126.2, 80.3, 23.0, 21.3.

HRMS (ESI) calcd. for C₂₄H₂₀NO₃S (M + H⁺) 366.1158. Found 366.1158.

Synthesis of 10-Methyl-5-tosyl-5,6-dihydrophenanthridin-6-ol. 32D



Following the general procedure described for *Method A*, starting from *N*-(2-bromo-3-methylphenyl)-4-methylbenzenesulfonamide **37a** and (2-formylphenyl)boronic acid **41c**, purification by column chromatography afforded **32D** as a white solid (220 mg, 66%).

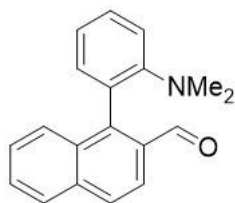
¹⁸⁴ Krolski, M. E.; Renaldo, A. F.; Rudisill, D. E.; Stille, J. K. *J. Org. Chem.* **1988**, *53*, 1170.

$^1\text{H-NMR}$ (400 MHz, CDCl_3) δ 7.87 (d, $J = 7.9$ Hz, 1H), 7.62 (d, $J = 7.9$ Hz, 1H), 7.41 (t, $J = 7.7$ Hz, 1H), 7.33 (t, $J = 7.6$ Hz, 1H), 7.18 (d, $J = 7.4$ Hz, 1H), 7.13 (t, $J = 7.5$ Hz, 1H), 7.05 (d, $J = 7.4$ Hz, 1H), 6.91 (d, $J = 7.9$ Hz, 2H), 6.72 (d, $J = 7.9$ Hz, 2H), 6.51 (d, $J = 4.5$ Hz, 1H), 2.68 (d, $J = 5.3$ Hz, 1H), 2.24 (s, 3H), 2.18 (s, 3H).

$^{13}\text{C-NMR}$ (100 MHz, CDCl_3) δ 143.0, 134.8, 134.5, 133.3, 132.2, 132.5, 129.5, 129.2, 128.9, 128.3, 128.2, 128.0, 127.5, 126.5, 125.4, 80.9, 22.3, 21.3.

HRMS (ESI) calcd. for $\text{C}_{24}\text{H}_{20}\text{NO}_3\text{S}$ ($\text{M} + \text{H}^+$) 366.1158. Found 366.1158.

Synthesis of 1-(2-(Dimethylamino)phenyl)-2-naphthaldehyde. **32E**



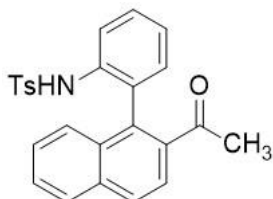
Following the general procedure described for *Method B*, starting from 2-bromo-*N,N*-dimethylaniline and **39**, purification by column chromatography afforded **32E** as a yellowish oil (144 mg, 69%).

$^1\text{H-NMR}$ (400 MHz, CDCl_3) δ 9.73 (br s, 1H), 8.09 (d, $J = 8.7$ Hz, 1H), 7.95 (d, $J = 8.4$ Hz, 1H), 7.91 (d, $J = 8.8$ Hz, 1H), 7.64 (t, $J = 7.5$ Hz, 1H), 7.55 – 7.42 (m, 2H), 7.27 (d, $J = 8.3$ Hz, 1H), 7.16 (t, $J = 8.5$ Hz, 1H), 2.40 (s, 3H).

$^{13}\text{C-NMR}$ (100 MHz, CDCl_3) δ 136.8, 133.2, 132.1, 130.1, 129.7, 128.4, 128.4, 128.1, 127.1, 127.1, 126.8, 122.5, 121.4, 117.9, 42.8.

HRMS (ESI) calcd. for $\text{C}_{19}\text{H}_{18}\text{NO}_3\text{S}$ ($\text{M} + \text{H}^+$) 276.1383. Found 276.1385.

Synthesis of N-(2-(2-Acetylnaphthalen-1-yl)phenyl)-4-methylbenzenesulfonamide. **32F**



Following the general procedure described for *Method C*, starting from pinacol borane **47** and triflate **48**, purification by column chromatography afforded **32F** as a yellowish amorphous solid (136 mg, 99%).

$^1\text{H-NMR}$ (400 MHz, CDCl_3) δ 7.97 (d, $J = 8.6$ Hz, 1H), 7.89 (d, $J = 8.3$ Hz, 1H), 7.76 (t, $J = 9.2$ Hz, 2H), 7.57 – 7.50 (m, 1H), 7.49 – 7.36 (m, 3H), 7.25 – 7.10 (m, 2H), 7.04 (d, $J = 7.8$ Hz, 2H), 6.97 (t, $J = 9.5$ Hz, 1H), 6.50 (s, 1H), 2.35 (s, 3H), 2.09 (s, 3H).

$^{13}\text{C-NMR}$ (100 MHz, CDCl_3) δ 202.8, 143.7, 138.0, 136.6, 135.6, 134.5, 132.9, 132.0, 131.2, 129.6, 129.5, 129.4, 128.9, 128.2, 127.6, 127.5, 127.2, 126.7, 124.4, 124.3, 119.9, 30.1, 21.6.

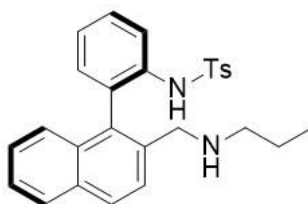
HRMS (ESI) calcd. for $\text{C}_{25}\text{H}_{22}\text{NO}_3\text{S}$ ($\text{M} + \text{H}^+$) 416.1315. Found 416.1318.

IV.4.3. Synthesis of axially chiral diamines via Asymmetric Transfer Hydrogenation

To a flame-dried Schlenk tube with 4Å molecular sieves, aldehyde **32A-E** (0.1 mmol), anhydrous 1,4-dioxane (1.0 mL), and amine **43a-i** (1.1 eq.) were sequentially added at room temperature and reaction mixture was stirred for 12-36h. Then, $[\text{RuCl}(\textit{p}\text{-cymene})(\textit{S,S}\text{-Ts-DPEN})]$ (5 mol%) followed by 1,4-dioxane (0.5 mL) and 5:2 $\text{HCO}_2\text{H}/\text{Et}_3\text{N}$ (40 μL) azeotropic mixture were added. Reaction mixture was stirred for 18-48h at room temperature. Then reaction was filtered through a short pad of celite, and solvent was removed under reduced pressure. The residue was purified by column chromatography on silica gel with *n*-hex/EtOAc or $\text{CH}_2\text{Cl}_2/\text{EtOAc}$ mixtures affording the resulting diamines.

Note. Racemic diamines were obtained by condensation of amine **43a-i** (1.0 eq.) with aldehyde **32A-E** (1.0 eq.) in toluene with 4Å MS and 5 mol% of *p*-toluenesulfonic acid for 2h. Then reaction mixture was extracted with EtOAc, dried over Na₂SO₄, filtered and solvent removed in vacuo. Reaction crude was dissolved in MeOH, and NaBH₄ (2.0 eq.) was added. Quenching with water, and EtOAc extraction afforded the racemic mixture of amines that were separated from reaction crude by preparative TLC prior to HPLC analysis.

Synthesis of (R)-4-Methyl-N-(2-(2-((propylamino)methyl)naphthalen-1-yl)phenyl)benzenesulfonamide. 34Aa



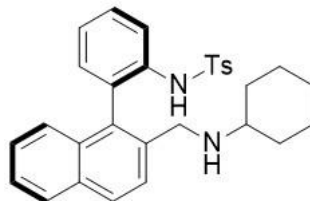
Following the general procedure from **32A** and *n*-propylamine **43a**, after 72 h and further purification by flash chromatography (3:1 *n*-hexane/EtOAc) afforded **34Aa** (40.0 mg, 90%) as a light-yellow solid. The pure product was crystallized by slow diffusion of *n*-pentane into a solution of the product in DCM to give **32Aa** as pale yellow prisms suitable for X-Ray analysis.

$[\alpha]_{\text{D}}^{20} +221.6$ (*c* 0.46, CHCl₃) for 98% *ee*.

¹H-NMR (400 MHz, CDCl₃) δ 7.88 (d, *J* = 8.1 Hz, 1H), 7.82 (d, *J* = 8.4 Hz, 1H), 7.75 (d, *J* = 8.2 Hz, 1H), 7.45 (d, *J* = 7.8 Hz, 1H), 7.41 (d, *J* = 8.5 Hz, 1H), 7.34 (t, *J* = 7.5 Hz, 1H), 7.22 (t, *J* = 7.5 Hz, 1H), 7.00 (d, *J* = 8.2 Hz, 1H), 6.96 (d, *J* = 7.4 Hz, 1H), 6.93 (d, *J* = 7.9 Hz, 2H), 6.65 (d, *J* = 8.6 Hz, 1H), 6.44 (d, *J* = 7.9 Hz, 2H), 3.76 (d, *J* = 11.4 Hz, 1H), 3.46 (d, *J* = 11.4 Hz, 1H), 2.74 (td, *J* = 10.1, 9.0, 6.1 Hz, 1H), 2.63 (td, *J* = 11.1, 10.2, 6.1 Hz, 1H), 2.06 (s, 3H), 1.68 (dt, *J* = 21.4, 13.9, 7.0 Hz, 2H), 0.97 (t, *J* = 7.4 Hz, 3H).

¹³C-NMR (100 MHz, CDCl₃) δ 141.6, 137.8, 136.5, 135.3, 134.0, 133.9, 133.3, 132.9, 132.2, 128.8, 128.5, 127.6, 127.4, 126.8, 126.7, 126.1, 126.0, 125.2, 125.1, 52.7, 51.6, 22.4, 21.4, 11.8.

Synthesis of (*R*)-*N*-(2-(2-((Cyclohexylamino)methyl)naphthalen-1-yl)phenyl)-4-methylbenzenesulfonamide. **34Ac**



Following the general procedure from **32A** and cyclohexylamine **43c**, after 72 h and further purification by flash chromatography (3:1 *n*-hexane/EtOAc) afforded **34Ac** (39.3 mg, 81%) as a light-yellow amorphous solid.

$[\alpha]_D^{20} +166.4$ (c 0.37, CHCl₃) for 99% *ee*.

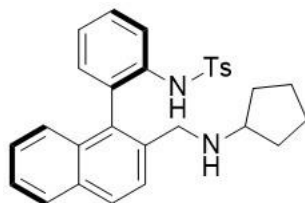
¹H-NMR (400 MHz, CDCl₃) δ 7.92 (dd, *J* = 8.1, 1.3 Hz, 1H), 7.86 (d, *J* = 8.3 Hz, 1H), 7.77 (d, *J* = 8.1 Hz, 1H), 7.47 (ddd, *J* = 8.2, 7.4, 1.6 Hz, 1H), 7.43 (d, *J* = 8.4 Hz, 1H), 7.37 (ddd, *J* = 8.1, 6.8, 1.2 Hz, 1H), 7.25 (td, *J* = 7.5, 1.3 Hz, 1H), 7.04 (dd, *J* = 7.6, 1.6 Hz, 1H), 6.99 (ddd, *J* = 8.3, 6.8, 1.3 Hz, 1H), 6.94 (d, *J* = 8.3 Hz, 2H), 6.69 (dd, *J* = 8.5, 1.0 Hz, 1H), 6.45 (d, *J* = 8.0 Hz, 2H), 3.81 (d, *J* = 11.0 Hz, 1H), 3.50 (d, *J* = 11.0 Hz, 1H), 2.58 (dt, *J* = 9.1, 5.6 Hz, 1H), 2.09 (s, 3H), 2.06 – 1.93 (m, 1H), 1.87 – 1.74 (m, 2H), 1.70 – 1.61 (m, 1H), 1.44 – 1.15 (m, 6H).

¹³C-NMR (100 MHz, CDCl₃) δ 141.6, 137.9, 136.4, 135.4, 134.3, 134.0, 133.3, 132.8, 132.2, 129.1, 128.8, 128.7, 128.5, 128.3, 127.9, 127.4, 126.8, 126.7, 126.1, 126.0, 125.3, 125.1, 57.1, 49.7, 33.2, 31.9, 25.9, 25.1, 25.1, 21.4.

HRMS (ESI) calcd. for C₃₀H₃₃O₂N₂S (M + H⁺) 485.2257. Found 485.2248.

HPLC (IA column, 85:15 *n*-Hex/*i*-PrOH, 30 °C, 1.0 mL/min): t_R 8.13 min (minor) and 16.02 min (major).

Synthesis of (*R*)-*N*-(2-(2-((Cyclopentylamino)methyl)naphthalen-1-yl)phenyl)-4-methylbenzenesulfonamide. **34Ae**



Following the general procedure from **32A** and cyclopentylamine **43d**, after 72 h and further purification by flash chromatography (3:1 *n*-hexane/EtOAc) afforded **34Ad** (36.2 mg, 77%) as a light-yellow amorphous solid.

$[\alpha]_D^{20} +179.4$ (c 0.61, CHCl₃) for 99% *ee*.

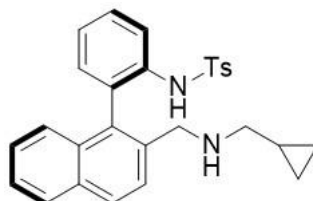
¹H-NMR (400 MHz, CDCl₃) δ 7.86 (dd, *J* = 8.2, 1.2 Hz, 1H), 7.83 (d, *J* = 8.3 Hz, 1H), 7.75 (d, *J* = 8.1 Hz, 1H), 7.45 (d, *J* = 8.4 Hz, 1H), 7.43 (ddd, *J* = 8.2, 7.4, 1.6 Hz, 1H), 7.35 (ddd, *J* = 8.0, 6.8, 1.2 Hz, 1H), 7.22 (td, *J* = 7.5, 1.3 Hz, 1H), 7.03 (dd, *J* = 7.6, 1.6 Hz, 1H), 7.01 – 6.96 (m, 1H), 6.95 (d, *J* = 8.2 Hz, 2H), 6.68 (d, *J* = 8.5 Hz, 1H), 6.47 (d, *J* = 7.9 Hz, 2H), 3.72 (d, *J* = 11.4 Hz, 1H), 3.47 (d, *J* = 11.3 Hz, 1H), 3.16 (p, *J* = 6.7 Hz, 1H), 2.08 (s, 3H), 1.96 – 1.73 (m, 4H), 1.61 – 1.47 (m, 3H), 1.50 – 1.38 (m, 1H).

¹³C-NMR (100 MHz, CDCl₃) δ 141.7, 137.9, 136.5, 135.5, 133.7, 133.6, 133.2, 132.9, 132.1, 128.9, 128.7, 128.6, 127.4, 126.9, 126.7, 126.2, 126.0, 125.2, 125.2, 60.0, 51.5, 32.9, 31.4, 24.1, 24.0, 21.4.

HRMS (ESI) calcd. for C₂₉H₃₁O₂N₂S (M + H⁺) 471.2101. Found 471.2095.

HPLC (IA column, 85:15 *n*-Hex/*i*-PrOH, 30 °C, 1.0 mL/min): *t*_R 7.82 min (minor) and 12.55 min (major).

Synthesis of (*R*)-*N*-(2-(2-(((Cyclopropylmethyl)amino)methyl)naphthalen-1-yl)phenyl)-4-methylbenzenesulfonamide. **34Ae**



Following the general procedure from **32A** and cyclopropanemethylamine **43e**, after 72 h and further purification by flash chromatography (3:1 *n*-hexane/EtOAc) afforded **34Ae** (33.8 mg, 74%) as a light-yellow amorphous solid.

$[\alpha]_D^{20} +197.6$ (c 0.38, CHCl₃) for 92% *ee*.

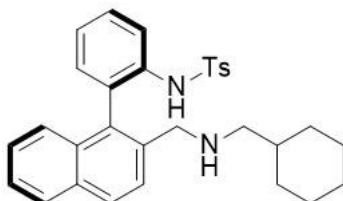
¹H-NMR (400 MHz, CDCl₃) δ 7.87 (d, *J* = 8.1 Hz, 1H), 7.83 (d, *J* = 8.3 Hz, 1H), 7.76 (d, *J* = 8.1 Hz, 1H), 7.44 (d, *J* = 8.8 Hz, 1H), 7.41 (t, *J* = 8.8 Hz, 1H), 7.35 (t, *J* = 7.5 Hz, 1H), 7.21 (t, *J* = 7.4 Hz, 1H), 7.00 (t, *J* = 7.5 Hz, 2H), 6.96 (d, *J* = 7.9 Hz, 2H), 6.66 (d, *J* = 8.6 Hz, 1H), 6.47 (d, *J* = 7.9 Hz, 2H), 3.78 (d, *J* = 11.5 Hz, 1H), 3.51 (d, *J* = 11.5 Hz, 1H), 2.62 (dd, *J* = 12.2, 6.7 Hz, 1H), 2.54 (dd, *J* = 12.2, 7.3 Hz, 1H), 2.08 (s, 3H), 1.22 – 1.11 (m, 1H), 0.53 (m, 2H), 0.23 – 0.12 (m, 2H). ¹

³C-NMR (100 MHz, CDCl₃) δ 141.7, 137.8, 136.5, 135.4, 133.8, 133.6, 133.3, 132.9, 132.2, 128.8, 128.6, 127.4, 127.3, 126.9, 126.6, 126.2, 126.0, 125.2, 125.2, 54.5, 52.3, 21.4, 10.2, 3.9, 3.5.

HRMS (ESI) calcd. for C₂₈H₂₉O₂N₂S (M + H⁺) 457.1944. Found 457.1941.

HPLC (IA column, 85:15 *n*-Hex/*i*-PrOH, 30 °C, 1.0 mL/min): *t*_R 8.26 min (minor) and 13.18 min (major).

Synthesis of (*R*)-*N*-(2-(2-(((Cyclohexylmethyl)amino)methyl)naphthalen-1-yl)phenyl)-4-methylbenzenesulfonamide. 34Af



Following the general procedure from **32A** and cyclohexanemethylamine **43f**, after 72 h and further purification by flash chromatography (3:1 *n*-hexane/EtOAc) afforded **34Af** (41.9 mg, 84%) as a light-yellow amorphous solid.

$[\alpha]_D^{20} +177.7$ (c 0.35, CHCl₃) for 98% *ee*.

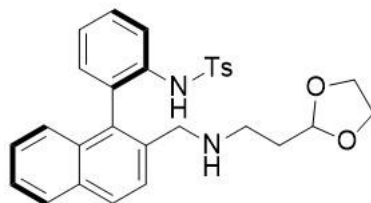
¹H-NMR (400 MHz, CDCl₃) δ 7.87 (d, *J* = 8.2 Hz, 1H), 7.83 (d, *J* = 8.4 Hz, 1H), 7.75 (d, *J* = 8.2 Hz, 1H), 7.44 (t, *J* = 7.6 Hz, 1H), 7.41 (d, *J* = 8.0 Hz, 1H), 7.35 (t, *J* = 7.5 Hz, 1H), 7.22 (t, *J* = 7.5 Hz, 1H), 7.01 (d, *J* = 8.0 Hz, 1H), 9.98 (t, *J* = Hz, 1H), 6.95 (t, *J* = 7.8 Hz, 2H), 6.67 (d, *J* = 8.6 Hz, 1H), 6.47 (d, *J* = 7.8 Hz, 2H), 3.72 (d, *J* = 11.5 Hz, 1H), 3.41 (d, *J* = 11.5 Hz, 1H), 2.63 – 2.48 (m, 2H), 2.08 (s, 3H), 1.90 – 1.60 (m, 6H), 1.27 (m, 3H), 0.96 (m, 2H).

¹³C-NMR (100 MHz, CDCl₃) δ 141.7, 137.8, 136.3, 135.6, 134.3, 133.8, 133.3, 132.9, 132.2, 128.8, 128.6, 127.4, 127.4, 126.8, 126.7, 126.2, 126.0, 125.3, 125.1, 56.4, 52.9, 36.8, 31.4, 31.3, 26.6, 25.9, 21.4.

HRMS (ESI) calcd. for C₃₁H₃₅O₂N₂S (M + H⁺) 499.2414. Found 499.2407.

HPLC (IA column, 85:15 *n*-Hex/*i*-PrOH, 30 °C, 1.0 mL/min): *t*_R 7.17 min (minor) and 8.96 min (major).

Synthesis of (*R*)-*N*-(2-(2-(((2-(1,3-Dioxolan-2-yl)ethyl)amino)methyl)naphthalen-1-yl)phenyl)-4-methylbenzenesulfonamide. **34Ag**



Following the general procedure from **32A** and 2-(1,3-dioxolan-2-yl)ethan-1-amine **43g**, after 72 h and further purification by flash chromatography (3:1 *n*-hexane/EtOAc) afforded **34Ag** (37.2 mg, 74%) as a light-yellow amorphous solid.

$[\alpha]_D^{20} +182.1$ (c 0.39, CHCl₃) for 96% *ee*.

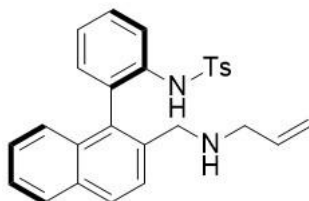
¹H-NMR (400 MHz, Chloroform-*d*) δ 7.85 (d, *J* = 9.1 Hz, 1H), 7.83 (d, *J* = 8.7 Hz, 1H), 7.74 (d, *J* = 8.1 Hz, 1H), 7.48 – 7.39 (m, 1H), 7.35 (ddd, *J* = 8.1, 6.8, 1.2 Hz, 1H), 7.21 (td, *J* = 7.5, 1.3 Hz, 1H), 7.02 – 6.97 (m, 2H), 6.95 (d, *J* = 8.1 Hz, 2H), 6.67 (d, *J* = 8.6 Hz, 1H), 6.46 (d, *J* = 8.1 Hz, 1H), 5.02 (t, *J* = 4.4 Hz, 1H), 4.07 – 3.97 (m, 2H), 3.96 – 3.83 (m, 2H), 3.77 (d, *J* = 11.5 Hz, 1H), 3.45 (d, *J* = 11.5 Hz, 1H), 2.92 (dt, *J* = 12.8, 6.5 Hz, 1H), 2.83 (dt, *J* = 12.3, 6.4 Hz, 1H), 2.07 (s, 3H), 2.06 (td, *J* = 6.7, 4.4 Hz, 2H).

¹³C-NMR (100 MHz, CDCl₃) δ 141.7, 137.8, 136.4, 135.3, 133.8, 133.6, 133.3, 132.9, 132.2, 128.8, 128.6, 128.6, 127.4, 127.4, 126.8, 126.8, 126.1, 126.0, 125.2, 125.2, 103.8, 103.8, 64.9, 64.8, 52.5, 44.3, 32.2, 21.4.

HRMS (ESI) calcd. for C₂₉H₃₁O₄N₂S (M + H⁺) 503.1999. Found 503.1995.

HPLC (IA column, 85:15 *n*-Hex/*i*-PrOH, 30 °C, 1.0 mL/min): t_R 13.25 min (minor) and 16.68 min (major).

Synthesis of (*R*)-*N*-(2-(2-((Allylamino)methyl)naphthalen-1-yl)phenyl)-4-methylbenzenesulfonamide. **34Ah**



Following the general procedure from **32A** and freshly distilled allylamine **43h**, after 72 h and further purification by flash chromatography (3:1 *n*-hexane/EtOAc) afforded **34Ah** (38.1 mg, 86%) as a light-yellow amorphous solid.

$[\alpha]_D^{20} +206.7$ (c 0.33, CHCl₃) for 97% *ee*.

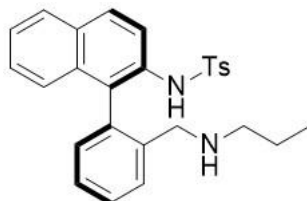
¹H-NMR (400 MHz, CDCl₃): δ 7.90 (d, *J* = 8.1 Hz, 1H), 7.87 (d, *J* = 7.3 Hz, 1H), 7.78 (d, *J* = 7.7 Hz, 1H), 7.47 (t, *J* = 8.1 Hz, 1H), 7.45 (d, *J* = 7.3 Hz, 1H), 7.38 (t, *J* = 7.7 Hz, 1H), 7.26 (t, *J* = 7.9 Hz, 1H), 7.04 (d, *J* = 7.9 Hz, 1H), 7.01 (d, *J* = 8.5 Hz, 1H), 6.99 (d, *J* = 8.1 Hz, 2H), 6.68 (d, *J* = 8.5 Hz, 1H), 6.51 (d, *J* = 7.7 Hz, 1H), 6.07 (tdd, *J* = 17.0, 7.5, 4.0 Hz, 0H), 5.28 (d, *J* = 17.1 Hz, 1H), 5.20 (d, *J* = 10.2 Hz, 1H), 3.80 (d, *J* = 11.4 Hz, 1H), 3.48 (d, *J* = 11.6 Hz, 1H), 3.44 – 3.32 (m, 1H), 2.12 (s, 1H).

¹³C-NMR (100 MHz, CDCl₃) δ 141.9, 137.6, 136.1, 135.3, 135.2, 134.1, 133.5, 133.3, 132.9, 132.2, 128.8, 128.6, 127.4, 127.2, 126.8, 126.7, 126.2, 126.0, 125.3, 125.2, 117.6, 52.1, 52.0, 21.4.

HRMS (ESI) calcd. for C₂₇H₂₇O₂N₂S (M + H⁺) 443.1788. Found 443.1780.

HPLC (IA column, 85:15 *n*-Hex/*i*-PrOH, 30 °C, 1.0 mL/min): *t*_R 8.10 min (minor) and 11.90 min (major).

Synthesis of (R)-4-Methyl-N-(1-(2-((propylamino)methyl)phenyl)naphthalen-2-yl)benzenesulfonamide. 34Ba



Following the general procedure from **32B** and *n*-propylamine **43a**, after 72 h and further purification by flash chromatography (3:1 *n*-hexane/EtOAc) afforded **34Ba** (35.1 mg, 79%) as a light-yellow amorphous solid.

$[\alpha]_D^{20} -86.9$ (c 0.39, CHCl₃) for 98% *ee*.

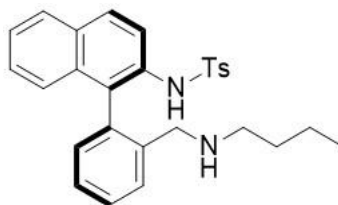
¹H-NMR (400 MHz, CDCl₃) δ 7.95 (d, *J* = 8.8 Hz, 1H), 7.87 (d, *J* = 8.9 Hz, 1H), 7.84 (d, *J* = 8.1 Hz, 1H), 7.39 (t, *J* = 7.5 Hz, 1H), 7.35 – 7.29 (m, 2H), 7.25 – 7.19 (m, 3H), 7.03 – 6.91 (m, 4H), 6.23 (d, *J* = 7.6 Hz, 1H), 3.57 (d, *J* = 11.6 Hz, 1H), 3.22 (d, *J* = 11.6 Hz, 1H), 2.63 (ddd, *J* = 11.5, 8.4, 6.3 Hz, 1H), 2.49 (ddd, *J* = 11.5, 8.7, 6.5 Hz, 1H), 2.34 (s, 3H), 1.61 (dp, *J* = 14.1, 6.9 Hz, 2H), 0.93 (t, *J* = 7.4 Hz, 3H).

¹³C-NMR (100 MHz, CDCl₃) δ 142.1, 138.2, 137.7, 136.0, 133.5, 133.1, 132.5, 131.9, 131.8, 129.4, 129.2, 128.7, 127.9, 127.8, 127.1, 126.7, 126.3, 126.1, 125.9, 125.3, 52.3, 51.2, 22.3, 21.5, 11.8.

HRMS (ESI) calcd. for C₂₇H₂₉O₂N₂S (M + H⁺) 445.1944. Found 445.1938.

HPLC (IA column, 85:15 *n*-Hex/*i*-PrOH, 30 °C, 1.0 mL/min): *t*_R 8.62 min (minor) and 12.76 min (major).

Synthesis of (R)-N-(1-(2-((butylamino)methyl)phenyl)naphthalen-2-yl)-4-methylbenzenesulfonamide. 34Bb



Following the general procedure from **32B** and *n*-butylamine **43b**, after 72 h and further purification by flash chromatography (3:1 *n*-hexane/EtOAc) afforded **34Bb** (37.9 mg, 98%) as a light-yellow amorphous solid.

$[\alpha]_D^{20} -62.5$ (c 0.38, CHCl₃) for 98% *ee*.

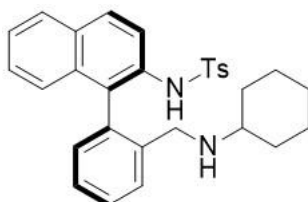
¹H-NMR (400 MHz, CDCl₃) δ 7.92 (d, *J* = 8.8 Hz, 1H), 7.86 (d, *J* = 9.3 Hz, 1H), 7.84 (d, *J* = 7.4 Hz, 1H), 7.43 (d, *J* = 7.2 Hz, 1H), 7.39 (ddd, *J* = 8.3, 6.9, 1.3 Hz, 1H), 7.35 (td, *J* = 7.5, 1.4 Hz, 1H), 7.29 – 7.21 (m, 3H), 7.03 – 6.96 (m, 4H), 6.30 (dd, *J* = 7.7, 1.3 Hz, 1H), 3.58 (d, *J* = 11.8 Hz, 1H), 3.24 (d, *J* = 11.8 Hz, 1H), 2.65 (ddd, *J* = 11.6, 8.5, 6.6 Hz, 1H), 2.50 (ddd, *J* = 11.7, 8.6, 6.5 Hz, 1H), 2.35 (s, 3H), 1.63 – 1.47 (m, 2H), 1.31 (dt, *J* = 14.9, 7.5 Hz, 3H), 0.90 (t, *J* = 7.3 Hz, 3H).

¹³C-NMR (100 MHz, CDCl₃) δ 142.3, 138.2, 136.9, 136.1, 133.4, 133.3, 131.8, 131.8, 129.6, 129.3, 128.8, 128.1, 127.9, 127.4, 126.7, 126.2, 126.2, 125.3, 51.8, 48.8, 30.7, 21.5, 20.4, 13.9.

HRMS (ESI) calcd. for C₂₇H₃₁O₂N₂S (M + H⁺) 459.2101. Found 459.2093.

HPLC (IA column, 85:15 *n*-Hex/*i*-PrOH, 30 °C, 1.0 mL/min): *t*_R 8.52 min (minor) and 12.51 min (major).

Synthesis of (*R*)-*N*-(1-(2-((Cyclohexylamino)methyl)phenyl)naphthalen-2-yl)-4-methylbenzenesulfonamide. **34Bc**



Following the general procedure from **32B** and cyclohexylamine **43c**, after 72 h and further purification by flash chromatography (3:1 *n*-hexane/EtOAc) afforded **34Bc** (44.1 mg, 91%) as a light-yellow amorphous solid.

$[\alpha]_D^{20} -59.0$ (c 0.69, CHCl₃) for 99% *ee*.

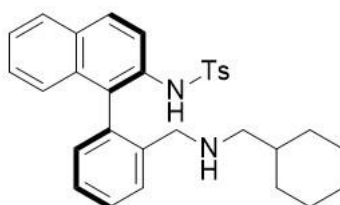
$^1\text{H-NMR}$ (400 MHz, CDCl_3) δ 7.95 (d, $J = 8.8$ Hz, 1H), 7.87 (d, $J = 9.0$ Hz, 1H), 7.84 (d, $J = 8.1$ Hz, 1H), 7.45 – 7.28 (m, 3H), 7.25 (d, $J = 6.8$ Hz, 1H), 7.22 (d, $J = 7.9$ Hz, 2H), 7.01 (d, $J = 8.5$ Hz, 1H), 6.98 (d, $J = 7.9$ Hz, 2H), 6.94 (d, $J = 7.3$ Hz, 1H), 6.24 (d, $J = 7.6$ Hz, 1H), 3.60 (d, $J = 11.2$ Hz, 1H), 3.22 (d, $J = 11.2$ Hz, 1H), 2.40 (t, $J = 10.5$ Hz, 1H), 2.34 (s, 3H), 1.92 – 1.80 (m, 2H), 1.78 – 1.64 (m, 2H), 1.59 (s, 1H), 1.25 – 1.05 (m, 5H).

$^{13}\text{C-NMR}$ (100 MHz, CDCl_3) δ 142.1, 138.3, 137.7, 136.1, 133.4, 133.2, 132.3, 131.9, 131.7, 129.4, 129.2, 128.7, 128.0, 127.9, 127.2, 126.7, 126.3, 126.1, 125.9, 125.3, 56.9, 49.1, 32.9, 31.6, 25.8, 25.0, 25.0, 21.5.

HRMS (ESI) calcd. for $\text{C}_{30}\text{H}_{33}\text{O}_2\text{N}_2\text{S}$ ($\text{M} + \text{H}^+$) 485.2257. Found 485.2251.

HPLC (IA column, 85:15 *n*-Hex/*i*-PrOH, 30 °C, 1.0 mL/min): t_{R} 7.85 min (minor) and 15.43 min (major).

Synthesis of (*R*)-*N*-(1-(2-(((Cyclohexylmethyl)amino)methyl)phenyl)naphthalen-2-yl)-4-methylbenzenesulfonamide. **34Bf**



Following the general procedure from **32B** and cyclohexanemethylamine **43f**, after 72 h and further purification by flash chromatography (3:1 *n*-hexane/EtOAc) afforded **34Bf** (39.9 mg, 90%) as a light-yellow amorphous solid.

$[\alpha]_{\text{D}}^{20} -54.1$ (c 0.38, CHCl_3) for 98% *ee*.

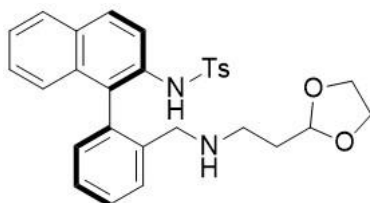
$^1\text{H-NMR}$ (400 MHz, CDCl_3) δ 7.96 (d, $J = 8.9$ Hz, 1H), 7.90 (d, $J = 9.0$ Hz, 1H), 7.87 (d, $J = 8.0$ Hz, 1H), 7.45 – 7.34 (m, 3H), 7.32 – 7.27 (m, 2H), 7.01 (ddd, $J = 14.8, 9.0, 5.9$ Hz, 4H), 6.29 (d, $J = 7.6$ Hz, 1H), 3.56 (d, $J = 11.6$ Hz, 1H), 3.20 (d, $J = 11.6$ Hz, 1H), 2.48 (dd, $J = 11.9, 6.7$ Hz, 1H), 2.39 (dd, $J = 11.9, 6.7$ Hz, 1H), 2.38 (s, 3H), 1.82 – 1.56 (m, 6H), 1.39 – 1.20 (m, 3H), 1.02 – 0.84 (m, 2H).

^{13}C -NMR (100 MHz, CDCl_3) δ 142.2, 138.1, 137.7, 135.9, 133.4, 133.0, 132.3, 131.9, 131.7, 129.5, 129.3, 128.7, 128.0, 127.9, 127.2, 126.8, 126.3, 126.2, 125.6, 125.4, 56.0, 52.3, 36.7, 31.4, 31.2, 26.6, 25.9, 21.5.

HRMS (ESI) calcd. for $\text{C}_{31}\text{H}_{35}\text{O}_2\text{N}_2\text{S}$ ($\text{M} + \text{H}^+$) 499.2414. Found 499.2408.

HPLC (IA column, 85:15 *n*-Hex/*i*-PrOH, 30 °C, 1.0 mL/min): t_{R} 7.91 min (minor) and 8.75 min (major).

Synthesis of (R)-N-(1-(2-(((2-(1,3-Dioxolan-2-yl)ethyl)amino)methyl)phenyl)naphthalen-2-yl)-4-methylbenzenesulfonamide. 34Bg



Following the general procedure from **32B** and 2-(1,3-dioxolan-2-yl)ethan-1-amine **43g**, after 72 h and further purification by flash chromatography (3:1 *n*-hexane/EtOAc) afforded **34Bg** (28.6 mg, 57%) as a light-yellow amorphous solid.

$[\alpha]_{\text{D}}^{20} -44.5$ (c 0.49, CHCl_3) for 98% *ee*.

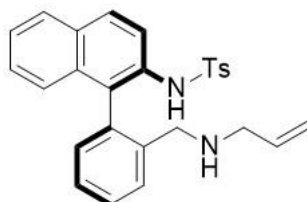
^1H -NMR (400 MHz, CDCl_3) δ 7.93 (d, $J = 8.8$ Hz, 1H), 7.86 (d, $J = 9.3$ Hz, 1H), 7.83 (d, $J = 7.8$ Hz, 1H), 7.43 – 7.34 (m, 2H), 7.33 (t, $J = 7.3$ Hz, 1H), 7.23 (d, $J = 7.6$ Hz, 3H), 6.98 (d, $J = 8.3$ Hz, 3H), 6.94 (d, $J = 7.4$ Hz, 1H), 6.25 (d, $J = 7.6$ Hz, 1H), 4.97 (t, $J = 4.5$ Hz, 1H), 4.05 – 3.92 (m, 2H), 3.91 – 3.80 (m, 2H), 3.59 (d, $J = 11.7$ Hz, 1H), 3.22 (d, $J = 11.6$ Hz, 1H), 2.81 (dt, $J = 12.5, 6.5$ Hz, 1H), 2.68 (dt, $J = 12.3, 6.5$ Hz, 1H), 2.34 (s, 3H), 2.04 – 1.95 (m, 2H).

^{13}C -NMR (100 MHz, CDCl_3) δ 142.3, 138.3, 137.4, 136.0, 133.5, 133.1, 132.2, 132.0, 131.9, 129.6, 129.3, 128.9, 128.0, 127.9, 127.3, 126.8, 126.4, 126.2, 125.8, 125.4, 103.8, 65.0, 64.9, 52.1, 44.1, 32.3, 21.6.

HRMS (ESI) calcd. for $\text{C}_{29}\text{H}_{31}\text{O}_4\text{N}_2\text{S}$ ($\text{M} + \text{H}^+$) 503.1999. Found 503.1991.

HPLC (IA column, 85:15 *n*-Hex/*i*-PrOH, 30 °C, 1.0 mL/min): t_R 14.32 min (minor) and 16.18 min (major).

Synthesis of (*R*)-*N*-(1-(2-((Allylamino)methyl)phenyl)naphthalen-2-yl)-4-methylbenzenesulfonamide. 34Bh



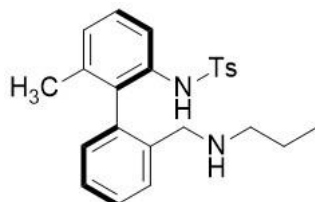
Following the general procedure from **32B** and freshly distilled allylamine **43h**, after 72 h and further purification by flash chromatography (3:1 *n*-hexane/EtOAc) afforded **34Bh** (10.2 mg, 29%) as a light-yellow amorphous solid.

$[\alpha]_D^{20}$ -48.2 (c 0.3, CHCl_3) for 99% *ee*.

HRMS (ESI) calcd. for $\text{C}_{27}\text{H}_{27}\text{O}_2\text{N}_2\text{S}$ ($\text{M} + \text{H}^+$) 443.1788. Found 443.1781.

HPLC (IA column, 85:15 *n*-Hex/*i*-PrOH, 30 °C, 1.0 mL/min): t_R 8.26 min (minor) and 10.06 min (major).

Synthesis of (*R*)-4-Methyl-*N*-(6-methyl-2'-((propylamino)methyl)-[1,1'-biphenyl]-2-yl)benzenesulfonamide. 34Ca



Following the general procedure from **32C** and propylamine **43a**, after 72 h and further purification by flash chromatography (3:1 *n*-hexane/EtOAc) afforded **34Ca** (24.9 mg, 61%) as a light-yellow amorphous solid.

$[\alpha]_{20}^D$ -7.2 (c 0.14, CHCl_3) for 96% *ee*.

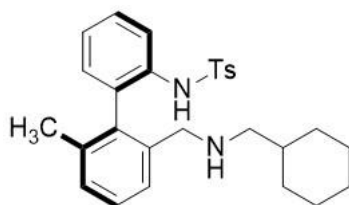
$^1\text{H-NMR}$ (400 MHz, CDCl_3) δ 7.60 – 7.53 (m, 1H), 7.38 – 7.22 (m, 5H), 7.08 (t, $J = 7.5$ Hz, 3H), 6.98 (td, $J = 7.5, 1.4$ Hz, 1H), 6.27 (dd, $J = 7.6, 1.3$ Hz, 1H), 3.59 (d, $J = 11.7$ Hz, 1H), 3.27 (d, $J = 11.7$ Hz, 1H), 2.67 (ddd, $J = 11.5, 8.5, 6.4$ Hz, 1H), 2.52 (ddd, $J = 11.5, 8.6, 6.4$ Hz, 1H), 2.41 (s, 3H), 1.83 (s, 3H), 1.69 – 1.57 (m, 2H), 0.95 (t, $J = 7.4$ Hz, 3H).

$^{13}\text{C-NMR}$ (100 MHz, CDCl_3) δ 142.2, 138.3, 137.3, 136.4, 136.0, 135.3, 130.6, 129.3, 129.2, 128.1, 127.7, 127.6, 127.5, 126.8, 124.0, 51.7, 51.1, 22.2, 21.5, 20.9, 11.7.

HRMS (ESI) calcd. for $\text{C}_{24}\text{H}_{29}\text{O}_2\text{N}_2\text{S}$ ($\text{M} + \text{H}^+$) 409.1944. Found 409.1938.

HPLC (IA column, 85:15 *n*-Hex/*i*-PrOH, 30 °C, 1.0 mL/min): t_{R} 8.69 min (minor) and 10.73 min (major).

Synthesis of (*R*)-*N*-(2'-(((Cyclohexylmethyl)amino)methyl)-6'-methyl-[1,1'-biphenyl]-2-yl)-4-methylbenzenesulfonamide. **34Df**



Following the general procedure from **32D** and cyclohexylmethanamine **43f**, after 72 h and further purification by flash chromatography (3:1 *n*-hexane/EtOAc) afforded **34Df** (26.8 mg, 58%) as a light-yellow amorphous solid.

$[\alpha]_{\text{D}}^{20} +61.4$ (c 0.17, CHCl_3) for 95% *ee*.

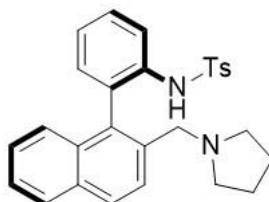
$^1\text{H-NMR}$ (400 MHz, CDCl_3) δ 7.71 (d, $J = 8.1$ Hz, 1H), 7.33 (dd, $J = 8.1, 1.6$ Hz, 3H), 7.23 (t, $J = 7.3$ Hz, 1H), 7.14 (d, $J = 7.5$ Hz, 2H), 7.02 (t, $J = 7.5$ Hz, 3H), 6.96 – 6.91 (m, 1H), 3.50 (d, $J = 1.6$ Hz, 1H), 3.22 (d, $J = 1.6$ Hz, 1H), 2.47 (dd, $J = 12.0, 6.8$ Hz, 1H), 2.40 (dd, $J = 12.3, 6.5$ Hz, 1H), 2.35 (s, 3H), 1.81 – 1.65 (m, 5H), 1.65 – 1.55 (m, 1H), 1.37 (s, 3H), 1.32 – 1.15 (m, 3H), 0.98 – 0.82 (m, 2H).

$^{13}\text{C-NMR}$ (100 MHz, CDCl_3) δ 142.3, 138.9, 138.1, 138.0, 137.2, 135.4, 135.2, 130.9, 129.7, 129.2, 128.4, 127.9, 126.9, 126.7, 126.5, 125.4, 56.2, 52.7, 36.8, 31.9, 31.3, 26.6, 25.9, 21.4, 20.7.

HRMS (ESI) calcd. for $\text{C}_{28}\text{H}_{35}\text{O}_2\text{N}_2\text{S}$ ($\text{M} + \text{H}^+$) 463.2414. Found 463.2407.

HPLC (IA column, 85:15 *n*-Hex/*i*-PrOH, 30 °C, 1.0 mL/min): t_R 7.28 min (minor) and 8.75 min (major).

Synthesis of (*R*)-4-Methyl-*N*-(2-(2-(pyrrolidin-1-ylmethyl)naphthalen-1-yl)phenyl)benzenesulfonamide. **34Ak**



Following the general procedure from **32A** and pyrrolidine **43k**, after 72 h and further purification by flash chromatography (3:1 *n*-hexane/EtOAc) afforded **34Ak** (38.4 mg, 84%) as a light-yellow amorphous solid.

$[\alpha]_D^{20} +192.6$ (c 0.38, CHCl₃) for 92% *ee*.

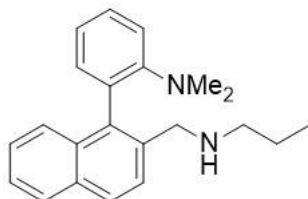
¹H-NMR (400 MHz, CDCl₃) δ 7.92 (dd, $J = 8.2, 1.3$ Hz, 1H), 7.83 (d, $J = 8.4$ Hz, 1H), 7.77 (d, $J = 8.2$ Hz, 1H), 7.54 – 7.41 (m, 2H), 7.37 (t, $J = 7.3$ Hz, 1H), 7.24 (td, $J = 7.5, 1.3$ Hz, 1H), 7.00 (dd, $J = 7.6, 1.7$ Hz, 2H), 6.93 (d, $J = 7.8$ Hz, 2H), 6.65 (d, $J = 8.6$ Hz, 1H), 6.42 (d, $J = 7.7$ Hz, 2H), 3.90 (d, $J = 11.9$ Hz, 1H), 3.32 (d, $J = 11.9$ Hz, 1H), 2.86 – 2.75 (m, 2H), 2.75 – 2.64 (m, 2H), 2.06 (s, 3H), 2.06 – 1.97 (m, 4H).

¹³C-NMR (100 MHz, CDCl₃) δ 141.4, 138.3, 136.9, 136.5, 134.5, 133.6, 133.0, 132.5, 132.3, 128.9, 128.4, 128.1, 127.8, 127.6, 127.2, 127.0, 126.1, 125.8, 125.1, 59.0, 53.5, 23.2, 21.3.

HRMS (ESI) calcd. for C₂₈H₂₉O₂N₂S (M + H⁺) 457.1944. Found 457.1944.

HPLC (IA column, 85:15 *n*-Hex/*i*-PrOH, 30 °C, 1.0 mL/min): t_R 7.22 min (minor) and 8.12 min (major).

Synthesis of *N,N*-Dimethyl-2-(2-((propylamino)methyl)naphthalen-1-yl)aniline. **34Ea**



Following the general procedure from **32E** and *n*-propylamine **43a**, after 72 h and further purification by flash chromatography (3:1 *n*-hexane/EtOAc) afforded **34Ea** (29.0 mg, 91%) as a light-yellow amorphous solid.

¹H-NMR (400 MHz, CDCl₃) δ 7.86 (d, *J* = 8.2 Hz, 2H), 7.68 (d, *J* = 8.4 Hz, 1H), 7.57 (d, *J* = 8.5 Hz, 1H), 7.49 – 7.33 (m, 3H), 7.14 (d, *J* = 8.2 Hz, 1H), 7.09 – 7.04 (m, 2H), 3.71 (d, *J* = 12.8 Hz, 1H), 3.63 (d, *J* = 12.9 Hz, 1H), 3.24 (br s, 1H), 2.49 (q, *J* = 7.1 Hz, 2H), 2.42 (s, 6H), 1.46 (h, *J* = 7.3 Hz, 2H), 0.85 (t, *J* = 7.3 Hz, 3H).

¹³C-NMR (100 MHz, CDCl₃) δ 152.0, 137.5, 134.8, 133.3, 133.0, 132.9, 131.0, 128.7, 128.0, 127.9, 127.6, 126.6, 126.0, 125.4, 121.4, 117.8, 52.2, 51., 43.3, 22.9, 11.8.

HRMS (ESI) calcd. for C₂₂H₂₆N₂ (M + H⁺) 318.2096. Found 318.2099.

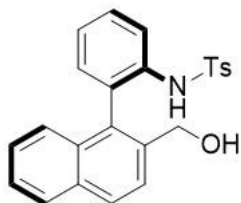
IV.4.4. General procedure for the reduction of carbonyls via asymmetric transfer hydrogenation.

To a flame-dried Schlenk tube with aldehyde **32A,E** or ketone **32F** (0.1 mmol) anhydrous 1,4-dioxane (1.0 mL), was added at room temperature. Then, [RuCl(*p*-cymene)(*S,S*-Ts-DPEN)] (5 mol%) followed by 1,4-dioxane (0.5 mL) and 5:2 HCO₂H/Et₃N (40 μL) azeotropic mixture were added, and reaction mixture was stirred for 36h. After that time, reaction brine was added and extracted with EtOAc, collected organic phases were dried over Na₂SO₄ and solvent was removed under reduced pressure. The residue was purified by column chromatography on silica gel with *n*-hex/EtOAc or CH₂Cl₂/EtOAc mixtures affording the resulting alcohols.

Note. Racemic alcohols were obtained by reduction of the aldehyde **32A,E** (1.0 eq.) in MeOH with NaBH₄ for 20 min. Quenching with water, and EtOAc extraction

afforded the racemic mixture of alcohols that were separated from reaction crude by preparative TLC prior to HPLC analysis.

Synthesis of (R)-N-(2-(2-(Hydroxymethyl)naphthalen-1-yl)phenyl)-4-methylbenzenesulfonamide. 42A



Following the general procedure from **32A**, purification by flash chromatography (3:1 *n*-hexane/EtOAc) afforded **42A** (39.7 mg, 98%) as a light-yellow amorphous solid.

$[\alpha]_D^{20} -23.4$ (c 0.40, CHCl₃) for 40% *ee*.

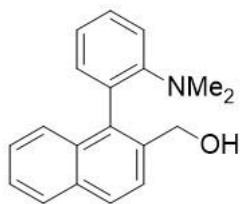
¹H-NMR (400 MHz, CDCl₃) δ 7.95 (d, *J* = 8.4 Hz, 1H), 7.88 (d, *J* = 8.0 Hz, 1H), 7.82 (d, *J* = 8.2 Hz, 1H), 7.69 (d, *J* = 8.5 Hz, 1H), 7.47 (q, *J* = 8.2 Hz, 2H), 7.36 (d, *J* = 7.8 Hz, 2H), 7.24 (t, *J* = 6.8 Hz, 1H), 7.17 (t, *J* = 7.2 Hz, 1H), 7.09 (d, *J* = 7.3 Hz, 1H), 7.01 (d, *J* = 7.8 Hz, 2H), 6.88 (d, *J* = 8.4 Hz, 1H), 6.81 (s, 1H), 4.39 (d, *J* = 12.4 Hz, 1H), 4.27 (d, *J* = 12.3 Hz, 1H), 2.36 (s, 3H), 2.07 (br s, 1H).

¹³C-NMR (100 MHz, CDCl₃) δ 143.6, 136.8, 136.4, 135.1, 133.1, 132.2, 131.5, 129.5, 129.4, 129.4, 129.2, 128.1, 127.0, 126.7, 126.4, 126.0, 125.5, 124.9, 121.4, 63.2, 21.6.

HRMS (ESI) calcd. for C₂₄H₂₂O₃NS (M + H⁺) 404.1315. Found 404.1313.

HPLC (IA column, 85:15 *n*-Hex/*i*-PrOH, 30 °C, 1.0 mL/min): t_R 12.20 min (major) and 16.48 min (minor).

Synthesis of (1-(2-(Dimethylamino)phenyl)naphthalen-2-yl)methanol. 42E



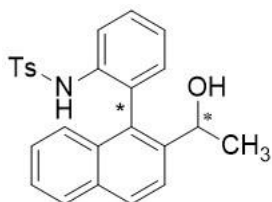
Following the general procedure from **32E**, purification by flash chromatography (3:1 *n*-hexane/EtOAc) afforded **42E** (21.9 mg, 79%) as a light-yellow amorphous solid.

¹H-NMR (400 MHz, CDCl₃) δ 7.91 (t, *J* = 7.5 Hz, 2H), 7.66 (dd, *J* = 8.4, 1.9 Hz, 1H), 7.58 (d, *J* = 8.4 Hz, 1H), 7.54 – 7.36 (m, 3H), 7.27 – 7.22 (m, 1H), 7.17 (ddd, *J* = 7.2, 6.0, 1.3 Hz, 1H), 7.11 (dt, *J* = 7.5, 2.0 Hz, 1H), 5.32 (br s, 1H), 4.39 (dd, *J* = 11.1, 1.9 Hz, 1H), 4.33 (dd, *J* = 11.0, 1.9 Hz, 1H), 2.42 (s, 6H).

¹³C-NMR (100 MHz, CDCl₃) δ 151.6, 136.6, 133.7, 133.2, 133.0, 132.1, 128.8, 128.4, 128.4, 128.2, 126.5, 126.3, 125.7, 122.7, 118.2, 65.3, 43.5.

HRMS (ESI) calcd. for C₁₉H₂₀ON (M + H⁺) 278.1539. Found 278.1540.

Synthesis of (+)-*N*-(2-(2-(1-Hydroxyethyl)naphthalen-1-yl)phenyl)-4-methylbenzenesulfonamide. 42F



Following the general procedure from **32E**, purification by flash chromatography (3:1 *n*-hexane/EtOAc) afforded **42E** (21.9 mg, 79%) as a light-yellow amorphous solid.

[α]_D²⁰ +64.8 (c 0.36, CHCl₃) for 83% *ee*.

¹H-NMR (400 MHz, CDCl₃) δ 8.03 (d, *J* = 8.7 Hz, 1H), 7.92 (d, *J* = 8.2 Hz, 1H), 7.83 (t, *J* = 8.1 Hz, 2H), 7.55 – 7.46 (m, 3H), 7.44 (t, *J* = 7.7 Hz, 1H), 7.24 – 7.10 (m, 5H), 6.80 (d, *J* = 8.4 Hz, 1H), 6.08 (s, 1H), 4.72 (d, *J* = 6.5 Hz, 1H), 2.44 (s, 3H), 1.71 (s, 1H), 1.44 (d, *J* = 6.3 Hz, 3H).

¹³C-NMR (100 MHz, CDCl₃) δ 144.0, 142.1, 136.1, 135.8, 133.1, 131.8, 131.0, 130.2, 130.0, 129.6, 129.3, 128.2, 127.4, 127.0, 126.9, 126.1, 125.4, 123.9, 123.7, 117.4, 67.1, 24.2, 21.6.

HRMS (ESI) calcd. for C₂₅H₂₄O₃NS (M + H⁺) 418.1471. Found 418.1473.

APPENDIX I: Abbreviations

AcO	Acetate
AcOEt	Ethyl Acetate
Alk	Alkyl
Aq	Aqueous
Ar	Aryl
Bn	Benzyl
Boc	<i>tert</i> -Butoxycarbonyl
B ₂ pin ₂	Bis(pinacolato)diboron
Bu	Butyl
^t Bu	<i>tert</i> -Butyl
<i>n</i> BuLi	<i>n</i> -Butyl lithium
Cat	Catalyst
Cat*	Chiral catalyst
cod	1,5-Cyclooctadiene
CPA	Chiral Phosphoric Acid
<i>m</i> -CPBA	<i>meta</i> -Chloroperbenzoic acid
dba	Dibenzylidenacetone
DBU	1,8-Diazabicyclo[5.4.0]undec-7-ene
DCE	1,2-Dichloroethane
DCM	Dichloromethane
DIPEA	<i>N,N</i> -Diisopropylethylamine
DKR	Dynamic Kinetic Resolution

DMAP	4-Dimethylaminopyridine
DME	1,2-Dimethoxyethane
DMF	<i>N,N</i> -Dimethylformamide
DMSO	Dimethylsulphoxide
DPPA	Diphenyl phosphoryl azide
dppp	1,3-Bis(diphenylphosphino)propane
dppf	1,1'-Bis(diphenylphosphino)ferrocene
DFT	Density Functional Theory
DYKAT	Dynamic Kinetic Asymmetric Transformation
<i>ent</i>	Enantiomer
eq.	Equivalents
Et	Ethyl
FG	Functional Group
HBpin	Pinacolborane
<i>n</i> -Hex	<i>n</i> -Hexane
HPLC	High Performance Liquid Chromatography
HRMS	High Resolution Mass Spectrometry
<i>i</i> Pr	<i>iso</i> -Propyl
IRC	Intrinsic Reaction Coordinate
L	Ligand
L*	Chiral ligand
LA	Lewis Acid
LB	Lewis Base

M	Metal
Me	Methyl
MeCN	Acetonitrile
MMPP	Magnesium monoperoxyphthalate
M.p.	Melting point
MS	Molecular sieve
Ms	Mesyl
n.d.	Not determined
n.r.	No reaction
Nf	Nonaflate
NHC	<i>N</i> -Heterocyclic carbene
NMP	<i>N</i> -Methylpyrrolidone
NMR	Nuclear Magnetic Resonance
Np	Naphthyl
Nu	Nucleophile
O ^t Bu	<i>tert</i> -Butoxide
Ph	Phenyl
PMHS	Polymethylhydrosiloxane
ppm	Parts per million
r.t.	Room temperature
R	General substituent
Tf	Triflate
TFA	Trifluoroacetic acid

TLC	Thin Layer Chromatography
THF	Tetrahydrofuran
Ts	Tosyl
X	Halogen
Xyl	Xylyl
δ	Chemical shift

APPENDIX II: General Methods

NMR Spectroscopy

¹H-NMR were recorded using a Bruker Advance DRX-500, and Bruker Advance DRX-400 spectrometers at 500 and 400 MHz respectively. ¹³C-NMR spectra were recorded using Bruker Advance DRX-400 spectrometer at 100 MHz. Solutions in commercial deuterated solvents were used to prepare samples, CDCl₃, CD₂Cl₂ or CD₃OD. Residual solvent peaks were used as an internal reference for ¹H-NMR spectra (CDCl₃ δ 7.26 ppm, CD₂Cl₂ δ 5.32 ppm, or CD₃OD δ 3.31 ppm) and ¹³C-NMR spectra (CDCl₃ δ 77.2 ppm, CD₂Cl₂ δ 53.8 ppm, or CD₃OD, 9.0 ppm). Coupling constants (J) are quoted to the nearest 0.1 Hz. The following abbreviations (or combinations thereof) were used to describe ¹H-NMR multiplicities: s = singlet, d = doublet, t = triplet, q = quartet, hept = heptet, m = multiplet, br = broad.

Mass Spectrometry

High Resolution Mass Spectrometry (HRMS) measurements were performed either by Kratos MS-80 RFA or Micromass AutoSpecQ (ESI) by General Services from University of Seville (CITIUS). In HRMS characterization, m/z found value for molecular peak was compared with that calculated from more abundant isotopes.

Chromatography

Analytical thin layer chromatography (TLC) was employed to monitor reactions progress. This technique was performed with commercial aluminium plates coated with 0.25 mm silica gel (Merck, silica gel 60 F254). Compounds were detected under UV-light at 254 nm and by dipping the plates in different home-made stains like mostain (20 g of ammonium molybdate tetrahydrate, 0.4 g of Ce(SO₄)₂ and 400 mL of 10% aqueous H₂SO₄), phosphomolybdic (5% solution of phosphomolybdic in EtOH), permanganate (10 g KMnO₄, 66 g K₂CO₃, 17 mL AcOH, 1 L H₂O), or ninhydrin (0.1% solution of ninhydrin in EtOH).

Flash chromatography purifications were performed with Merck silica gel 60 (0.040-0.063 μm grade), and eluting by gravity or using compressed air pressure. As eluents, solvent mixtures are indicated for each case.

Melting Points

Melting points were measured on a Gallenkamp MFB-595 apparatus, and are uncorrected.

Optical Rotations

Optical rotations were measured on a Perkin-Elmer 341 MC using a 1.0 cm cell with a Na ($\lambda = 589 \text{ nm}$) yellow light.

X-ray Analysis

X-ray diffraction analyses were performed by Dr Javier Iglesias Sigüenza at the X-ray services from Centro de Investigación, Tecnología e Innovación de la Universidad de Sevilla (CITIUS), equipped with a BRUKER APEX II diffractometer. This equipment has the possibility of employ three different irradiation lamps: copper, tungsten, or silver. Furthermore, it includes a four circles goniometer with Kappa geometry, and a high sensitivity CCD detector. It is also possible to cool the samples thanks to a liquid nitrogen cooling system Cryostream 700 Plus from Oxford, which allows the execution of experiments from 80 to 500 K, with a 0.1 K stability.

Experimental procedures, reagents and glassware

Commercially available chemicals were used as purchased, or where specified, purified by standard techniques. Solvent compositions are given in (v/v). All reactions were carried out under an atmosphere of nitrogen in flame-dried glassware with magnetic stirring, unless otherwise indicated. MeCN, THF, DCM, and DMF were purified by an Innovative Technology Solvent Delivery System. All other solvents were used as purchased.

Anhydrous solvents

Anhydrous toluene and DCM were directly used after collection from PureSolv MD3 Solvent Purification System. THF was dried over Na with benzophenone as indicator, and distilled just before every single use. 1,4-Dioxane was dried over CaH and distilled.